Naval Research Laboratory
Stennis Space Center, MS 39529-5004

NRL/MR/7331--93-7074

Characterization and Evaluation of the At-Sea Performance of the Airborne Expendable K_d and Temperature Probe

ALAN WEIDEMANN

Ocean Science Branch
Oceanography Division

MICHAEL WILCOX

Planning Systems, Inc.
Slidell, LA 70458

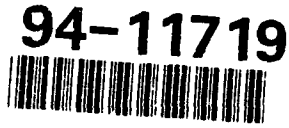

March 21, 1994

REPORT DOCUMENTATION PAGE

Form Approved
OBM No. 0704-0188

1. Agency Use Only *(Leave blank).*	2. Report Date.	3. Report Type and Dates Covered.
	March 21, 1994	Final

4. Title and Subtitle.

Characterization and Evaluation of the At-Sea Performance of the Airborne Expendable K_d and Temperature Probe

5. Funding Numbers.

Program Element No. 0604704N
Project No.
Task No.
Accession No.
Work Unit No. 735136B4

6. Author(s).

Alan Weidemann and *Michael Wilcox

7. Performing Organization Name(s) and Address(es).

Naval Research Laboratory
Oceanography Division
Stennis Space Center, MS 39529-5004

8. Performing Organization Report Number.

NRL/MR/7331--93-7074

9. Sponsoring/Monitoring Agency Name(s) and Address(es).

Naval Research Laboratory
Tactical Oceanographic Warfare Support Office
Stennis Space Center, MS 39529-5004

10. Sponsoring/Monitoring Agency Report Number.

NRL/MR/7331--93-7074

11. Supplementary Notes.

*Planning Systems, Inc.
Slidell, LA 70458

12a. Distribution/Availability Statement.

Approved for public release; distribution is unlimited.

12b. Distribution Code.

13. Abstract *(Maximum 200 words).*

This report documents the performance of the Airborne Expendable Vertical Attenuation (K_d) and Temperature (AXKT) Probe manufactured by Sippican Incorporated during three at-sea evaluation tests. The tests include clear and overcast sky conditions with relatively calm seas for all tests. The test locations include a Norwegian fjord and nearshore and offshore sites in the Northwest Pacific Ocean. The performance of the AXKT is evaluated relative to shipboard measurements of the vertical attenuation coefficient, K_d, from 15 to 100 m. Despite several potential design weaknesses that can be corrected, the AXKT showed that it has potential to measure K_d to 200 m in waters with K_d values less than 0.06 m^{-1}. This is a detection range of 12 (product of K_d and maximum depth of valid signal). In comparison with shipboard measurements, the AXKT: (1) exceeded the depth capabilities of shipboard measurement systems; (2) was generally within 10% of the shipboard-derived K_d when multiple probes were used, with departures of 20 to 40% for a single probe in regions of high optical or temperature variability; and (3) exhibited trends for unresolved systematic departure of K_d relative to those obtained with shipboard systems.

14. Subject Terms.	15. Number of Pages.
AXKT, Shipboard Measurement System	177
	16. Price Code.

17. Security Classification	18. Security Classification of Report.	19. Security Classification of This Page.	20. Limitation of Abstract. of Abstract.
Unclassified	Unclassified	Unclassified	SAR

CONTENTS

CONTENTS (cont.)

CHARACTERIZATION AND EVALUATION OF THE AT-SEA PERFORMANCE OF THE AIRBORNE EXPENDABLE K_d AND TEMPERATURE PROBE

1.0 Introduction

The determination of the vertical attenuation coefficient for light propagation in the open ocean is, at present, an important input parameter for passive and active system performance modeling for nonacoustical Antisubmarine Warfare (ASW), Amphibious Warfare, and Special Warfare. To meet the wide spatial and temporal coverage necessary to encompass the large variability in this parameter, an air expendable unit was developed for the Naval Research Laboratory (NRL) by Sippican Incorporated (Marion, Massachusetts). The Sippican Airborne Expendable Vertical Attenuation (K_d) and Temperature (AXKT) Probe has been evaluated by NRL, Codes 7331 and 7332, for its performance and ability to yield an accurate representation of the vertical attenuation coefficient as a function of depth.

This report summarizes the performance evaluation of the AXKT probe and examines data collected during three Performance-Evaluation studies made by NRL and the Naval Oceanographic Office (NAVOCEANO). The performance of the probe was evaluated in the following areas:

(1) Achievement of requested performance levels in scuttle time, failure rate, multichannel reception, and temperature profile response;

(2) Comparability of air and shipboard signals;

(3) Ability to accurately yield the vertical structure of the diffuse light attenuation coefficient (K_d) as compared to standard shipboard measurements of the diffuse attenuation coefficient;

(4) Depth range over which an "acceptable" K_d profile is obtained: nominally from the surface to 200 m;

(5) Optical characterization of the AXKT probe including cosine response, linearity, and spectral response;

(6) Techniques for processing relative irradiance to yield a K_d profile with removal of system noise;

(7) Near-surface K_d (0 to 10 m) determination; and

(8) Fall-rate equation versus shipboard temperature profiles.

Under normal incident irradiance (sun and sky contributions combined) and deep enough below the surface to be free from boundary effects, the cosine irradiance $E_d(z,\lambda)$ decreases approximately with an exponential decay rate with increasing depth. It is the derivative of this exponential decay that is calculated as the vertical attenuation coefficient $K_d(z,\lambda)$. The vertical

attenuation coefficient is an apparent optical property; thus, its value can be altered by the geometry of the measurement. The orientation for measurement of the vertical attenuation coefficient is with the diffuse cosine collector in the horizontal plane, parallel to the ocean surface. Mathematically, the vertical attenuation coefficient is defined by:

$$K_d(z,\lambda) = -\frac{1}{E_d}\frac{dE_d(z,\lambda)}{dz}.$$

Operationally, $K_d(z,\lambda)$ is calculated over a depth increment, Δz, as

$$K_d = \frac{\ln E_d(z_1,\lambda) - \ln E_d(z_2,\lambda)}{(z_2 - z_1)}.$$

The wavelength dependency is henceforth assumed.

There are several difficulties in using K_d as an optical property. The vertical attenuation coefficient varies not only with the geometry of measurement, but also with the constituents of the water as well. It is dependent on the solar zenith angle, the radiance distribution of incident light (i.e., the solar and sky contributions of photons to the downwelling stream), and surface phenomena (wavefocusing). Equally important is that K_d is operationally calculated over a depth increment. Since K_d is not constant with depth due to an ever changing inwater radiance field, the value of K_d is dependent on the depth increment used in the calculation. In addition, K_d is determined for a waveband from λ_1 to λ_2, not for a single wavelength; thus, K_d represents the convolution of the changing spectral characteristics of the water with the spectral response function of the sensor. Stavn (1982; 1988) has shown that a more accurate determination of the optical properties of water would be a measurement of absorption combined with a measurement of average cosine. To measure the average cosine, however, both the scalar and cosine irradiances for the up- and downwelling light streams are required. So while being sound theoretically, derivation of K_d from the average cosine and absorption is impractical because four irradiance measurements are required, all intercalibrated. In addition, an accurate method to measure absorption continues to be problematic.

The most common method employed to calculate K_d is to use regression analysis of $\ln E_d$ versus depth over a depth increment between 4 and 20 m. Smoothing the irradiance profile to remove noise, wavefocusing, and high-frequency ship motion effects normally proceeds the regression. A more recent technique developed by Mueller (1991) uses Hermitian polynominals over finite depth elements to analytically express the irradiance profile and derive K_d. The nodes (endpoints) for the function are selected based on ancillary information about the chlorophyll structure, thermocline or isopicnal position, and beam transmission structure

in the water column. But because of the recursive nature of the Hermitian polynomial, the method is sensitive to boundary conditions. The resulting K_d is also sensitive to node position. While yielding a good representation of the irradiance profile, and showing subtle structures in the K_d profile, the method has not been shown to be robust in its application. This is most notable when no ancillary oceanographic data is available, and the results become biased by any preconceived notion that the data analyst may have concerning the locations of changes in K_d with depth.

2.0 Test Site Conditions and Instrument Comparison

2.1 Test Site Conditions

2.1.1 Vestfjord, Norway

The first field test took place on 23 September 1990 in Vestfjord, Norway aboard the R/V *Bartlett* (Cruise 1310-90) between the hours of 1000 and 1300 (l.s.t.). The ship position was approximately 68°15'N and 15°49'E. Optical profiles were taken between AXKT drops as time permitted using a MER 2040 (Biospherical Instruments Incorporated, San Diego, California). The sea-state and weather conditions were ideal for the field evaluation. The sea state was 1 to 2 and skies were clear at the time of the deployment. The wave-height fluctuations as measured from pressure changes in the MER pressure sensor were <1 m. Because of the optimal weather and sea-state conditions, this deployment is weighted more heavily in showing the "at-sea" characteristics of the AXKT in the absence of overcast skies.

2.1.2 Pacific 1990 and 1992

The second and third field deployments were conducted on the shelf-break area (near the shore) of the Northeast Pacific during December 1990 and April 1992. For the 1990 cruise, all AXKT drops except one were made with the sun obscured by high altocirrus clouds. The sea condition for the 1990 test was about sea state 1 to 2 with winds 0 to 5 kt, wave height of <0.5 m, and a swell of 1 m. The sky conditions were variable during this test with clouds covering 60 to 80% of the sky. As a consequence of the overcast conditions, this deployment shows the impact of "no surface reference" on the derived K_d profiles.

The weather conditions during the Pacific 1992 deployment were much more favorable with only 20 to 40% of the sky overcast during the AXKT test. Observational reports indicated a dominance of high cumulus clouds. The wave height was <0.5 m with a swell of 1.3 m. The weather observations also indicated that the sun was unobscured during most of this test.

2.2 Instrument Comparison

2.2.1 Vestfjord, Norway

The optical characteristics for the AXKT are discussed in Sec. 4.3. In general, the central waveband for the AXKT probe is between 490 nm (as determined by the Center for Hydro-optics and Remote Sensing, CHORS, San Diego, California, during AXKT characterization tests) and 494 nm (reported to Sippican in Pierson Scientific Associates Incorporated 1989), with a 39 to 44 nm Full Width Half Maximum (FWHM) (bandwidth at one-half peak responsitivity). By comparison, the central peak for the MER 2040 is 488 (±3 nm) with a 10 to 12 nm FWHM bandwidth (Biospherical Instrument's Users Manual for MER 2040). Therefore, exact agreement between the vertical attenuation coefficients (K_d) is not expected, particularly near the surface where the spectral characteristics of the water may vary significantly spatially, temporally, and spectrally. Because K_d is near a minimum at 490 nm for most "blue" open ocean water (~0.03 to 0.04 m^{-1}), the broader band in the AXKT probe could lead to K_d values that are slightly higher than those measured by the MER; the magnitude will be a function of the particulate and dissolved substances in the water column and the waveband response of the AXKT. An end-to-end calibration of the AXKT probe has never been performed so that some error in K_d may arise due to the uncertainty in the irradiance/frequency conversion. This is discussed in greater detail in Sec. 4.0.

The data acquisition and fall (descent) rates for the MER 2040 and the AXKT are also different. Consequently, the spatial resolution (i.e., the average number of data points collected per meter) differs between the two instruments. The AXKT acquires data at a rate of 10 Hz and has a projected fall rate of about 1.65 m/sec. In contrast, the MER 2040 fall rate is approximately 0.8 m/sec and collects data at 13 Hz. Therefore the MER will acquire, on average, 2 to 3 times more points per meter than the AXKT probe. But the MER 2040 has potential ship motion and ship reflection/shadow restraints that the AXKT does not.

2.2.2 Pacific 1990 and 1992

Throughout the evaluation tests, the only aspect of the AXKT optical configuration that changed was the response time of the probe. However, for the Pacific 1990 and 1992 deployments a slightly different optical package (the MER 1032) was used for shipboard measurements taken by NAVOCEANO personnel. This model's optical characteristics are similar to the MER 2040 with a centerband at 488 (±3 nm) and a 12-nm FWHM. Like the MER 2040 used in Vestfjord, the spectral characteristics of the AXKT do not match the AXKT and exact agreement in K_d profiles is not expected. In addition, the NAVOCEANO instrument deployed during these tests has a fall rate of 0.33 m/sec and acquired data at a speed of 1.67 Hz.

There are several potential sources of error in the shipboard measurements. These include: (1) ship shadow interference, which

is very important under cloudy conditions or low sun angle (Gordon 1985; Voss 1986); (2) high-frequency wavefocusing effects, which are averaged over space and time in the near-surface data; (3) instrument self-shading (Gordon and Ding 1991); and (4) wave effects due to the wire angle and tilting of the package as the ship oscillates with gravity waves and swell.

3.0 AXKT Fall Rate and Temperature Profile Analysis

A cursory examination of AXKT fall rate was made by comparing the predicted depth position of the AXKT (shipboard received data) as determined using the fall-rate equation:

$$\text{Depth} = 1.65t - 0.001634t^2$$
(t in seconds, depth in meters),

with the depth measured by the MER 2040 or 1032 with Seabird conductivity-temperature-depth (CTD) unit auxiliary sensors. Temperature structures that appeared to be common to most of the MER and AXKT profiles are used as depth-mark indicators.

3.1 Vestfjord, Norway

Figures 1-3 show the temperature profiles for the AXKT and the MER and corresponding mean temperature profiles. The temperature features common to both data sets include: (1) a slight temperature increase (maximum) near 40 m; (2) a temperature minimum at about 48 to 50 m; and (3) a greatly reduced rate of change beginning at the bottom of the thermocline. Due to an electrical problem, there is high-frequency noise in the MER 2040 temperature profile; however, the identified features can be clearly delineated in the mean profile. The large standard deviation bars on the MER are a consequence of this electrical noise.

All AXKT temperature profiles for Vestfjord are plotted in Fig. 1. There is remarkable consistency in the position of the temperature increase near 40 m. On the other hand, the transition zone from the sharp thermocline to deep layer shows considerable variability. This is not surprising given that this test was conducted in a fjord, where mixed-layer depths may change over short distances (Lavoie et al. 1993). There is good agreement between the MER and the AXKT depths for both the 40- and 48-m structures. But there is a discernable difference between the depth of the third feature in the AXKT probes and that determined from the MER. This is the bottom of the thermocline where the steep decline in temperature seen in the upper portion of the water column ceases. The depth of this transition varies from 62 to 72 m in the AXKT profiles with a median at about 70 m, whereas the MER profiles suggest that this break occurs at about 65 m. By 70 m, the AXKT depth is approximately 5 m greater than that measured on the MER. This 5- to 10-m difference by 70 m between the MER and the AXKT is prevalent in the other tests as well.

3.2 Pacific 1990

There are two features in the AXKT (Fig. 4) and MER (Fig. 5) temperature profiles that are common for this test. The structures identified to compare the MER with the AXKT temperature profiles for the Pacific 1990 cruise include the location of the bottom of the thermocline near 67 m and a temperature inversion between 95 and 115 m. Because these features are somewhat variable in location, the mean and standard deviation for all shipboard (MER) optical profiles are compared to the mean and standard deviation for the AXKT probes (Fig. 6). In the AXKT profiles, there is a sudden drop in temperature near the surface suggesting that equilibration with sea temperature is problematic. The temperature measured by the AXKT is systematically 0.5°C higher than that measured by the MER system. The position of the thermocline and the temperature inversion at 115 m in the MER profiles are 10 m shallower for the AXKT probe; suggesting that the fall rate was in error by about 10% for the Pacific 1990 cruise.

3.3 Pacific 1992

For the Pacific 1992 cruise, the difference between the temperature profile as measured by the AXKT probe (Fig. 7) and that measured by the MER (Fig. 8) was less than observed during the two previous analyses. The comparison of mean AXKT and MER temperature profiles is presented in Fig. 9. At depths greater than 100 m, the disparity in depth measurements taken by the AXKT and the MER is greater than that observed between the surface and 100 m. However, the 10-m-depth difference evident in the 1990 deployments is only 0 to 5 m in this test. There is also at least a 0.2°C offset in temperature between the AXKT and the MER-CTD package at depths >100 m.

3.4 Conclusion

Both the Pacific 1990 and the Vestfjord experiments yielded depth values for the AXKT that are higher than two independent MER-CTD systems at depths of 70 to 100 m. This result suggests that either the predicted AXKT fall rate is about 10% too high or the secondary term in the fall-rate equation, which takes into account the slowing of the AXKT due to increased drag by the wire, is too low. For all three tests one can project that the AXKT probes may err by 5 to 15 m upon reaching a depth of 200 m. Of more concern is the apparent offset between the calibrated CTD packages used in the MER configurations versus the recorded AXKT temperature at a fixed depth. If the AXKT temperature had been less than the MER, then one could speculate that the mass of the MER contributed to an increased temperature; however, since the deviations are in the opposite direction, the cause of the offset remains a point of uncertainty in the overall performance of the AXKT.

4.0 AXKT Probe Evaluation Results

4.1 Probe Failure Rate

4.1.1 General Probe Failure

For this evaluation, general probe failure is identified by the loss of an interpretable signal in the aircraft and the shipboard systems. Due to a deficiency in the scuttling mechanism, probe failure that can be directly attributed to an overlap of radio frequency (RF) signals from subsequent AXKT probes is treated separately in Sec. 4.2. Because the 1992 drop contained so much RF interference, it is not considered in this analysis; although 5 of the 20 probes (25%) show evidence of an irradiance profile and are used in the K_d and temperature comparisons. Tables 1a and 1b summarize the qualitative acceptability of the probe signals.

Table 1a. Probe failure rate for Vestfjord, Norway (23 September 1990), test series. AXKT signal versus aircraft signal comparison. * denotes profile not used in data analysis. ** denotes that the profile shows temperature dependency through the thermocline (discussed in Sec. 4.1.2).

Drop	Channel	S/N	Ship Traces	Aircraft Traces	Comments
1	12	002	Good	None	
1	14	019	Good	None	
1	16	021	None	None	Probe failure*
2	12	007	Good	Good	Traces similar
2	14	003	Good	Good	Traces similar
2	16	001	Good	Good	Traces similar
3	12	016	Good	Good	Traces similar
3	14	018	Good	Erratic	
3	16	020	None	None	Probe failure*
4	12	006	Good	Good below 20 m	
4	14	010	None	Noisy 90-120 m	Increasing irradiance w/depth
4	16	017	Good, some	Good	
5	12	009	Breaks at	Occasional spikes	*
5	14	004	Good	None	
5	16	013	None	None	Probe failure*
6	14	011	Good	Good below 10 m	Both traces exhibit steps
6	16	005	Good	Good below 10 m	Both traces exhibit steps
7	12				AXBT
7	14	014	Good	Noisy	
7	16	012	None	Noisy	

Summary Vestfjord test:
Failure rate: 3 out of 20 = 15%
Probe data judged unacceptable: 14 out of 20 = 70%

Table 1b. Probe failure rate for the Pacific 1990 test series sponsored by NAVOCEANO.

Drop	Channel	S/N	Ship Traces	Aircraft Traces	Comments
1	12	210	Good	Good	Traces similar
2	14	209	Good	Good	Traces similar
3	12	221	Good	Occasional spikes (10)	
4	12	217	Noisy 120-170 m	Noisy	
4	14	205	Noisy 140-180 m	Noisy 140-180 m	Traces similar
4	16	214	Good	Good	Traces similar
5	12	218	Good	Noisy to 140 m	Ship started late*
5	14	215	None	None	Probe failure*
5	16	208	Good to 160 m,	Noisy to 110 m	Ship started late*
6	12	223	Constant signal	Clipped 0-25 m,	Aircraft traces exhibits
6	14	207	Good	Good	Traces similar
6	16	202	Good	Noisy to 40 m	Aircraft started late
7	12	220	Good	Good	Traces similar
7	14	216	Poor	Poor	Possibility of clouds*
7	16	206	Good	Numerous spikes	
8	12	219	Good	Good	Traces similar
8	14	222	Good	Good	Traces similar
8	16	204	No irradiance,	No irradiance, Fair	Probe failure*

Summary Pacific 1990 test:

Failure rate: 2 out of 18 = 11%
Probe data judged unacceptable: 12 out of 18 = 67%

A good probe signal was identified as one in which exponential decay is obvious and contained less than 10 spikes. Signals that met this test but contained spikes could have processing techniques applied to them to remove the spikes. Using signal loss as a criterion, it is clear to see that the probe failure rate for the 1990 deployments ranges from 11 to 15% (Tables 1a and 1b). However, many AXKT profiles were considered too erratic and questionable to be included in the analysis of the K_d profiles. The Vestfjord and Pacific 1990 tests had about a 70% success rate for acceptable and interpretable irradiance profiles. Many of the exclusions are due to RF interference in part of the profile.

4.1.2 Temperature Dependency

In one Vestfjord probe (Channel 12, Drop 5; 12:5), there is an apparent "increase" in irradiance between the depths of 50 and 70 m. One reason for this could be "cloudy skies" becoming clear followed by the sudden onset of overcast skies again; however, observational notes indicate conditions were clear throughout the entire exercise. Upon further examination, it is evident that the "deviation" in the decay rate for irradiance coincides with the position of the thermocline (Fig. 10). The profiles of temperature and irradiance in Fig. 10 show the close relationship between the sharp increase in irradiance (five-fold increase) and the sudden

drop in temperature change as the probe falls through the thermocline. This magnitude of irradiance increase cannot be accounted for by phytoplankton fluorescence, and it is improbable that a bioluminescent organism adhering to the probe would yield such a signal. More likely is that this probe exhibited a strong temperature sensitivity in either the optical components (interference filters) or electrical components, or both. This large temperature dependency is evident in only one probe and is therefore believed to be an isolated case and not ubiquitous to the system. If consideration is given to the differences in response time of the MER and the AXKT probe, then overall, the performance of the AXKT near the thermocline equals that of the MER.

4.2. Scuttling Deficiencies

4.2.1 New Navy Mission

As ASW declines in importance and Special Operations Warfare, Mine Countermeasures, and Amphibious Warfare increase, the scenario for use of the AXKT probe switches from one of large areal coverage in the open ocean to localized concentrated assessment of environmental properties and their variability. With the latter focus of many Navy missions, the utilization of the AXKT will tend toward small areal coverage over various lengths of time. Because the signal of the probe is a frequency modulation, there must be assurance that a probe dropped at a specific time will cease transmission within a known time interval. If a signal does not stop after completion of a profile, then it may carry over into subsequent probes being recorded on the same channel. With closely spaced, concentrated sampling, or with drop patterns that may repeat over an identified area, there is a high requirement for the timely scuttling of a probe. In the open ocean and for ASW scenarios, this requirement is not as vital because drop patterns are large enough that spacing between the probes seldom yields signal overlap.

4.2.2 RF Interference in AXKT Probes

The initial design specification for the AXKT was for a 6-min scuttle time. However, during the course of the AXKT evaluation, a design flaw that has probably persisted for many years in another expendable probe, the Airborne Expendable Bathythermograph (AXBT), was uncovered. An attempt was made to document the extent of the scuttling problem in the Vestfjord and Pacific 1990 evaluation tests. During playback of the recorded data signals, three time intervals were recorded: (1) the time from detection of carrier to onset of modulation; (2) the length of time of modulation; and (3) the time period from the end of modulation to loss of carrier (start of background RF). The results are presented in Table 2. Note the prevalence at which the signal from one probe set persists into the next set. The key point is that the scuttle time is within the 6 min indicated by Sippican Incorporated, in only 2 of 32 probes launched. Several probes even show the "lack of scuttling sequence" after 15 min.

Between the second and third tests, Sippican reported that the apparent lack of scuttling within the 6-min time period was due to a master timer on the circuit board that was set for 12 min in test boards and never changed to the correct setting. The circuit board for the float was modified and the clock set to its proper activation time. These modifications were in place for the Pacific 1992 evaluation test.

During the Pacific 1992 test, the probes were dropped in close proximity to one another in a scenario that is representative of localized environmental characterization as defined by NAVOCEANO. Most of the probes, however, showed severe RF interference. All of the "interpretable data" for the Pacific 1992 test is presented in Appendix A; however, interpretable does not imply "acceptable" irradiance profiles, as the figures demonstrate. In many cases, only "portions" of a profile are evident. The operator noted that it was difficult, if not impossible, to discern the onset of modulation in many of the probes, or to determine when the carrier signal reception was lost from a particular probe and background RF levels achieved. Some probes stayed at the surface and were retrieved by NAVOCEANO for further examination. The RF interference is clearly evident in the profile traces after about six probes had been launched (Channel 14, Drop 4). The RF interference increases in magnitude in later probes as exemplified by Channel 12, Drop 7; Channel 14, Drop 7; and Channel 12, Drop 9. For probes such as these, no attempt to produce a K_d profile is made since the RF interference critically masks the irradiance decay signal.

Upon examination of the units retrieved by NAVOCEANO that failed to scuttle, Sippican reported that enough air is trapped in the unit after burning a hole in the bag that, under calm conditions, such as present in Vestfjord and Pacific 1992 test, there is sufficient buoyancy remaining to keep the bag afloat. The entrapment of air is apparently an inherent design flaw that has been with this scuttling mechanism for over a number of years. Since the probe is still floating, the RF carrier continues to cycle through the 6-min sequence until the sea battery is exhausted (several hours). This phenomenon is consistent with the "transient nature of the scuttling problem" because some probes would have insufficient buoyancy (i.e., enough trapped air) to keep them afloat. The severity of the scuttling problem would be dependent on test environmental conditions (sea state, wind, etc.), and the drop pattern for the probes. The net effect is that when dropping the probes in a concentrated area versus long track lines such as for open ocean, the scuttling problem is more pronounced. The evidence for this design oversight is present in data from the Vestfjord and Pacific 1992 evaluation tests.

Table 2. Scuttle times for Vestfjord and Pacific 1990 tests. T1 = time from carrier up to modulation; T2 = time of start of modulation to end of modulation; T3 = time of start of background RF and carrier lost. All time in minutes: seconds. + indicates that carrier continued into next probe launch.

Vestfjord Aircraft replay

Channel	S/N	T1	T2	T3
12	002	NOT ON TAPE		
14	019	NOT ON TAPE		
16	021	BAD PROBE		
12	007	0:45	2:08	9:12
14	003	0:45	2:15	8:55
16	001	0:45	2:15	8:55
12	016	0:43	2:51	18:55
14	018	0:43	1:07	? Uncertain due to bad signal
16	020	0:45	1:00	10:00+
12	006	0:42	2:17	9:16
14	010	0:45	2:17	9:10
16	017	0:46	2:16	9:13
12	009	0:43	2:14	8:45
14	004	NO AIRCRAFT DATA		
16	013	NO AIRCRAFT DATA		
12	008	0:42	2:40	25:23
14	011	0:45	2:15	9:15
16	005	0:46	2:16	9:13
14	014	0:43	2:15	? Noisy signal
16	012	0:38	2:09	13:19 Noisy signal

Pacific 1990 replay

12	210	0:43	3:37	6:57
14	209	0:46	2:20	9:03
12	221	0:43	3:14	5:34+
12	217	?	2:19	7:16+
14	205	1:05	2:55	Carrier from previous probe
16	214	0:43	2:15	Carrier from previous probe
12	218	?	2:03	30:39+
14	215	NO AIRCRAFT DATA		
16	208	BAD MODULATION BEGINNING		
12	223	?	4:53	8:11+
14	207	?	5:04	8:52+
16	202	?	3:51	6:55
12	220	?	2:18	10:41
14	216	0:43	4:52	8:52+
16	206	1:28	5:08	4:14? Noisy signal
12	219	0:42	4:27	Stopped tape before scuttling
14	222	0:42	?	? Noisy signal
16	204	0:43	4:10	? Bad probe

4.3 Optical Characterization

4.3.1 Staircase Step Function

4.3.1.1 Step Function Manifestation in Irradiance Profiles

A transient phenomenon appears in all three field tests that is characteristic of a digitization resolution limitation. The effect gives the irradiance profile the appearance of a "staircase" in which discontinuities in the decay rate of irradiance are observable. The magnitude of the effect is dependent on the absolute irradiance, with the effect most prevalent at low irradiance values. Four examples from the Vestfjord test (Fig. 11-14) and two from the Pacific 1992 (Fig. 15 and 16) test are presented to show the potential seriousness of this problem. Then irradiance profiles for Channel 14, Drop 6 and Channel 16, Drop 6 for the Vestfjord AXKT test (Fig. 11 and 12) are typical staircase profiles. In these profiles there are instances in the trace where there is no change in irradiance over a 5-m-depth interval (see inset over the 140- to 160-m-depth interval). The calculation of K_d over 5-m intervals in these regions leads to K_d values of zero (i.e., no change in irradiance). Note in both Fig. 11 and Fig. 12 that the staircasing decreases in severity as one approaches the surface (higher irradiances).

For the other two Vestfjord AXKT irradiance profiles presented, Channel 12, Drop 3 and Channel 12, Drop 4 (Fig. 13 and 14), the staircase effect is only about 1 to 2 m long and is obscured somewhat by high-frequency noise. The Pacific data from the third test (Channel 14, Drop 2 and Channel 14, Drop 5; Fig. 15 and 16) more closely approximate these examples. In the third deployment, the staircase step function is indistinct. One reason for this outcome is that by a depth of 140 to 150 m, irradiance levels in the Vestfjord test were lower than those at an equal depth in the Pacific 1992 test. For example, in the 140- to 150-m-depth range, the natural logarithm of irradiance is 2.5 to 3.5 for the Vestfjord drop versus 5.5 to 6.5 for the same depths in the Pacific. Since these probes are not individually calibrated, this is a crude comparison. But never the less, the large change does represent a significant disparity in irradiance levels.

The dependence in the magnitude of the staircase effect on ambient irradiance values is further evidence that the root of the problem may be digitization resolution or instability in the logging function. Instability in the logging function is supported by the transient nature of this problem. The problem is not always present and seems to be more prevalent in some profiles over others even though irradiance levels are similar. For example, in the Vestfjord test, Channel 16, Drop 6 (Fig. 12) has a much better defined "staircase effect" than that exhibited by Channel 12, Drop 3 (Fig. 13) even though both have relative irradiance values of ln 3 to ln 4 between 140 and 160 m.

4.3.1.2 Laboratory Manifestation of the Staircase Effect

The staircase effect is also a prevalent feature in the results from linearity tests that were conducted as part of the AXKT probe characterization by CHORS. Linearity measurements of the AXKT response to slowly changing irradiance were conducted on an optical rail by changing the distance between the source and the detector. The discontinuities are clearly evident in the scaled response (Fig. 17a and 17b). While linearity is indicated when viewed over a large dynamic range (Fig. 17a), it is clear from the data that for smaller and slowly varying irradiances, there is a shift in frequency in the AXKT output per unit change in the log of irradiance. Furthermore, this shift does not appear to be constant. The result is a linearity plot that shows a staircase step function with no change in the AXKT response over measurable changes in irradiance. In Fig. 17b, the impact of the staircase effect on fine resolution measurements of linearity is demonstrated. The irradiance scale for the step function, observed in the laboratory, is consistent with those observed in the AXKT irradiance profiles determined from at-sea test data.

The staircase function not only impacts the linearity determination, but also prevents an accurate determination of the immersion coefficient for the AXKT probe. When immersed in water, the transmittance characteristics of the diffusing material change. Therefore, in order to use an AXKT probe to measure "absolute" irradiance, the magnitude of this change is required. The presence of the staircase effect, however, precludes any accurate determination of this change in transmittance characteristics. During measurement of the immersion coefficient, the discontinuities due to the staircase effect are convolved into the transmittance changes of the diffuser, and consequently, large errors in the immersion coefficient calculation result. Attempts to measure the immersion coefficient by CHORS were unsuccessful.

4.3.2 Spectral Characterization

CHORS measured the spectral response (Fig. 18 and 19) for two AXKT probes. These spectral response plots show the relative response of a probe as a function of wavelength from 400 to 700 nm. The spectra identify three points:

(1) the central wavelength is about 491 nm;

(2) the FWHM is approximately 39-44 nm; and

(3) a high response to red wavelengths (>540 nm).

The high red responsivity is a function of the filters used and creates a "red tail" in the spectral response. This red tail can adversely influence the AXKT performance in estimating $K_d(488)$. Water is a strong absorber in the red region of the spectrum with absorption coefficients ranging from 0.06 m^{-1} at 540 nm to 0.65 m^{-1} at 700 nm, compared to 0.02 m^{-1} at 488 nm. Due to the red tail and as long as there is red light present, such as is common near the

surface, the AXKT will detect it and the rate of decay for irradiance will be influenced. The value for K_d at a wavelength will be proportionately weighted by the relative response at that specific wavelength. The reported "K_d" will be an overestimate near the surface where red light still represents a significant portion of the spectrum. On the other hand, in those coastal areas with high concentrations of colored dissolved organic material, the $K_d(488)$ may be slightly underestimated. In these environments the colored dissolved organic acids absorb light in the blue and shift the most penetrating wavelength from 490 nm toward 530 or 540 nm. In this case, too much weighting of the red region will yield K_d values that are too low. The amount of the error will depend on the overall spectral characteristics of the water and the absorbing constituents which are not known a priori. In both cases, the "red tail" is an AXKT optical characteristic that degrades the probes performance. This problem could be eliminated with a change in the filter selection or possibly modeled. Before any new filters are accepted for the probe, the transmission characteristics as measured IN THE AXKT PROBE ASSEMBLY should be determined and reported.

4.3.3 Cosine Response

The relative angular response was measured for one AXKT detector by CHORS. The angular response measurement determines the proximity of the detector's response (in the housing) to an ideal cosine response. The closer to the ideal cosine response, the easier to relate the probe response to measurement of downwelling irradiance. Fig. 20 shows the results of the cosine response measurement of CHORS. Note that the actual AXKT angular response exhibits a significant deviation from either that of an ideal cosine response or from an unshielded cylinder response. Mueller (1993) reported that an unshielded cylinder closely describes the AXKT diffuser/detector assembly configuration when in its housing.

Because of the unique and unusual results, measurements of the angular response were repeated by CHORS for any systematic errors. The resulting angular responses varied considerably (as indicated by measurements 1-4 in Fig. 20). While the data represents only a single probe, the conclusion drawn is that **THE AXKT DOES NOT HAVE A GOOD COSINE RESPONSE AS IT IS NOW CONFIGURED**. The deviation from the theoretical cosine curve is significant even at departures of less than 45° from normal. As a consequence, improper weighting is being given to the light incident from more oblique angles.

There is clearly azimuthal asymmetry in the cosine response. This is believed to be caused by the mechanical assembly of the AXKT diffuser/detector. There is a slot approximately 2 mm wide in the holder tube assembly that exposes the diffuser block to external illumination (see Mueller 1993; page 6 and 7 for details). This slot allows external stray light at specific azimuthal angles near the slot to hit the detector causing a 50% deviation from the ideal cosine response near 45°. The azimuthal anisotropy probably results in cyclic fluctuations in irradiance as the AXKT rotates during descent. The error in K_d will depend on the rotational

speed relative to the sampling frequency and the ambient radiance distribution.

The CHORS angular response data is significantly different than that published by Pierson Scientific Associates (Report to Sippican Incorporated 1989). The Pierson conclusion was that the AXKT probes exhibit good cosine response (Fig. 21). However, of some concern in their measurement was "shadowing and vignetting by the black body" since the diffuser was 0.025 in. below the AXKT housing. Sippican did not apparently characterize the "final" AXKT design (diffuser, detector, and housing).

4.3.4 Response Time and Effect on K_d Profile

4.3.4.1 Response Time Characteristics

The response time is operationally defined as the length of time necessary to decrease the amplitude by 3 dB when going from high light to "dark" conditions. The response time of the AXKT is the integrated response of several electronic systems, each with their own characteristic signal response. The response time of the AXKT was about 700 to 1000 msec for deployments one and two. This was decreased by the manufacturer to 400 to 500 msec for the Pacific 1992 test. The main electronic component dominating the response time is a capacitor response that is required in the circuit just before the log amplifier. This aids in achieving the high gains necessary at low irradiance levels. Even the 500 to 1000 msec response is slow, however, compared to wavefocusing time scales (tens of msec; Stramski and Dera 1988).

The response time for deployments one and two is a critical issue. The slow response time effects both the near-surface area, as well as irradiance changes at the "boundary layers." In the first two deployments an opaque launch tube was employed; therefore, the irradiance rapidly increased after exiting the launch tube. The time required for the irradiance to reach ambient levels was about 3 sec, based on acceleration time and fall rate. The near-surface effect is offset somewhat by the acceleration time (2 to 3 sec) required to reach terminal velocity in the AXKT (depending on entry orientation). In the third deployment, a more translucent tube was used. The effectiveness of the translucent tube in the third deployment and the near-surface irradiance problems will be discussed in greater detail in Sec. 4.4.

4.3.4.2 Response Time Effect on K_d Profile

The conditions under which a K_d profile is influenced by the relatively slow response time include: (1) descent through turbid water (uniformly high K_d); (2) descent through a penetrating layer with a different "attenuation"; and (3) exposure to varying incident light levels (e.g., clouds). Under each of these conditions, a finite amount of time passes before the AXKT yields the correct relative irradiance. The 1-sec response time for the first two deployments can potentially cause a "smearing" of the K_d profile in regions of rapid transition. This smearing has been

found to be negligible relative to the uncertainties inherent in the calculation of K_d. The effect of this smearing is manifest in the K_d profile for the Vestfjord data by a systematic 5% overestimate in K_d determined for a rapidly changing irradiance field (see Appendix B). For the Pacific 1990 data, the deviation was as large as 40% (Appendix C).

The overestimations of K_d by the AXKT relative to the MER are partially resolved by improper depth determination. In a region with a rapidly changing K_d, a 10% error in depth can easily lead to an additional 20% error in K_d (Fig. 23). The error in the Vestfjord and Pacific 1990 data can be reduced by assuming that the AXKT depth is in error by 5 to 10 m at the thermocline boundary during these two tests. The uncertainty in depth suggested by the temperature data (i.e., a 10% error at 70 m) is sufficient to explain some of the deviation between the Vestfjord and Pacific 1990 K_d values and those collected from the MER system data. The error in K_d due to the 1-sec response time increases the deviation in K_d. The mean slope of the K_d through the thermocline as estimated from the average AXKT and MER profiles are presented for the three tests in Fig. 22-24. For the Vestfjord test, the mean slope is 0.0014 (AXKT) versus 0.0016 (MER), and 0.0008 (AXKT) versus 0.0010 (MER) for the Pacific 1990 test. There is no difference in the rate of change in K_d through the thermocline in Pacific 1992 AXKT and MER average profiles. K_d is calculated as described in Sec. 4.6.1.

In the Pacific 1992 test, the smearing due to the response time of the probe is much less obvious. The AXKT and the MER exhibit approximately the same transition regions (Fig. 23). However, postprocessing was necessary to reduce the offset between the MER and AXKT K_d values at depths below 70 m (Sec. 4.6.2). Since only 5 AXKT profiles were useable for the Pacific 1992 test, the performance of the AXKT in an environment with a large or sharp optical boundary, such as that present in many coastal areas, has not been determined.

4.4 Near-surface Response

Errors in the near-surface K_d profile may be the result of several mechanisms: (1) the blockage of the incident light by the launch tube; (2) the response time of the AXKT sensor package; (3) surface saturation at high light intensities; and/or (4) acceleration of the probe (leading to an inaccurate depth interval prior to the AXKT reaching terminal velocity). It is often difficult to separate these factors since the signal at depth is affected by all of these mechanisms.

4.4.1 Opaque Tube Versus Translucent Tube

The deployment methodology and the slow response time of the AXKT probe influence the type of launch tube and methodology required. Fig. 25 and 26 show the combined effect of the opaque launch tube and the slow response time for four AXKT probes deployed in Vestfjord, Norway (Channel 12, Drop 1; Channel 16, Drop

2; Channel 14, Drop 3; and Channel 12, Drop 4). Evident in these figures is a "dip" in the relative irradiance near the surface (0 to 3 m). Even though the opaque tube extends less than a meter into the water, low irradiances are persistent to a depth of 2 to 3 m. At depths greater than 3 m, irradiance increases and recovers to "ambient" levels. The discrepancy between the 1-m launch tube and the 3-m depth of recovery is due to an approximate 2-sec acceleration time of the probe to terminal velocity and the near 1-sec response time of the probe.

The net result of this irradiance "dip" at the surface on the K_d profile is dramatic. Because light is increasing with depth as the probe is launched and ambient light levels are reached, K_d will have the opposite sign normally associated with it (i.e., light intensity is not decaying with depth but rather increasing). The K_d profile is therefore contaminated over a depth range that depends on how quickly ambient light is reached, as well as the depth increment (processing window) used in calculating K_d. With the standard processing techniques applied to AXKT data for this report, K_d values are unacceptable from the surface to 15 m for most profiles.

To alleviate the problems introduced by the opaque launch tube, a translucent tube was adopted by Sippican for the Pacific 1992 evaluation test. However, the lack of "good" probes precludes any conclusions to be drawn on the effectiveness of the new tube. The results are mixed on the effectiveness of the translucent tube. All acceptable near-surface profiles have been plotted (Fig. 27-30). The profiles for Channel 12, Drop 6 and Channel 14, Drop 8, while being used in the overall profile analysis, are not shown due to large surface noise and surface irradiance saturation, respectively. In three of the eight probes presented, the "dip" in irradiance near the surface typical of deployments one and two is still evident. Thus, one can conclude that the opaque versus translucent tube is not the only factor contributing to the low irradiance observed. The problem is confined to the upper 2 m and is possibly due to faster response time of the AXKT probes used in the 1992 deployment.

4.4.2 Surface Saturation

Several AXKT probes from the Pacific 1992 test that have acceptable irradiance profiles below 10 m show evidence of saturation near the surface. Saturation is marked by a clipped appearance in irradiance with an upper limit evident. Clear cases are the profiles from AXKT probes for Channel 14, Drop 5; Channel 14, Drop 8; and Channel 16, Drop 3 (Fig. 28-30). In each of these plots, there is a definite upper limit (13.8) that is not exceeded even though extrapolation of the irradiance below 10 m suggests that higher values would be expected. The cause of this upper limit is presumably the manufacturer's dynamic range setting. Therefore, the upper limit (i.e., the saturation) is correctable through an adjustment to the dynamic range of the AXKT. There is a trade-off, since some probes with the saturation correction may not yield valid irradiances at depths approaching 200 m.

Saturation at the surface is distinct in the Vestfjord and Pacific 1990 data as well. Figure 31 shows three near-surface profiles for these tests (Vestfjord AXKT Channel 16, Drop 6; AXKT Channel 14 Drop 1; and Pacific 1990 Channel 12, Drop 7). These irradiance profiles also exhibit the "clipped" irradiance characteristic of saturation. The conclusion is that surface saturation is not a problem isolated to a few probes, but rather is ubiquitous in the AXKT design and circuitry. There is a high probability that saturation of the probes will take place in areas near the equator where irradiances near the surface exceed those in either the Pacific or Vestfjord tests. In Vestfjord, the solar elevation was low, and in the Pacific 1990 test, which was conducted in late fall, overcast skies were prevalent. Since neither of these cases is representative of high solar intensity, saturation of the probe is very likely for most water types. Generally irradiances just below the ocean surface are 200 $\mu W\ cm^{-2}\ nm^{-1}$ with occasional spikes, under conditions where the sun is at the fringe of a cloud and for a wind-blown surface. However, in Vestfjord, surface irradiances were in the range of 150 to 200 $\mu W\ cm^{-2}\ nm^{-1}$, and even lower for the Pacific 1990 test.

The phenomenon that enhances irradiance below the surface to saturation levels when a wind-roughened surface is present is wavefocusing. Under such environmental conditions, increases in downwelling irradiance due to wavefocusing can be as high as a factor of 3 above the mean irradiance (Dera and Stramski 1986; Stramski and Dera 1988). However, the slow AXKT response time and large surface area of the detector lessen the impact of wavefocusing to a range commonly exhibited by collectors of 1 cm or greater in size. The irradiance increases for instruments of this size are about 1.5 to 2.0 fold in the upper 2 m. While wavefocusing is a feature in the MER data, it is not found in the AXKT irradiance profiles. This is most likely due to the slow response time of the sensor relative to high-frequency surface phenomena.

4.5 Apparent Improper Frequency/Log Irradiance Setting

Two probes deployed during the Pacific 1992 cruise have calculated K_d values that are approximately a factor of 2 too low. A plot of the irradiance as a function of depth for these two AXKT probes (Channel 12, Drop 1 and Channel 16, Drop 7) is presented in Fig. 32, together with a more typical irradiance profile (Channel 12, Drop 4). Note that the rate of change in irradiance over any specific depth increment for probe 12:4 is much greater than that for either probe 12:1 or probe 16:7. There is no apparent problem with measurement of surface irradiance in either probe 12:1 or 16:7; their surface values are about the same as those recorded for all the other probes (relative values between 12 and 14 on ln scale). The temperature profiles for probes 16:7 and 12:1 expose no abnormalities. These factors suggest that the functional relationship between the change in frequency output of the AXKT and irradiance differed by approximately a factor of 2 for these probes (df/dE_d). Even though the resultant K_d profiles look similar in "structure" (Fig. 33), as a result of this changed frequency/

irradiance relationship, the magnitude for K_d differs by about a factor of 2 from other K_d profiles. The shift in calculated K_d is continuous over the entire profile and expressed even at the subsurface chlorophyll (i.e., K_d) maximum (about 35 m). However, the percent deviation is not constant for all K_d values. For K_d values of 0.04 m^{-1}, the disparity is a factor of 2 (100- to 200-m-depth interval), by comparison, the disagreement at the subsurface K_d peak (35 m) is 0.07 versus 0.04 or a factor of 1.75 too low. The cause for the shift in the frequency/irradiance relationship is unknown.

4.6 Comparison of AXKT and Shipboard K_d Profiles

4.6.1 Method for K_d Calculation

High-frequency noise in the AXKT and MER was removed using a lowpass digital filter with a Hamming window (Matlab). The same approach was used for both systems. The high-frequency noise was common through the entire AXKT profile and at low irradiances for the MER system. Filter windows of 250 (old method) and 100 points (new method) were used with a 4-m linear regression at 1-m intervals on the filtered irradiance data to calculate K_d. Data points that exceeded +/- 1 standard deviation from the mean irradiance for a 1-m bin were removed. Irradiance profiles are reconstructed after application of a high-frequency lowpass filter with either a 100-point or 250-point window (Fig. 34). The lowpass filter eliminates spikes in the data. Examples of resultant derived K_d profiles using these two window sizes are presented in Fig. 35. Windows of these sizes are consistent with the 21-m window used in processing at NAVOCEANO; however, recently Mueller (1991) has proposed a change to processing methodology. These large windows have a residual influence in the resulting K_d profile. Using the 100-point filter, Fig. 36 illustrates that normally, AXKT K_d profiles are influenced to a depth of about 16 m. The extent of the contamination is largely dependent on the "dip" in the near-surface irradiance.

Efforts are underway to determine optimal windows for both the MER and the AXKT employing either a lowpass filter or using the Mueller technique. Since the staircase effect can expand a depth interval of 5 m, it is speculated that for batch processing, use of a lowpass filter with a 50-point window (about 8 m) will be the optimal. A study of various window sizes and processing indicates that a 50-point window with deletion of the upper 0 to 5 m of data, provides the best K_d profile in the upper 25 m. To achieve accurate K_d values over the 0- to 5-m-depth interval, the low irradiance during launch (tube and warm-up) must be eliminated. The Mueller technique describes the irradiance profile in terms of optical depth and with $K_d(z)$ represented by Hermitian cubic polynomials defined over a set of finite depth elements. The Mueller technique allows for the interactive editing of data, such as the near-surface contamination that is an artifact of the system and not representative of the actual irradiances. Employing the Mueller methodology with fixed depth elements that are based on the irradiance profile from AXKT data has yet to be evaluated.

For each test cruise, AXKT irradiance profiles that show significant RF interference or exhibit clear contamination from atmospheric, ship, or probe effects are discarded from the analysis. From the resulting AXKT and MER K_d profiles, mean profiles and standard deviations are calculated. Because the irradiance measurements for the MER are seldom reliable for depths <5 m, and the processing techniques introduces errors in the "recovered" irradiance in the upper 16 m (see insert Fig. 34). The data above 16 m for the AXKT and MER K_d profiles is neglected in the overall comparison of K_d calculations.

The total number of AXKT profiles used for Vestfjord is 14, 12 for the Pacific 1990 test and 5 for the Pacific 1992 test (Table 3). Figures 36 through 44 show the processed K_d profiles used in the comparison for the AXKT, the MER, and the mean profile and standard deviation for each system. The performance of the AXKT is evaluated by comparing the processed K_d below 16 m for the AXKT with average K_d depth profile derived from all MER data.

Table 3. AXKT profiles used in the MER versus AXKT comparison.

Vestfjord 1990	Pacific 1990	Pacific 1992
12:1	12:1	12:4
12:2	12:3	12:6
12:3	12:4	14:2
12:4	12:7	14:5
14:1	12:8	14:8
14:2	14:2	
14:3	14:4	
14:5	14:6	
14:6	14:8	
14:7	16:4	
16:2	16:6	
16:4	16:7	
16:6		
16:7		

4.6.2 AXKT K_d Versus MER K_d Profiles

Appendices B, C, and D present the graphical results for the percent deviation of each AXKT relative to the mean MER profile for the Vestfjord test, the Pacific 1990 test, and the Pacific 1992 test, respectively. In the upper 16 m, the deviation of the AXKT from the MER reflects the effect of the processing methodology, the opaque launch tube for Vestfjord, the slow response time, as well as real differences in the K_d profiles. Therefore the analysis excludes the 0- to 16-m data.

4.6.2.1 Vestfjord Profiles

Below 16 m, there is an approximate overestimate in K_d by the AXKT of as much as 10% throughout the water column in most of the profiles. This overestimation is enlarged to 15 to 20% in the region of the thermocline where the second derivative in irradiance

exhibits its greatest value (the rate of change in K_d/m is the largest). The systematic 10% error in K_d is unexplainable by a constant 10% overestimation in the depth interval (i.e., fall rate uncertainty) since this would tend to yield lower K_d values for the AXKT, not higher values. In addition, inaccuracies in depth position, while influencing K_d near the thermocline where K_d varies with depth, cannot explain the 10% deviation at depths below 70 m. The low standard deviation in the AXKT profiles indicates that, in general, the AXKT profiles are consistent from profile to profile and agree well with the MER data (within the 10%). It should be noted that these data were collected under sunny conditions and therefore fluctuations in the incident irradiance during a profile were minimal.

4.6.2.2 Pacific 1990 Profiles

The Pacific 1990 test took place under overcast skies and the effect of such conditions is reflected in the K_d profiles. In contrast to the MER data, which can be normalized to a deck cell, and therefore many of the large deviations removed, the AXKT cannot. Even K_d derived from normalized MER data shows more profile-to-profile variability in this exercise than in either of the other two tests (a good example of this can be found in Fig. 40). Most K_d profiles for the AXKT display large oscillations (Fig. 39) brought about by erratic irradiance fluctuations. These large deviations apparently result from a changing incident light field during overcast skies. Even after taking the larger standard deviations into account, the mean profile for the AXKT and the MER differ substantially between 40 and 80 m (Fig. 41). In this region, K_d measured by the AXKT is frequently 20 to 40% greater than that determined with the MER system. This difference is a combination of the slow response time of the AXKT, possible inaccuracies in AXKT depth, and the impact of variable sky conditions.

There is some evidence that variability in K_d for the 40- to 80-m region may represent real differences in local optical properties. Major oscillations in the AXKT profiles (Fig. 39) occur in the region of the thermocline. In this region, even though AXKT response is the poorest, local variability in optical properties is likely to be the highest. Below the rapid transition of the thermocline and into the deep layer (> 70 m), the AXKT and the MER both yield values for K_d of about 0.04 m^{-1}. This value is close to that measured for clear ocean water at 488 nm and is consistent with low chlorophyll, low particle water (Jerlov 1976; Weidemann and Stavn - unpublished data analyses). A comparison of local fluctuations in temperature and K_d suggest there is internal consistency within the data itself, with moderate deviations in K_d occurring at depths around the region of rapid temperature change. Since moderate deviations in K_d (about 20 to 40% change in K_d from AXKT relative to the MER) coincide with temperature changes, an argument can be made that they represent actual variability in K_d together with some sensor temperature sensitivity. One MER cast has a K_d profile is nearly identical to the mean for the AXKT profiles, while others fluctuate throughout the thermocline. There are many profiles, however, that have sporadic fluctuations

(Channel 14, Drop 7 and Channel 16, Drop 7) that likely represent changes in incident irradiance during probe deployment.

4.6.2.3 Pacific 1992 Profiles

The data from the Pacific 1992 test is the most troublesome. For this test, new calibration coefficients were employed for the NAVOCEANO MER data. Mean profiles for the MER and the AXKT are within 10% of each other at depths less than 70 m, but differ by about 20% for depths greater than 70 m (below the thermocline). In contrast to deployments one (Vestfjord) and two (Pacific 1990), this test yielded K_d values for the AXKT that underestimated those of the MER system below depths of 60 m. Above 60 m, the two systems exhibited similar trends, although the AXKT was on average underestimated, by about 10% between 16 and 30 m. A fall rate that is slightly too high will result in K_d values that are underestimated, since irradiance values believed to be at depth z are actually those at z + 0.1z. Even though the cause of the systematic underestimate of K_d below 60 m cannot be determined, fall rate inaccuracies undoubtedly contribute to the disparity. Error in the measurement of irradiance by the MER system at low light levels is also a possibility. The MER system had a post calibration that differed significantly in dark values over those of previous calibrations. Because the AXKT and the MER are close and only differ in "low light regime," there is good reason to question the accuracy of the dark current correction for the MER. In addition, at depths below 70 m, the MER yielded values of K_d on the order of 0.05 m^{-1}, whereas, the AXKT probes had values close to 0.04 m^{-1}, which are similar to the Pacific 1990 deployment.

Because the data at depth give the appearance of an "offset" in K_d, a less likely source of error may be in the irradiance/ frequency relationship, whereby the apparent loss in irradiance is not as great as the actual change over a fixed distance, but this is only speculative. It is noteworthy that the Pacific 1992 test contains only a small sample size and is the only deployment where the AXKT and the MER differed significantly in the low light regime. This suggests that inaccuracies in the MER dark current are the most likely cause for the AXKT-MER disparity.

4.7 Conclusion

Overall, the AXKT compares favorably to shipboard MER profiles. Disregarding the near-surface data, the two systems generally were within 10% of each other, with some occasional deviations of 20 to 40% in the thermocline region. This is, however, an area where localized deviations in K_d are also expected to be the greatest, and where small deviations in actual depth may yield large deviations in K_d of the AXKT relative to the MER. The AXKT demonstrated that, to a first order, it could yield a K_d profile similar to that of the more expensive MER system. However, the Pacific 1992 data is suspect when compared to deployments in Vestfjord and Pacific 1990, since the AXKT was systematically lower than the MER system. The AXKT does have several distinct advantages over the MER. The depth range over which it yields an

interpretable signal was impressive. The AXKT almost always yielded a K_d value to 200 m with little indication of reaching the lower light limit. The MER has been shown to have some low light difficulty. The depth performance of the AXKT is up to a factor of 2 greater than that of the MER (Vestfjord test). This suggests that with a faster response time, these probes may be useful in Case 2 waters (coastal regimes) where K_d is high and light extinction is rapid. The low light range of the AXKT would be beneficial under such environmental conditions. A noteworthy point is that the AXKT almost always tended toward a value of 0.04 m^{-1} for measurements below 100 m. This value is consistent with Monte Carlo predictions for extremely clear oceanic environments (Jerlov 1976, Weidemann and Stavn - unpublished data analyses).

5.0 Recommendations for AXKT

The AXKT has been shown to yield reproducible profiles of the vertical attenuation, K_d, when examined at scales of 25 m or more. Over this scale, the AXKT can discern overall trends in K_d, as well as the value of K_d generally within 20% for a single probe, or within 10% with the use of multiple probes. For many applications, this level of precision is adequate and is equivalent to, or better than, values of K_d that can be derived from remote sensing platforms such as the upcoming ocean color satellite SEASTAR. The potential of the AXKT is not fully utilized for "coastal applications" since there are near- surface problems with the probe. However, with these problems overcome, the AXKT could be very useful in turbid water with high K_d values.

There are six areas in which the AXKT shows deficiencies and modifications to improve its performance are strongly advised. These are (in descending priority):

(1) RF interference and scuttling failures;
(2) Near-surface (0 to 10 m) K_d determination;
(3) Lack of incident irradiance information;
(4) Red tail on the spectral response;
(5) "Staircase effect"; and
(6) Mechanical design flaw leading to anisotropy in cosine response function.

Scuttling failure. A mechanism to insure proper scuttling should be implemented in any future design. The mechanism must be tested in calm seas, as well as normal seas. The interference caused by the failure to scuttle in the allotted time negatively impacts use of the AXKT in shallow-water and coastal applications.

Near-surface K_d. Sufficient time to achieve ambient light levels must be available in order to minimize near-surface contamination. The translucent launch tube shows some promise, but the solution may also require separation of the irradiance transmission initiation and launch out of the tube, as well as a faster response time for the probe.

Incident irradiance. It is suggested that either an upward-viewing cosine sensor be positioned on a surface mount (or the antenna), or that a downward-viewing radiance sensor be mounted on the launch tube. Either of these options will yield a surface radiance/irradiance that can be employed as a surface reference to normalize AXKT irradiances. While an upward-viewing cosine collector on the buoy is the easiest to develop, the downward-viewing radiance collector will probably be more stable over the 10 to 20° roll common in moderate seas. An alternative approach would be a sampling strategy whereby 3 probes are dropped in the same vicinity and clouds are disseminated by the temporal variation in the position of the irradiance fluctuations in AXKT profiles. However, this technique is presumptive about the spatial variability in K_d.

Red tail in response. This is best solved by more careful selection of filters used in the system. For several applications, the 10 to 20% difference that the red tail may cause is small when compared to errors due to near-surface effects and incident irradiance. But for coastal applications where the potential for high colored dissolved organic concentration exists, this problem must be addressed.

Staircase effect. The source of this problem should be found. While the effect of this nonlinearity over large depth intervals is small, this problem does limit the vertical resolution of the probe. Furthermore, since the relative importance of the staircase effect is dependent upon atmospheric and water properties (K_d and incident light levels), the impact of this problem unpredictable until initial probes are launched.

Cosine response. The cosine response anisotropy can be corrected by the addition of a collar designed to block the entrance of light along the side of the diffuser or from light leakage and subsequent reflections from the holder assembly for the sensor package. This should be a relatively easy and inexpensive fix that should improve the cosine response. It is suggested that the manufacturer have the cosine response of the complete AXKT unit tested in the future.

6.0 Acknowlegments

This research was supported by the Tactical Oceanographic Warfare Support (TOWS) Office, NRL Code 7410 under Program Element 0604704N, Harry Selsor, Program Manager. The AXKT was developed under sponsorship of the TOWS Office as well; Ken Ferer, Program Manager. The authors wish to thank Dr. Rudolph Hollman (NRL Code 7332) for collection of the in situ optical data in Vestfjord and Kimberly Davis (NAVOCEANO) for collection of the in situ data for the Northeastern Pacific sea evaluation tests.

7.0 References

Dera, J. and D. Stramski 1986. "Maximum Effects of Sunlight Focusing Under a Wind-disturbed Sea Surface," Oceanologia 23:15-27.

Gordon, H.R. 1985. "Ship Perturbations of Irradiance Measurements and Methodology at Sea, 1: Monte Carlo Simulations," Applied Optics 24:4172-4182.

Gordon, H.R. and K. Ding 1991. "Self Shading of In-water Optical Instruments," Limnology and Oceanography 37:491-500.

Jerlov, N.G. 1976. Marine Optics (Elsevier Scientific Publishing Company, Amsterdam) 231 pp.

Lavoie, D.M., A. Green, I. DePalma, and D. Young 1993. "Influence of the Norwegian Coastal Current on the Hydrography of Vestfjord, Norway in October 1989," Continental Shelf Research In Press.

Mueller, J. 1991. "Integral Method for Irradiance Profile Analysis," CHORS Tech. Mem. 007-91, San Diego State University, 10 pp.

Mueller, J. 1993. "Radiometric Characterization of an Airborne Expendable K and Temperature (AXKT) Meter," CHORS Tech. Mem. 006-93, San Diego State University, 16 pp.

Pierson Scientific Associates Inc. 1989. "A Measurement of Spectral and Angular Response of a Photometric Detector," report for Sippican Inc., 15 pp.

Stavn, R. 1982. "The Three-parameter Model of the Submarine Light Field: Radiant Energy-Absorption and Energy Trapping in Nepheloid Layers," J. Geophysical Research 87(C3):2079-2082.

Stavn, R. 1988. "Lambert-Beer Law in Ocean Waters: Optical Properties of Water and of Dissolved/Suspended Material, Optical Energy Budgets," Applied Optics 27(2):222-231.

Stramski, D. and J. Dera 1988. "On the Mechanism for Producing Flashing Light Under a Wind-disturbed Water Surface," Oceanologia 25:5-21.

Voss, K., J. Nolten, and G. Edwards 1986. "Ship Shadow Effects on Apparent Optical Properties," Proceedings of the International Society for Optical Engineering, Ocean Optics VIII 637:186-190.

8.0 Figures

1. Temperature profiles for all AXKT probes used in Vestfjord, Norway, analysis.

2. Temperature profiles for all MER profiles used in Vestfjord, Norway, analysis.

3. Mean and standard deviation for MER and AXKT temperature profiles used in Vestfjord, Norway, analysis.

4. Temperature profile for all AXKT probes used in Pacific 1990 analysis.

5. Temperature profile for all MER profiles used in Pacific 1990 analysis.

6. Mean and standard deviation for MER and AXKT temperature profiles used in Pacific 1990 analysis.

7. Temperature profiles for all AXKT probes used in Pacific 1992 analysis.

8. Temperature profiles for all MER data used in Pacific 1992 analysis.

9. Mean and standard deviation for MER and AXKT temperature profiles used in Pacific 1992 analysis.

10. Temperature and Irradiance profile (ln) as function of depth for Channel 12, Drop 5, in Vestfjord showing irradiance irregularity.

11. Staircase effect in Channel 14, Drop 6; Vestfjord test.

12. Staircase effect in Channel 16, Drop 6; Vestfjord test.

13. Staircase effect in Channel 12, Drop 3; Vestfjord test.

14. Staircase effect in Channel 12, Drop 4; Vestfjord test.

15. Staircase effect in Channel 14, Drop 2; Pacific 1992 test.

16. Staircase effect in Channel 14, Drop 5; Pacific 1992 test.

17a. Laboratory manifestation of staircase effect in AXKT.
b. Enlargement of staircase effect as a function of irradiance.

18. Normalized wavelength responsivity of AXKT probe 1 sent to CHORS, with "red tail contamination evident."

19. Normalized wavelength responsivity of AXKT probe 2 sent to CHORS, showing some "red tail" contamination.

20. Cosine response function of AXKT as measured by CHORS, compared to tilted cylinder and ideal cosine curve.

21. Cosine response function as reported by Pierson Scientific Incorporated.

22. Vestfjord mean profile of K_d for MER and AXKT systems.

23. Pacific 1990 mean profile of K_d for MER and AXKT systems.

24. Pacific 1992 mean profile of K_d for MER and AXKT systems.

25. Irradiance dip for the AXKT between 0 and 10 m for Channel 12, Drop 1, and Channel 16, Drop 2; Vestfjord 1990.

26. Irradiance dip for the AXKT between 0 and 10 m for Channel 14, Drop 3, and Channel 12, Drop 4; Vestfjord.

27. Irradiance dip for the AXKT between 0 and 10 m for Channel 12, Drop 1, and Channel 14, Drop 2; Pacific 1992 (with translucent tube).

28. Irradiance for the AXKT between 0 and 10 m for Channel 16, Drop 3, and Channel 12, Drop 4; Pacific 1992 (with translucent tube).

29. Irradiance for the AXKT between 0 and 10 m for Channel 14, Drop 5, and Channel 12, Drop 7; Pacific 1992 (with translucent tube and surface saturation).

30. Irradiance for AXKT between 0 and 10 m for Channel 16, Drop 7 (no saturation at the surface), and Channel 14, Drop 8 (saturation of surface irradiance).

31. Surface saturation in Vestfjord probes 16:6, 14:1, and 12:7.

32. Irradiance profiles for two probes (12:1 and 16:7) that show slower rate of change per unit depth than more typical probe (12:4); Pacific 1992.

33. Derived K_d profiles from Fig. 32 demonstrating a factor of 2 difference in K_d for 12:1 and 16:7 versus probe 12:4; Pacific 1992.

34. Reconstructed irradiance curve versus raw data for Channel 14, Drop 2; 1992 Pacific.

35. Comparison of 100 point (new) and 250 point (old) processing methodology for calculation of K_d (Pacific 1992; probe 14:2).

36. All processed AXKT K_d profiles used in AXKT/MER comparison for Vestfjord evaluation.

37. All processed MER K_d profiles used in AXKT/MER comparison for Vestfjord evaluation.

38. Mean K_d profile for AXKT and MER for Vestfjord.

39. All processed AXKT K_d profiles used in AXKT/MER comparison for Pacific 1990 evaluation.

40. All processed MER K_d profiles used in AXKT/MER comparison for Pacific 1990 evaluation.

41. Mean K_d profile for AXKT and MER for Pacific 1990.

42. All processed AXKT K_d profiles used in AXKT/MER comparison for Pacific 1992 evaluation.

43. All processed MER K_d profiles used in AXKT/MER comparison for Pacific 1992 evaluation.

44. Mean K_d profile for AXKT and MER for Pacific 1992.

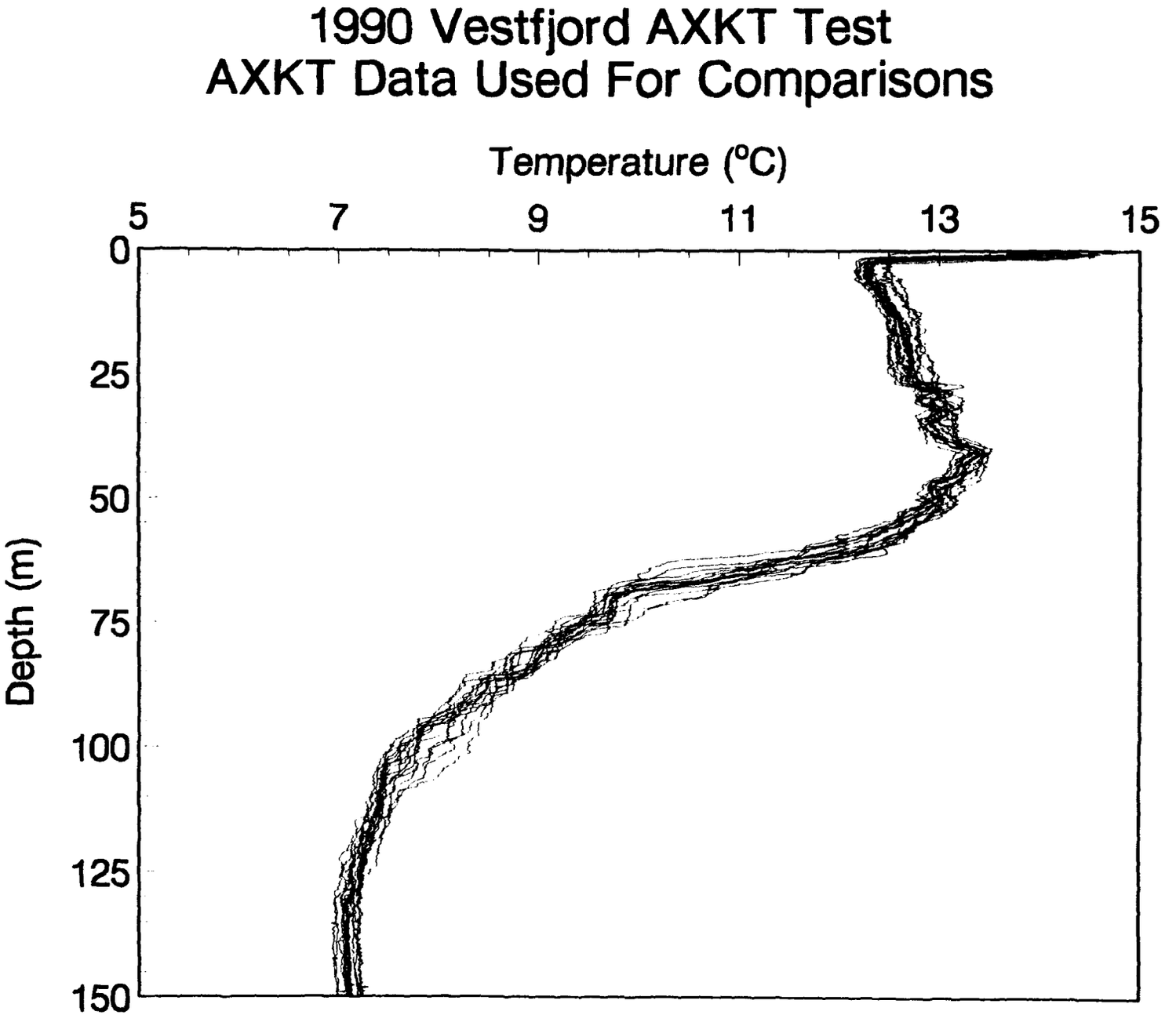
1990 Vestfjord AXKT Test
AXKT Data Used For Comparisons
Temperature (°C)
5
7
9
11
13
15
Depth (m)
0
25
50
75
100
125
150

Figure 1.

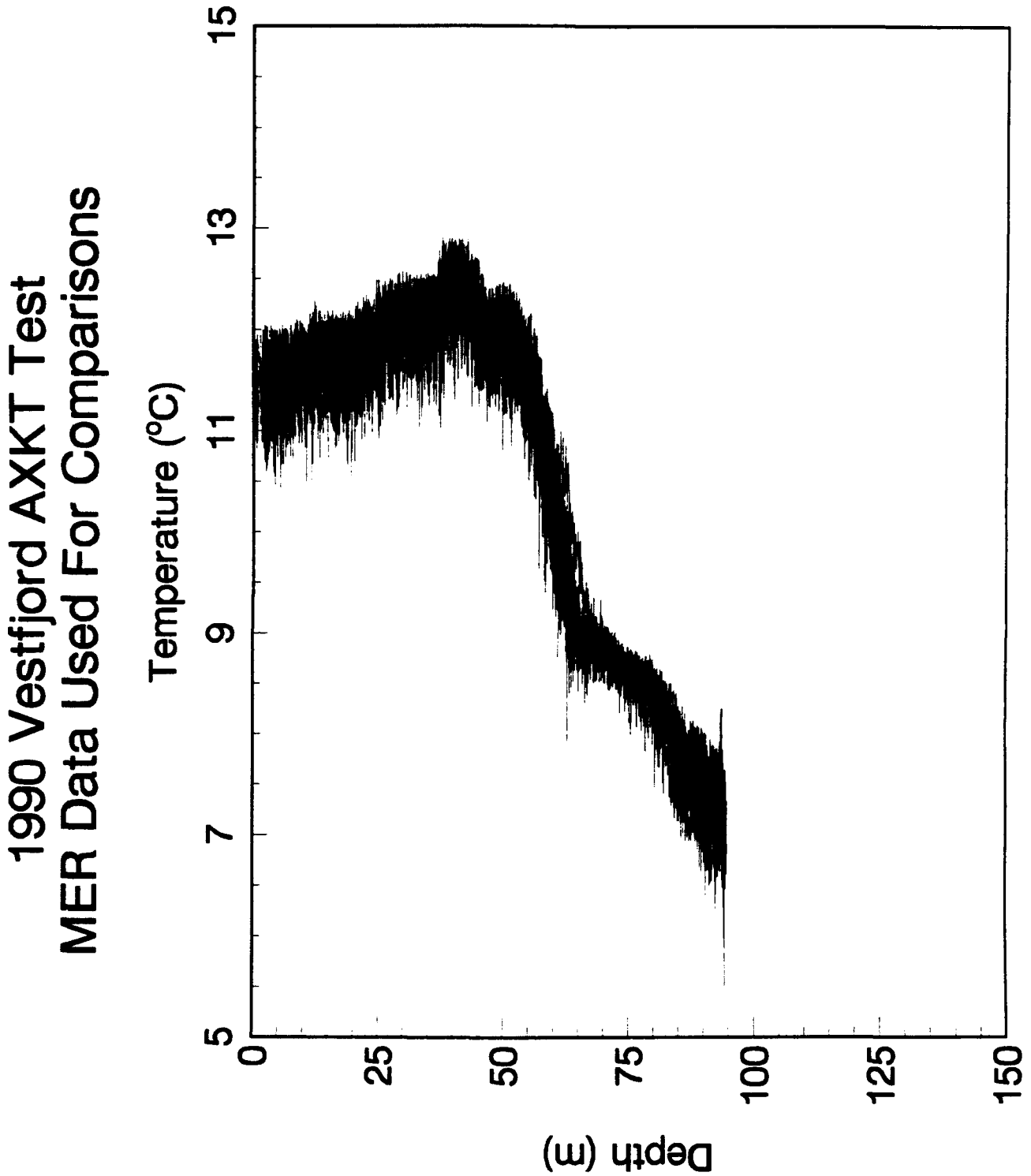
1990 Vestfjord AXKT Test
MER Data Used For Comparisons
Temperature (°C)
5
7
9
11
13
15
0
25
50
75
100
125
150
Depth (m)

Figure 2.

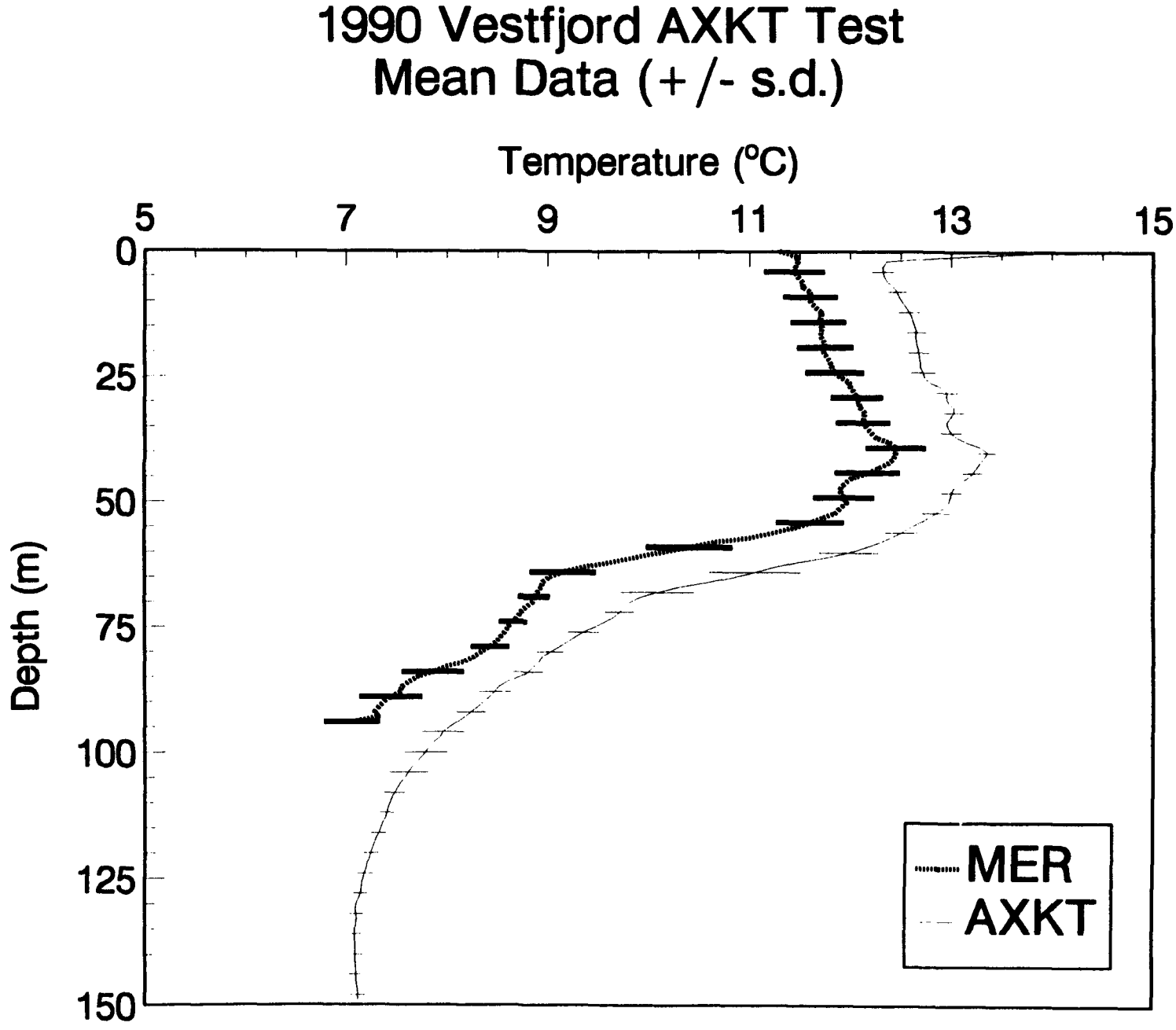
1990 Vestfjord AXKT Test
Mean Data (+/- s.d.)
Temperature (°C)
5
7
9
11
13
15
0
25
50
75
100
125
150
Depth (m)
MER
AXKT

Figure 3.

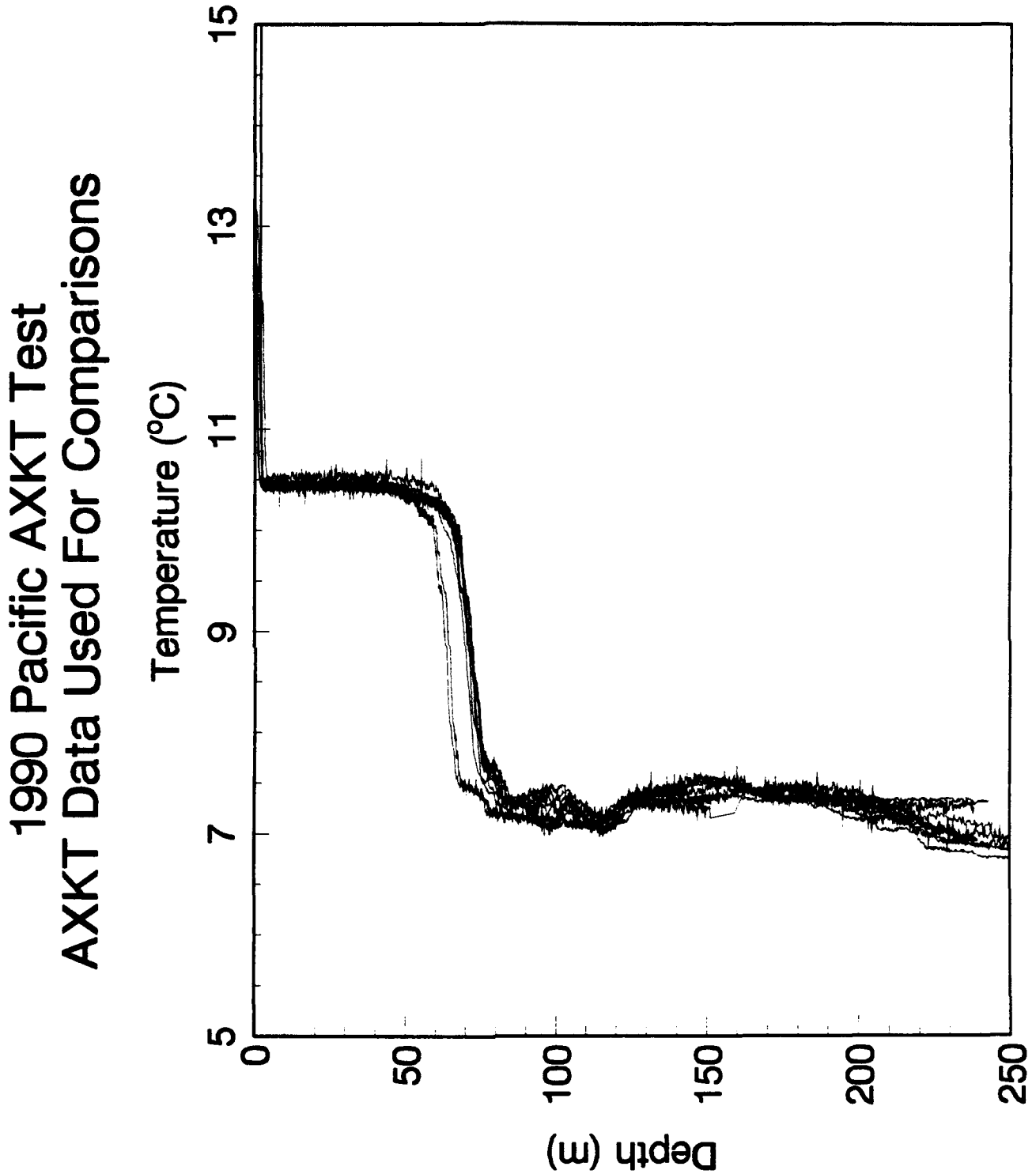
1990 Pacific AXKT Test
AXKT Data Used For Comparisons
Temperature (°C)
5
7
9
11
13
15
0
50
100
150
200
250
Depth (m)

Figure 4.

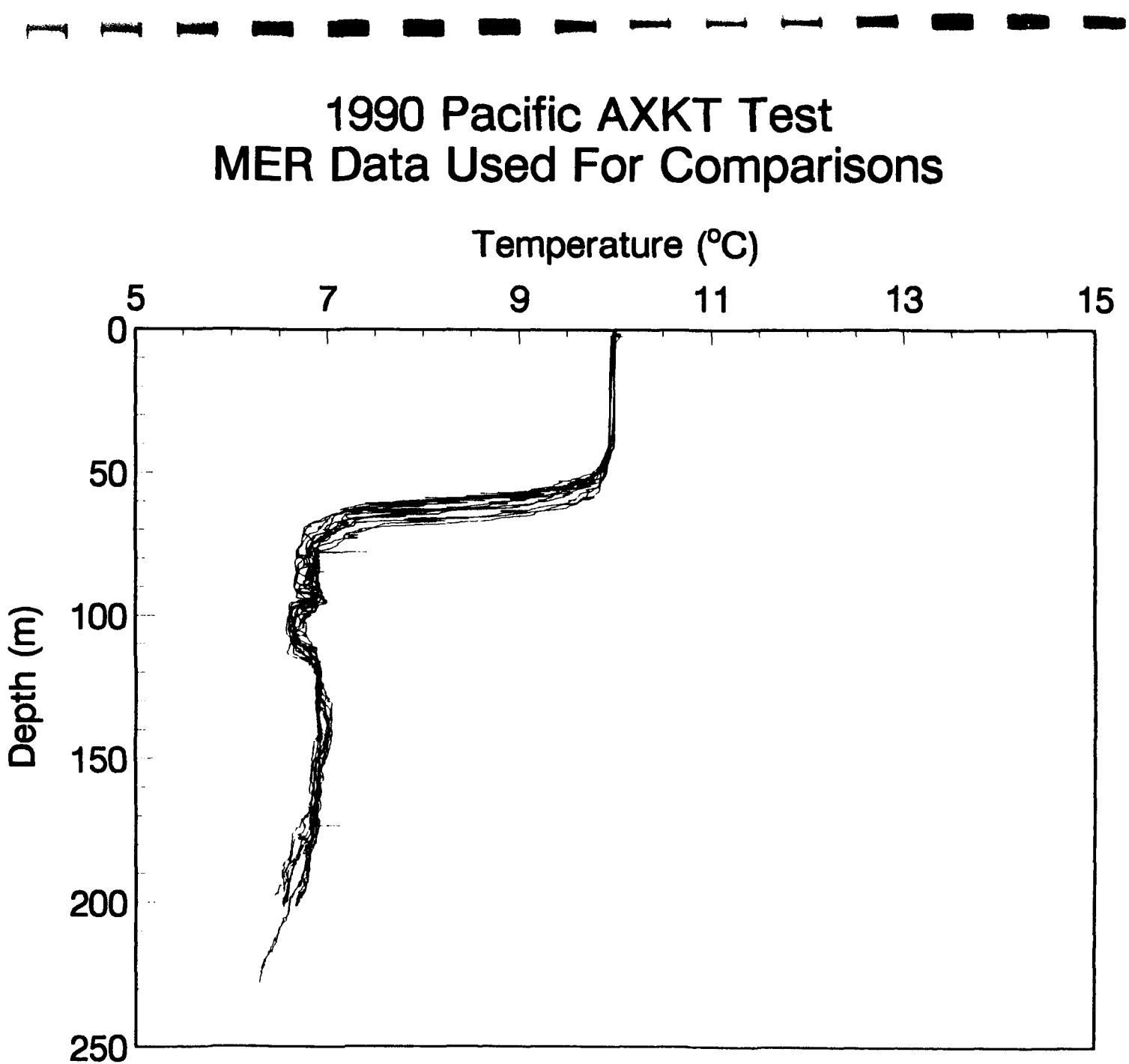
1990 Pacific AXKT Test
MER Data Used For Comparisons
Temperature (°C)
5
7
9
11
13
15
0
50
100
150
200
250
Depth (m)

Figure 5.

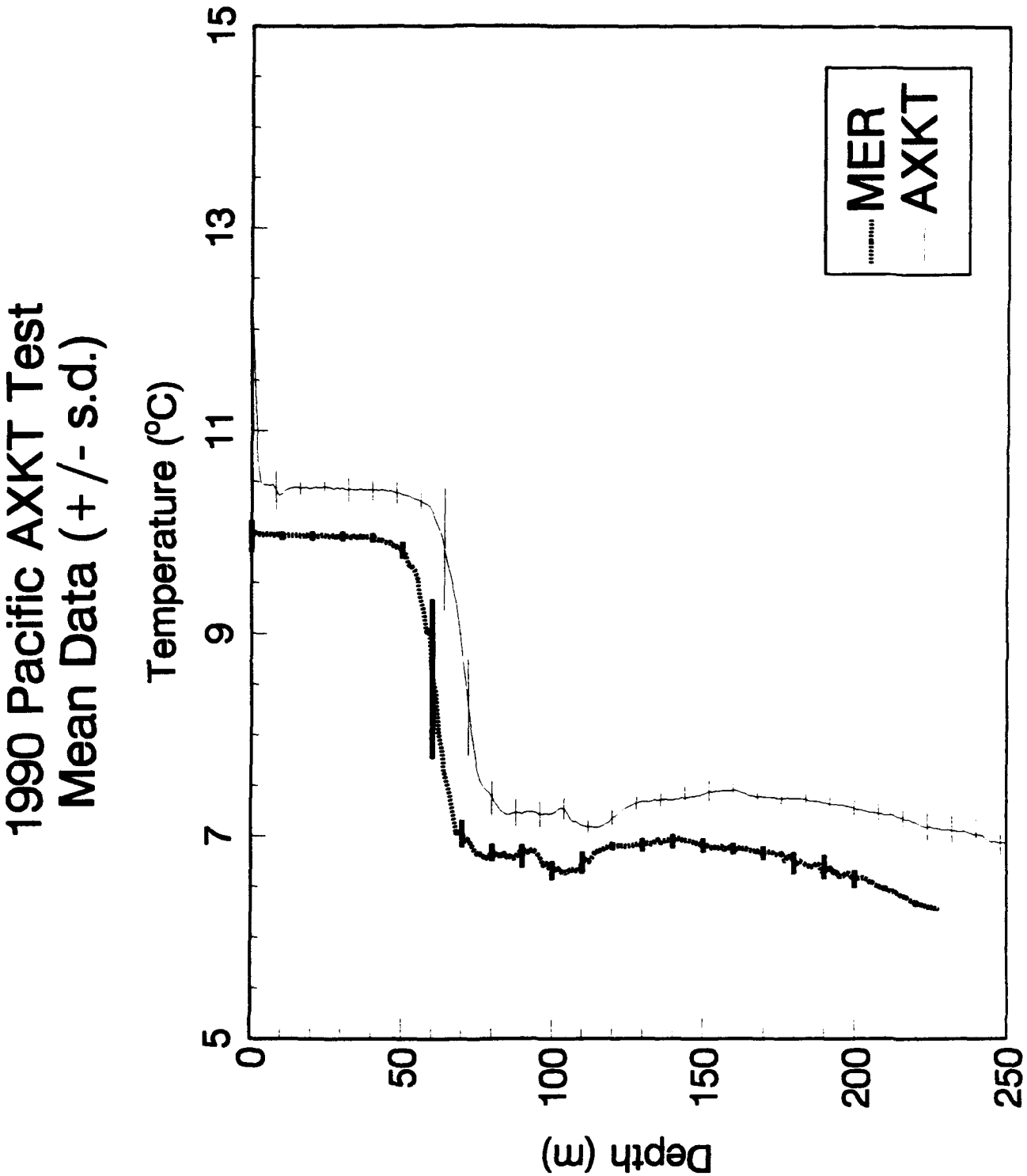
1990 Pacific AXKT Test
Mean Data (+/- s.d.)
Temperature (°C)
Depth (m)
MER
AXKT
5
7
9
11
13
15
0
50
100
150
200
250

Figure 6.

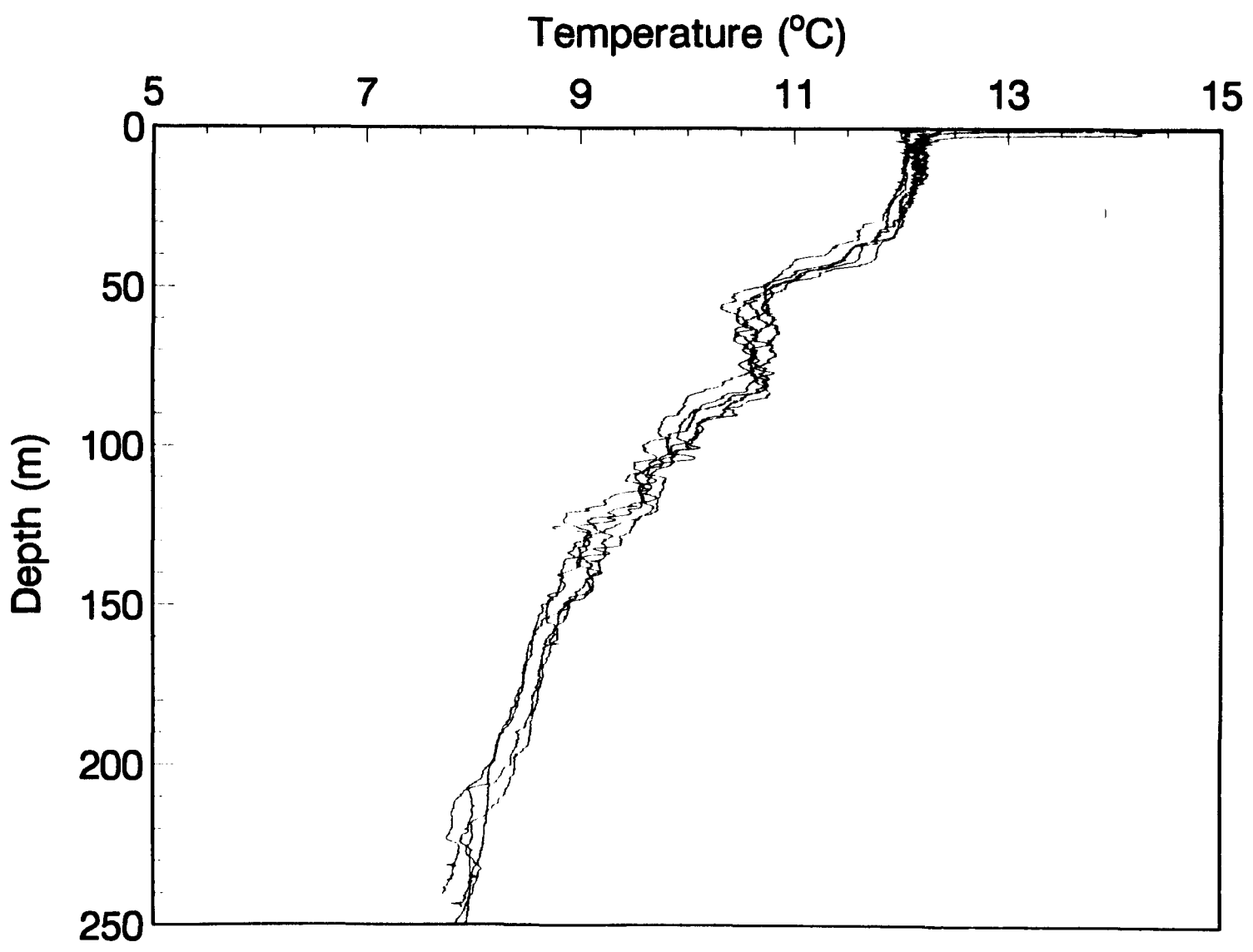
1992 Pacific AXKT Test
AXKT Data Used For Comparisons
Temperature (°C)
5
7
9
11
13
15
0
50
100
150
200
250
Depth (m)

Figure 7.

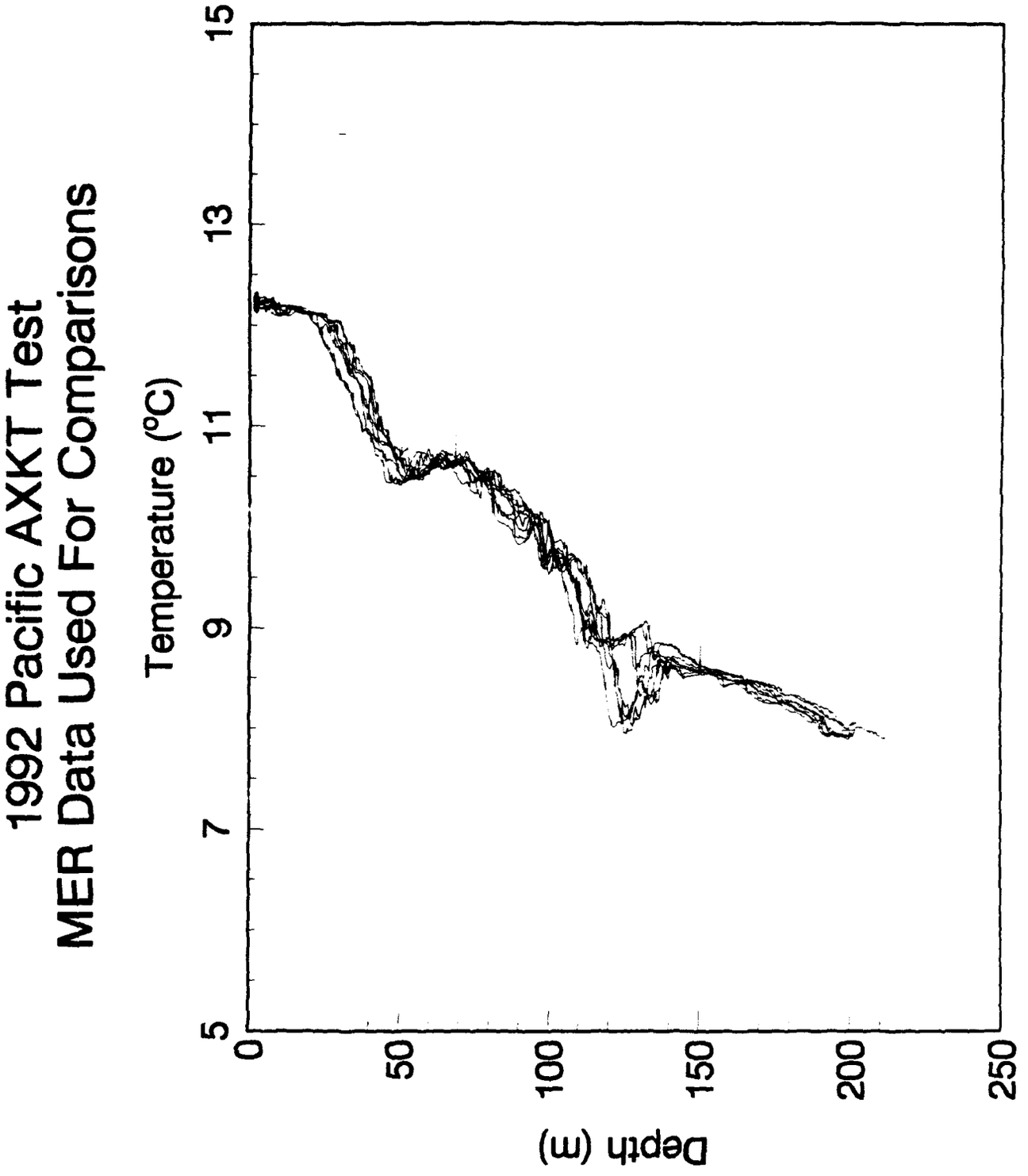
1992 Pacific AXKT Test
MER Data Used For Comparisons
Temperature (°C)
5
7
9
11
13
15
0
50
100
150
200
250
Depth (m)

Figure 8.

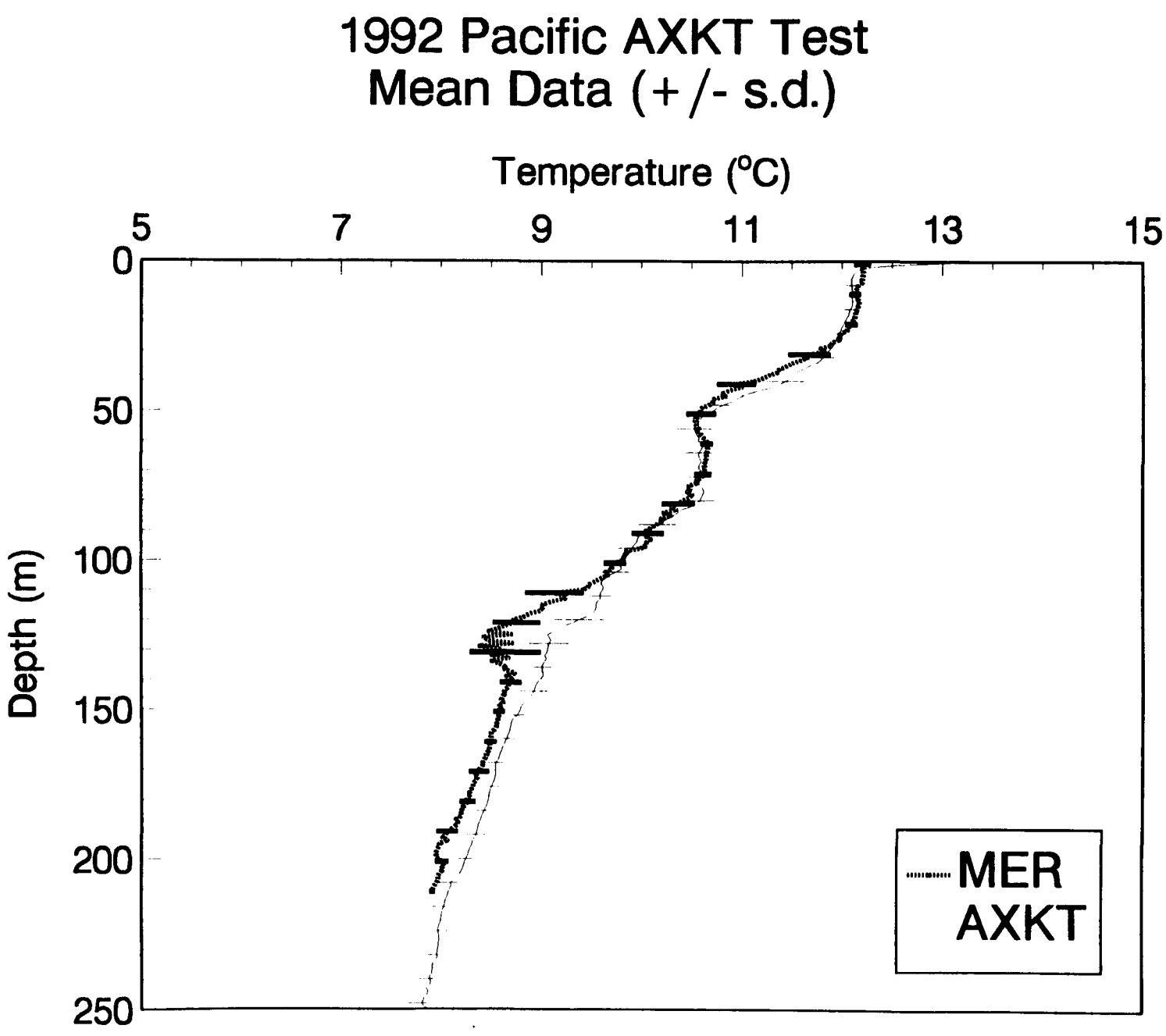
1992 Pacific AXKT Test
Mean Data (+/- s.d.)
Temperature (°C)
5
7
9
11
13
15
0
50
100
150
200
250
Depth (m)
MER
AXKT

Figure 9.

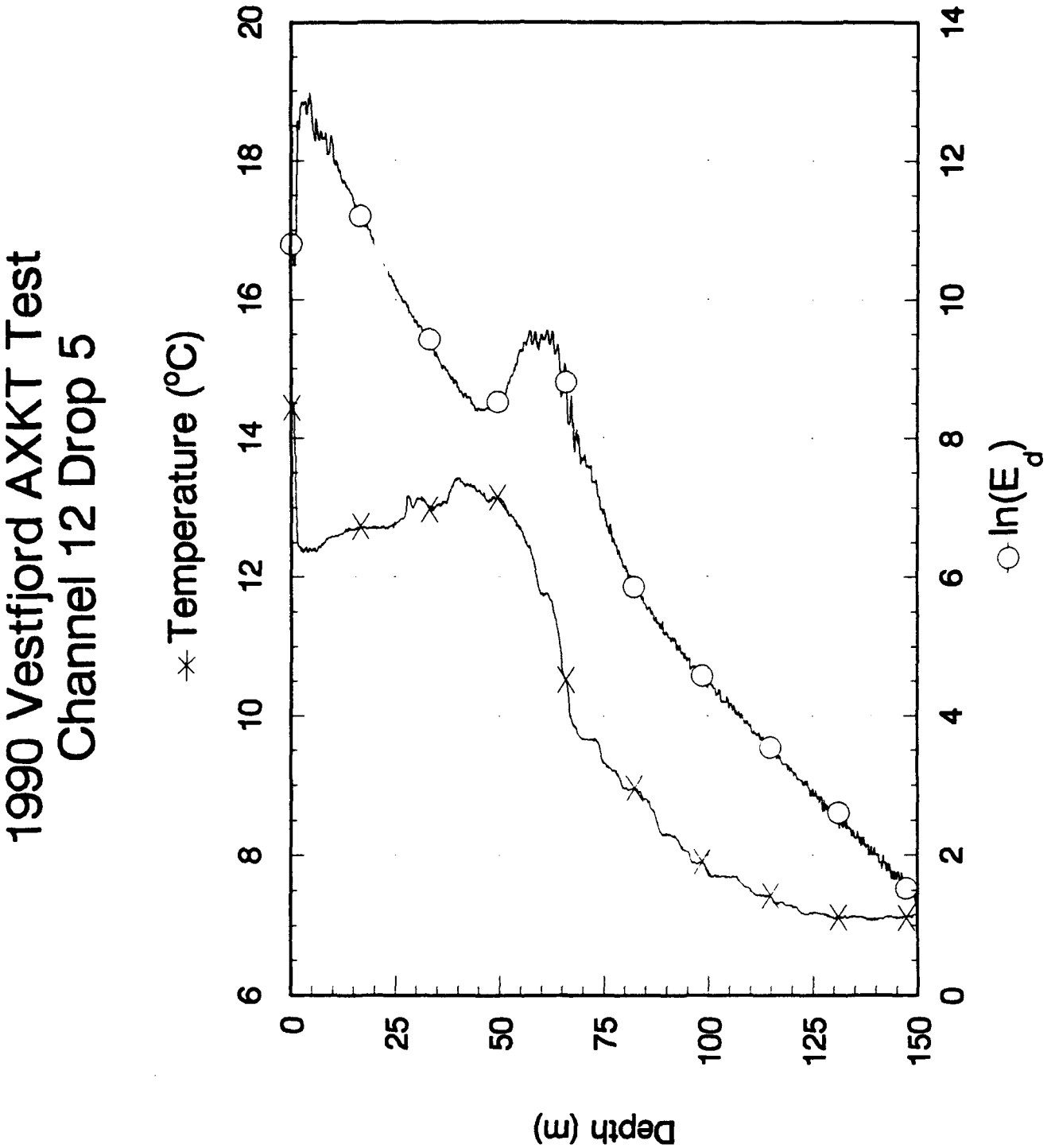
1990 Vestfjord AXKT Test
Channel 12 Drop 5
Temperature (°C)
ln(E_d)
Depth (m)
6
8
10
12
14
16
18
20
0
2
4
6
8
10
12
14
0
25
50
75
100
125
150

Figure 10.

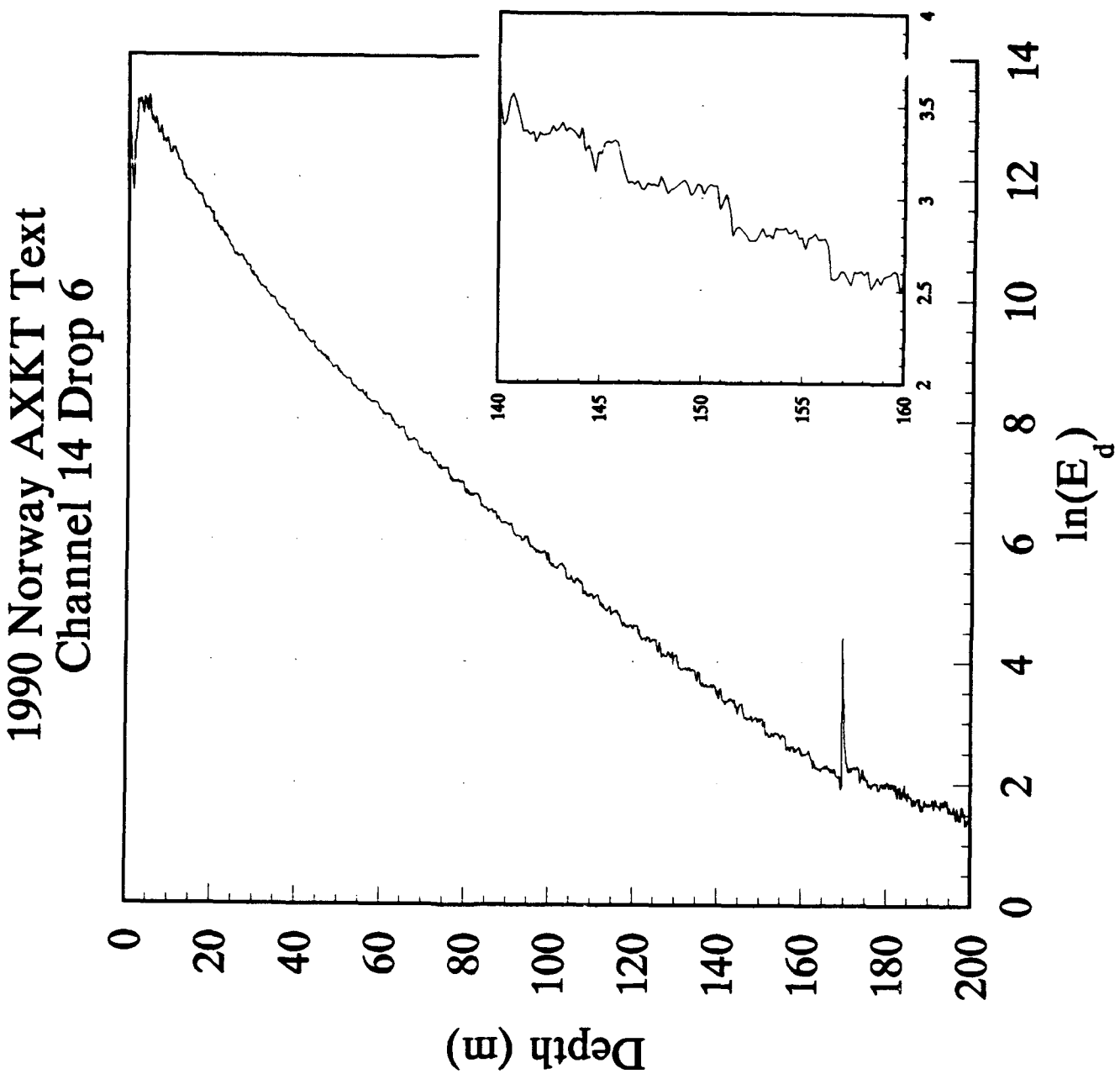
1990 Norway AXKT Text
Channel 14 Drop 6
Depth (m)
0
20
40
60
80
100
120
140
160
180
200
ln(E_d)
0
2
4
6
8
10
12
14
140
145
150
155
160
2
2.5
3
3.5
4

Figure 11.

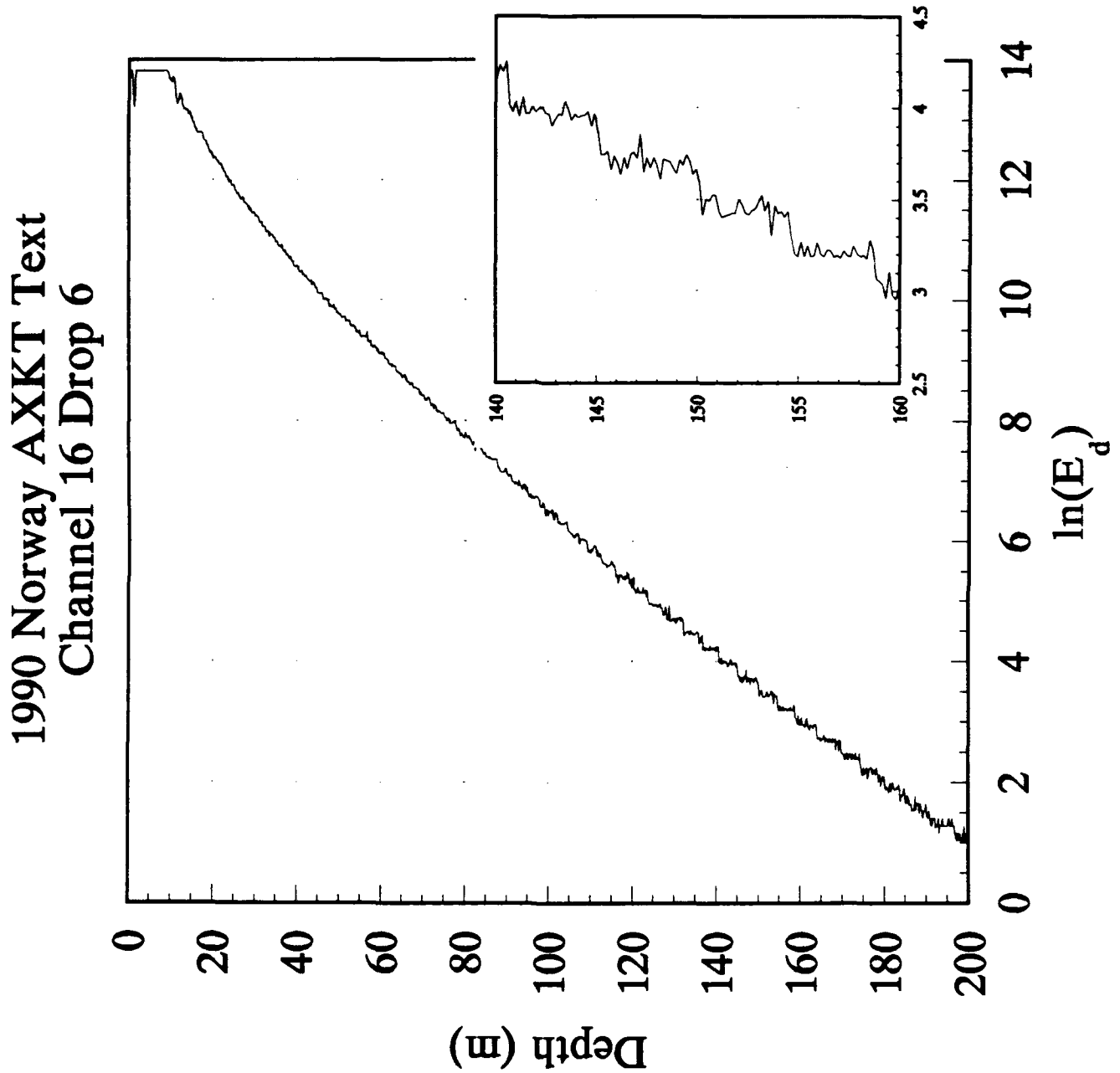
1990 Norway AXKT Text
Channel 16 Drop 6
Depth (m)
0
20
40
60
80
100
120
140
160
180
200
ln(E_d)
0
2
4
6
8
10
12
14
140
145
150
155
160
2.5
3
3.5
4
4.5

Figure 12.

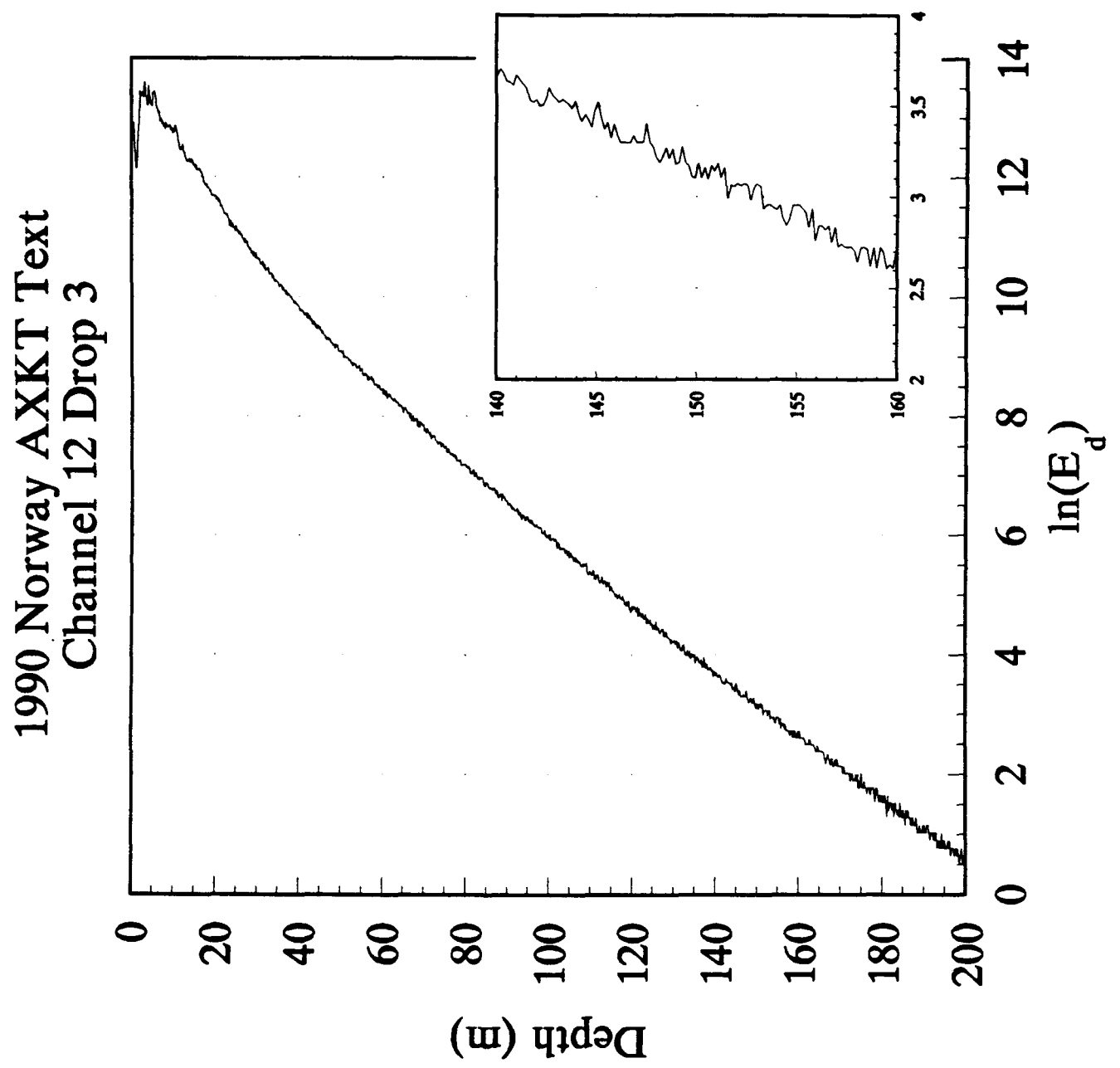
1990 Norway AXKT Text
Channel 12 Drop 3
Depth (m)
0
20
40
60
80
100
120
140
160
180
200
0
2
4
6
8
10
12
14
ln(E_d)
140
145
150
155
160
2
2.5
3
3.5
4

Figure 13.

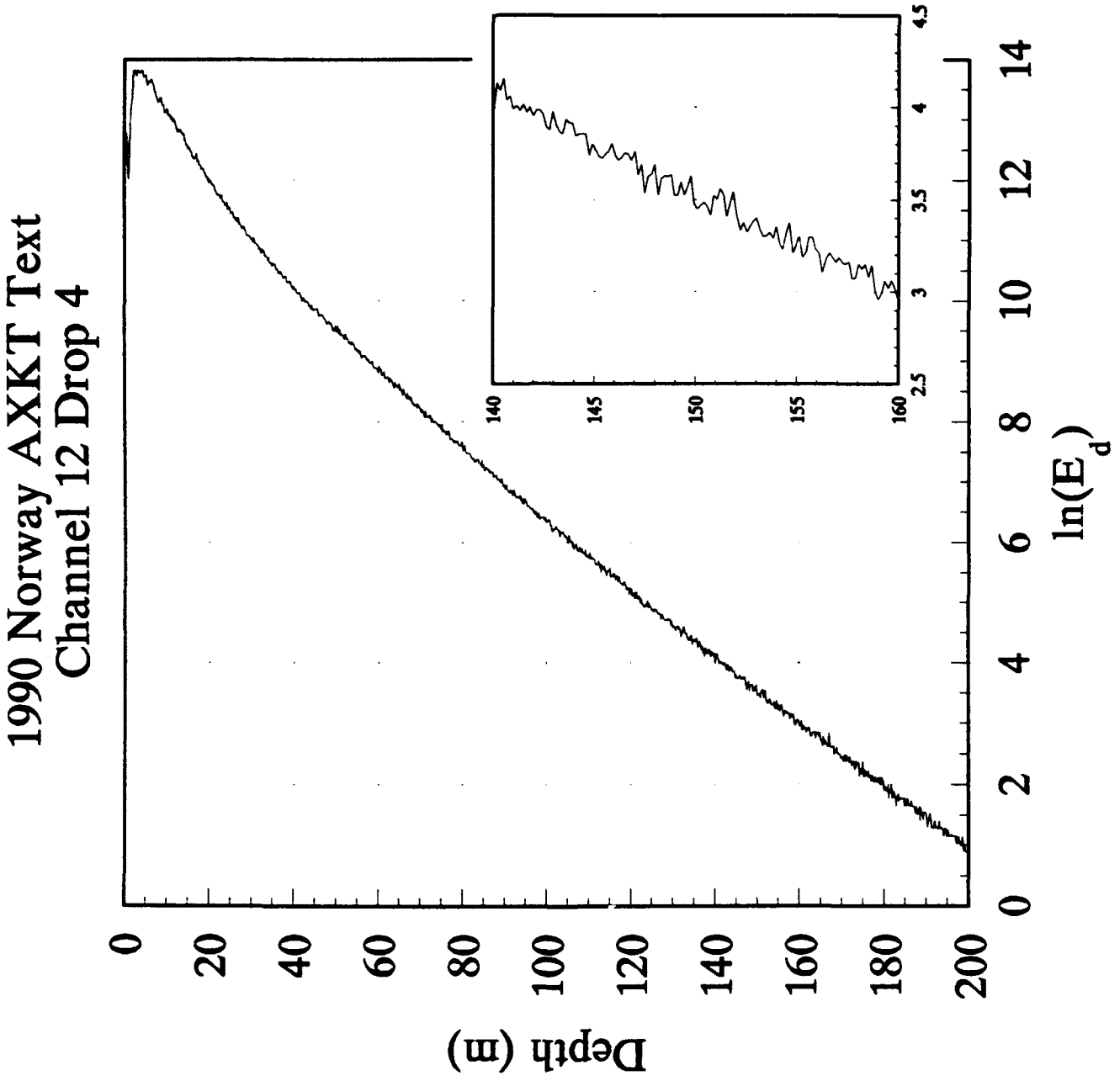
1990 Norway AXKT Text
Channel 12 Drop 4
Depth (m)
0
20
40
60
80
100
120
140
160
180
200
0
2
4
6
8
10
12
14
ln(E_d)
140
145
150
155
160
2.5
3
3.5
4
4.5

Figure 14.

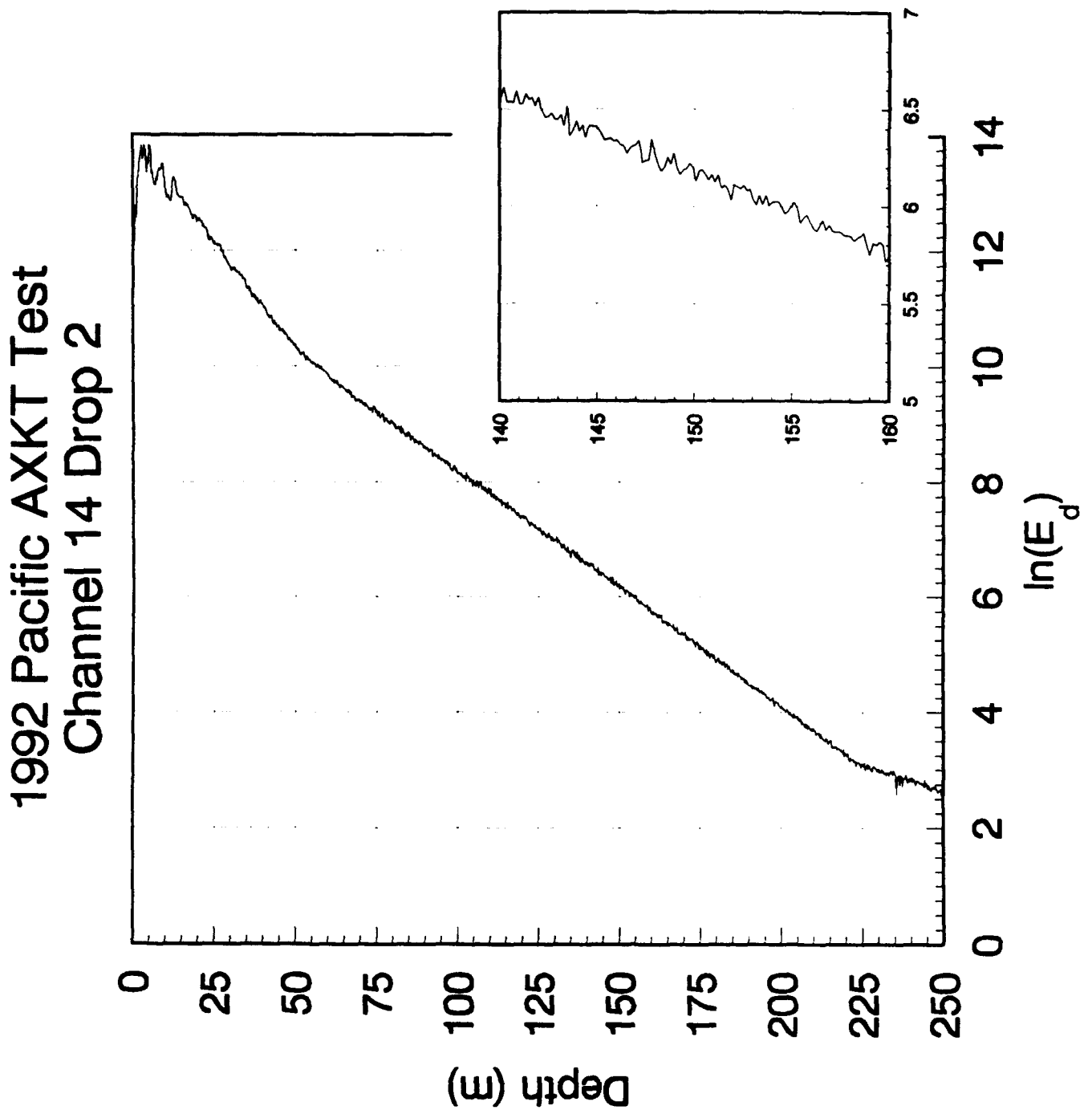
1992 Pacific AXKT Test
Channel 14 Drop 2
Depth (m)
0
25
50
75
100
125
150
175
200
225
250
ln(E_d)
0
2
4
6
8
10
12
14
140
145
150
155
160
5
5.5
6
6.5
7

Figure 15.

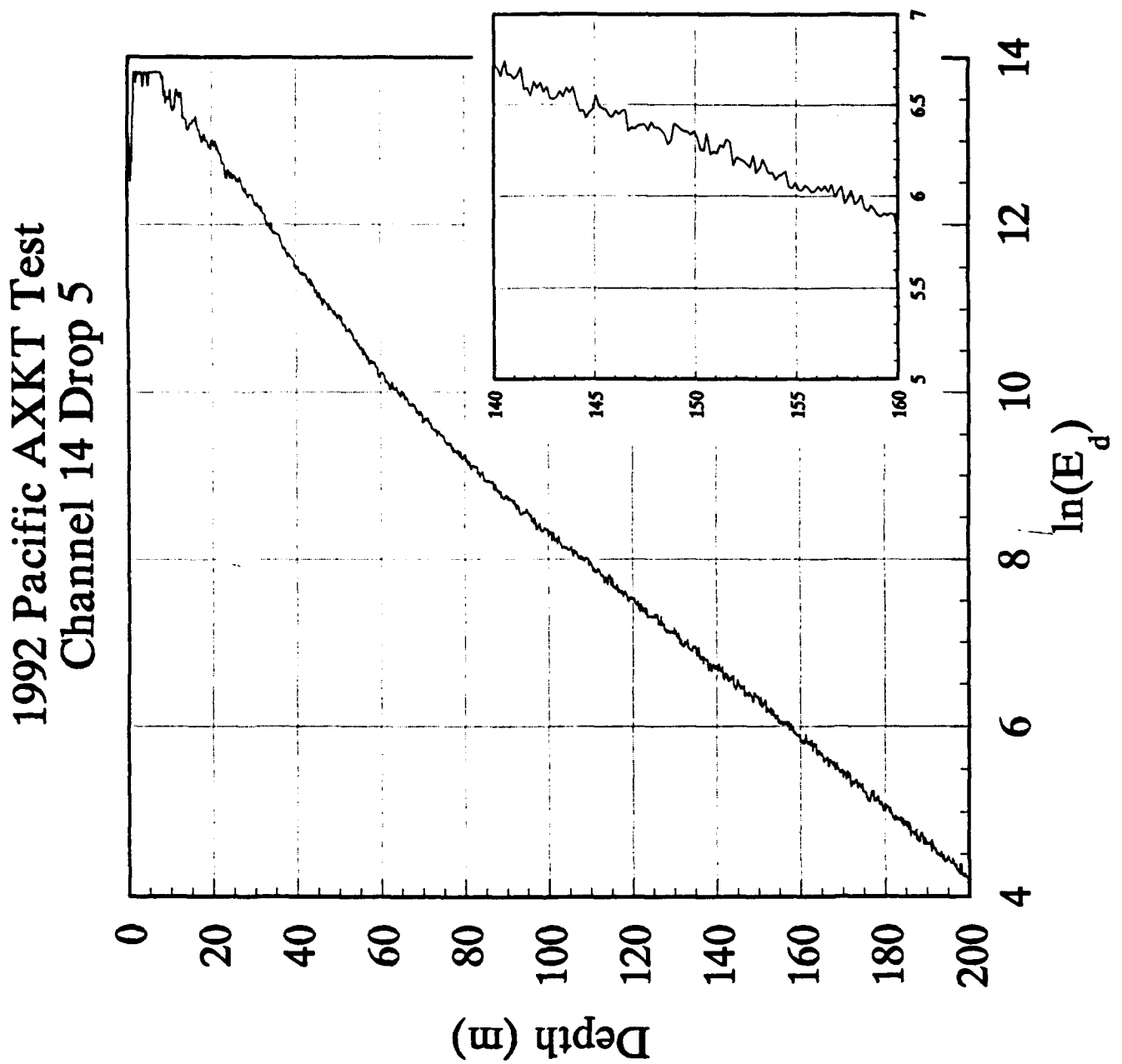
1992 Pacific AXKT Test
Channel 14 Drop 5
Depth (m)
0
20
40
60
80
100
120
140
160
180
200
4
6
8
10
12
14
ln(E_d)
140
145
150
155
160
5
5.5
6
6.5
7

Figure 16.

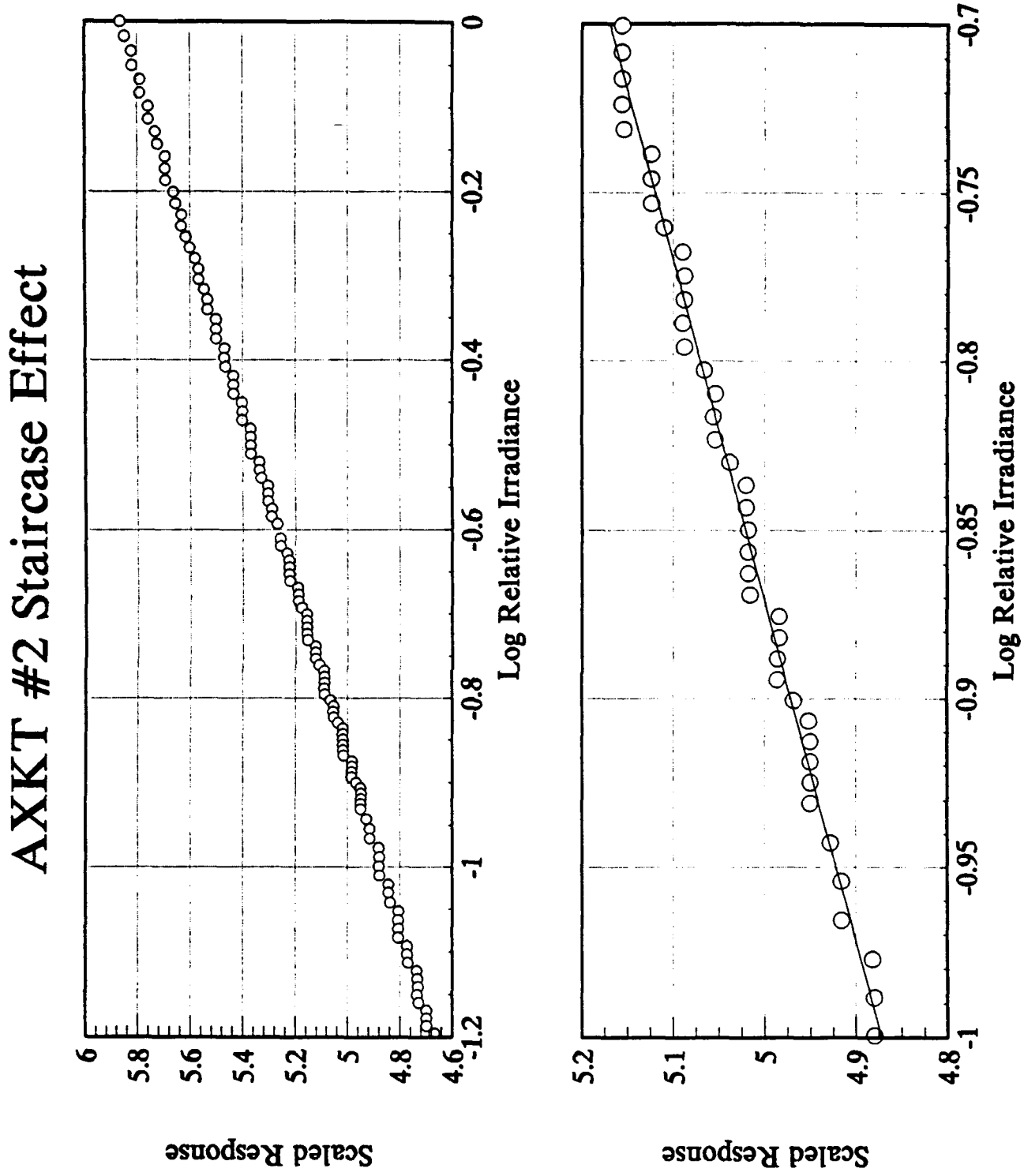
AXKT #2 Staircase Effect
Scaled Response
6
5.8
5.6
5.4
5.2
5
4.8
4.6
-1.2
-1
-0.8
-0.6
-0.4
-0.2
0
Log Relative Irradiance
Scaled Response
5.2
5.1
5
4.9
4.8
-1
-0.95
-0.9
-0.85
-0.8
-0.75
-0.7
Log Relative Irradiance

Figure 17.

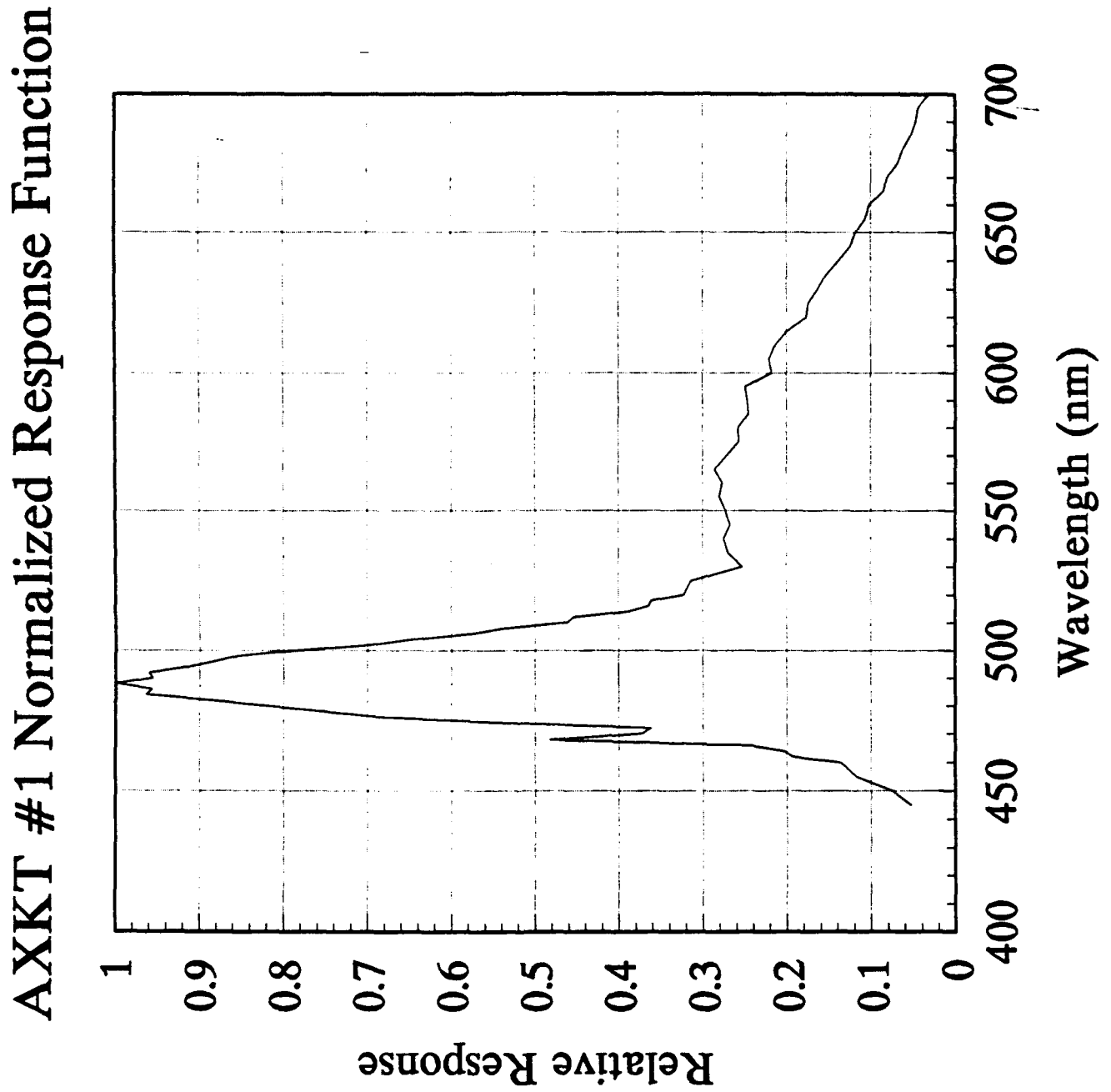
AXKT #1 Normalized Response Function
Relative Response
1
0.9
0.8
0.7
0.6
0.5
0.4
0.3
0.2
0.1
0
400
450
500
550
600
650
700
Wavelength (nm)

Figure 18.

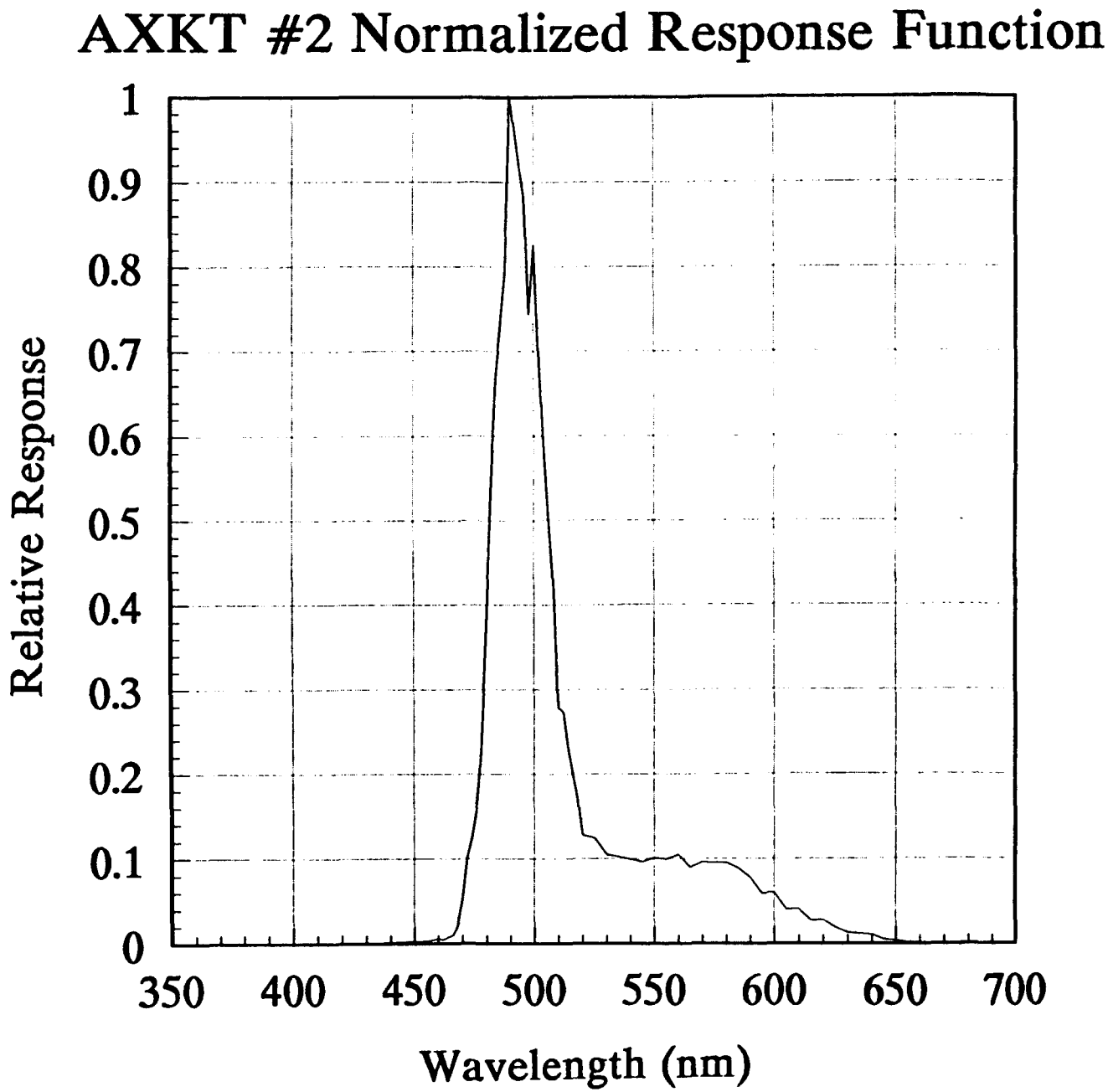
AXKT #2 Normalized Response Function
Relative Response
1
0.9
0.8
0.7
0.6
0.5
0.4
0.3
0.2
0.1
0
350
400
450
500
550
600
650
700
Wavelength (nm)

Figure 19.

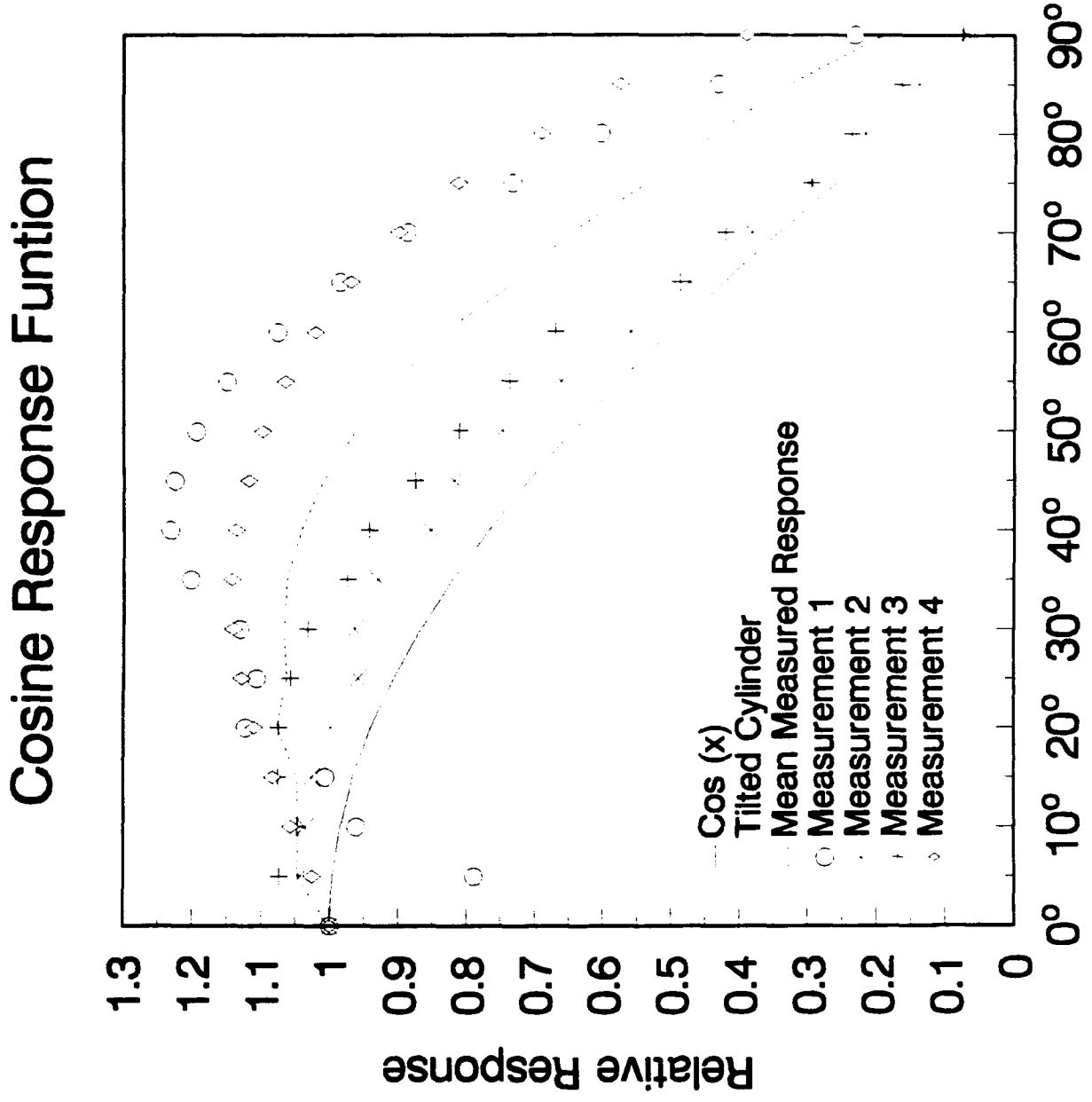
Cosine Response Funtion
Relative Response
1.3
1.2
1.1
1
0.9
0.8
0.7
0.6
0.5
0.4
0.3
0.2
0.1
0
0°
10°
20°
30°
40°
50°
60°
70°
80°
90°
Incidence Angle
Cos (x)
Tilted Cylinder
Mean Measured Response
Measurement 1
Measurement 2
Measurement 3
Measurement 4

Figure 20.

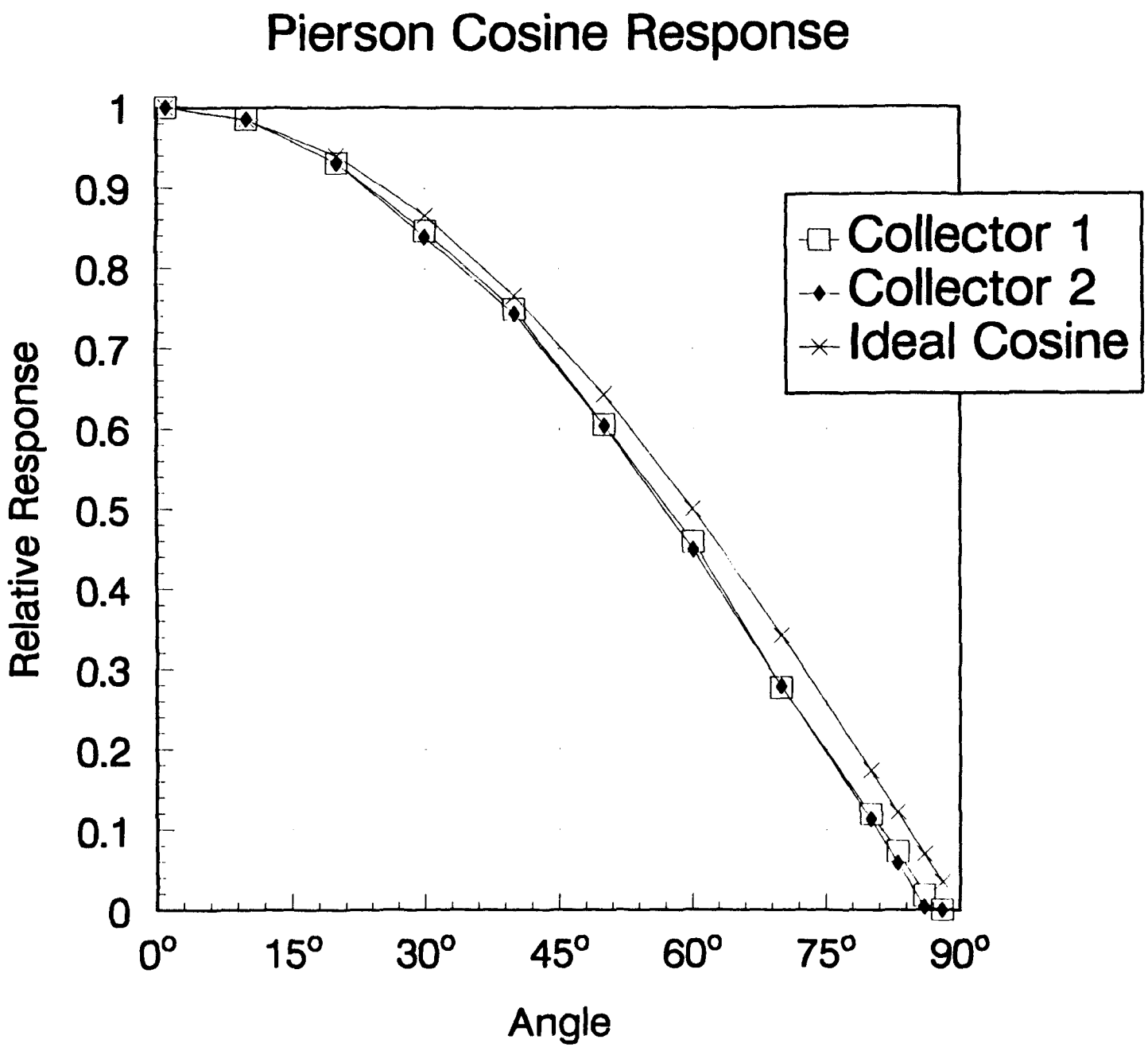
Pierson Cosine Response
Relative Response
1
0.9
0.8
0.7
0.6
0.5
0.4
0.3
0.2
0.1
0
0°
15°
30°
45°
60°
75°
90°
Angle
Collector 1
Collector 2
Ideal Cosine

Figure 21.

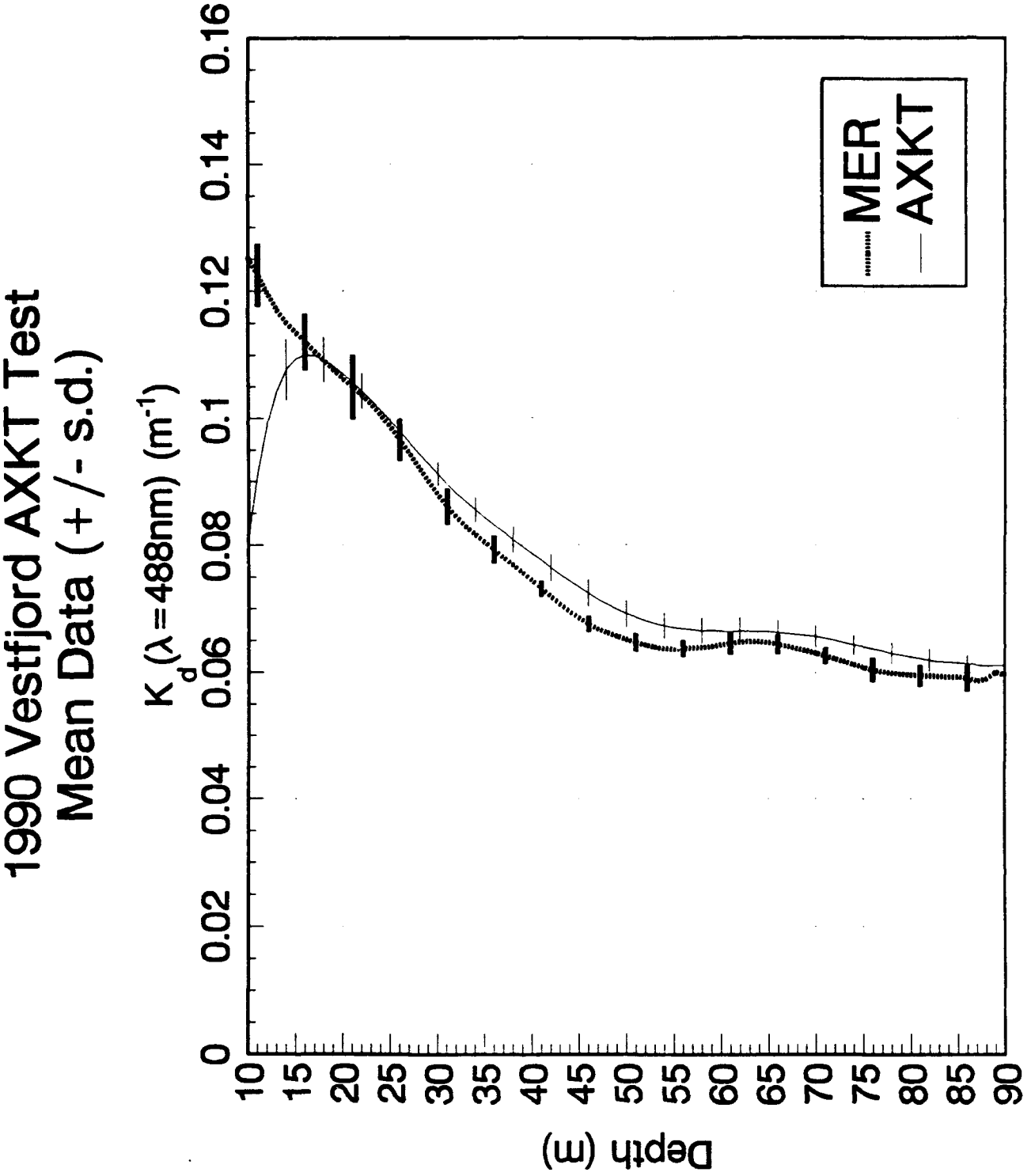
1990 Vestfjord AXKT Test
Mean Data (+/- s.d.)
$K_d(\lambda=488nm)$ (m^{-1})
0
0.02
0.04
0.06
0.08
0.1
0.12
0.14
0.16
10
15
20
25
30
35
40
45
50
55
60
65
70
75
80
85
90
Depth (m)
MER
AXKT

Figure 22.

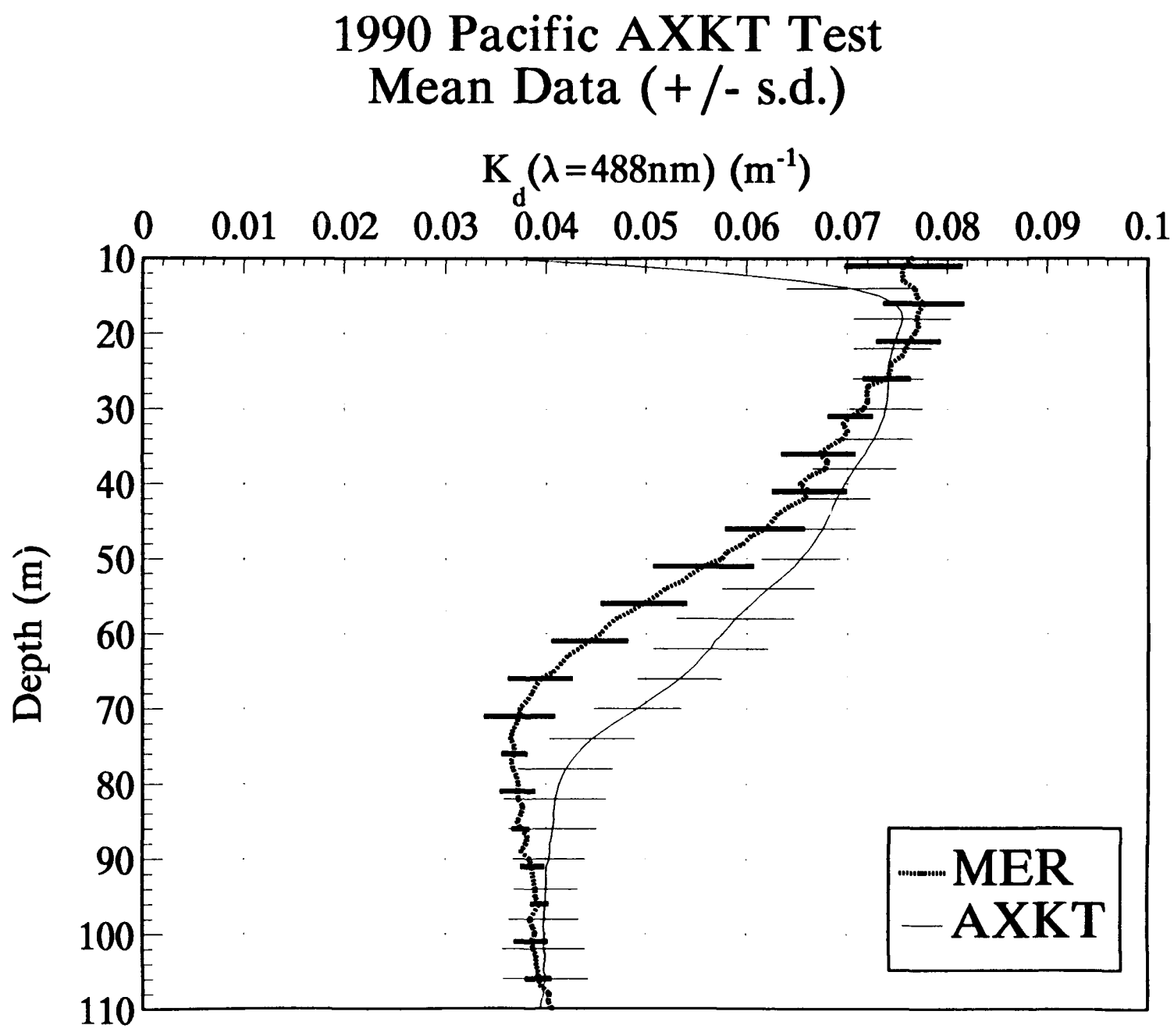
1990 Pacific AXKT Test
Mean Data (+/- s.d.)
K d (λ=488nm) (m-1)
0
0.01
0.02
0.03
0.04
0.05
0.06
0.07
0.08
0.09
0.1
Depth (m)
10
20
30
40
50
60
70
80
90
100
110
MER
AXKT

Figure 23.

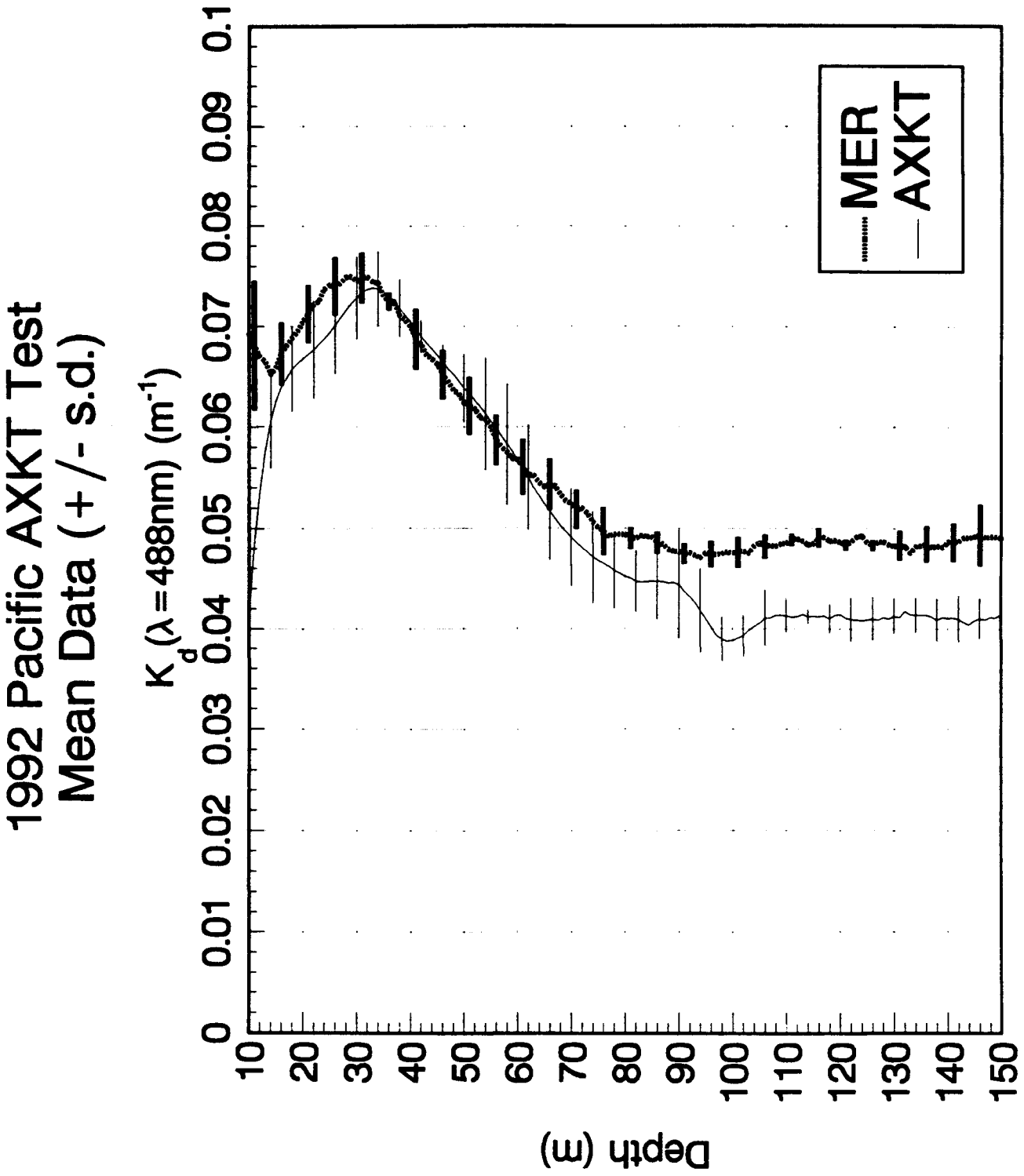
1992 Pacific AXKT Test
Mean Data (+/- s.d.)
$K_d(\lambda=488nm)$ (m^{-1})
0
0.01
0.02
0.03
0.04
0.05
0.06
0.07
0.08
0.09
0.1
10
20
30
40
50
60
70
80
90
100
110
120
130
140
150
Depth (m)
MER
AXKT

Figure 24.

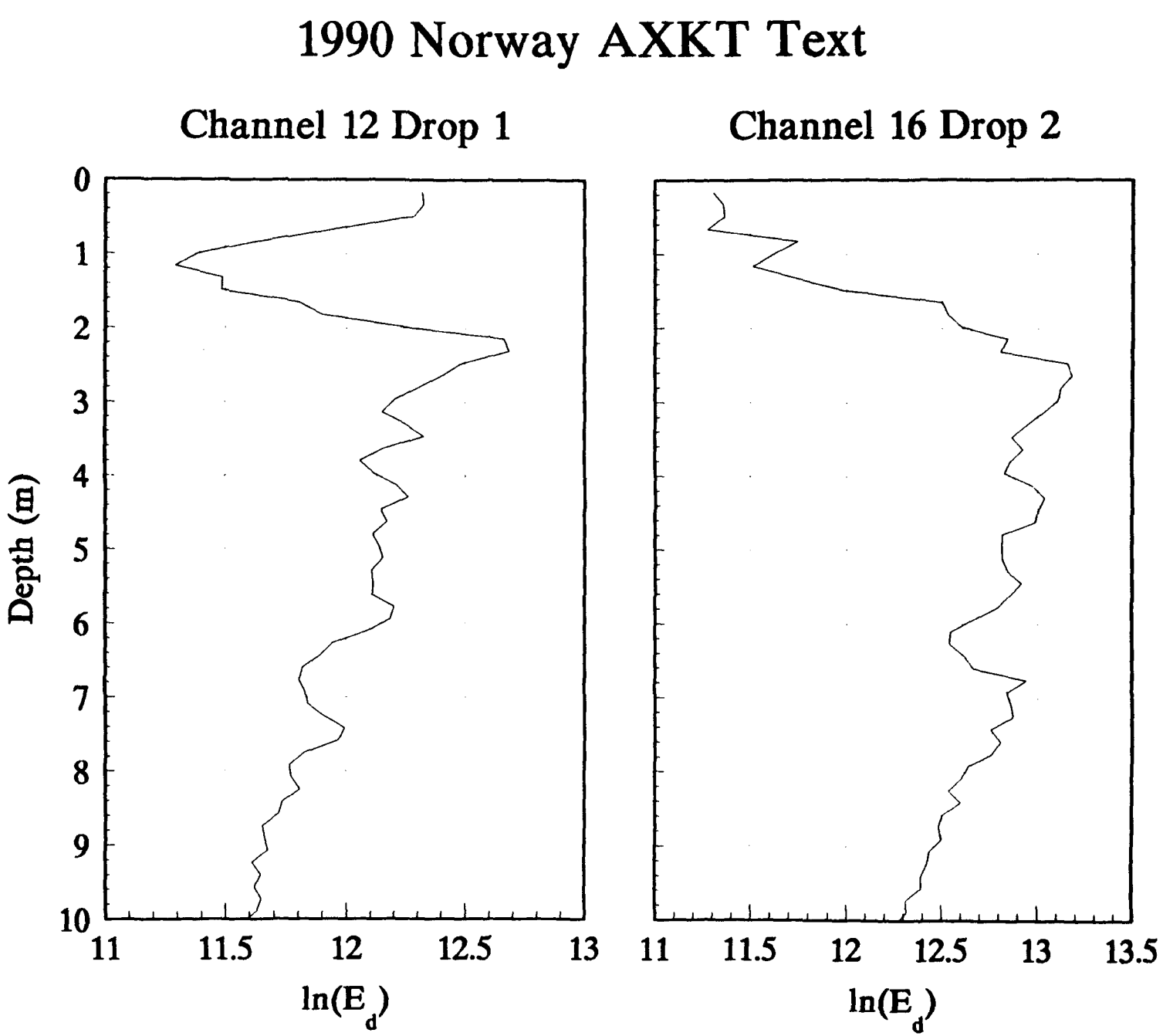
1990 Norway AXKT Text
Channel 12 Drop 1
Channel 16 Drop 2
Depth (m)
0
1
2
3
4
5
6
7
8
9
10
11
11.5
12
12.5
13
13.5
ln(E_d)
ln(E_d)

Figure 25.

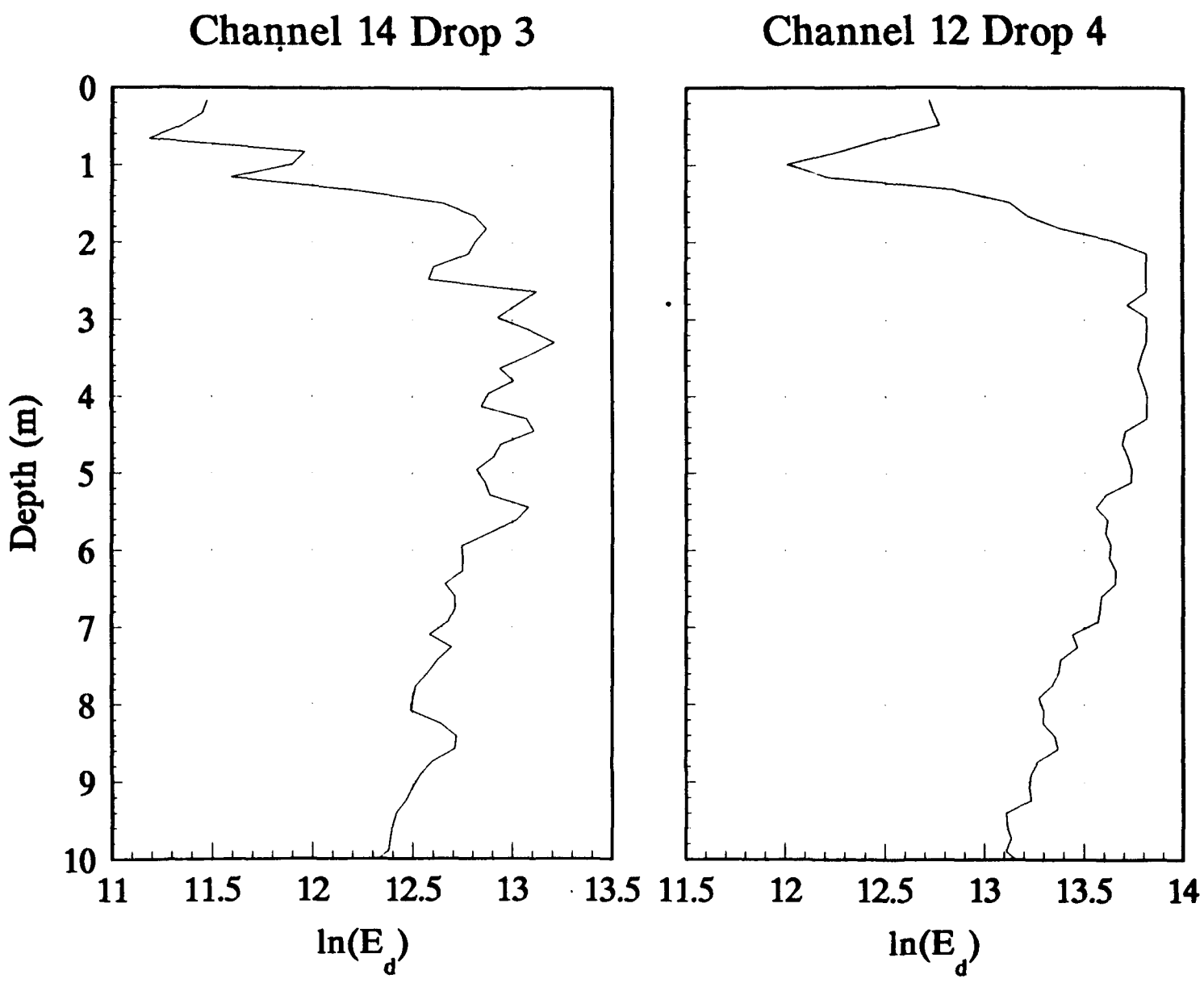
1990 Norway AXKT Text
Channel 14 Drop 3
Channel 12 Drop 4
Depth (m)
0
1
2
3
4
5
6
7
8
9
10
11
11.5
12
12.5
13
13.5
14
ln(E_d)
ln(E_d)

Figure 26.

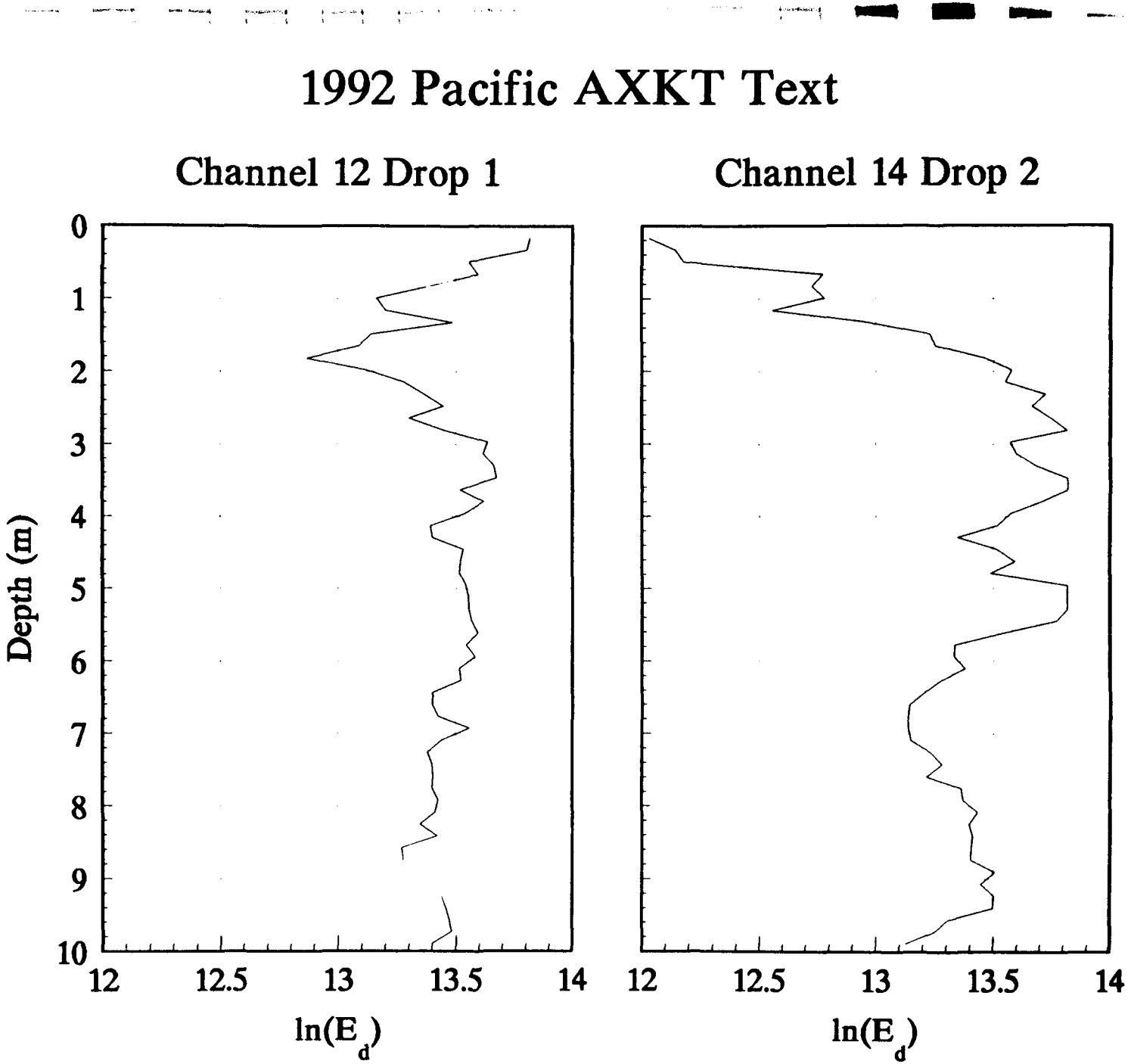
1992 Pacific AXKT Text
Channel 12 Drop 1
Channel 14 Drop 2
Depth (m)
0
1
2
3
4
5
6
7
8
9
10
12
12.5
13
13.5
14
ln(E_d)
12
12.5
13
13.5
14
ln(E_d)

Figure 27.

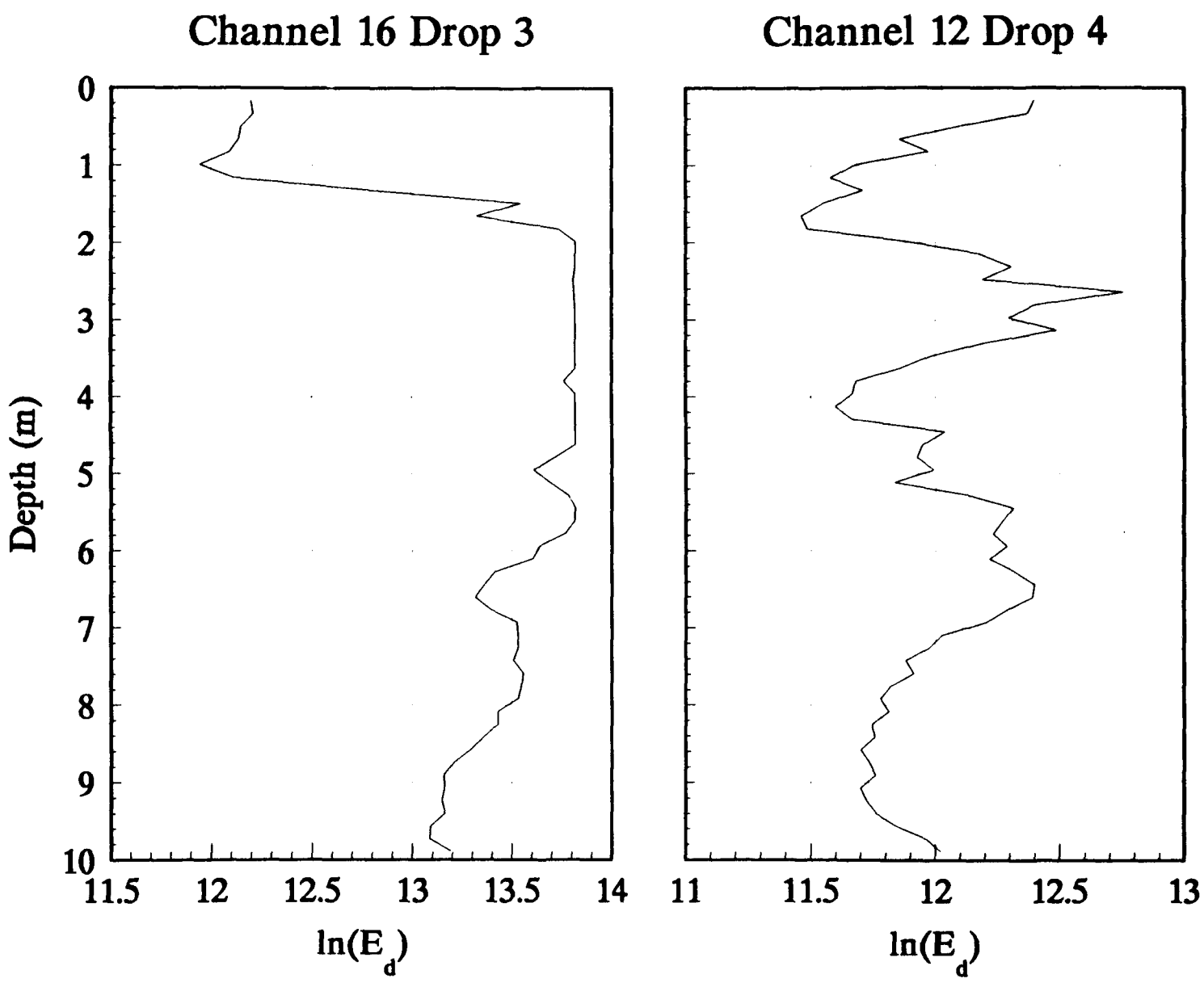
1992 Pacific AXKT Text
Channel 16 Drop 3
Channel 12 Drop 4
Depth (m)
0
1
2
3
4
5
6
7
8
9
10
11.5
12
12.5
13
13.5
14
11
11.5
12
12.5
13
ln(E_d)
ln(E_d)

Figure 28.

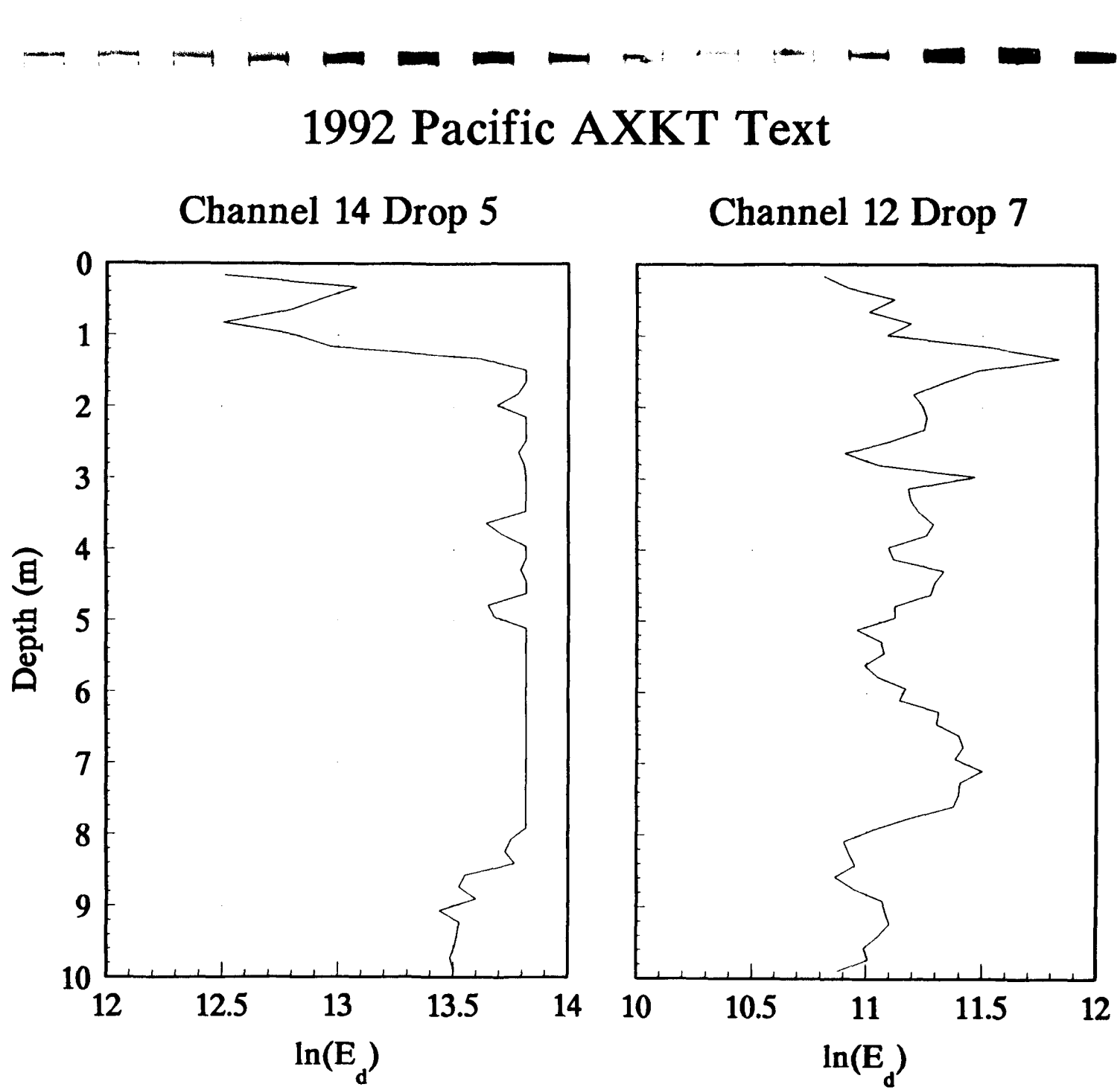
1992 Pacific AXKT Text
Channel 14 Drop 5
Channel 12 Drop 7
Depth (m)
0
1
2
3
4
5
6
7
8
9
10
12
12.5
13
13.5
14
10
10.5
11
11.5
12
ln(E_d)
ln(E_d)

Figure 29.

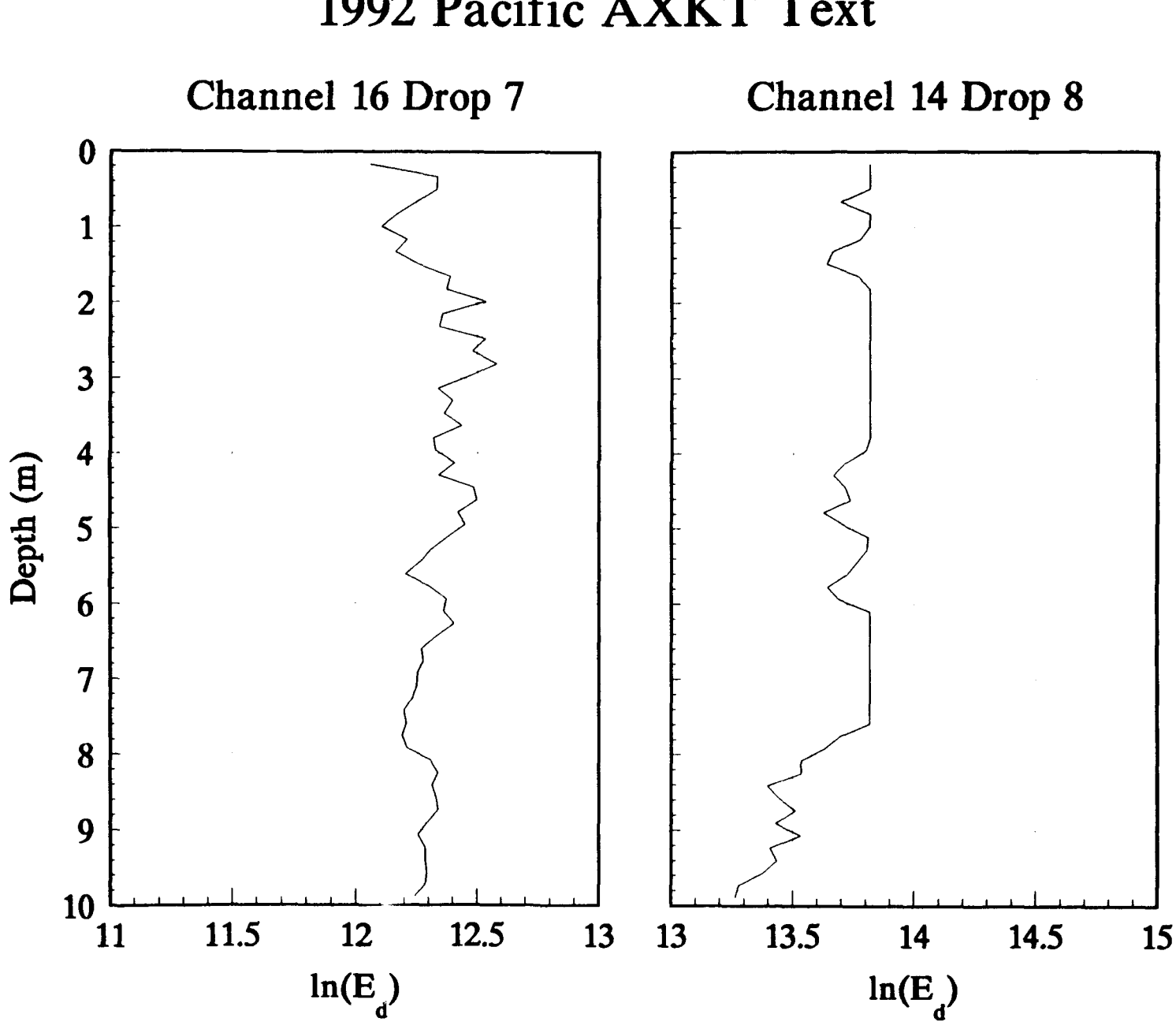
1992 Pacific AXKT Text
Channel 16 Drop 7
Channel 14 Drop 8
Depth (m)
0
1
2
3
4
5
6
7
8
9
10
11
11.5
12
12.5
13
13
13.5
14
14.5
15
ln(E_d)
ln(E_d)

Figure 30.

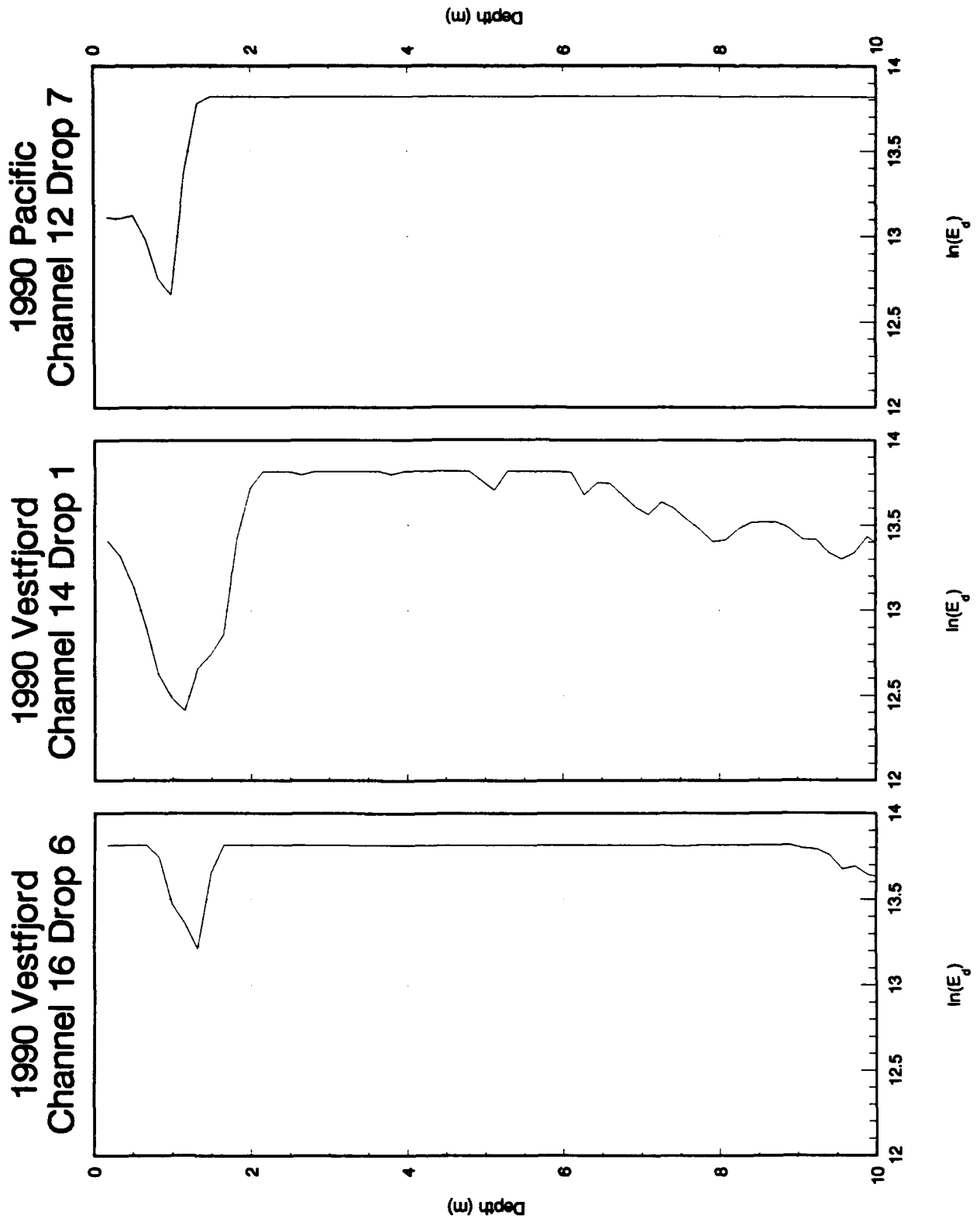
1990 Pacific
Channel 12 Drop 7
1990 Vestfjord
Channel 14 Drop 1
1990 Vestfjord
Channel 16 Drop 6
Depth (m)
0
2
4
6
8
10
12
12.5
13
13.5
14
ln(E_d)

Figure 31.

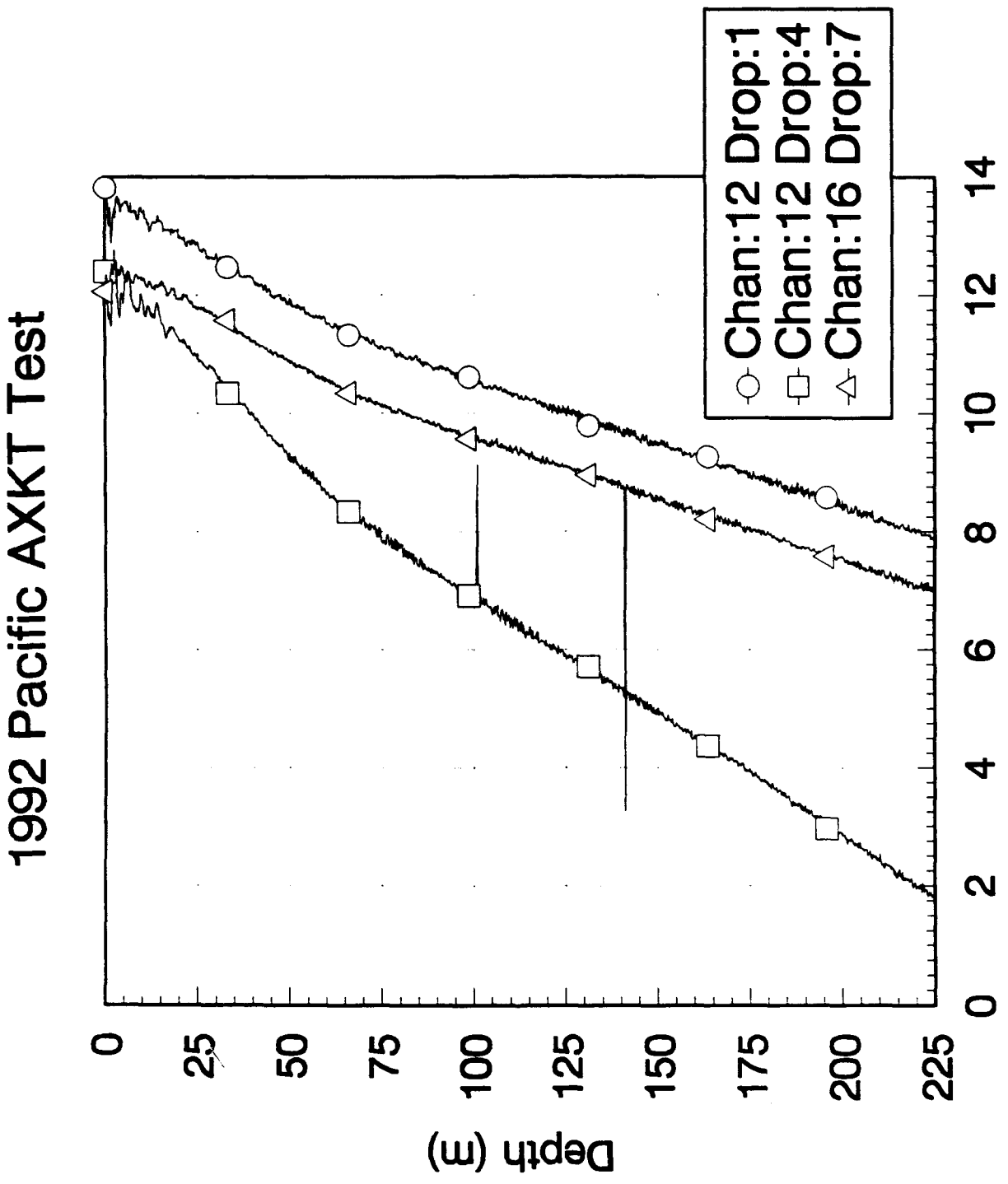
1992 Pacific AXKT Test
Chan:12 Drop:1
Chan:12 Drop:4
Chan:16 Drop:7
Depth (m)
0
25
50
75
100
125
150
175
200
225
ln(E_d)
0
2
4
6
8
10
12
14

Figure 32.

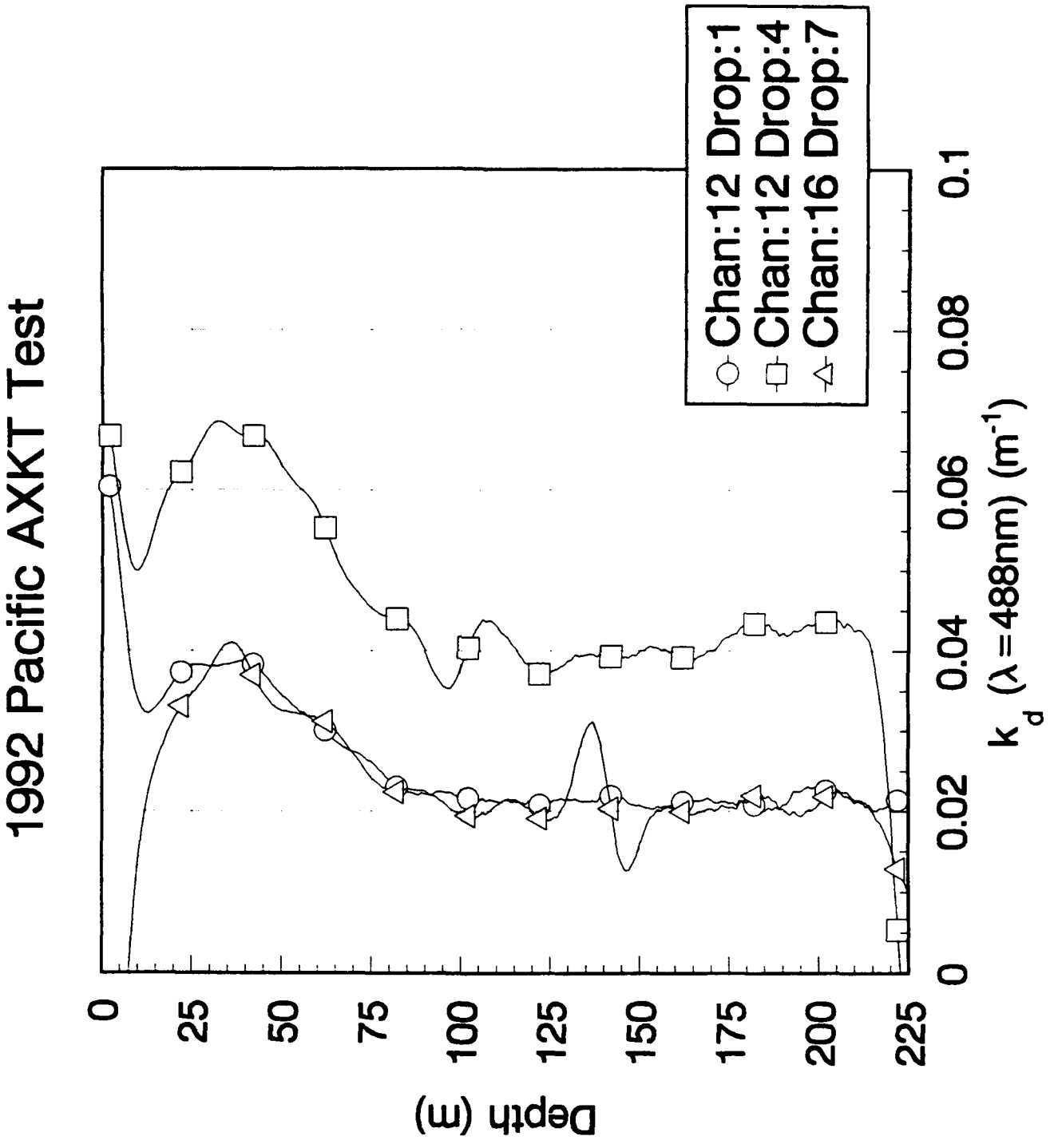
1992 Pacific AXKT Test
Chan:12 Drop:1
Chan:12 Drop:4
Chan:16 Drop:7
Depth (m)
0
25
50
75
100
125
150
175
200
225
0
0.02
0.04
0.06
0.08
0.1
k_d (λ=488nm) (m^{-1})

Figure 33.

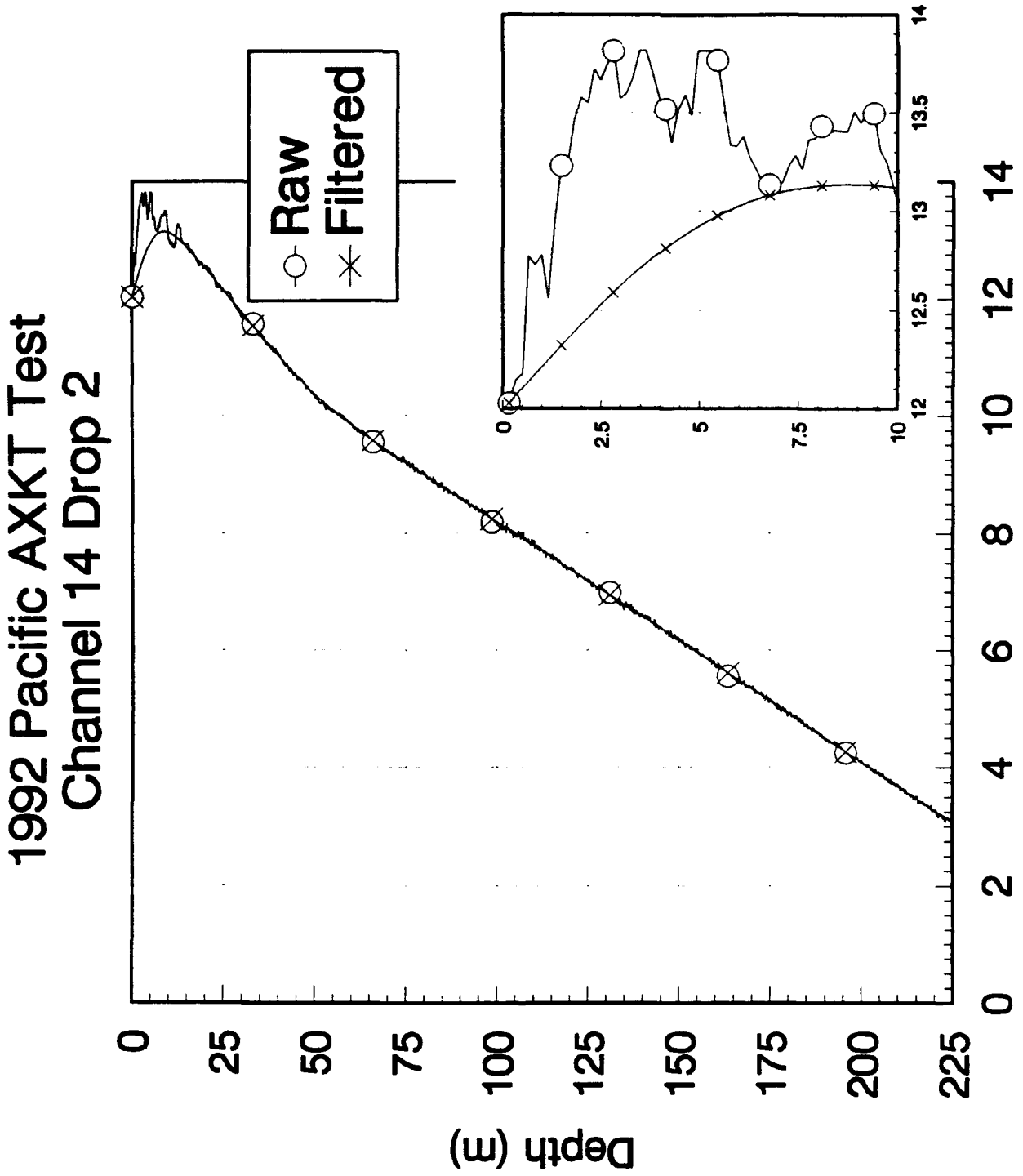
1992 Pacific AXKT Test
Channel 14 Drop 2
Raw
Filtered
Depth (m)
ln(E_d)
0
25
50
75
100
125
150
175
200
225
0
2
4
6
8
10
12
14
0
2.5
5
7.5
10
12
12.5
13
13.5
14

Figure 34.

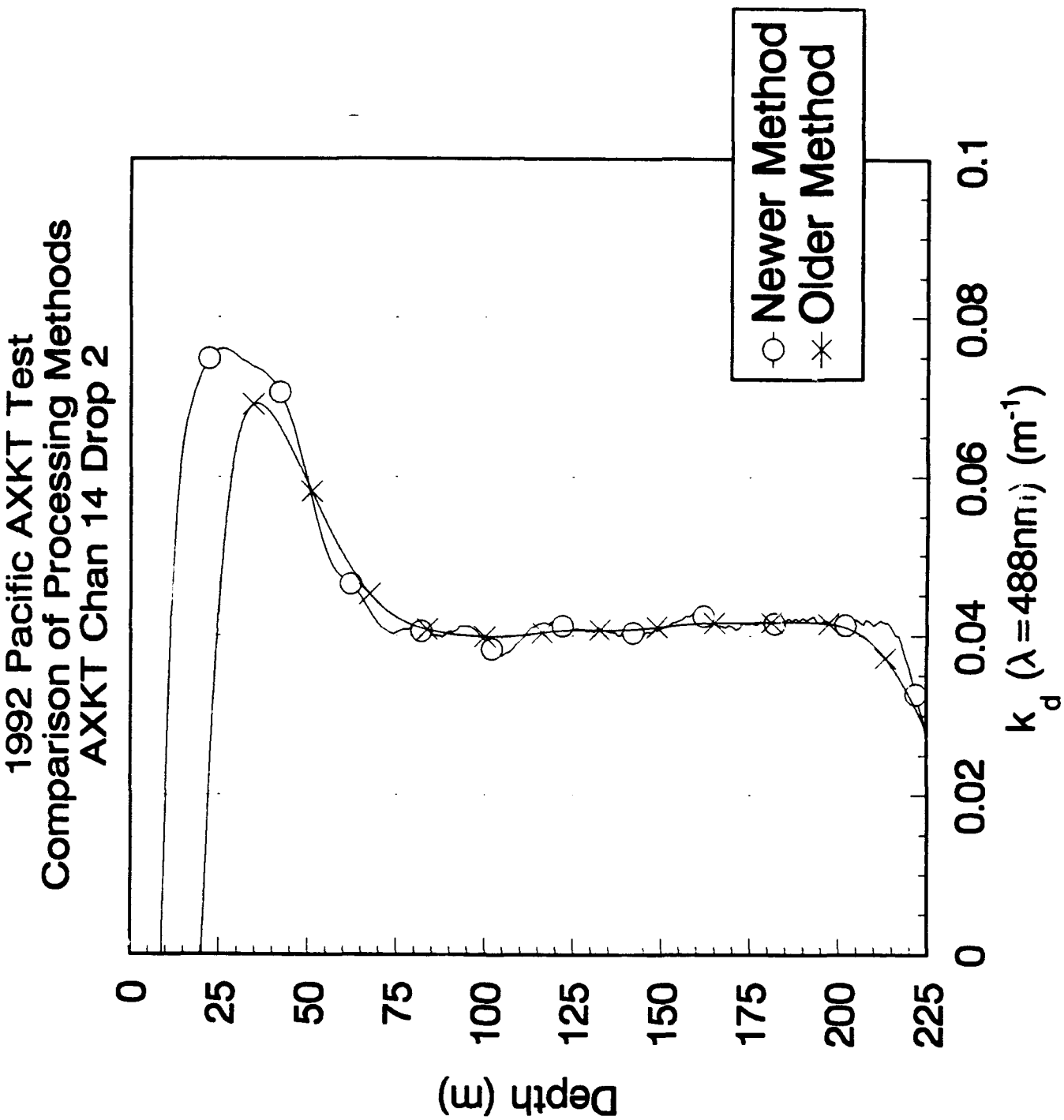
1992 Pacific AXKT Test
Comparison of Processing Methods
AXKT Chan 14 Drop 2
Newer Method
Older Method
Depth (m)
0
25
50
75
100
125
150
175
200
225
0
0.02
0.04
0.06
0.08
0.1
k_d (λ=488nm) (m^{-1})

Figure 35.

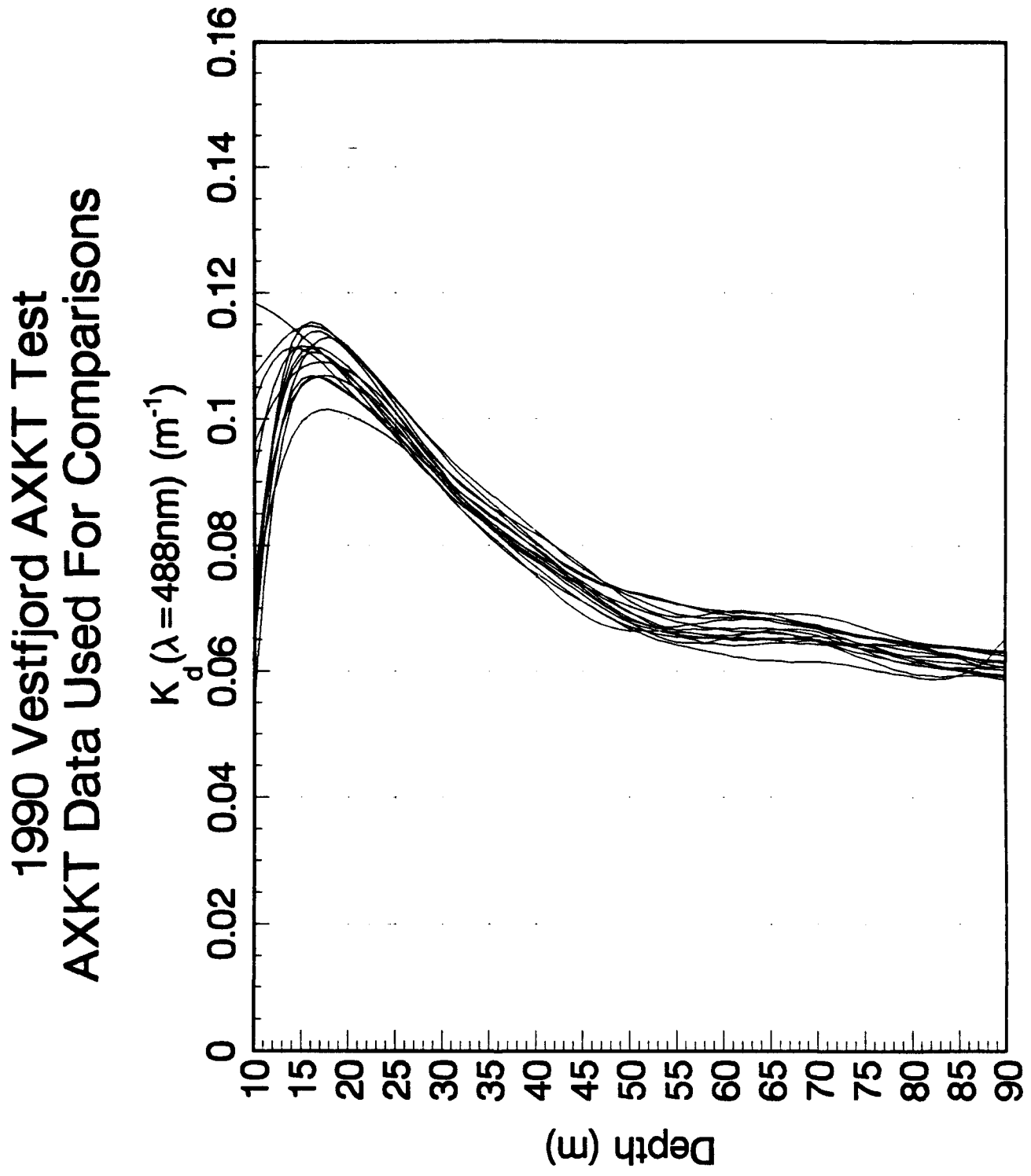
1990 Vestfjord AXKT Test
AXKT Data Used For Comparisons
$K_d(\lambda=488nm)$ (m^{-1})
0
0.02
0.04
0.06
0.08
0.1
0.12
0.14
0.16
10
15
20
25
30
35
40
45
50
55
60
65
70
75
80
85
90
Depth (m)

Figure 36.

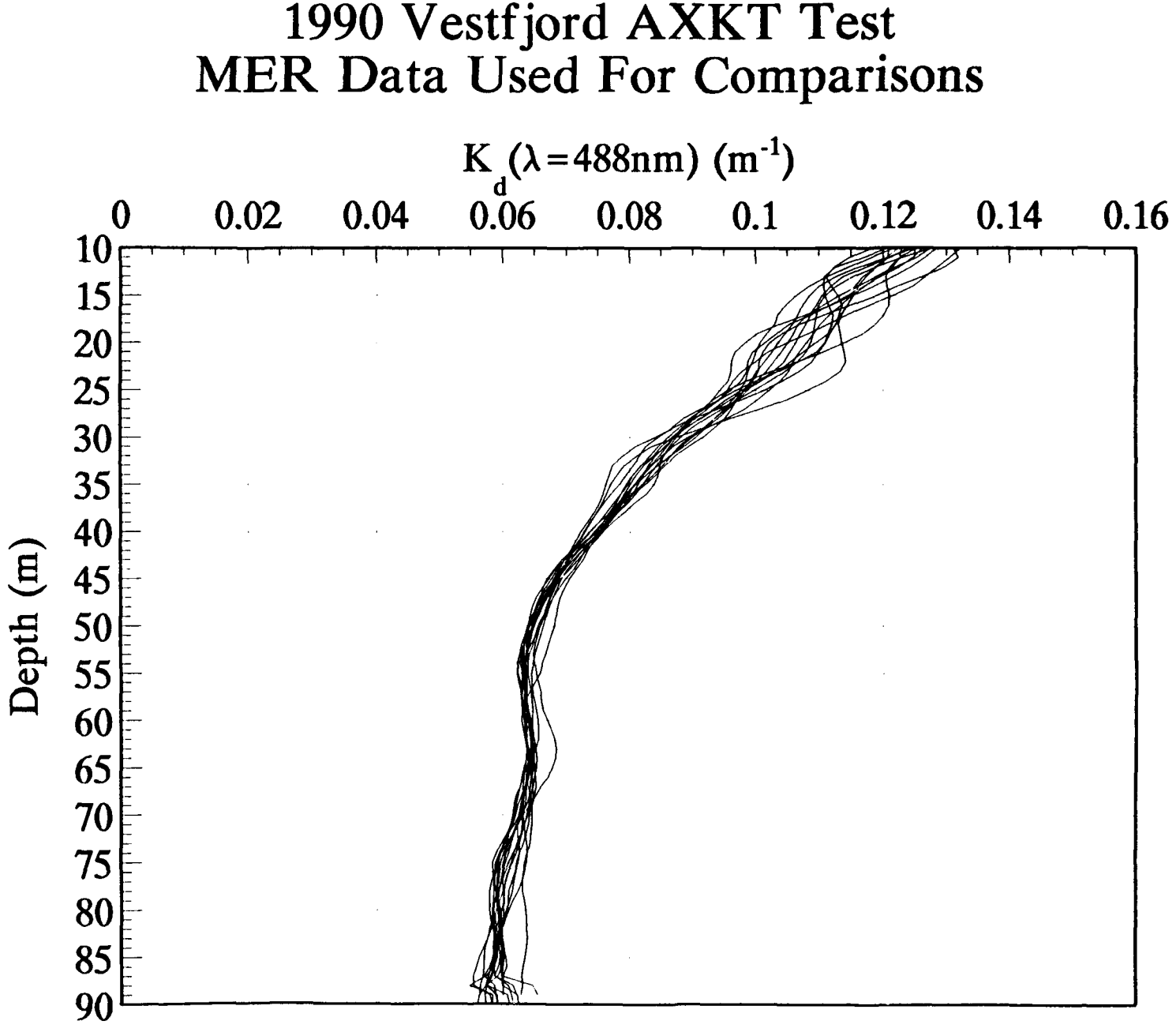
1990 Vestfjord AXKT Test
MER Data Used For Comparisons
K d (λ=488nm) (m-1)
0
0.02
0.04
0.06
0.08
0.1
0.12
0.14
0.16
Depth (m)
10
15
20
25
30
35
40
45
50
55
60
65
70
75
80
85
90

Figure 37.

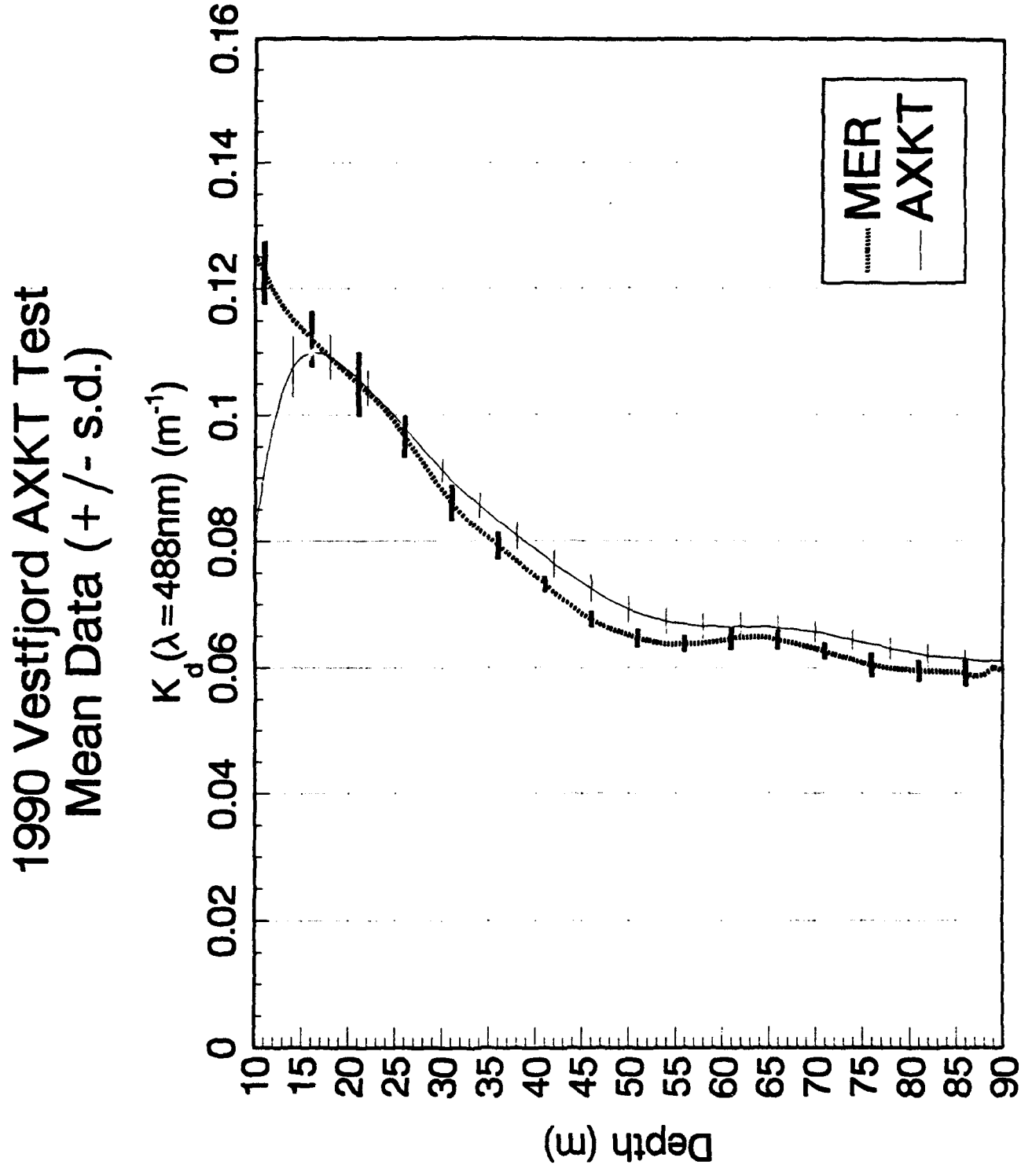
1990 Vestfjord AXKT Test
Mean Data (+/- s.d.)
$K_d(\lambda=488nm)$ (m^{-1})
0
0.02
0.04
0.06
0.08
0.1
0.12
0.14
0.16
Depth (m)
10
15
20
25
30
35
40
45
50
55
60
65
70
75
80
85
90
MER
AXKT

Figure 38.

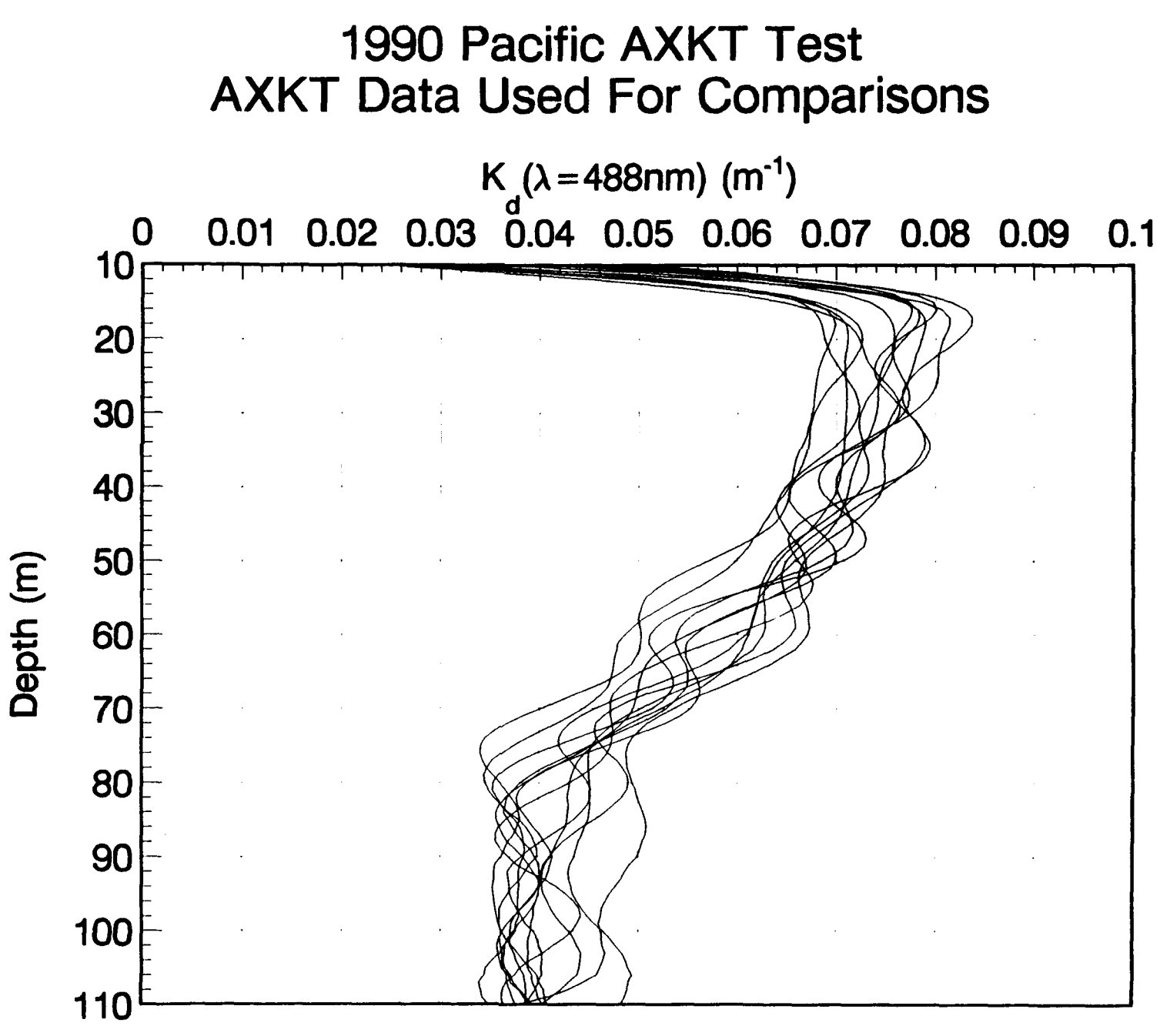
1990 Pacific AXKT Test
AXKT Data Used For Comparisons
K d (λ=488nm) (m-1)
0
0.01
0.02
0.03
0.04
0.05
0.06
0.07
0.08
0.09
0.1
Depth (m)
10
20
30
40
50
60
70
80
90
100
110

Figure 39.

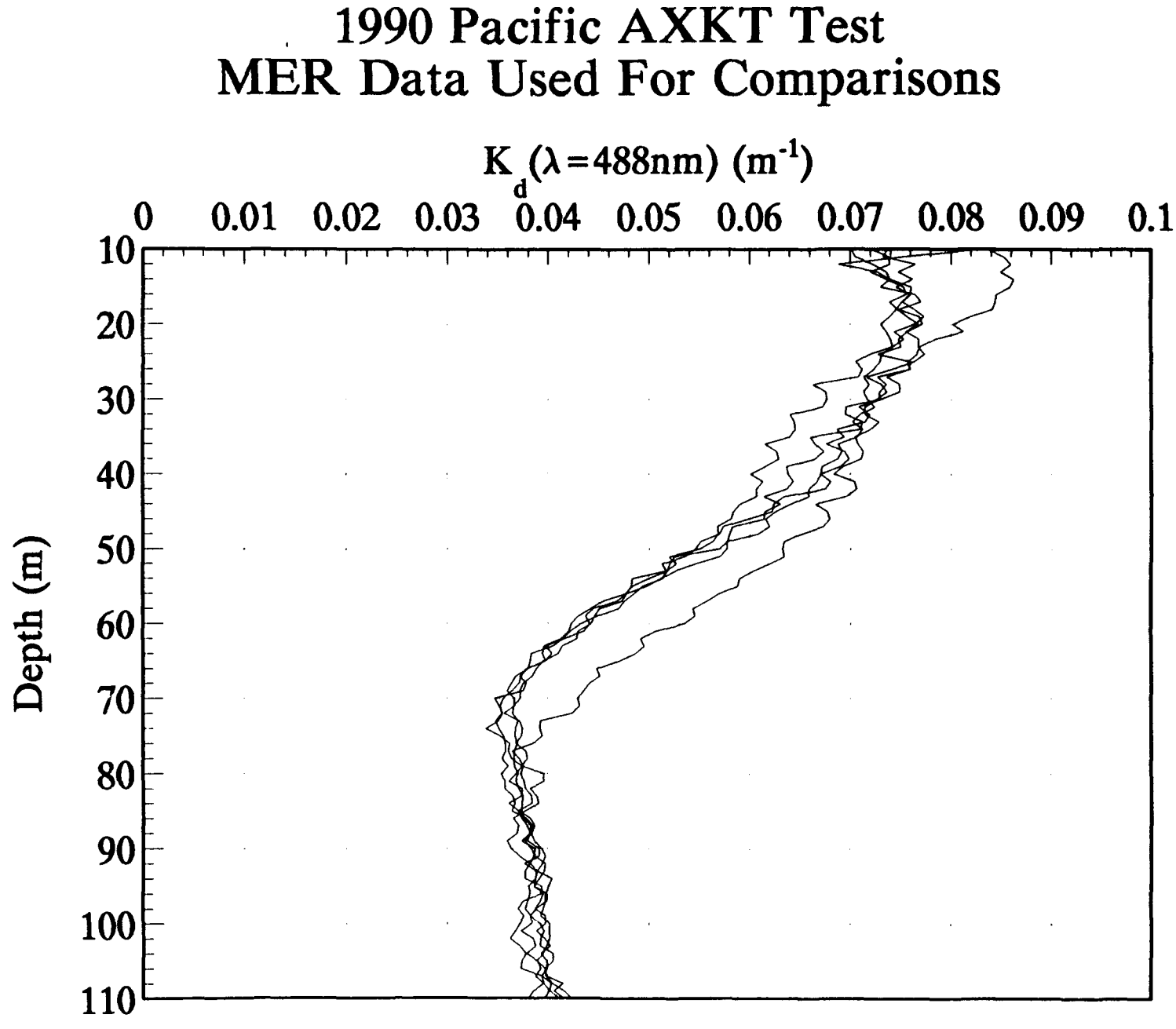
1990 Pacific AXKT Test
MER Data Used For Comparisons
K d (λ=488nm) (m-1)
0
0.01
0.02
0.03
0.04
0.05
0.06
0.07
0.08
0.09
0.1
Depth (m)
10
20
30
40
50
60
70
80
90
100
110

Figure 40.

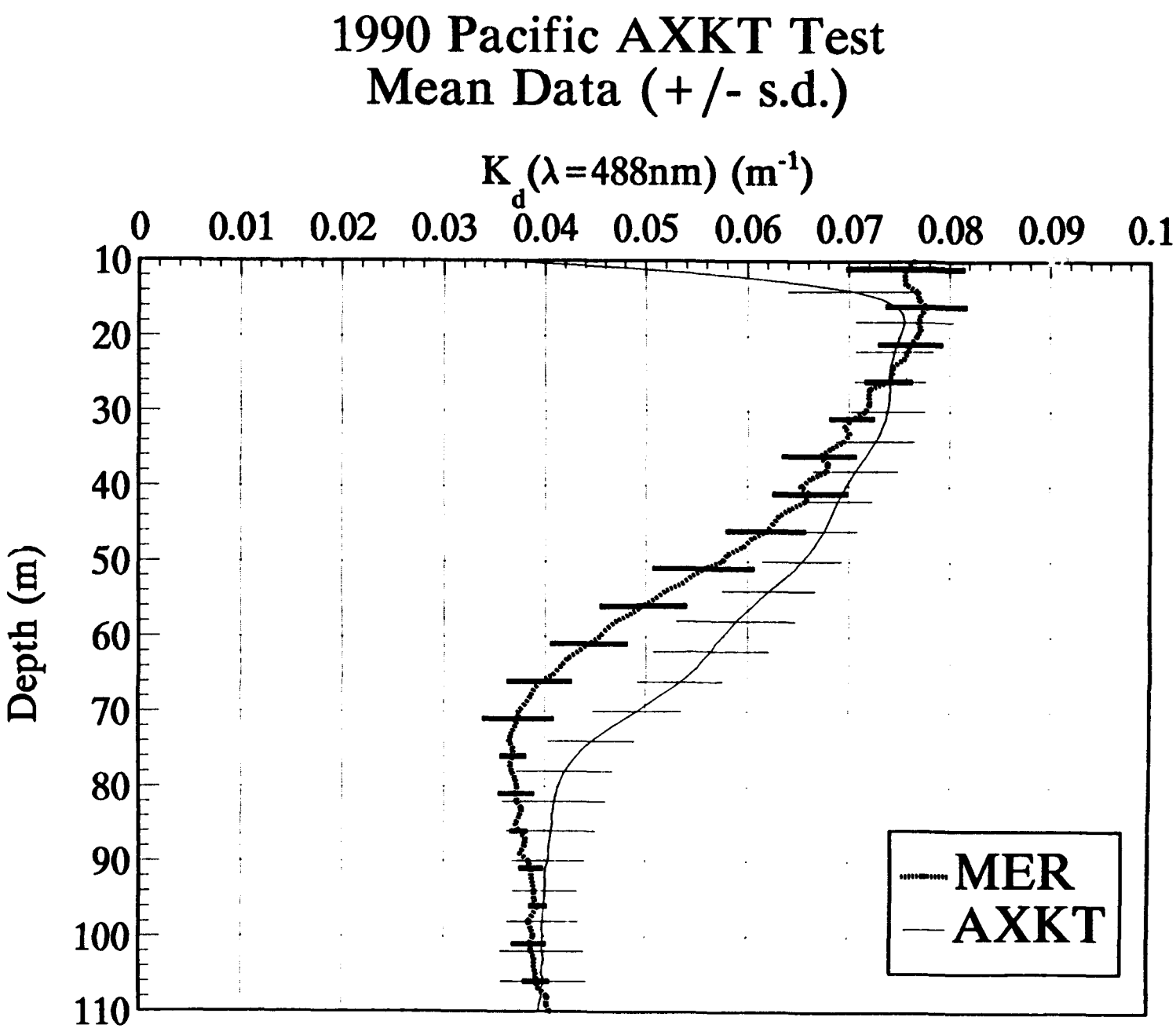
1990 Pacific AXKT Test
Mean Data (+/- s.d.)
K d (λ=488nm) (m-1)
0
0.01
0.02
0.03
0.04
0.05
0.06
0.07
0.08
0.09
0.1
Depth (m)
10
20
30
40
50
60
70
80
90
100
110
MER
AXKT

Figure 41.

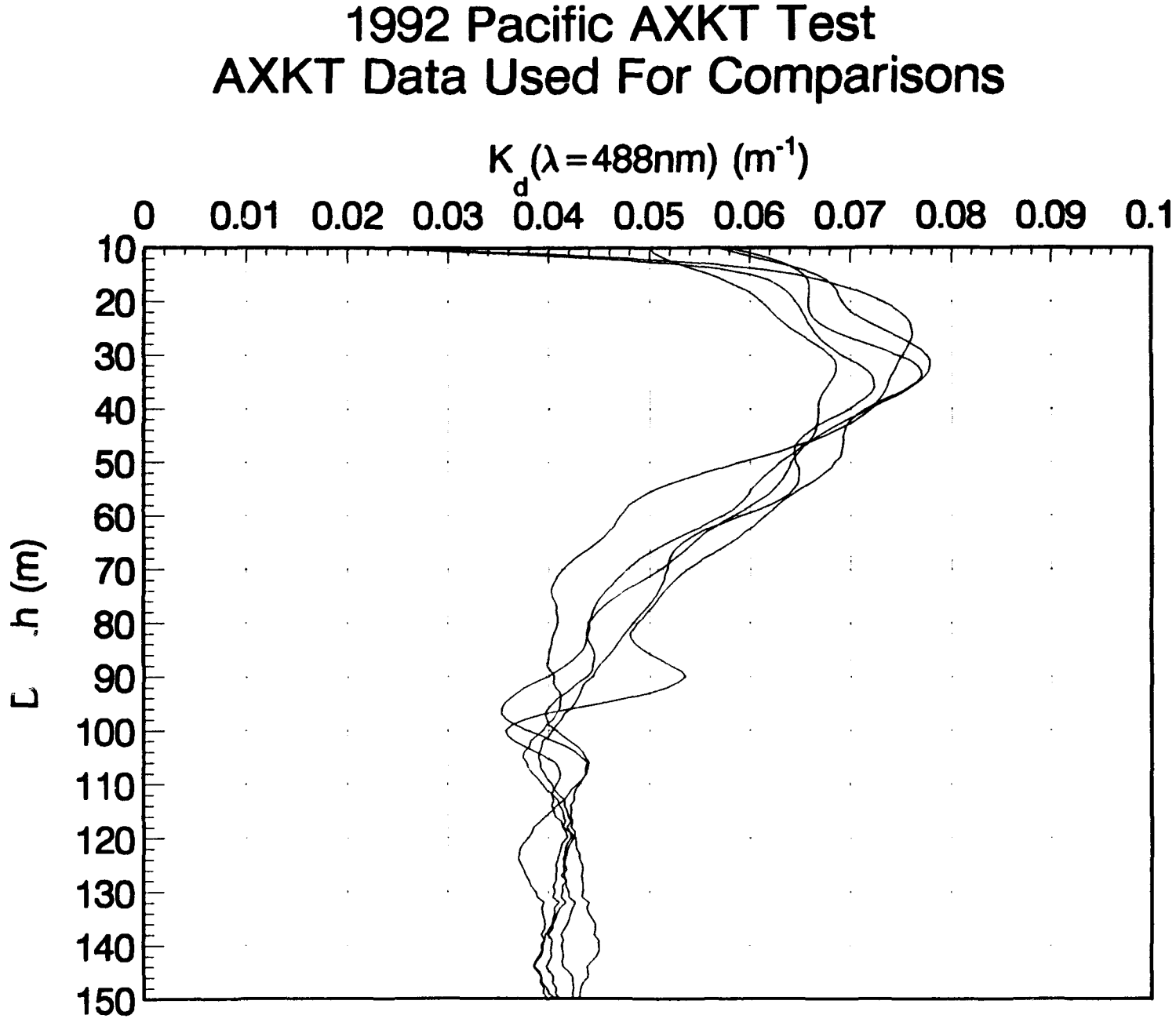
1992 Pacific AXKT Test
AXKT Data Used For Comparisons
K d (λ=488nm) (m-1)
0
0.01
0.02
0.03
0.04
0.05
0.06
0.07
0.08
0.09
0.1
10
20
30
40
50
60
70
80
90
100
110
120
130
140
150
h (m)

Figure 42.

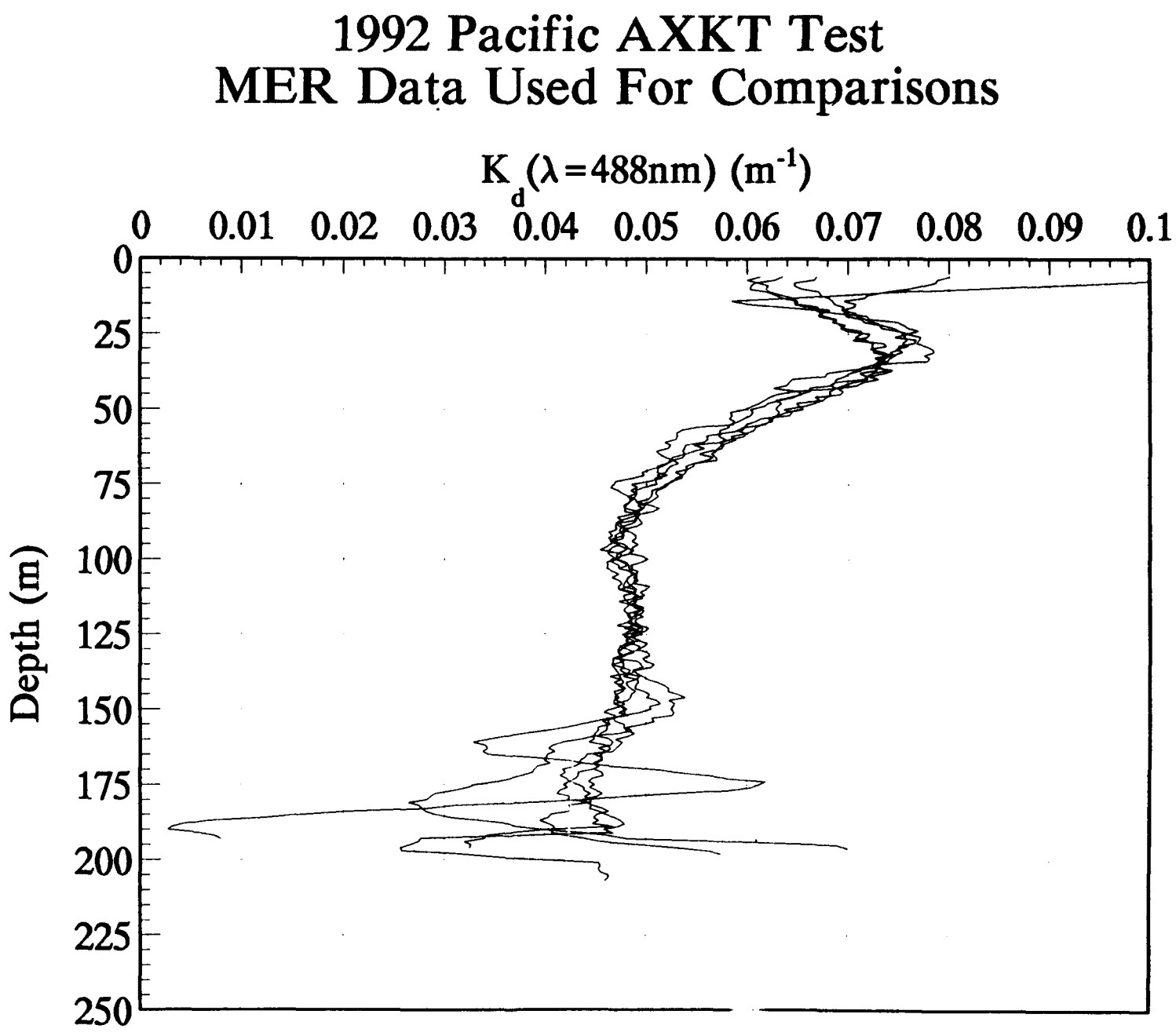
1992 Pacific AXKT Test
MER Data Used For Comparisons
K d (λ=488nm) (m-1)
0
0.01
0.02
0.03
0.04
0.05
0.06
0.07
0.08
0.09
0.1
Depth (m)
0
25
50
75
100
125
150
175
200
225
250

Figure 43.

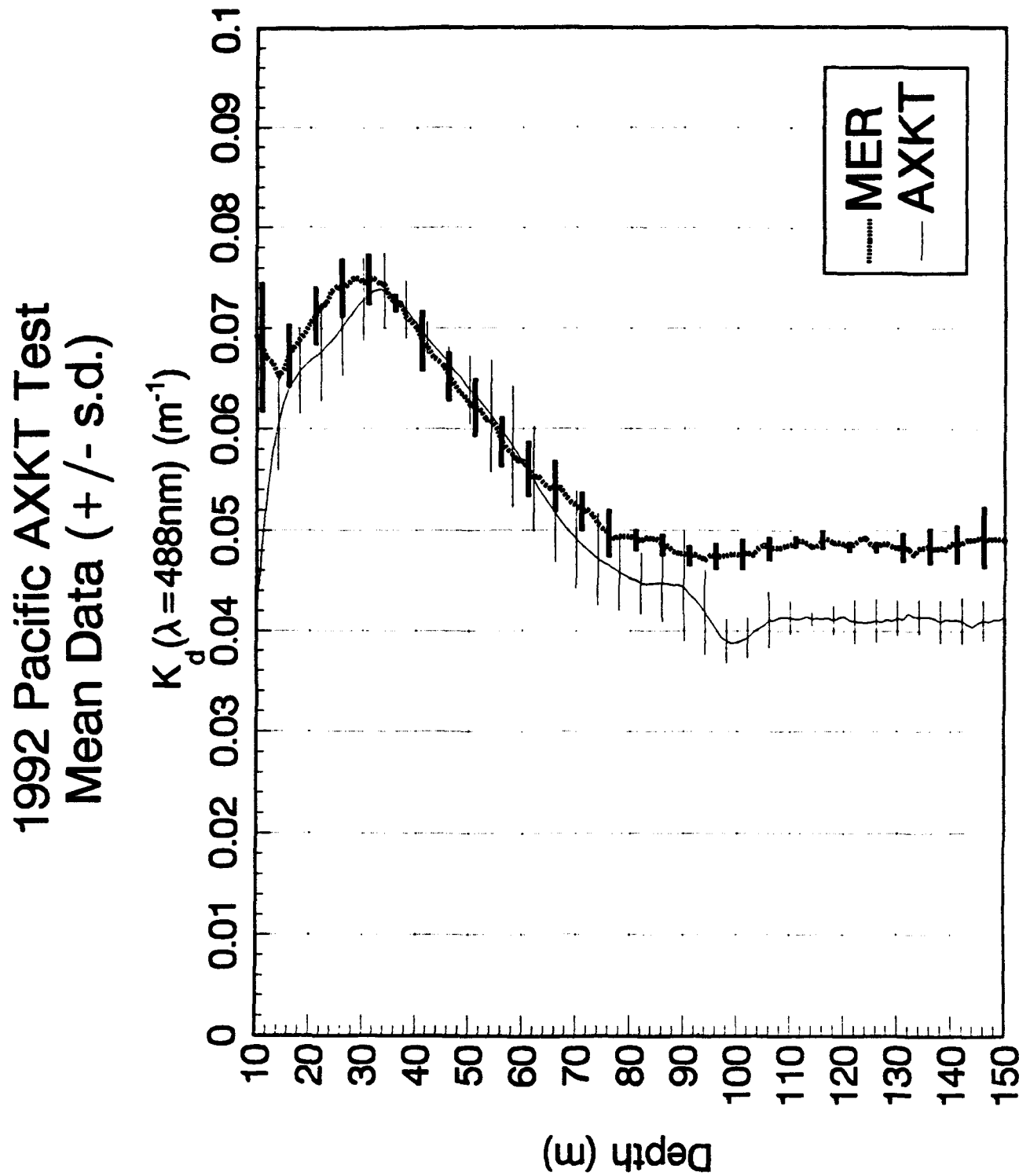
1992 Pacific AXKT Test
Mean Data (+/- s.d.)
$K_d(\lambda=488nm)$ (m^{-1})
0
0.01
0.02
0.03
0.04
0.05
0.06
0.07
0.08
0.09
0.1
10
20
30
40
50
60
70
80
90
100
110
120
130
140
150
Depth (m)
MER
AXKT

Figure 44.

Appendix A

All Interpretable Data from Pacific 1992 AXKT Probes

1992 AXKT Test Channel 12 Drop 1 Realtime
(All Data)
k 21 pt regress and filtfilt(250,.01)
Depth (meters)
0
50
100
150
200
250
300
ln (Ed)
0
2
4
6
8
10
12
14
K
0
0.01
0.02
0.03
0.04
0.05
0.06
0.07
Temperature
0
2
4
6
8
10
12
14

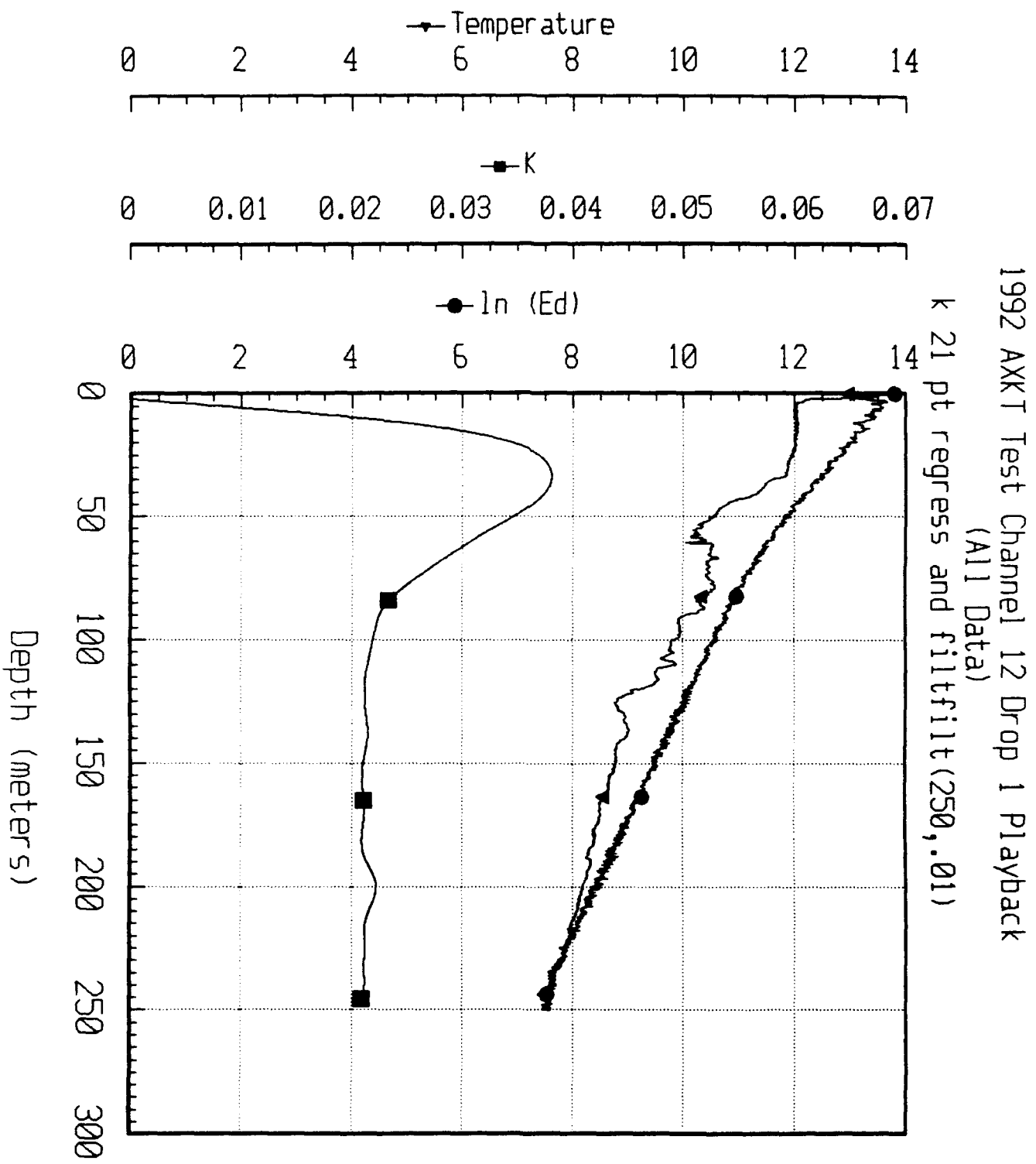
Temperature
0 2 4 6 8 10 12 14
K
0 0.01 0.02 0.03 0.04 0.05 0.06 0.07
ln (Ed)
0 2 4 6 8 10 12 14
0 50 100 150 200 250 300
Depth (meters)
1992 AXKT Test Channel 12 Drop 1 Playback
(All Data)
k 21 pt regress and filtfilt(250,.01)

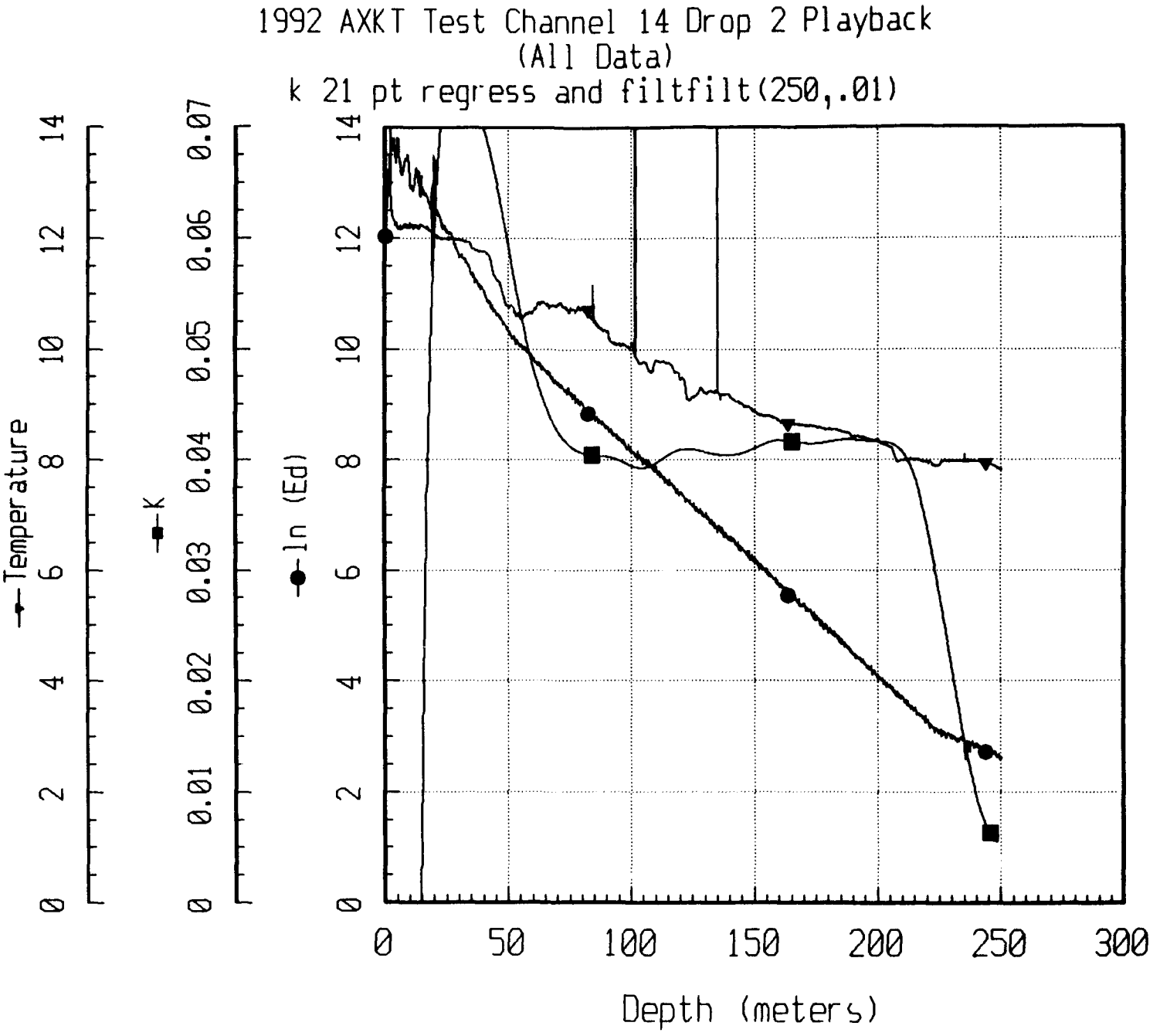
1992 AXKT Test Channel 14 Drop 2 Playback
(All Data)
k 21 pt regress and filtfilt(250,.01)
Temperature
K
ln (Ed)
0
2
4
6
8
10
12
14
0.01
0.02
0.03
0.04
0.05
0.06
0.07
0
50
100
150
200
250
300
Depth (meters)

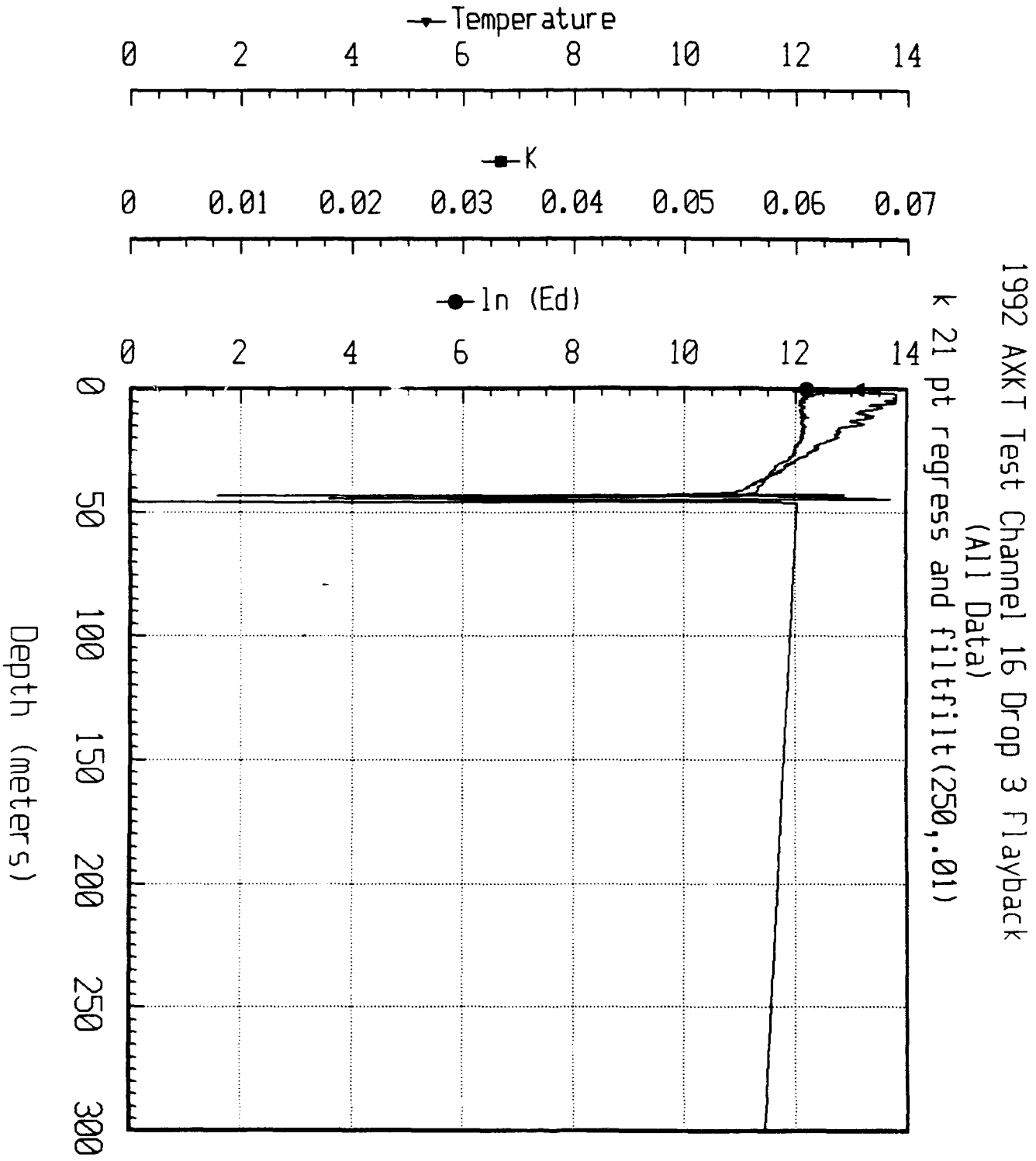
Temperature
0 2 4 6 8 10 12 14
K
0 0.01 0.02 0.03 0.04 0.05 0.06 0.07
ln (Ed)
0 2 4 6 8 10 12 14
0 50 100 150 200 250 300
Depth (meters)
1992 AXKT Test Channel 16 Drop 3 Playback
(All Data)
k 21 pt regress and filtfilt(250,.01)

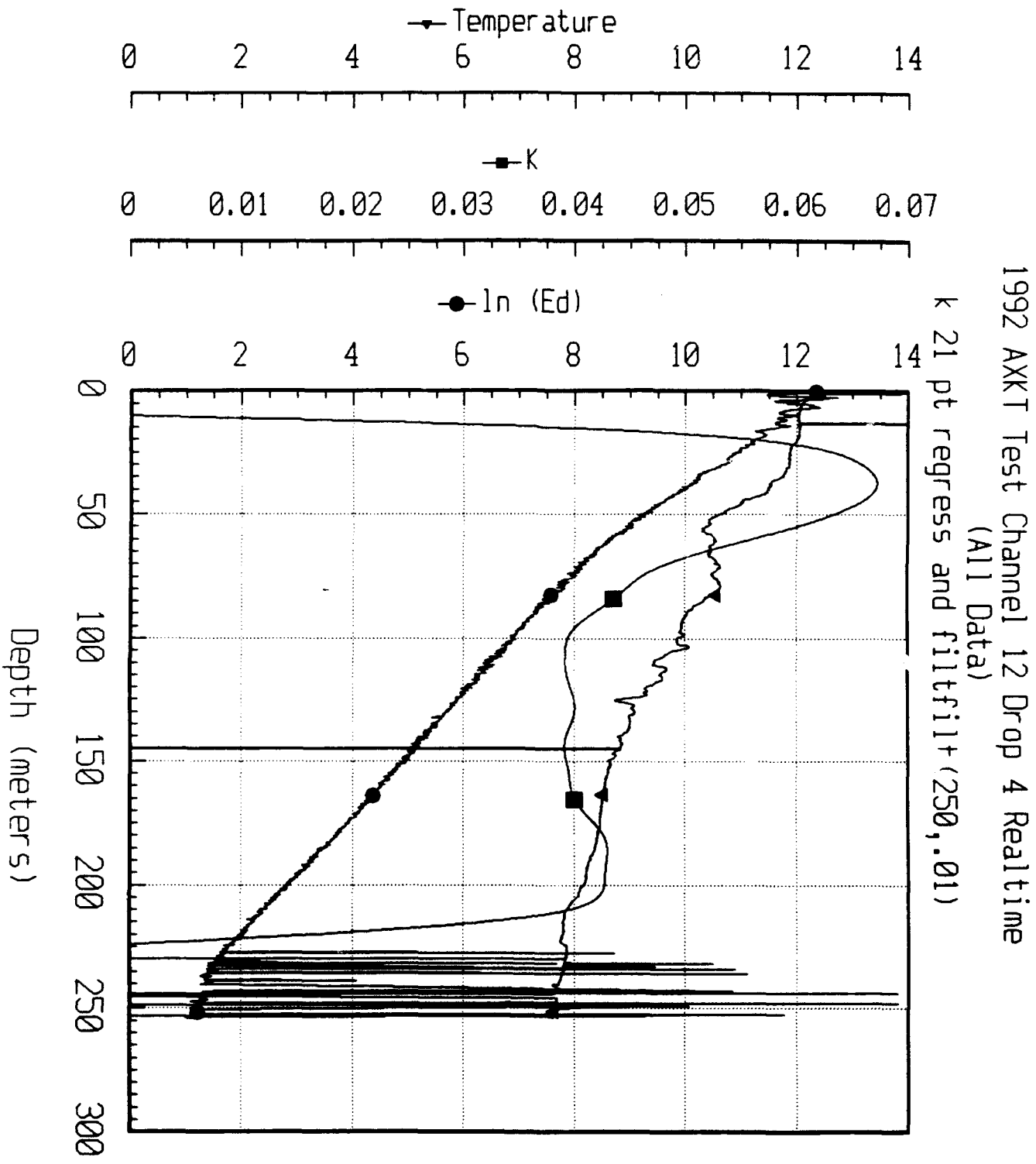
Temperature
0 2 4 6 8 10 12 14
K
0 0.01 0.02 0.03 0.04 0.05 0.06 0.07
ln (Ed)
0 2 4 6 8 10 12 14
0 50 100 150 200 250 300
Depth (meters)
1992 AXKT Test Channel 12 Drop 4 Realtime
(All Data)
k 21 pt regress and filtfil+(250,.01)

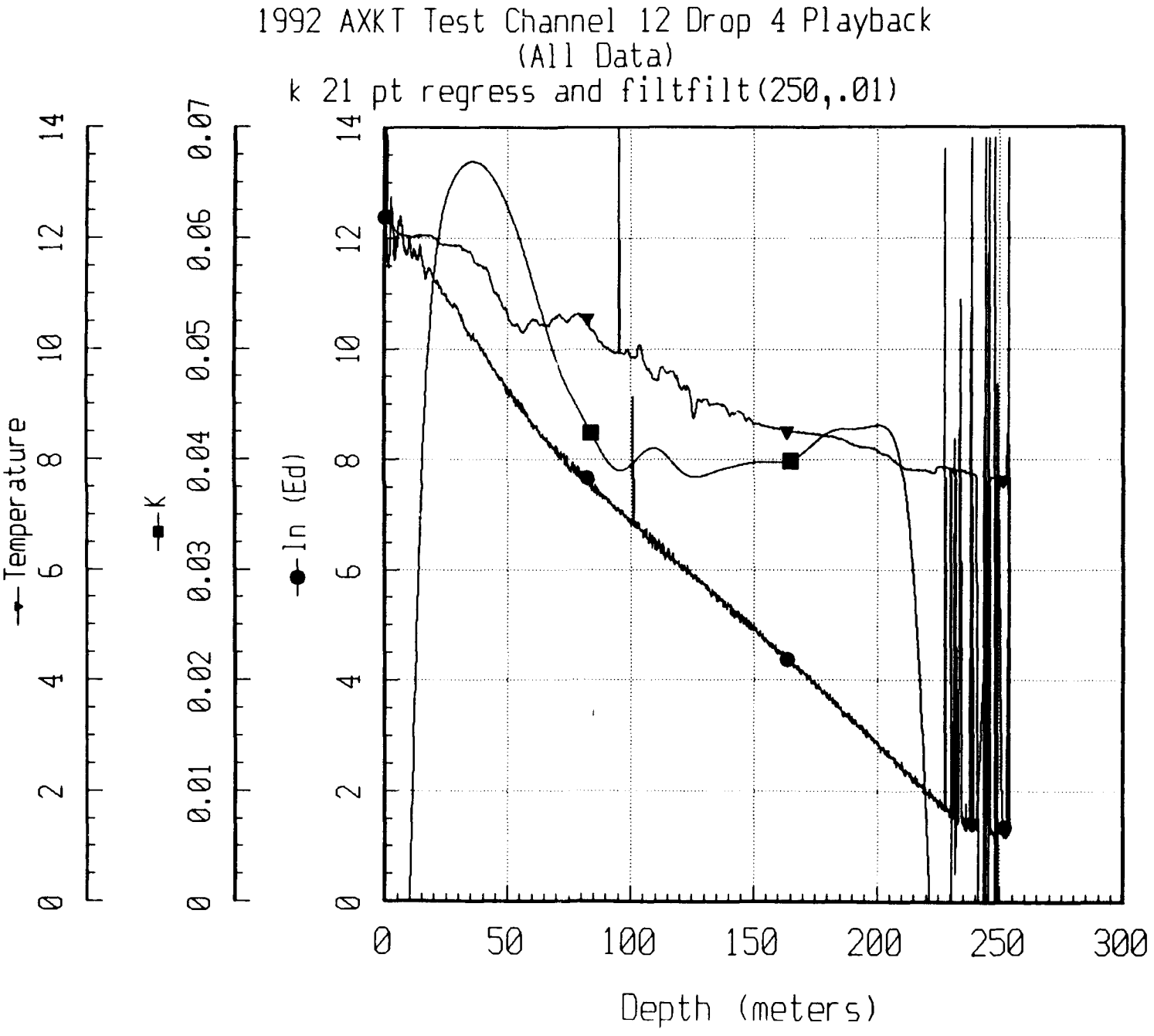
1992 AXKT Test Channel 12 Drop 4 Playback
(All Data)
k 21 pt regress and filtfilt(250,.01)
Temperature
K
ln (Ed)
0
2
4
6
8
10
12
14
0.01
0.02
0.03
0.04
0.05
0.06
0.07
0
50
100
150
200
250
300
Depth (meters)

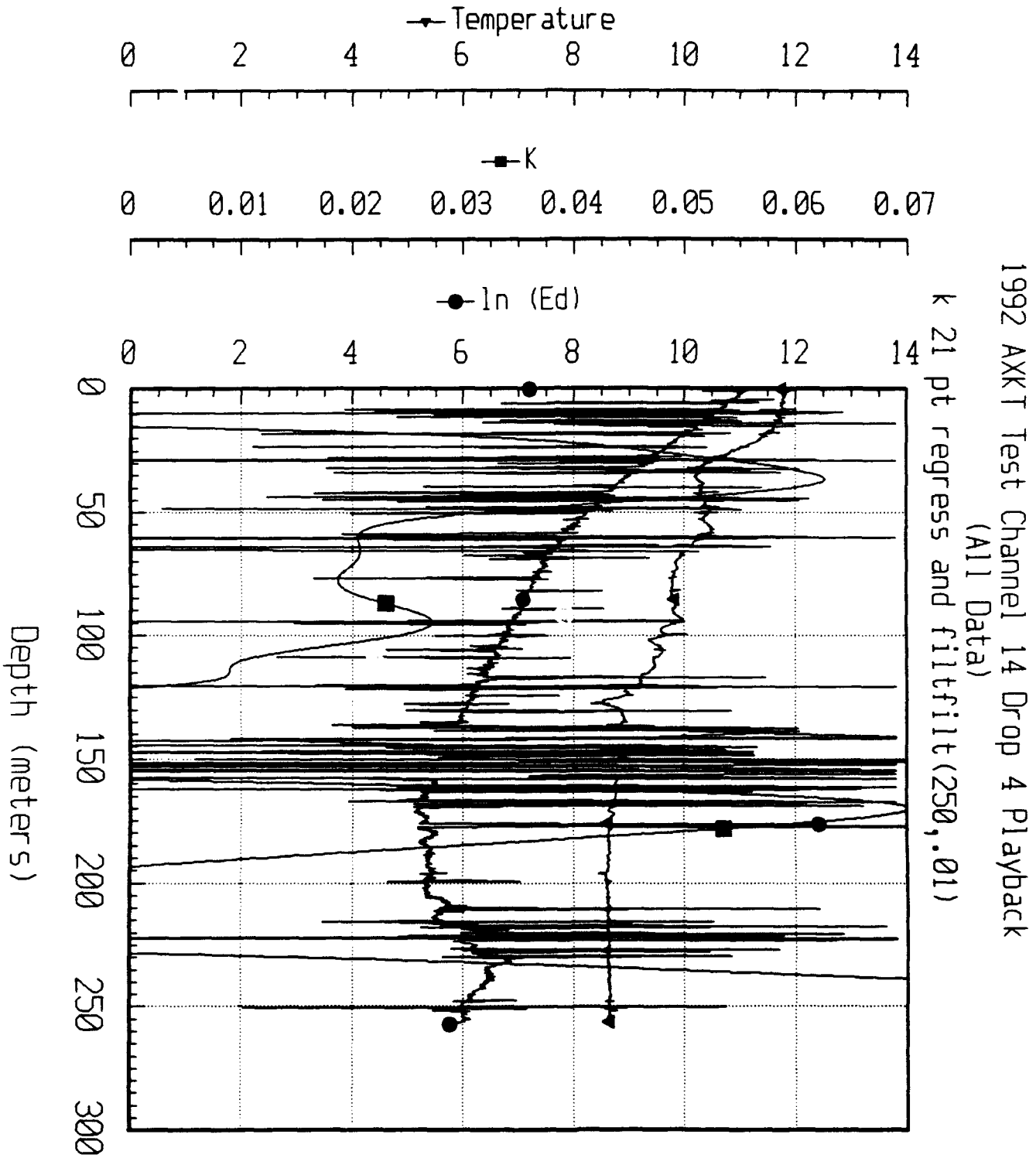
Temperature
0 2 4 6 8 10 12 14
K
0 0.01 0.02 0.03 0.04 0.05 0.06 0.07
ln (Ed)
0 2 4 6 8 10 12 14
0 50 100 150 200 250 300
Depth (meters)
1992 AXKT Test Channel 14 Drop 4 Playback
(All Data)
k 21 pt regress and filtfilt(250,.01)

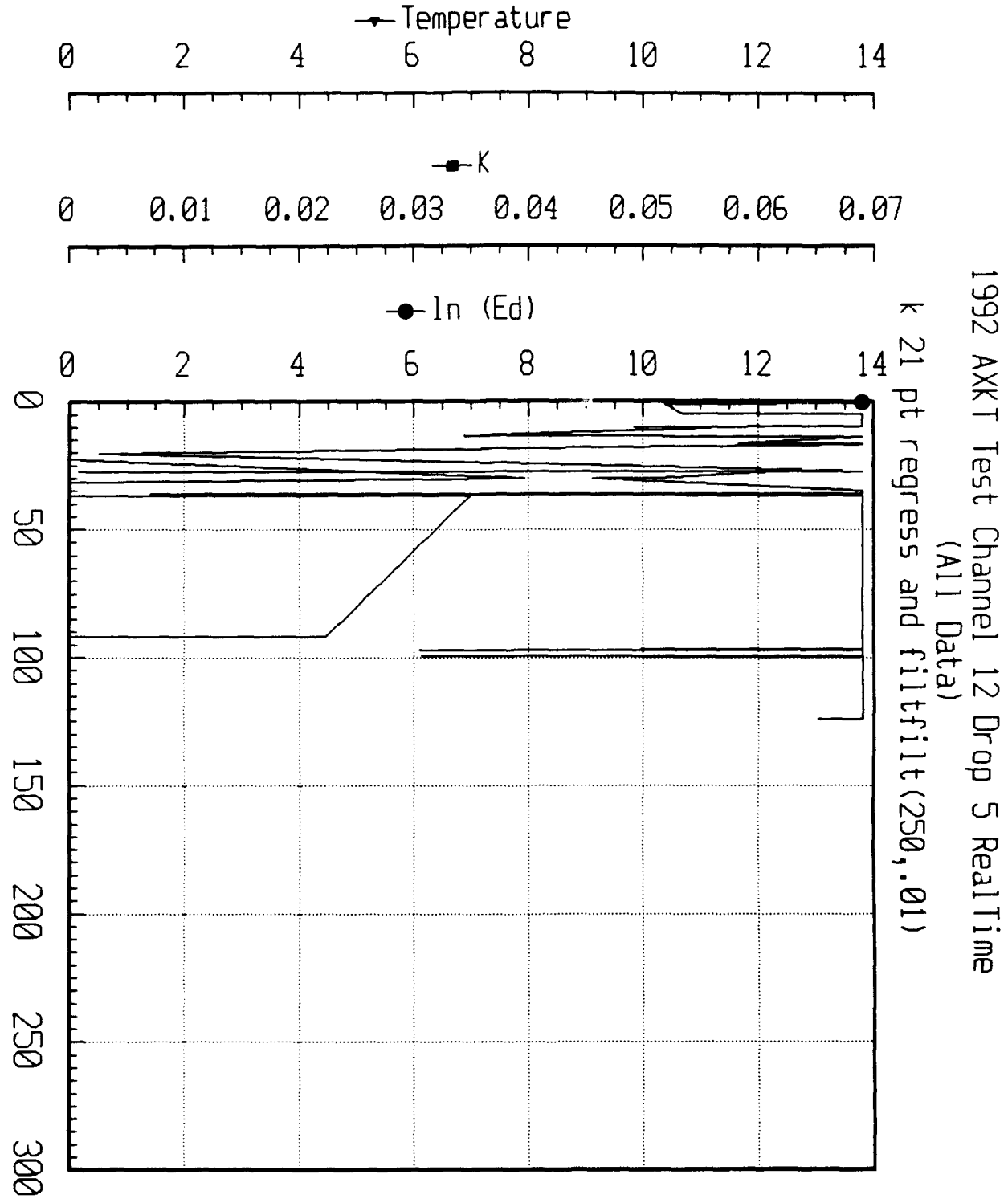
Temperature
0 2 4 6 8 10 12 14
K
0 0.01 0.02 0.03 0.04 0.05 0.06 0.07
ln (Ed)
0 2 4 6 8 10 12 14
0 50 100 150 200 250 300
Depth (meters)
1992 AXKT Test Channel 12 Drop 5 RealTime
(All Data)
k 21 pt regress and filtfilt(250,.01)

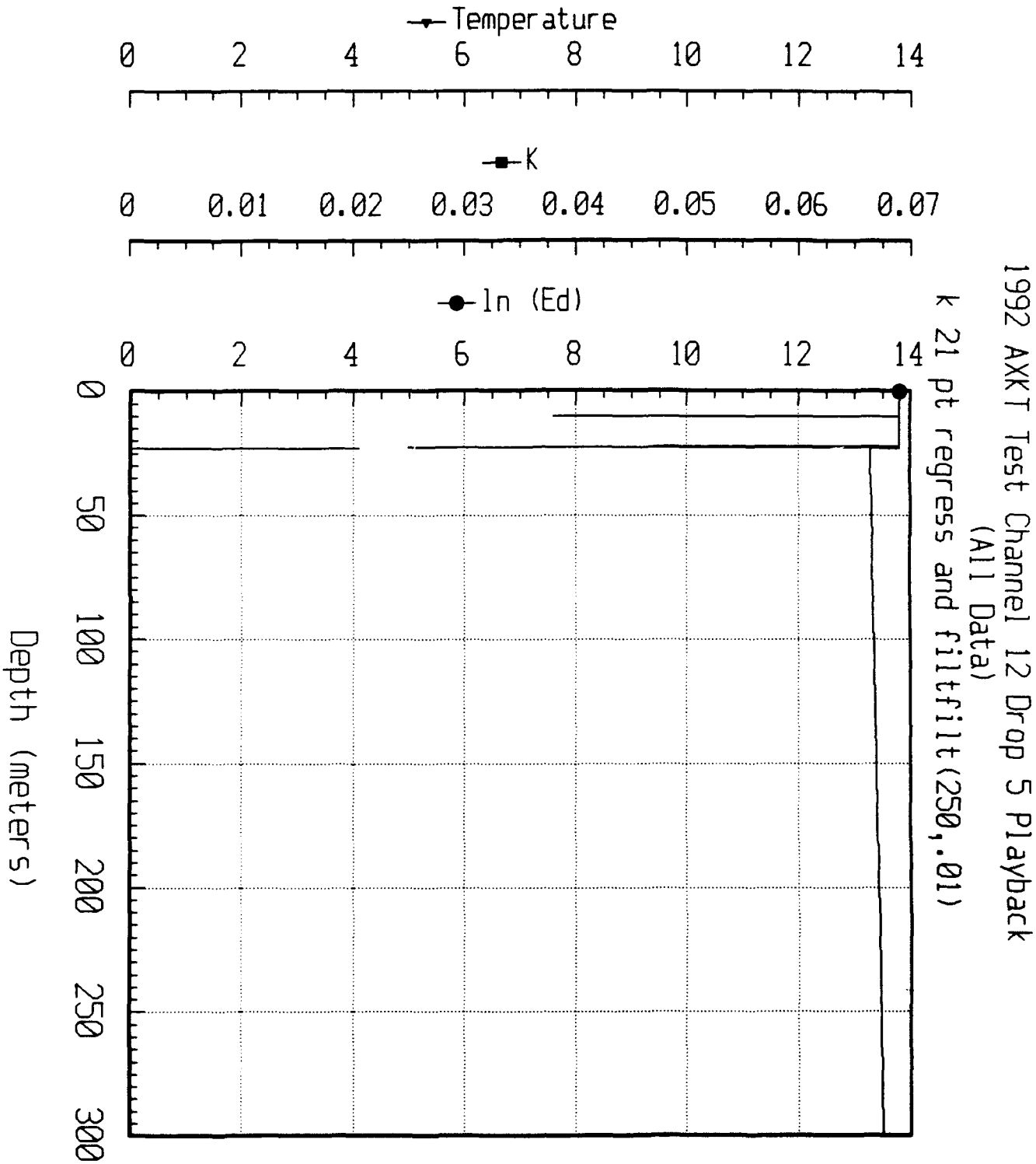
Temperature
0 2 4 6 8 10 12 14
K
0 0.01 0.02 0.03 0.04 0.05 0.06 0.07
ln (Ed)
0 2 4 6 8 10 12 14
0 50 100 150 200 250 300
Depth (meters)
1992 AXKT Test Channel 12 Drop 5 Playback
(All Data)
k 21 pt regress and filtfilt(250,.01)

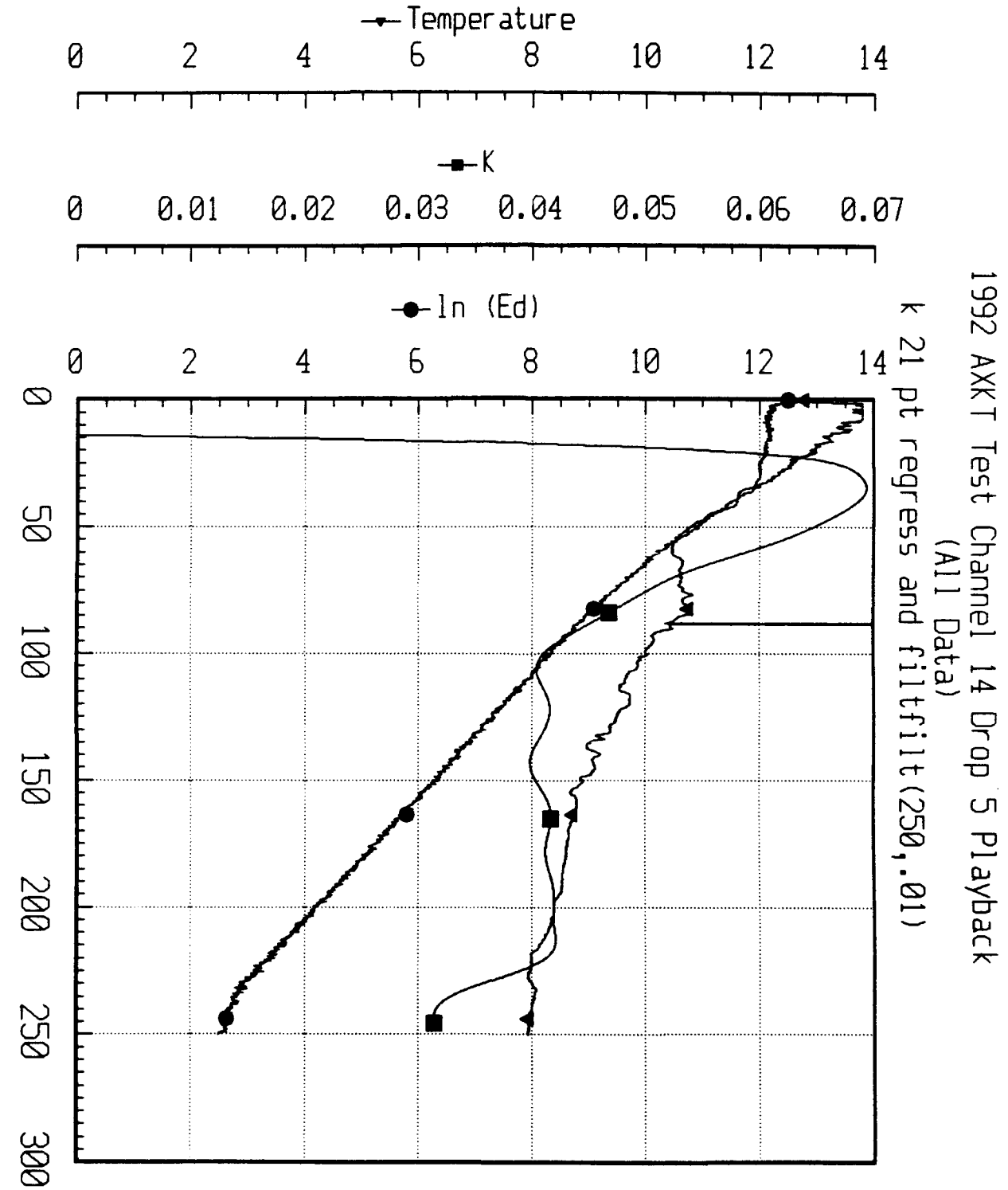
Temperature
0 2 4 6 8 10 12 14
K
0 0.01 0.02 0.03 0.04 0.05 0.06 0.07
ln (Ed)
0 2 4 6 8 10 12 14
0 50 100 150 200 250 300
Depth (meters)
1992 AXKT Test Channel 14 Drop 5 Playback
(All Data)
k 21 pt regress and filtfilt(250,.01)

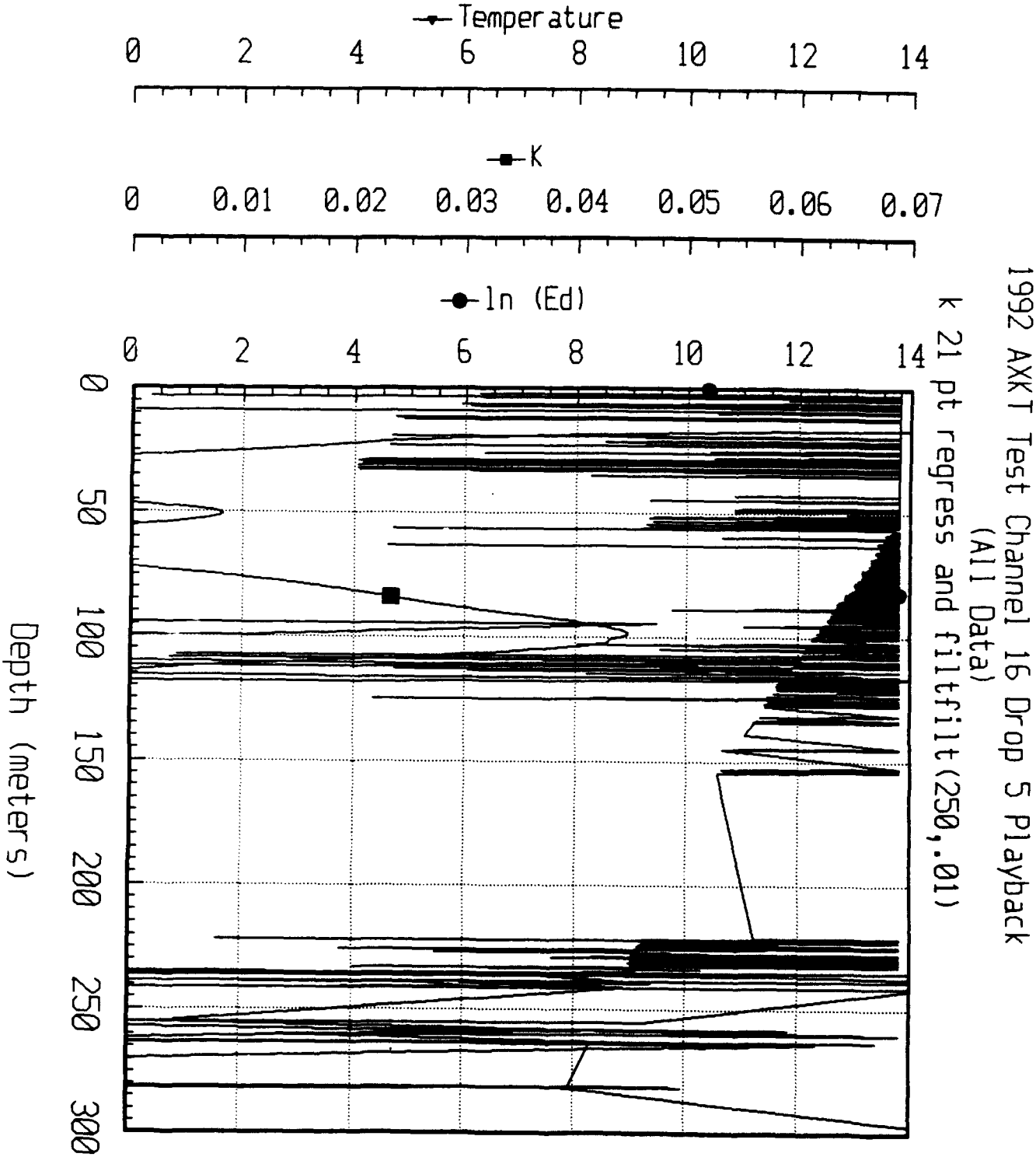
Temperature
0 2 4 6 8 10 12 14
K
0 0.01 0.02 0.03 0.04 0.05 0.06 0.07
ln (Ed)
0 2 4 6 8 10 12 14
0 50 100 150 200 250 300
Depth (meters)
1992 AXKT Test Channel 16 Drop 5 Playback
(All Data)
k 21 pt regress and filtfilt(250,.01)

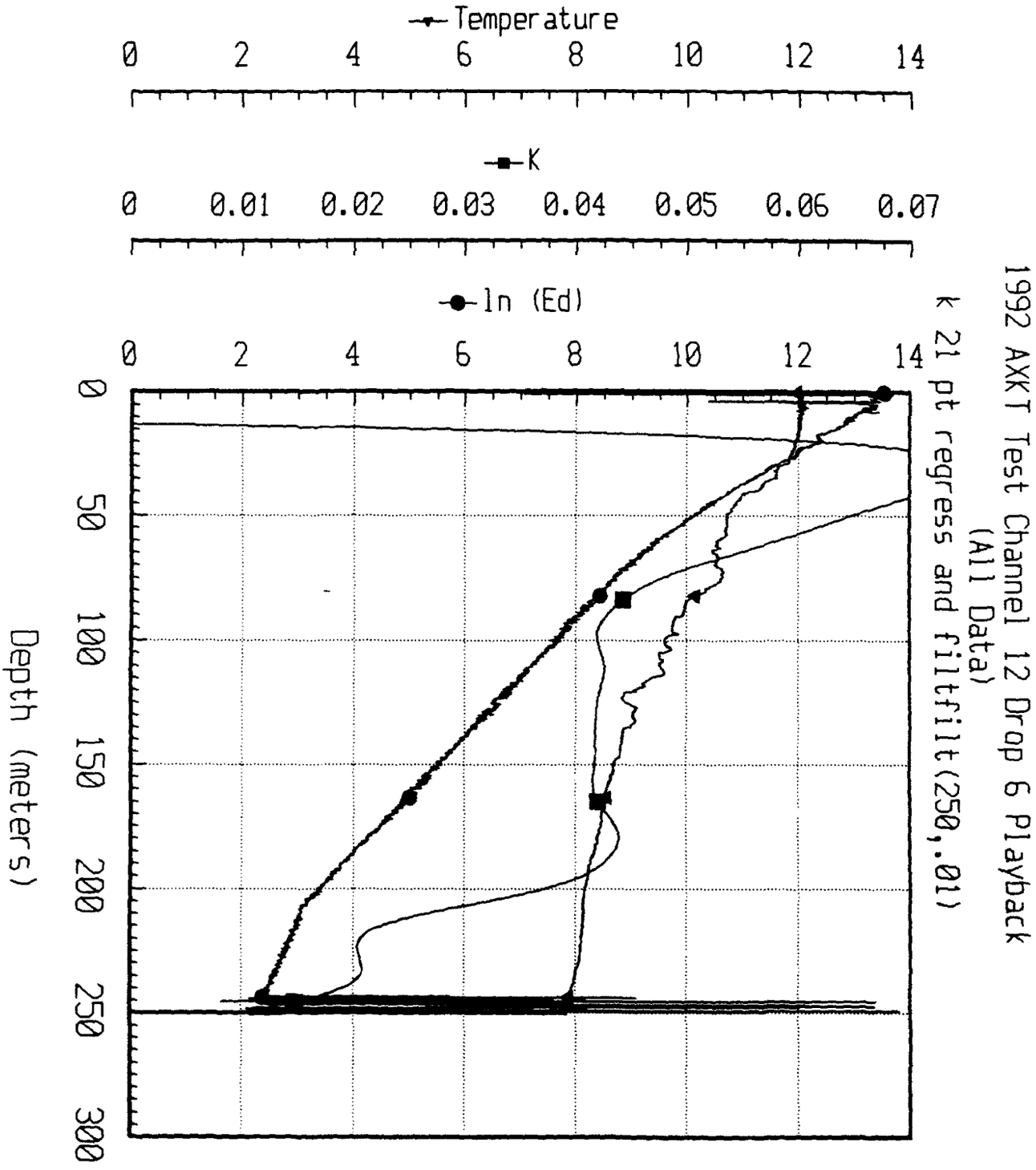
Temperature
0 2 4 6 8 10 12 14
K
0 0.01 0.02 0.03 0.04 0.05 0.06 0.07
ln (Ed)
0 2 4 6 8 10 12 14
0 50 100 150 200 250 300
Depth (meters)
1992 AXKT Test Channel 12 Drop 6 Playback
(All Data)
k 21 pt regress and filtfilt(250,.01)

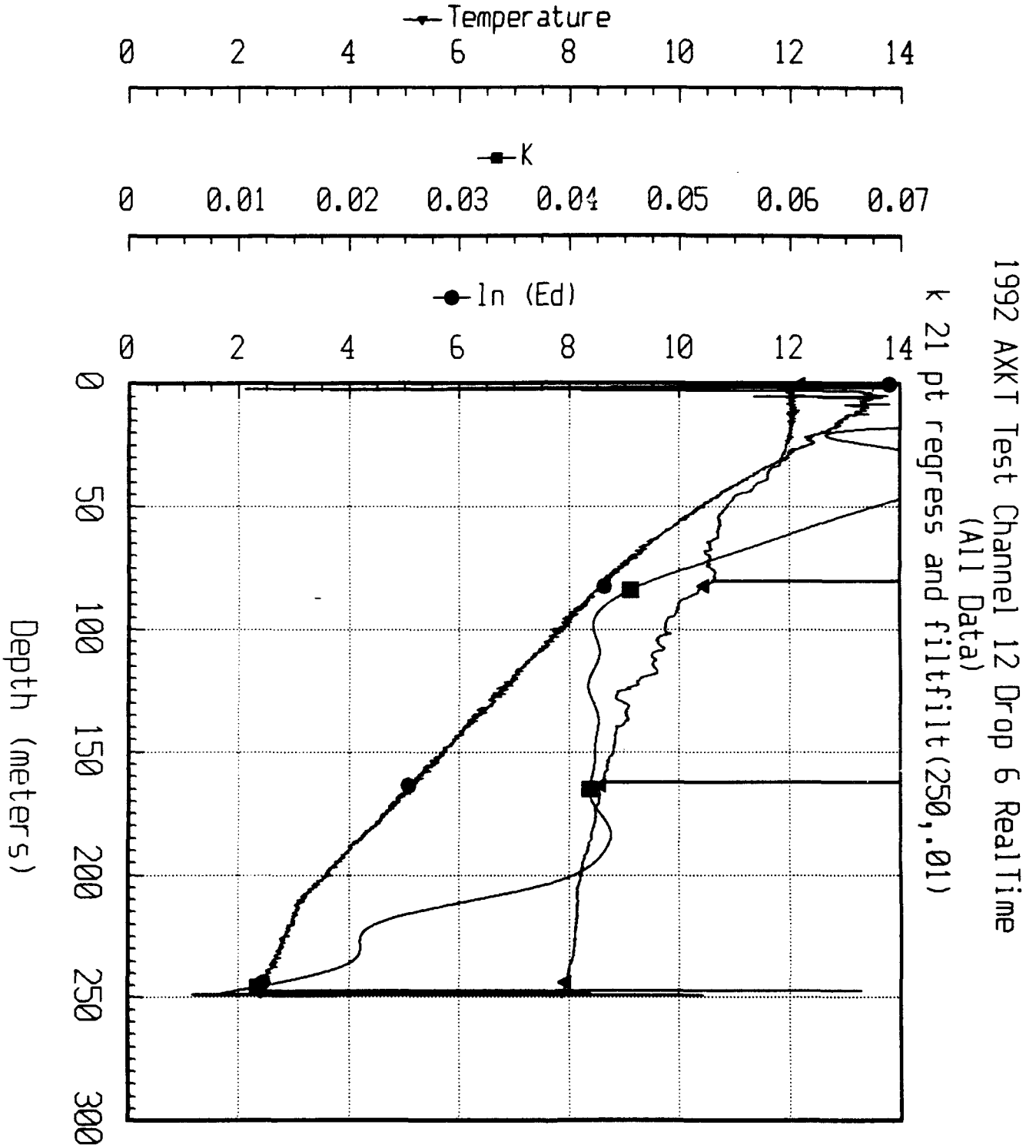
Temperature
0 2 4 6 8 10 12 14
K
0 0.01 0.02 0.03 0.04 0.05 0.06 0.07
ln (Ed)
0 2 4 6 8 10 12 14
0 50 100 150 200 250 300
Depth (meters)
1992 AXKT Test Channel 12 Drop 6 RealTime
(All Data)
k 21 pt regress and filtfilt(250,.01)

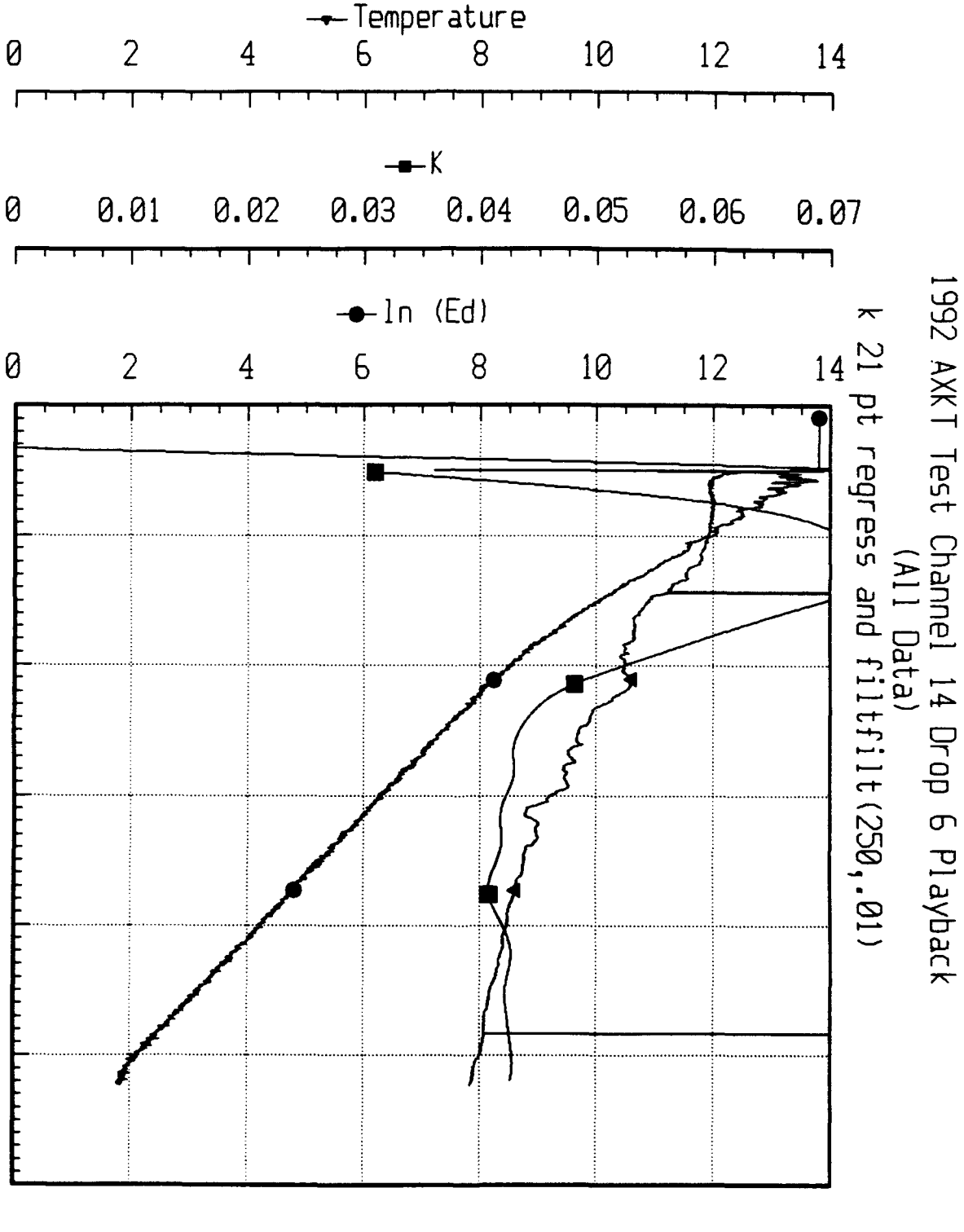
Temperature
0 2 4 6 8 10 12 14
K
0 0.01 0.02 0.03 0.04 0.05 0.06 0.07
ln (Ed)
0 2 4 6 8 10 12 14
0 50 100 150 200 250 300
Depth (meters)
1992 AXKT Test Channel 14 Drop 6 Playback
(All Data)
k 21 pt regress and filtfilt(250,.01)

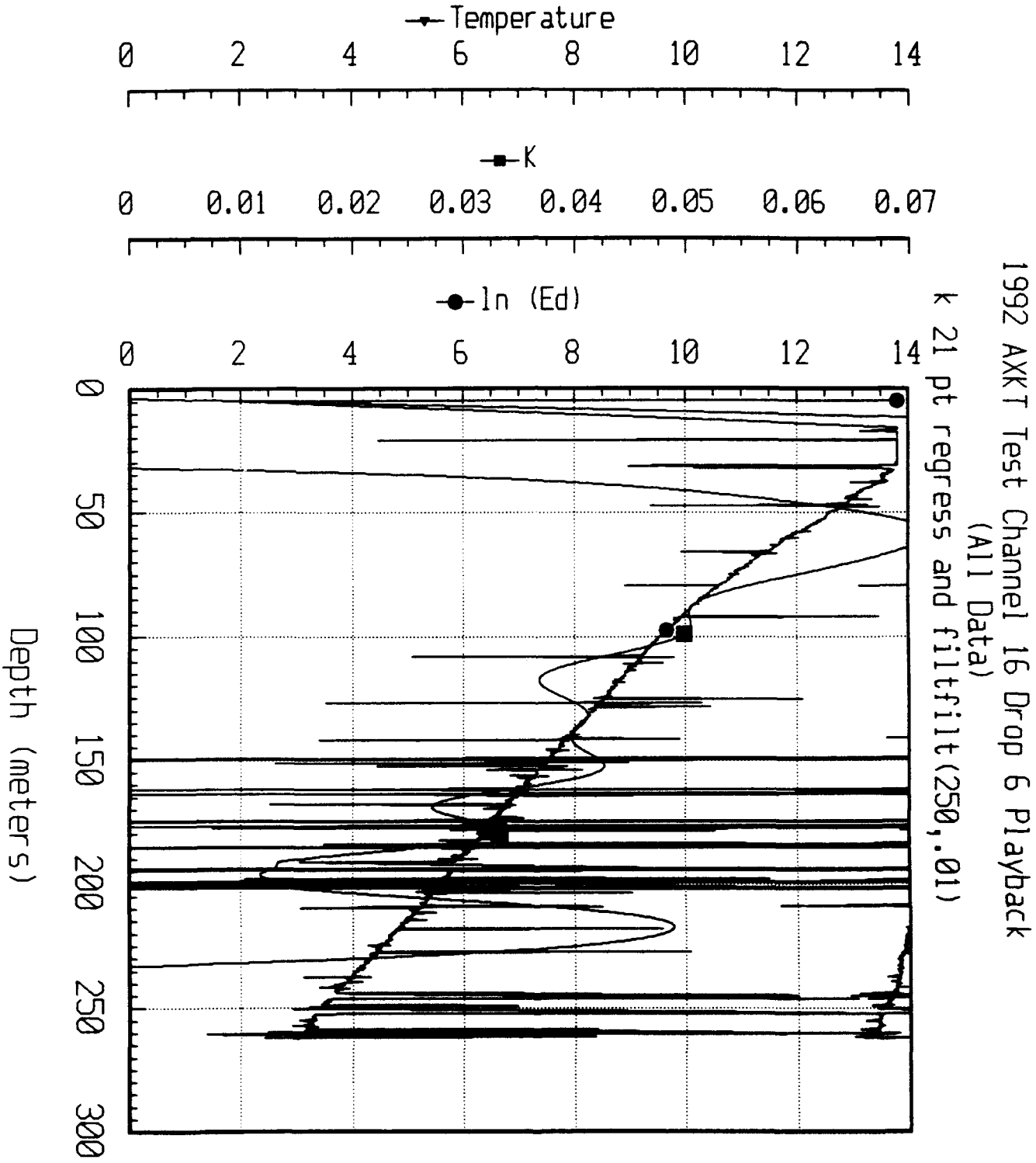
Temperature
0 2 4 6 8 10 12 14
K
0 0.01 0.02 0.03 0.04 0.05 0.06 0.07
ln (Ed)
0 2 4 6 8 10 12 14
0 50 100 150 200 250 300
Depth (meters)
1992 AXKT Test Channel 16 Drop 6 Playback
(All Data)
k 21 pt regress and filtfilt(250,.01)

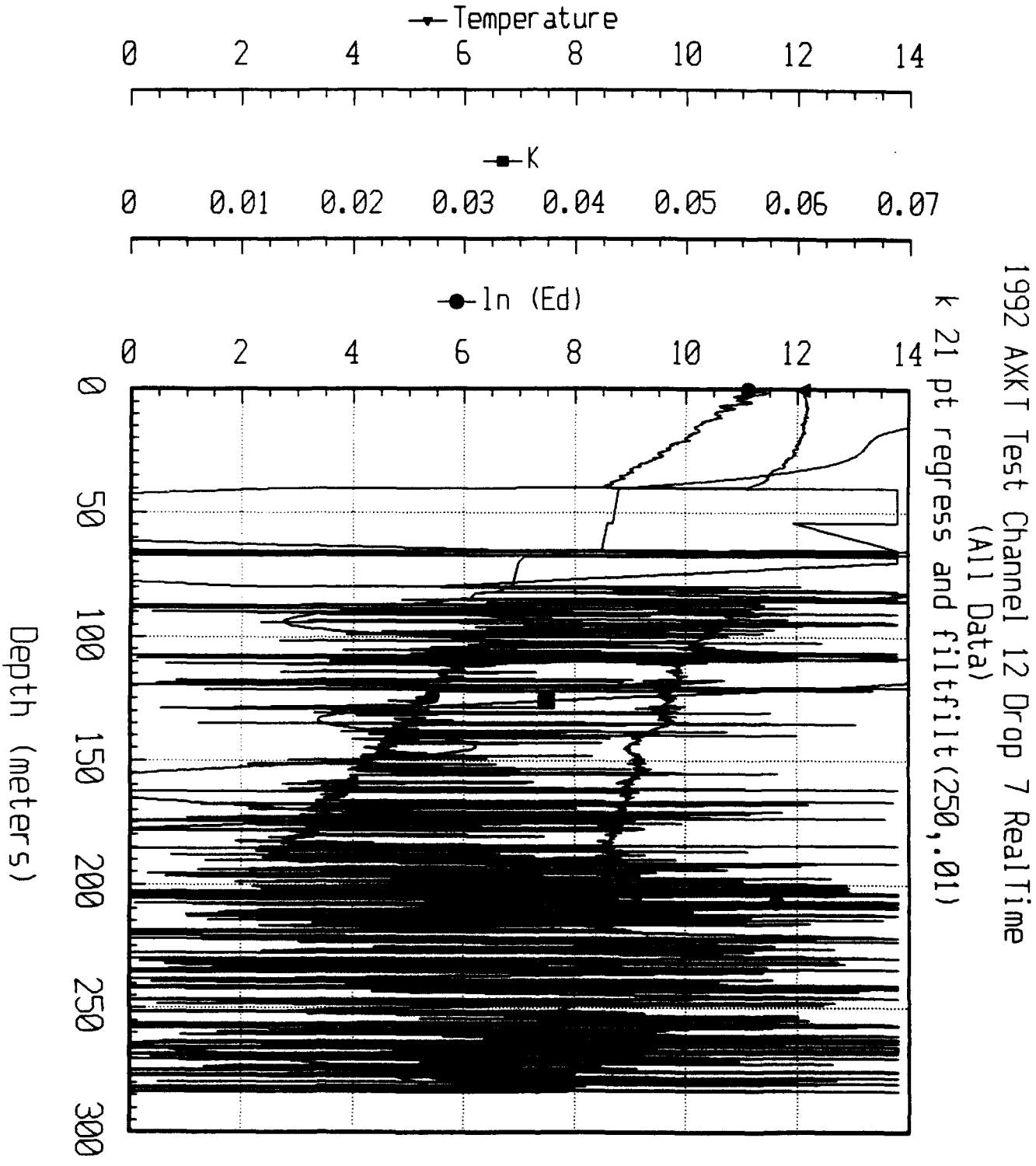
Temperature
0 2 4 6 8 10 12 14
K
0 0.01 0.02 0.03 0.04 0.05 0.06 0.07
ln (Ed)
0 2 4 6 8 10 12 14
0 50 100 150 200 250 300
Depth (meters)
1992 AXKT Test Channel 12 Drop 7 RealTime
(All Data)
k 21 pt regress and filtfilt(250,.01)

1992 AXKT Test Channel 12 Drop 7 Playback
(All Data)
k 21 pt regress and filtfilt(250,.01)
Depth (meters)
0
50
100
150
200
250
300
ln (Ed)
0
2
4
6
8
10
12
14
K
0
0.01
0.02
0.03
0.04
0.05
0.06
0.07
Temperature
0
2
4
6
8
10
12
14

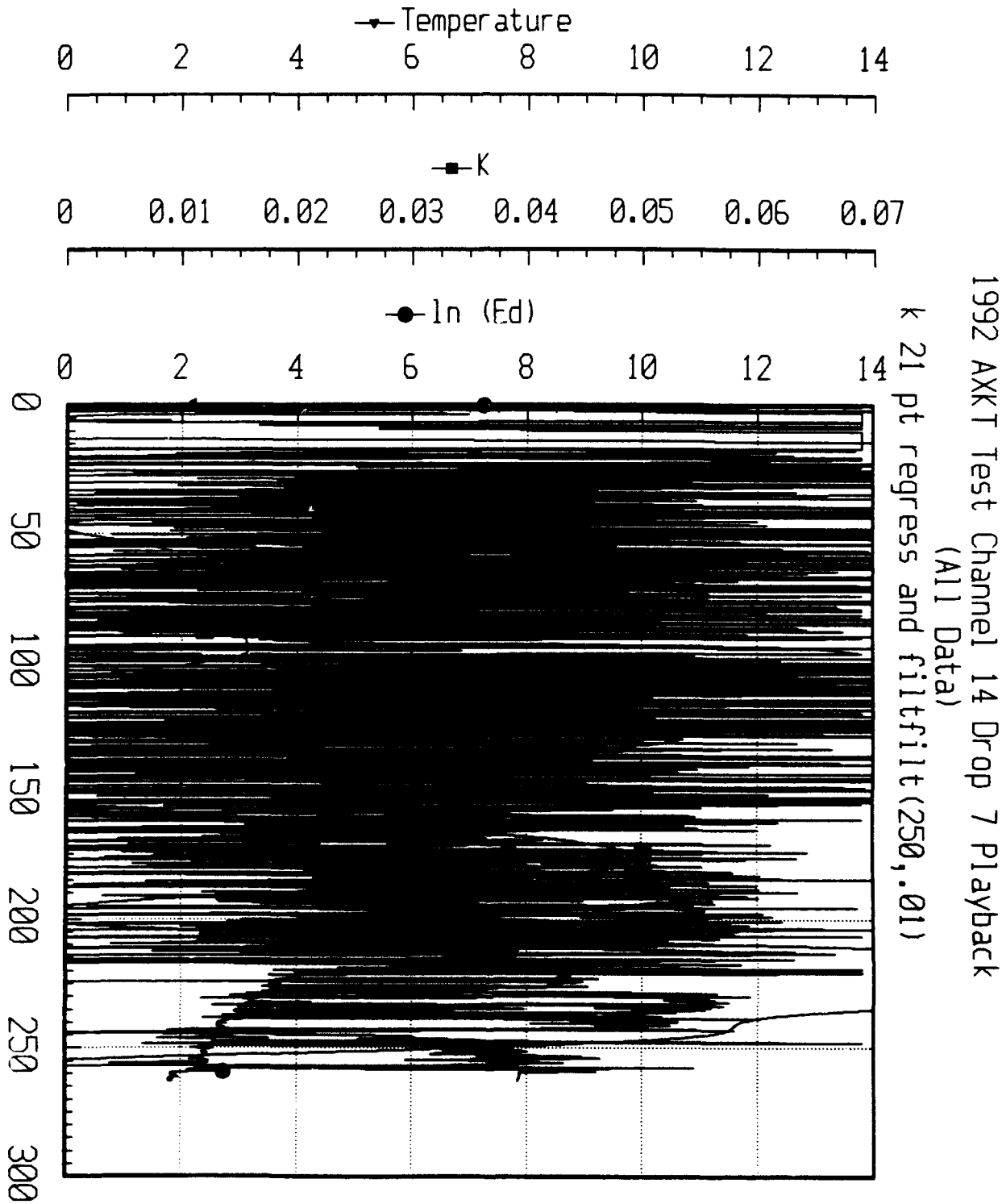
Temperature
0 2 4 6 8 10 12 14
K
0 0.01 0.02 0.03 0.04 0.05 0.06 0.07
ln (Ed)
0 2 4 6 8 10 12 14
0 50 100 150 200 250 300
Depth (meters)
1992 AXKT Test Channel 14 Drop 7 Playback
(All Data)
k 21 pt regress and filtfilt(250,.01)

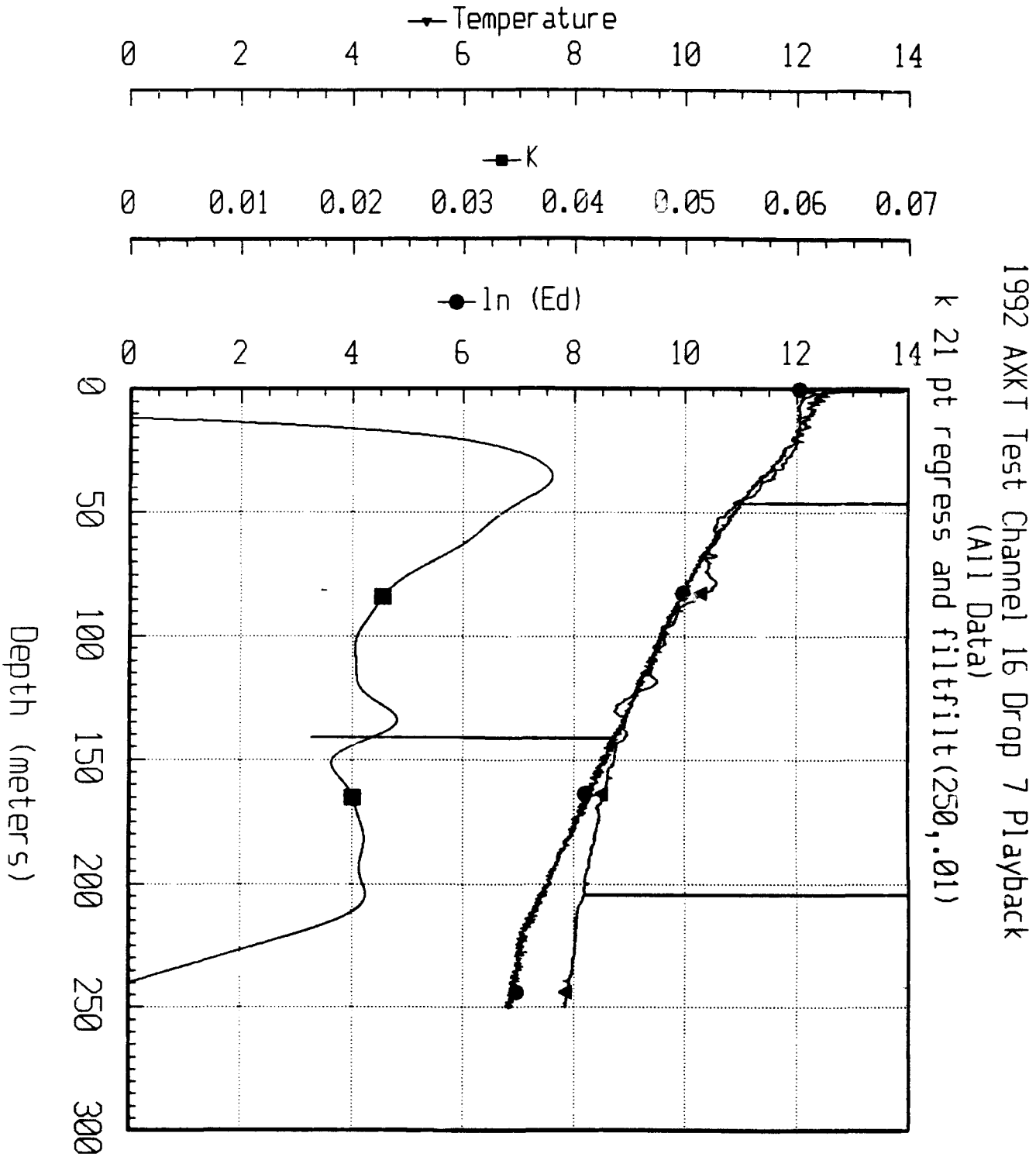
Temperature
0 2 4 6 8 10 12 14
K
0 0.01 0.02 0.03 0.04 0.05 0.06 0.07
ln (Ed)
0 2 4 6 8 10 12 14
0 50 100 150 200 250 300
Depth (meters)
1992 AXKT Test Channel 16 Drop 7 Playback
(All Data)
k 21 pt regress and filtfilt(250,.01)

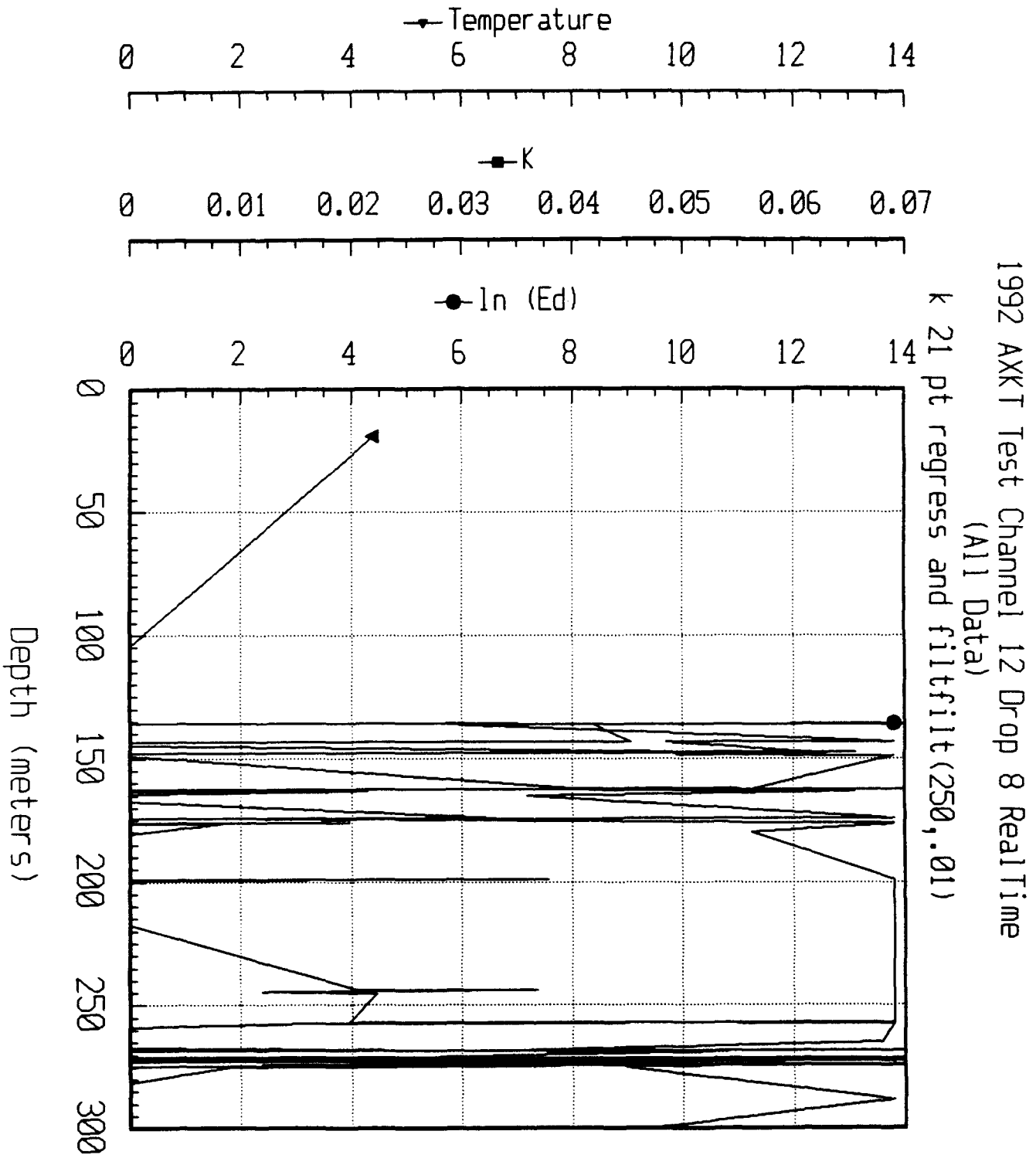
Temperature
0 2 4 6 8 10 12 14
K
0 0.01 0.02 0.03 0.04 0.05 0.06 0.07
ln (Ed)
0 2 4 6 8 10 12 14
0 50 100 150 200 250 300
Depth (meters)
1992 AXKT Test Channel 12 Drop 8 RealTime
(All Data)
k 21 pt regress and filtfilt(250,.01)

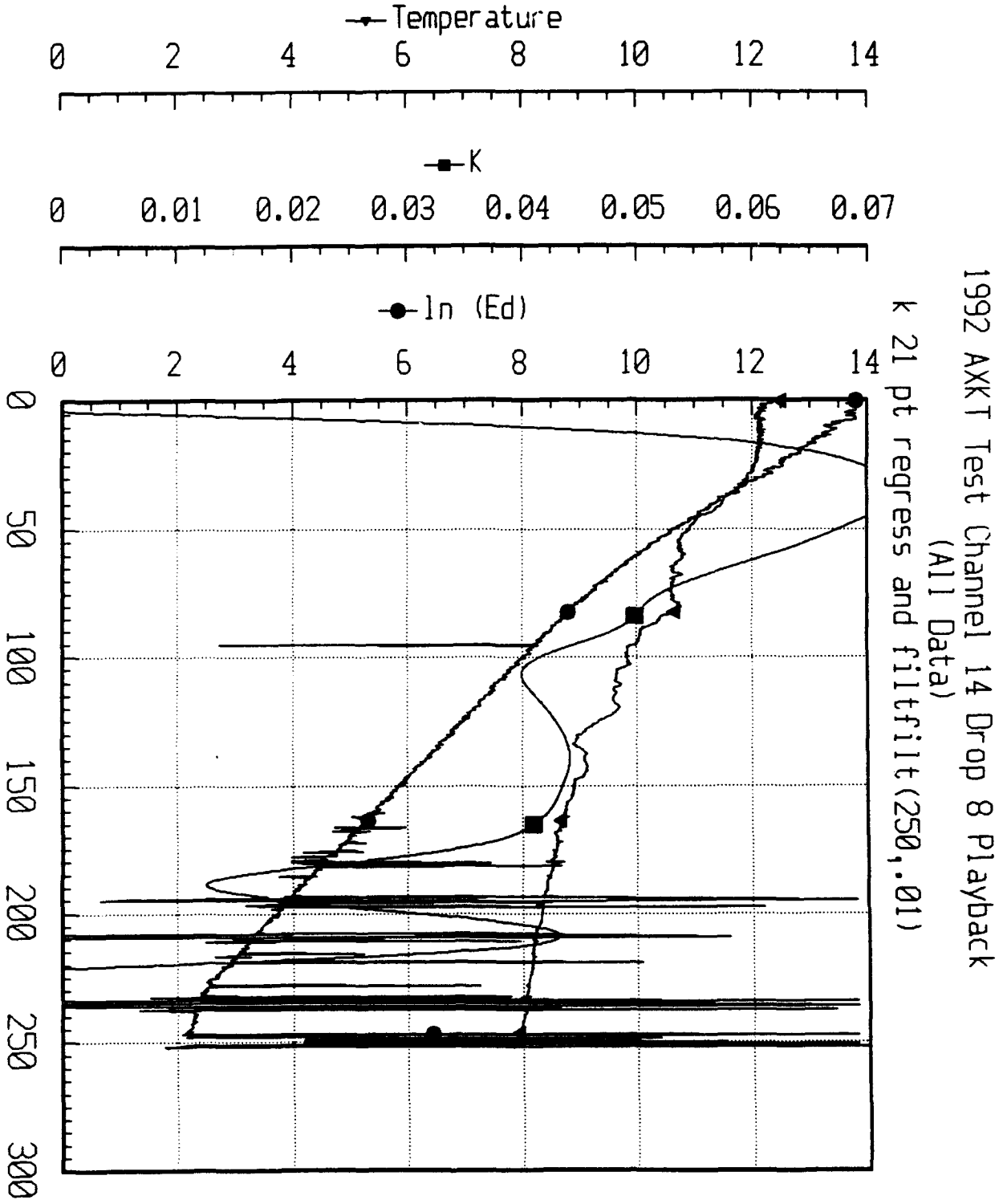
Temperature
0 2 4 6 8 10 12 14
K
0 0.01 0.02 0.03 0.04 0.05 0.06 0.07
ln (Ed)
0 2 4 6 8 10 12 14
0 50 100 150 200 250 300
Depth (meter
1992 AXKT Test Channel 14 Drop 8 Playback
(All Data)
k 21 pt regress and filtfilt(250,.01)

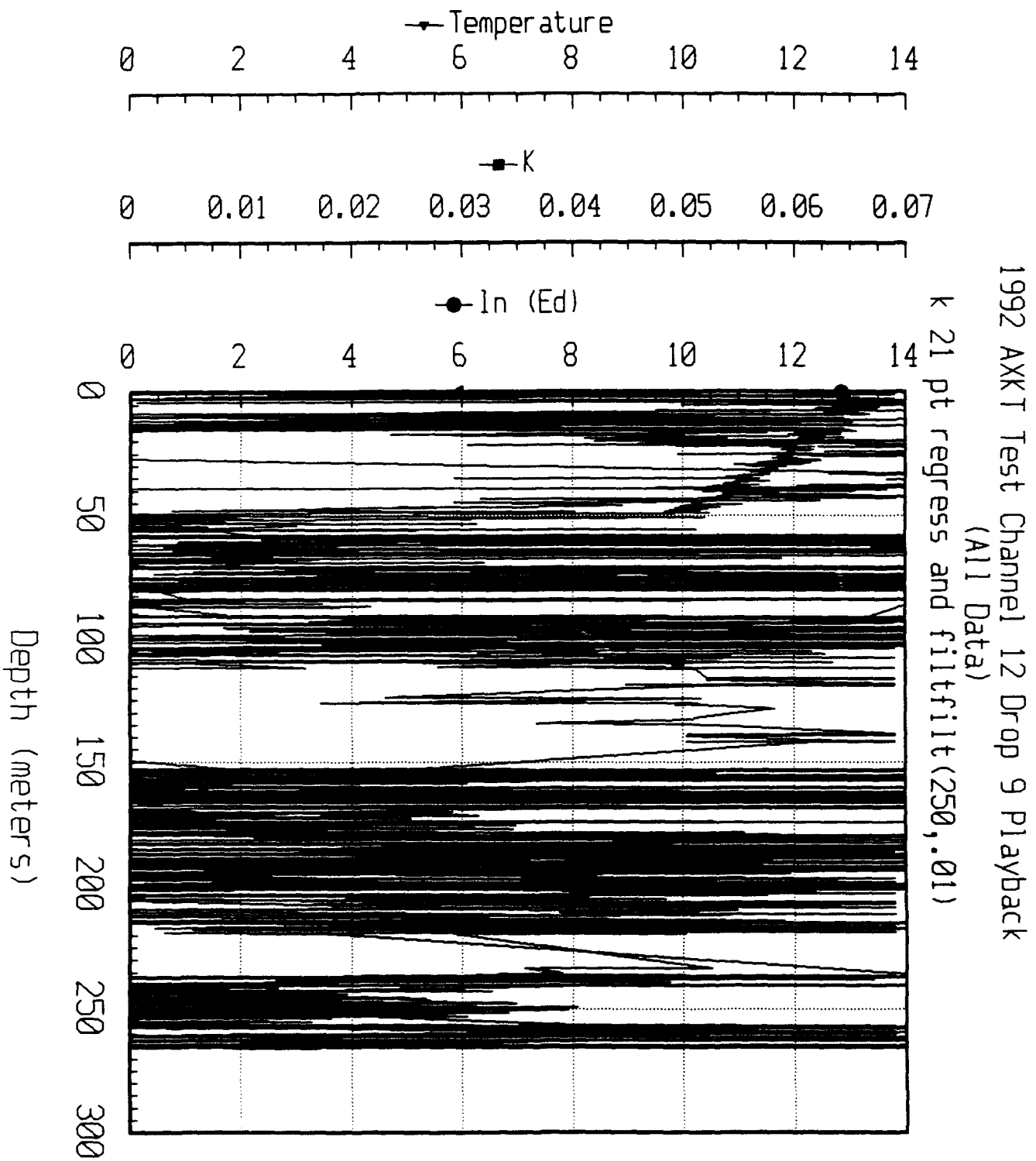
Temperature
0 2 4 6 8 10 12 14
K
0 0.01 0.02 0.03 0.04 0.05 0.06 0.07
ln (Ed)
0 2 4 6 8 10 12 14
0 50 100 150 200 250 300
Depth (meters)
1992 AXKT Test Channel 12 Drop 9 Playback
(All Data)
k 21 pt regress and filtfilt(250,.01)

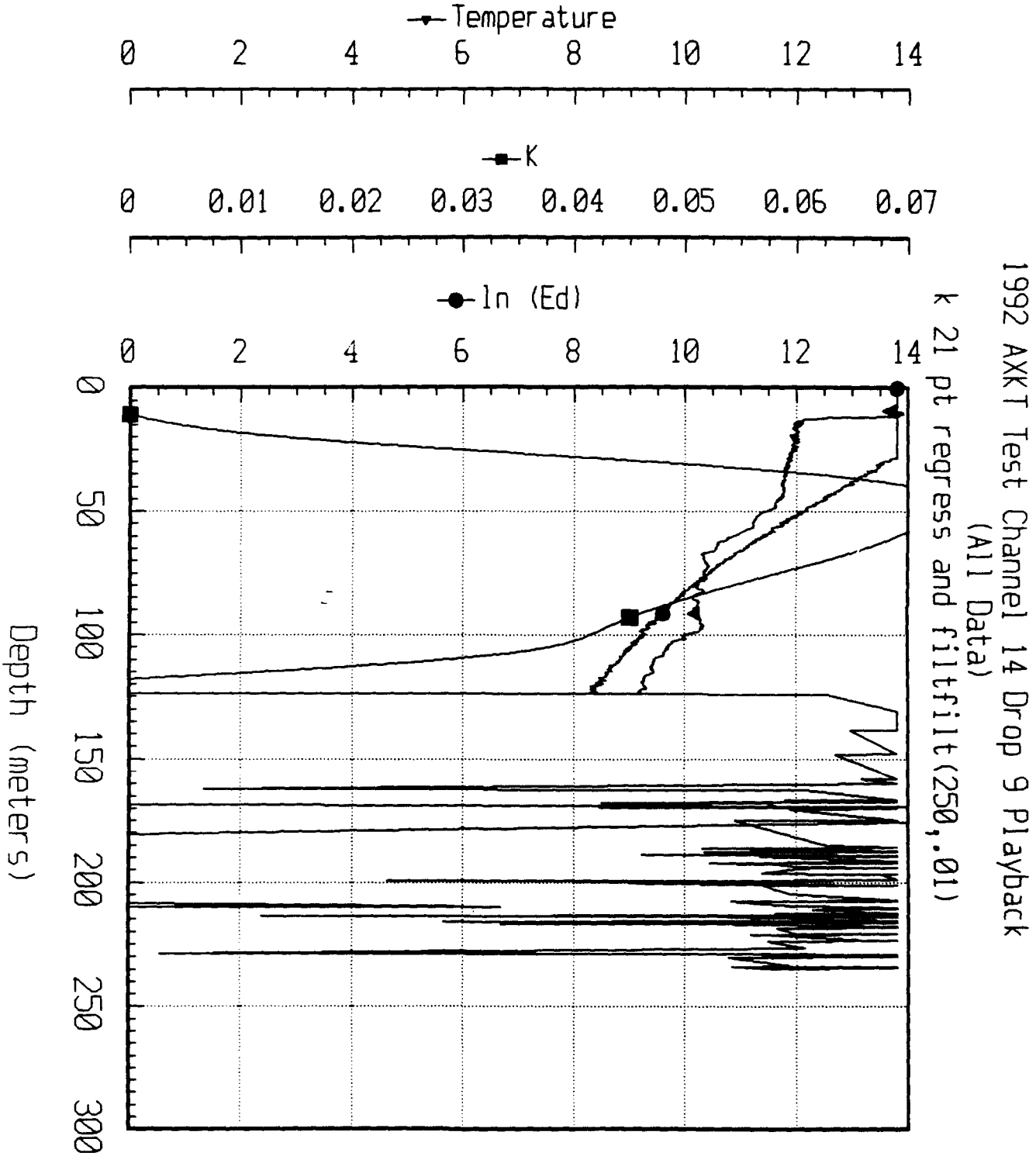
Temperature
0 2 4 6 8 10 12 14
K
0 0.01 0.02 0.03 0.04 0.05 0.06 0.07
ln (Ed)
0 2 4 6 8 10 12 14
0 50 100 150 200 250 300
Depth (meters)
1992 AXKT Test Channel 14 Drop 9 Playback
(All Data)
k 21 pt regress and filtfilt(250,.01)

Appendix B

Comparison of MER and AXKT K_d Profiles for Vestfjord Test

1990 Vestfjord AXKT Test
MER Mean Data (+/- s.d.)

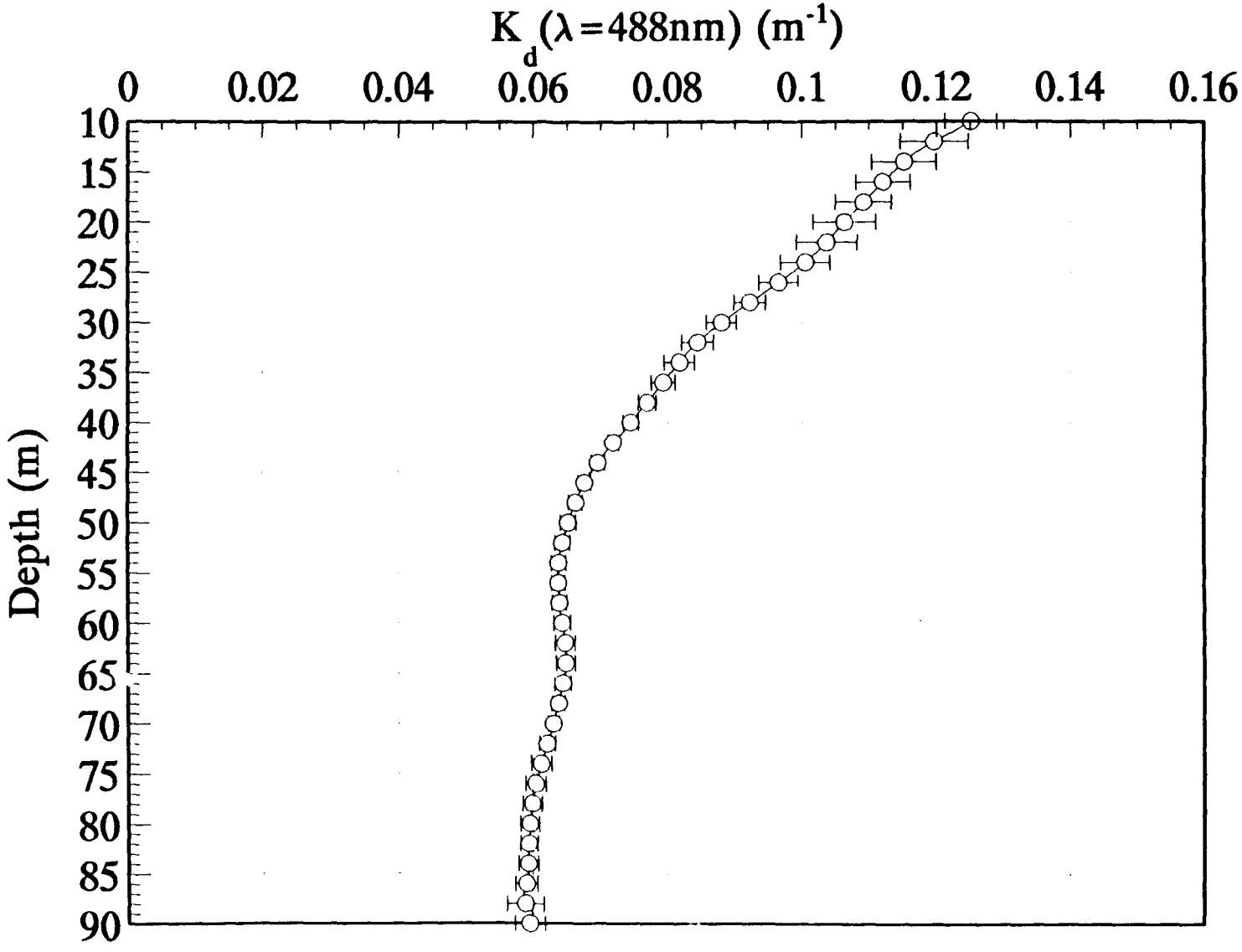

1990 Vestfjord AXKT Test
AXKT Channel 12 Drop 1

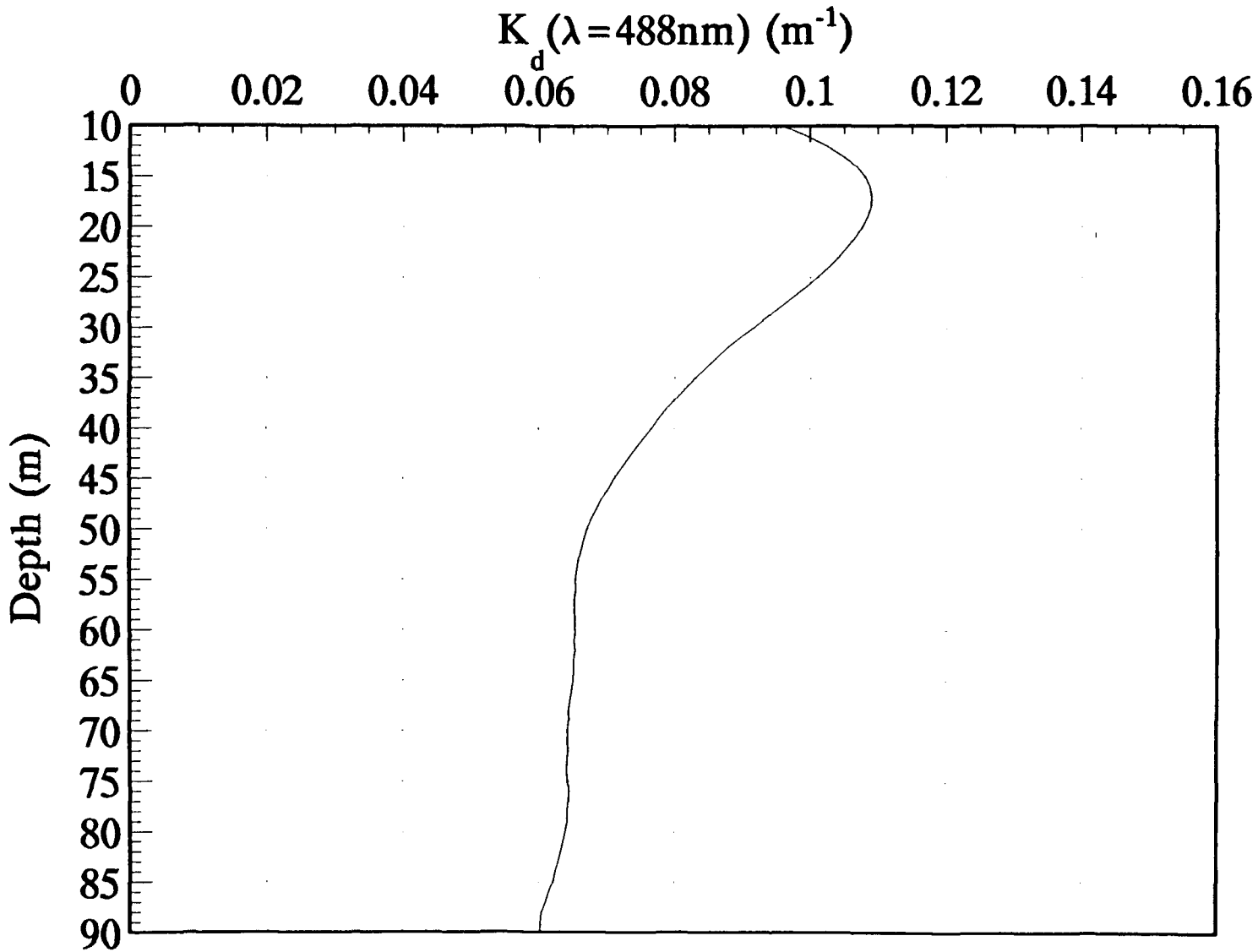

1990 Vestfjord AXKT Test
AXKT Channel 12 Drop 1 (% Difference From MER Data)

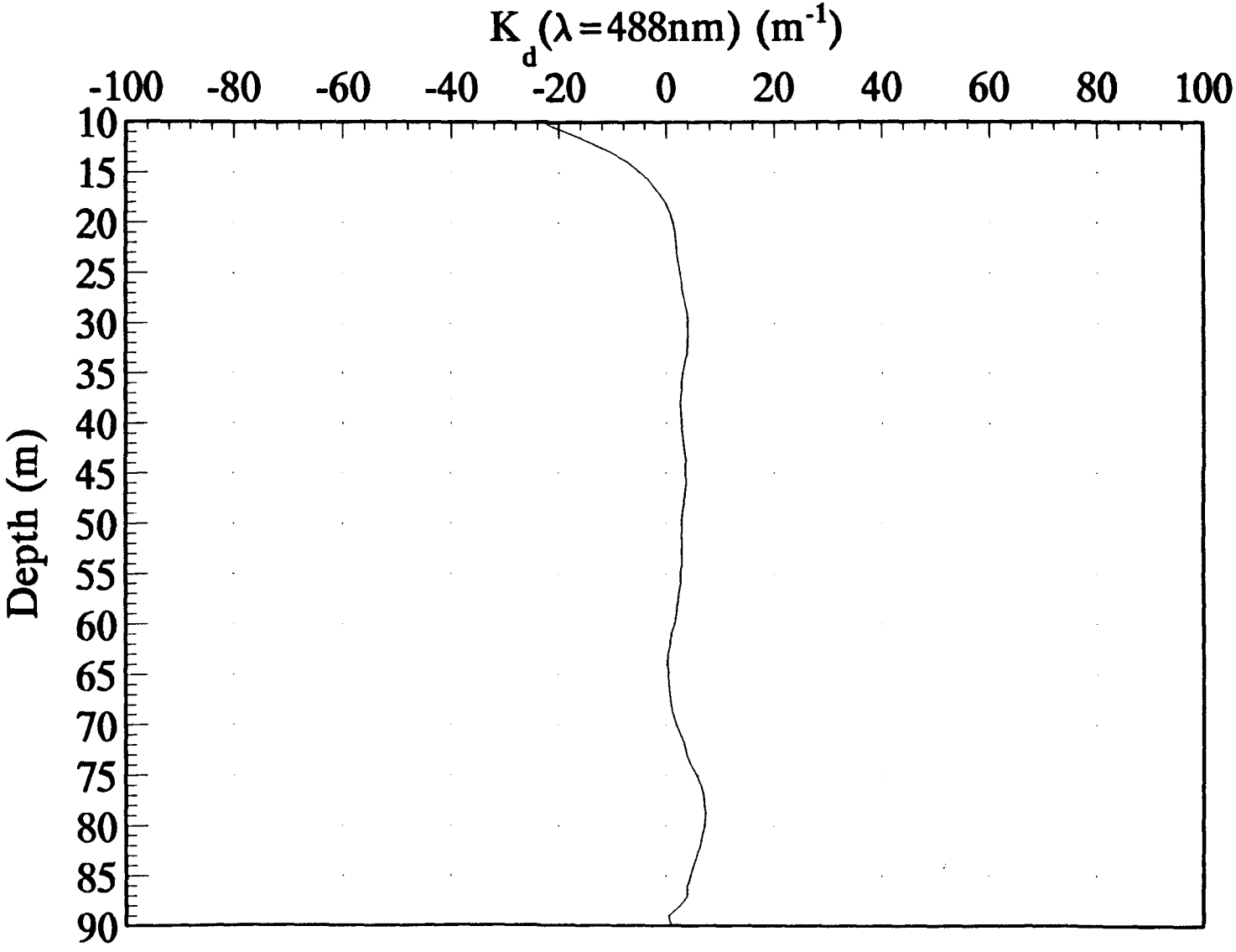

1990 Vestfjord AXKT Test
AXKT Channel 12 Drop 2

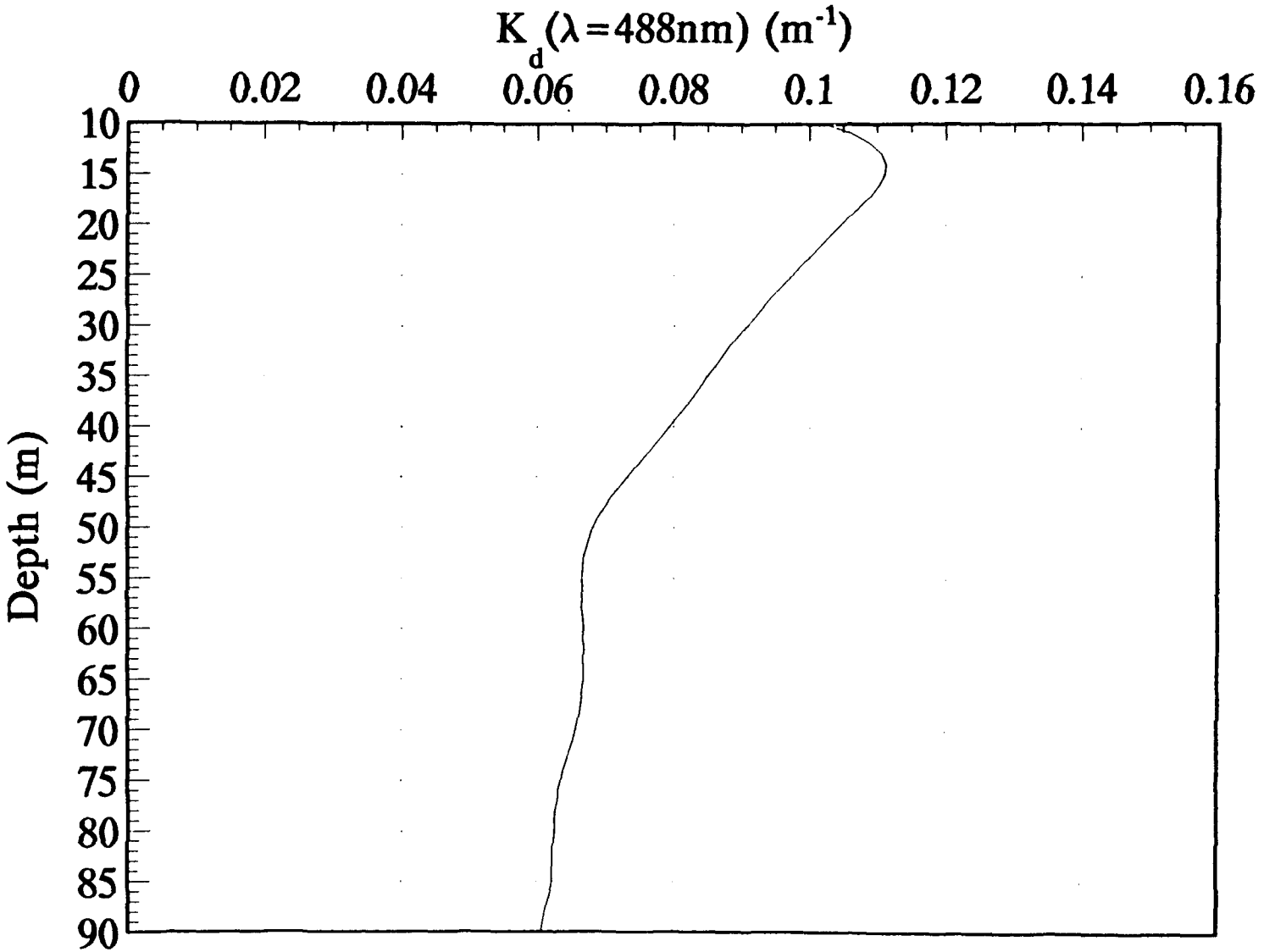

1990 Vestfjord AXKT Test
AXKT Channel 12 Drop 2 (% Difference From MER Data)

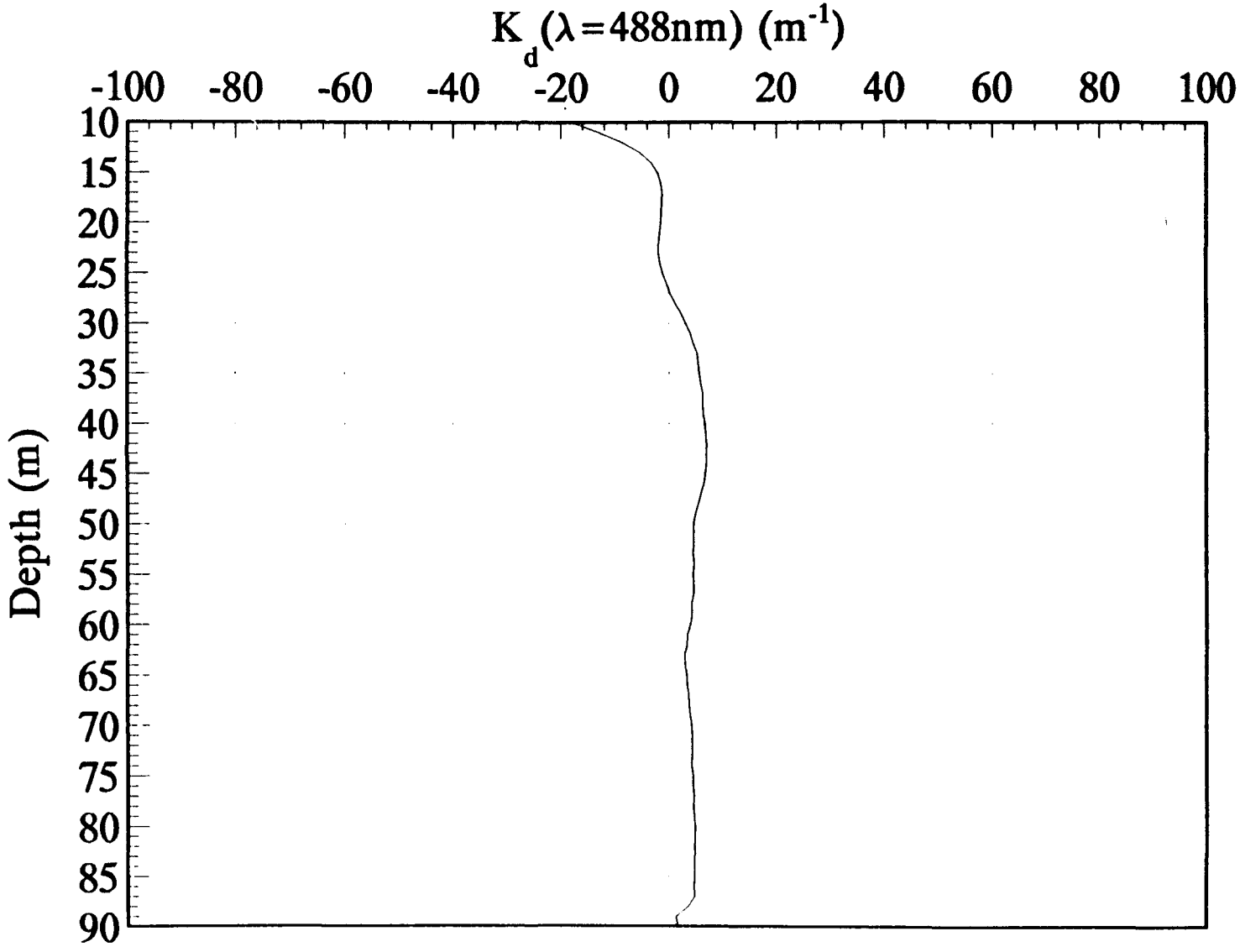

1990 Vestfjord AXKT Test
AXKT Channel 12 Drop 3

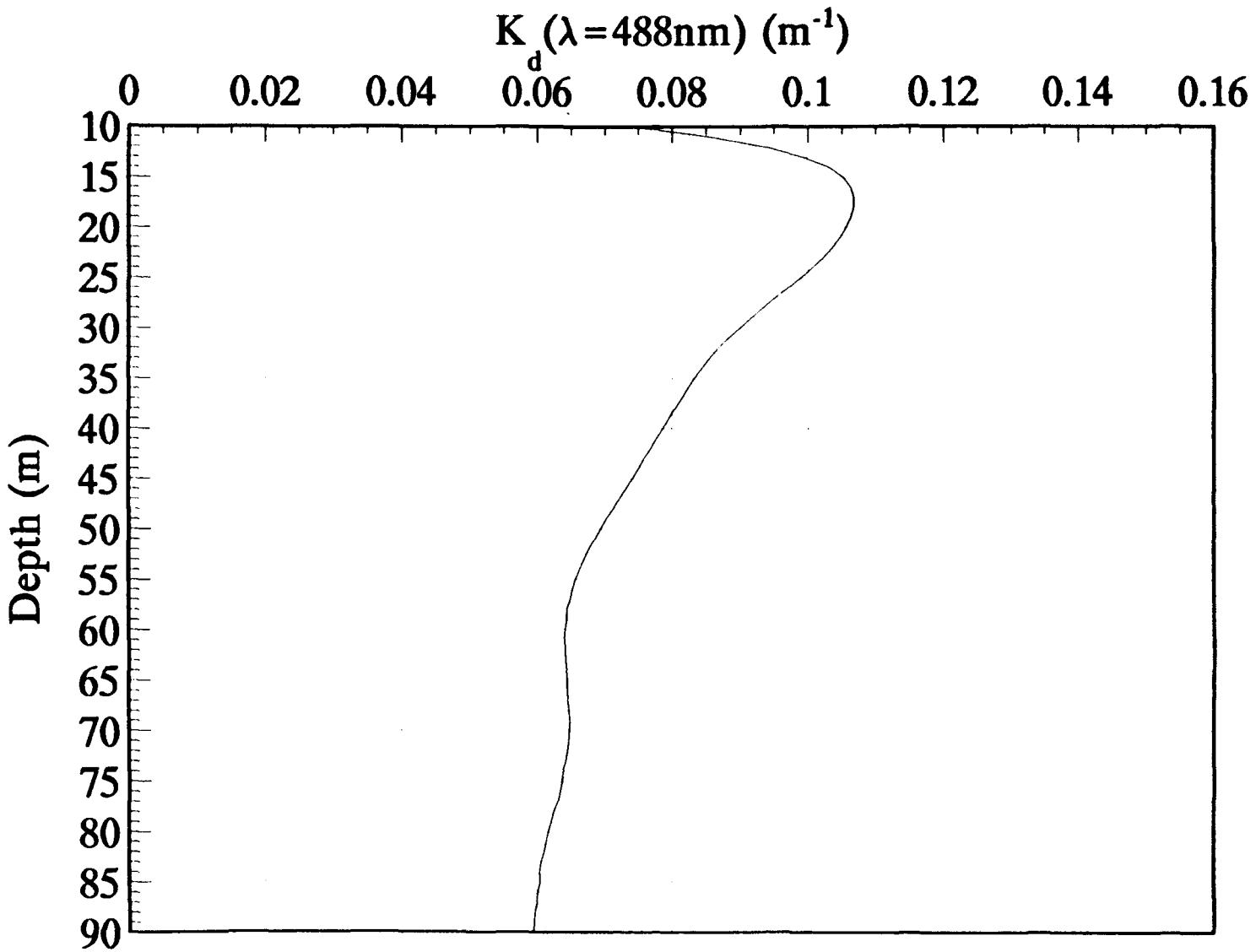

ta)

100

1990 Vestfjord AXKT Test
AXKT Channel 12 Drop 3 (% Difference From MER Data)

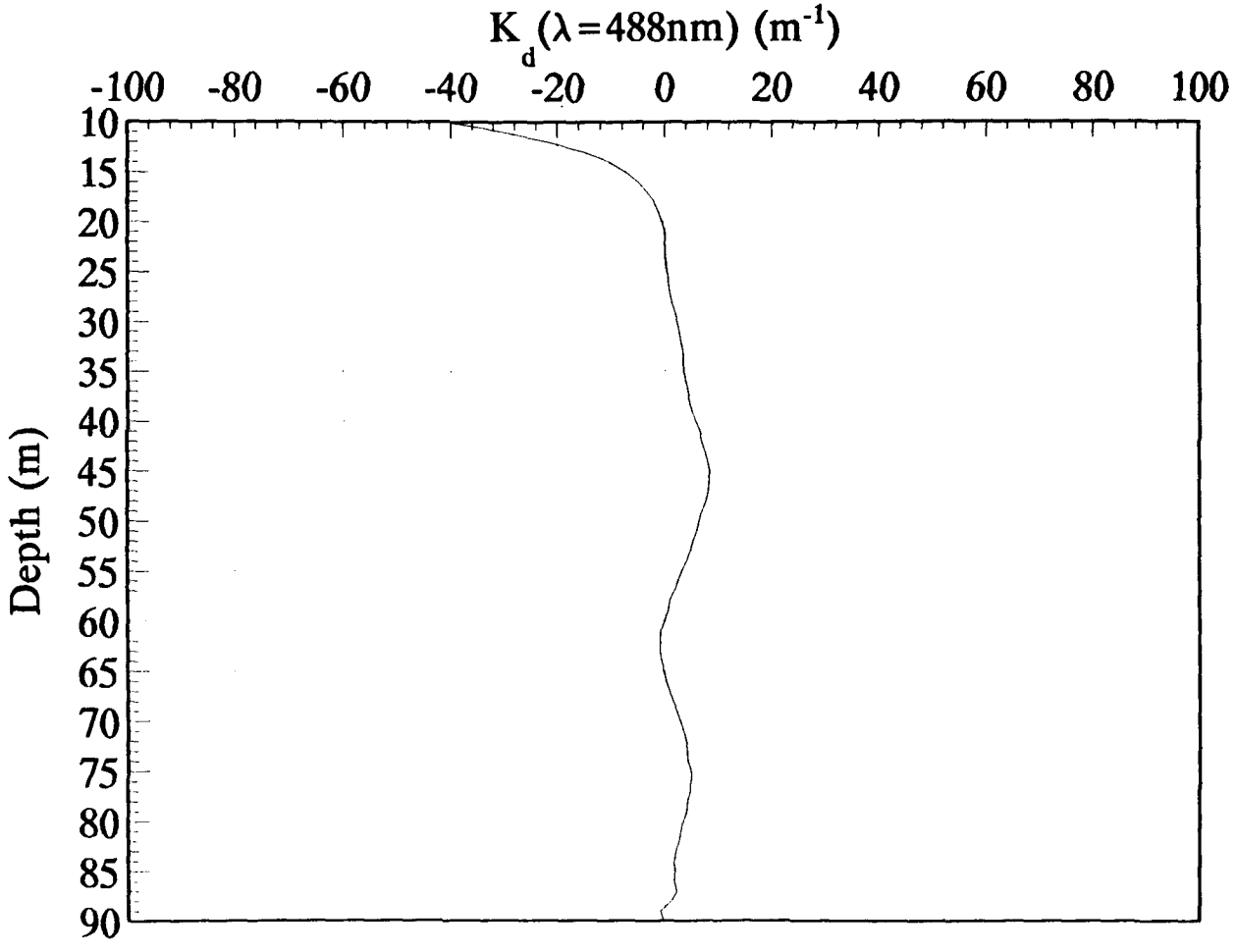

1990 Vestfjord AXKT Test
AXKT Channel 12 Drop 4

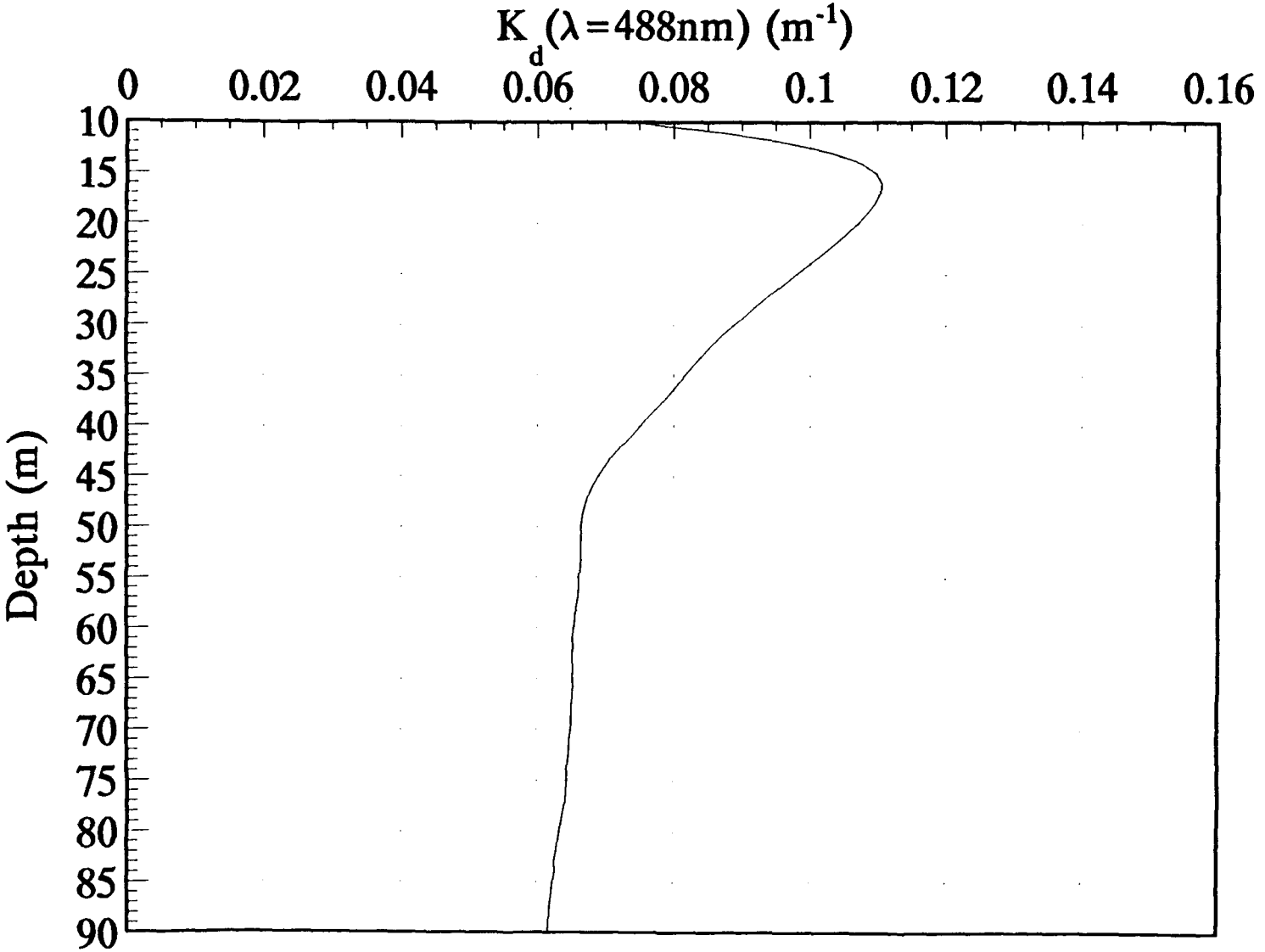

1990 Vestfjord AXKT Test
AXKT Channel 12 Drop 4 (% Difference From MER Data)

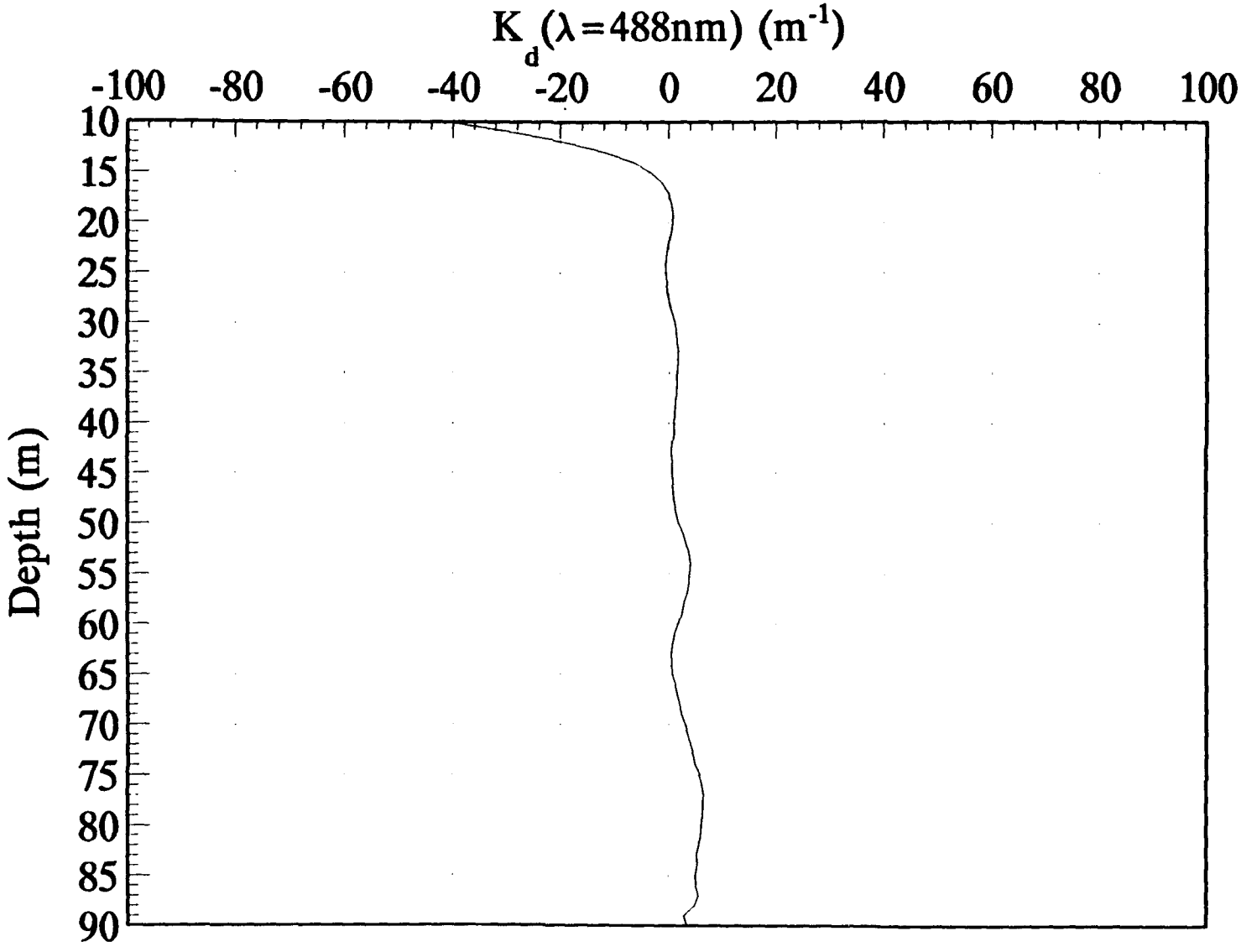

1990 Vestfjord AXKT Test
AXKT Channel 14 Drop 1

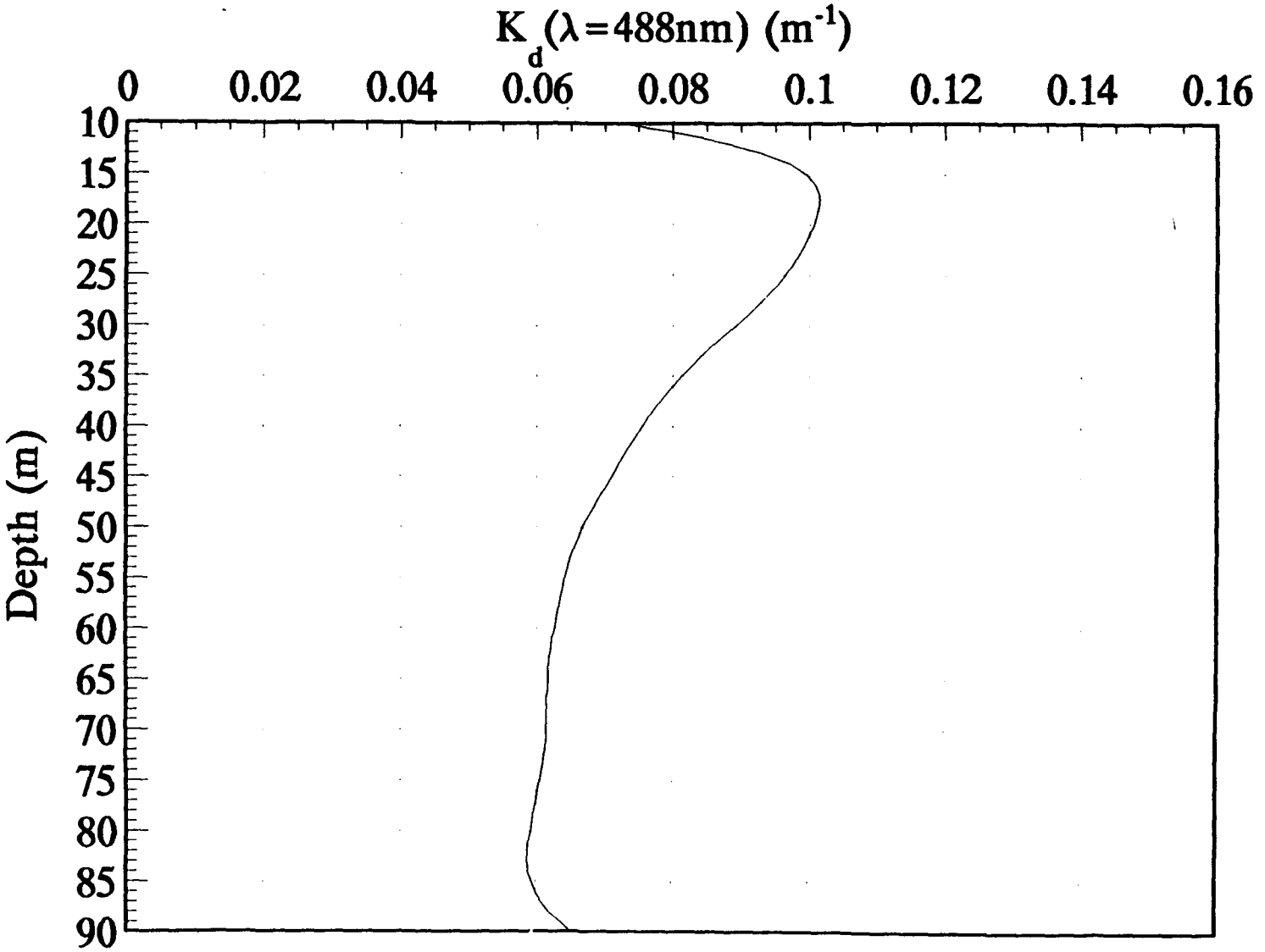

1990 Vestfjord AXKT Test
AXKT Channel 14 Drop 1 (% Difference From MER Data)

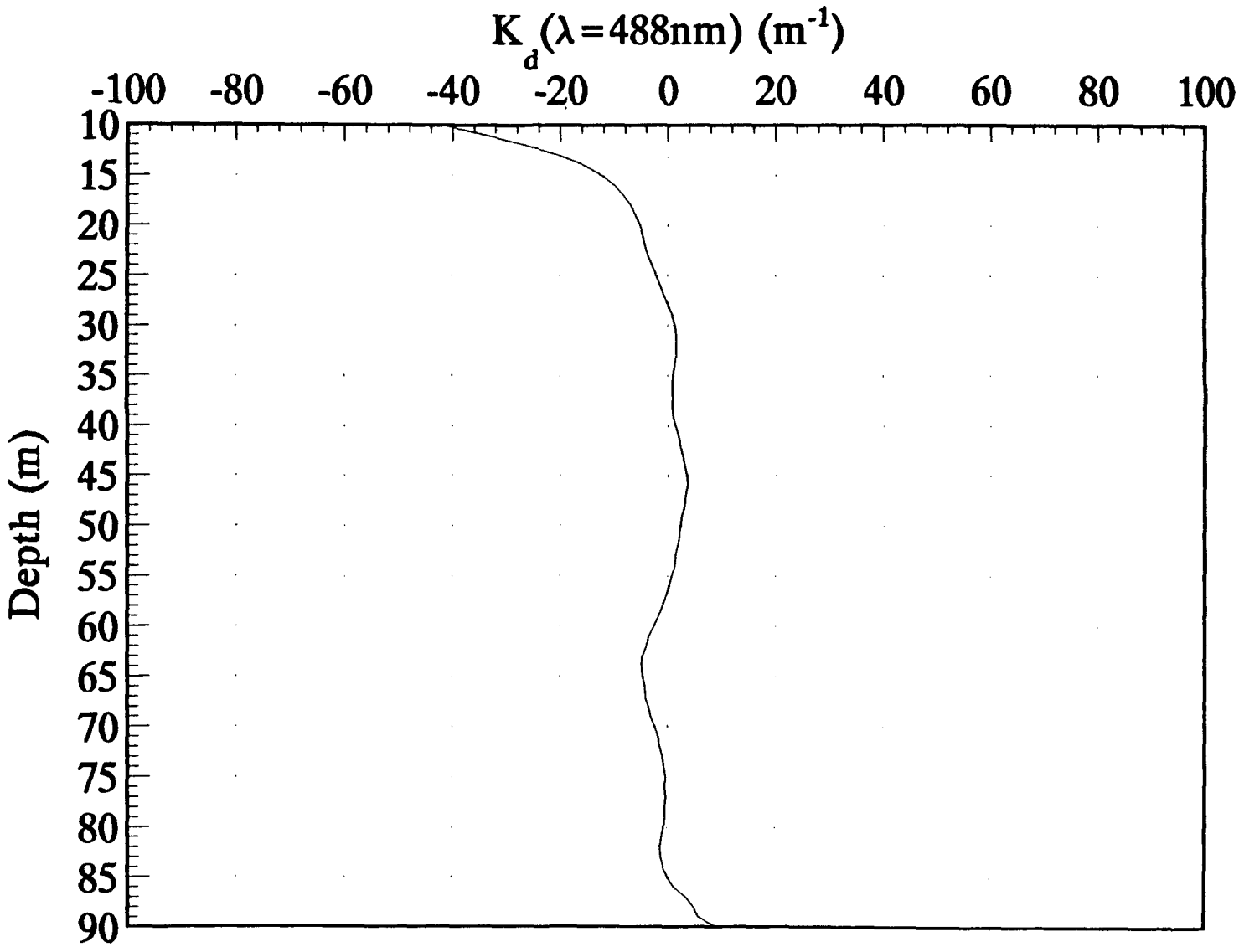

1990 Vestfjord AXKT Test
AXKT Channel 14 Drop 2

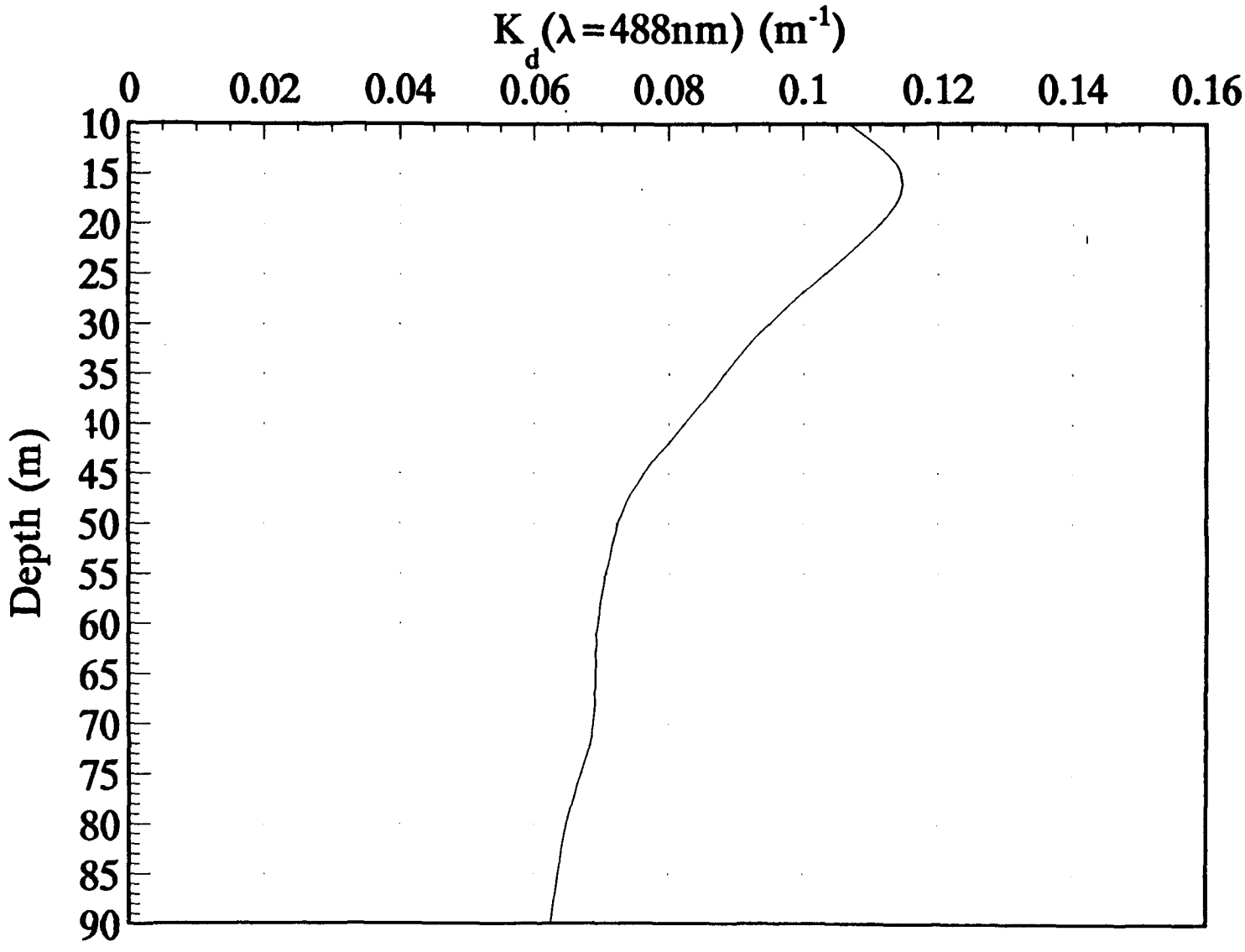

1990 Vestfjord AXKT Test
AXKT Channel 14 Drop 2 (% Difference From MER Data)

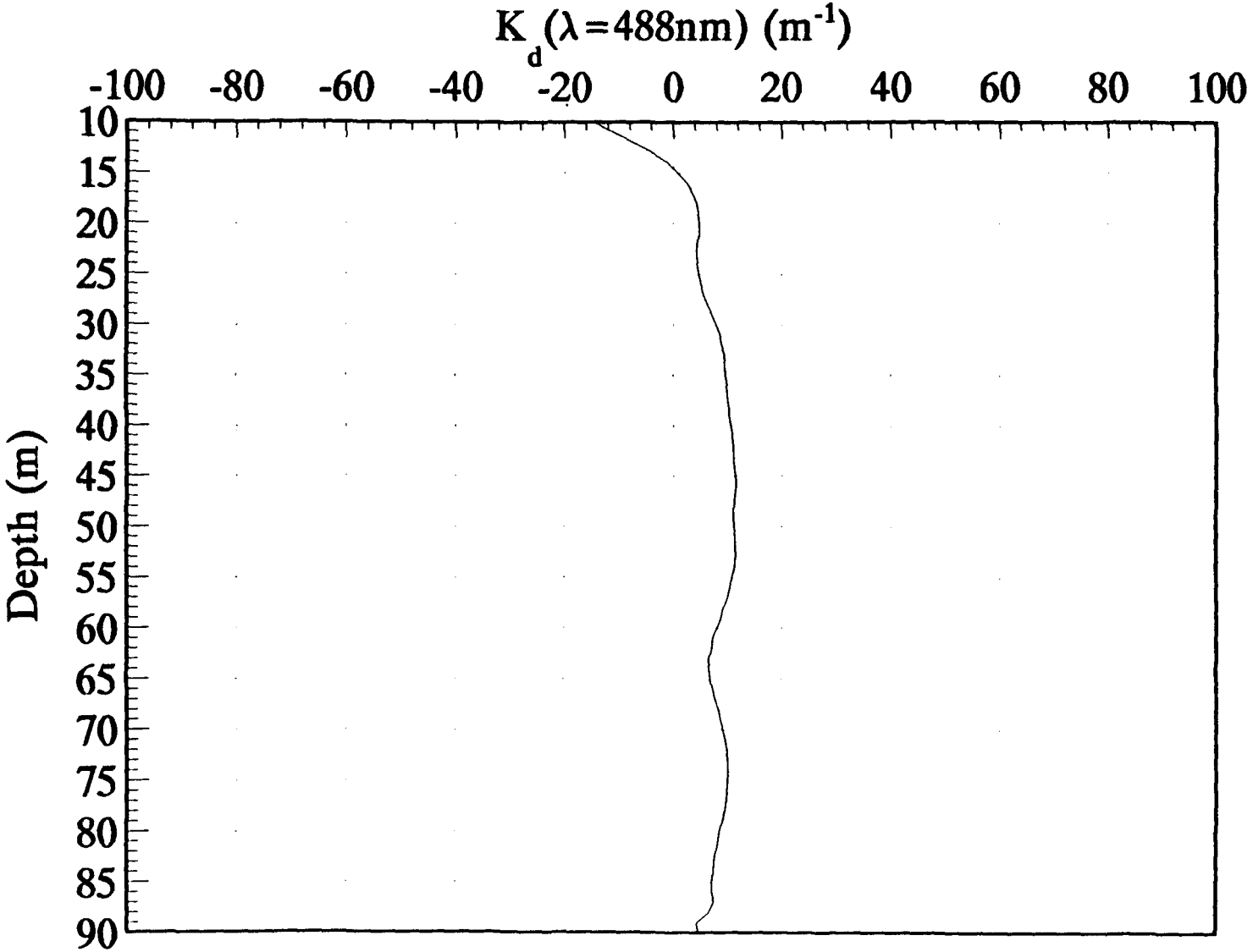

1990 Vestfjord AXKT Test
AXKT Channel 14 Drop 3

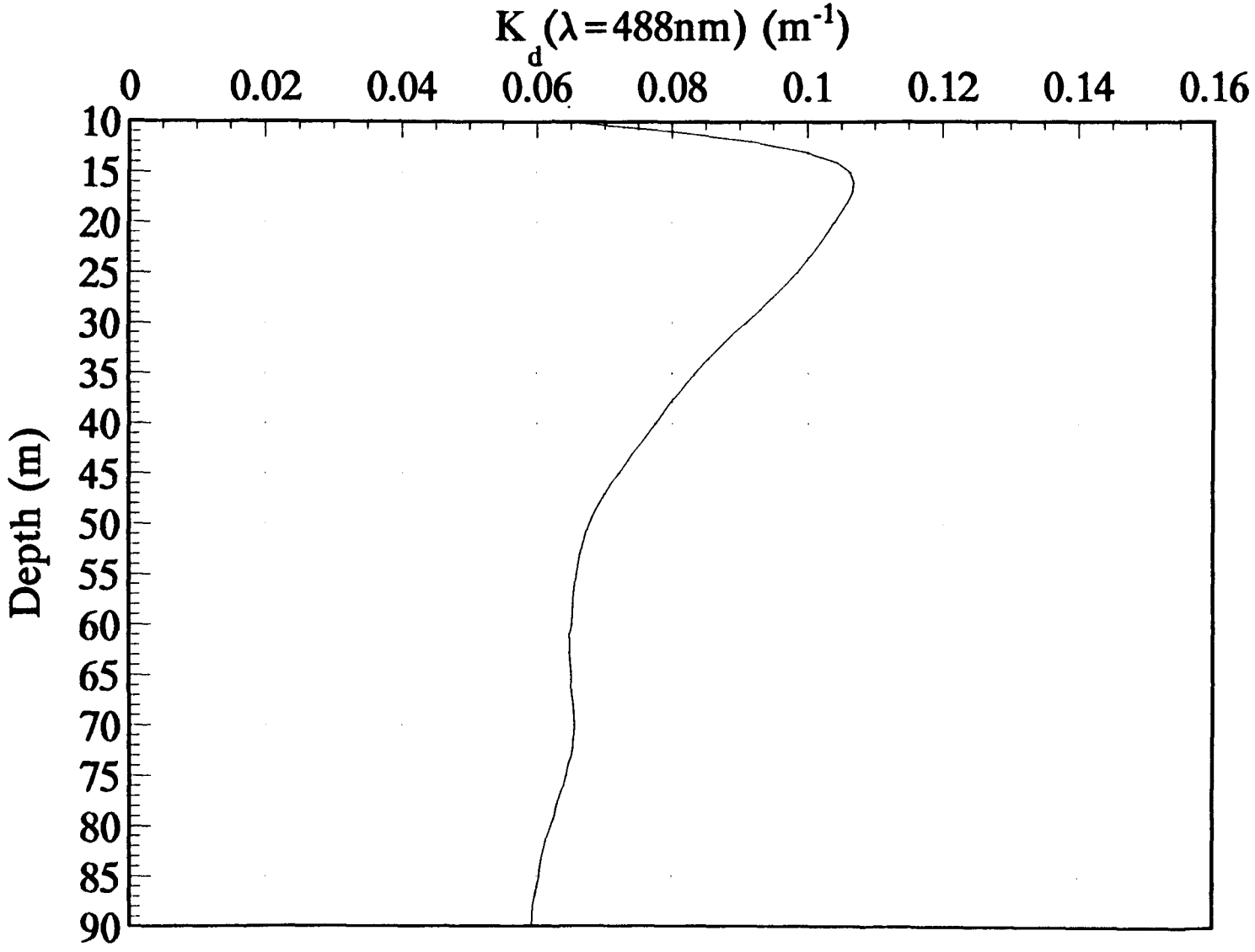

1990 Vestfjord AXKT Test
AXKT Channel 14 Drop 3 (% Difference From MER Data)

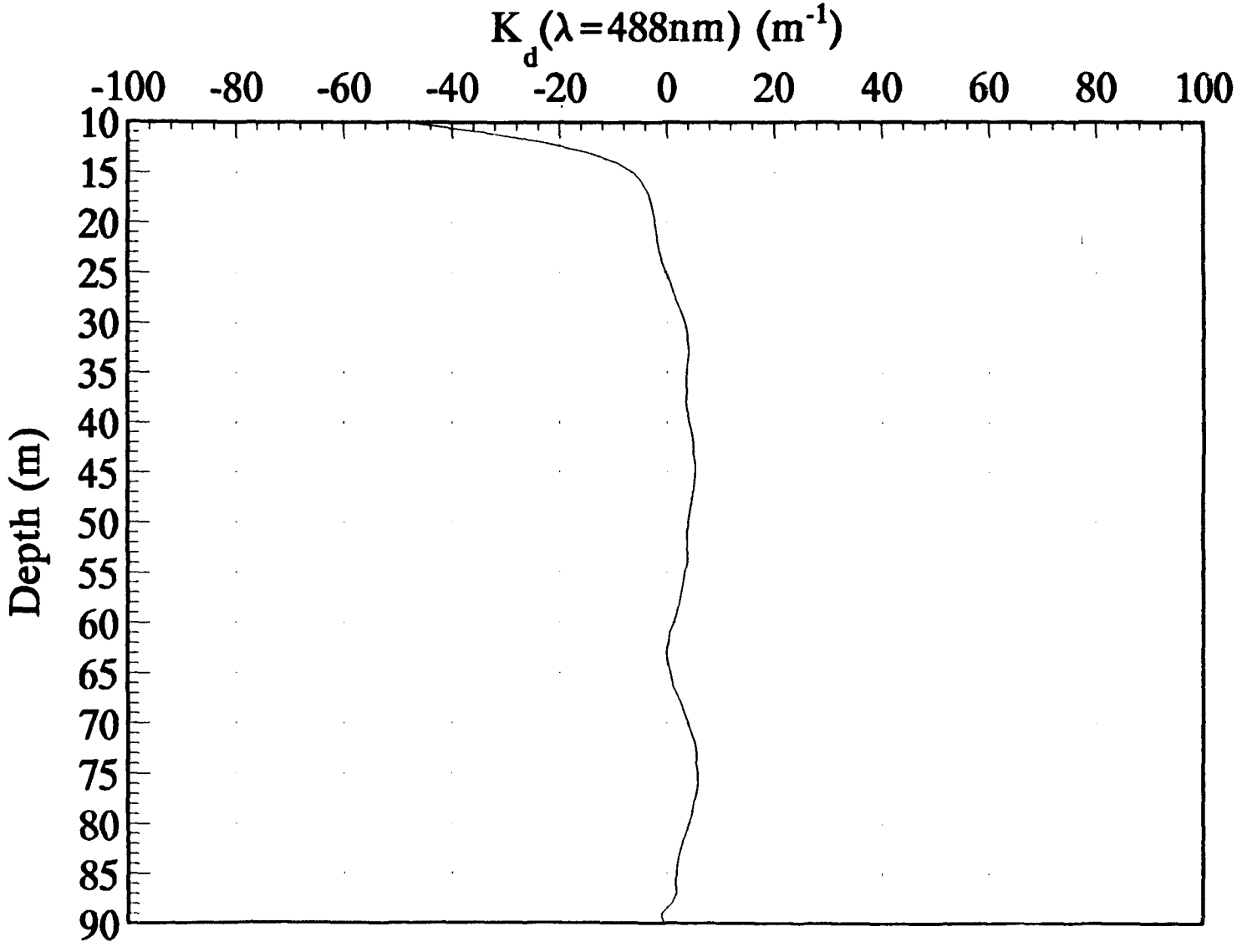

1990 Vestfjord AXKT Test
AXKT Channel 14 Drop 5

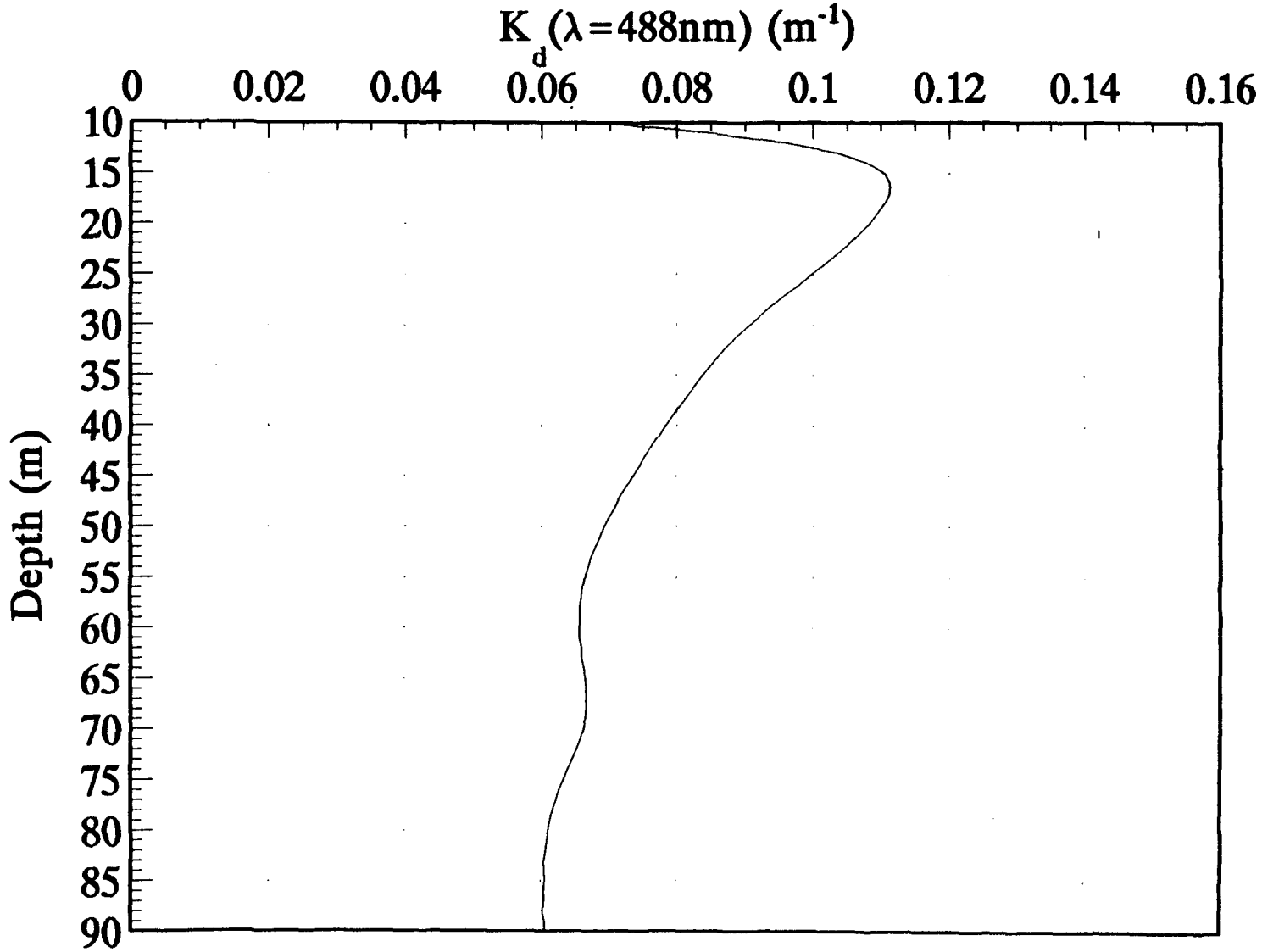

1990 Vestfjord AXKT Test
AXKT Channel 14 Drop 5 (% Difference From MER Data)

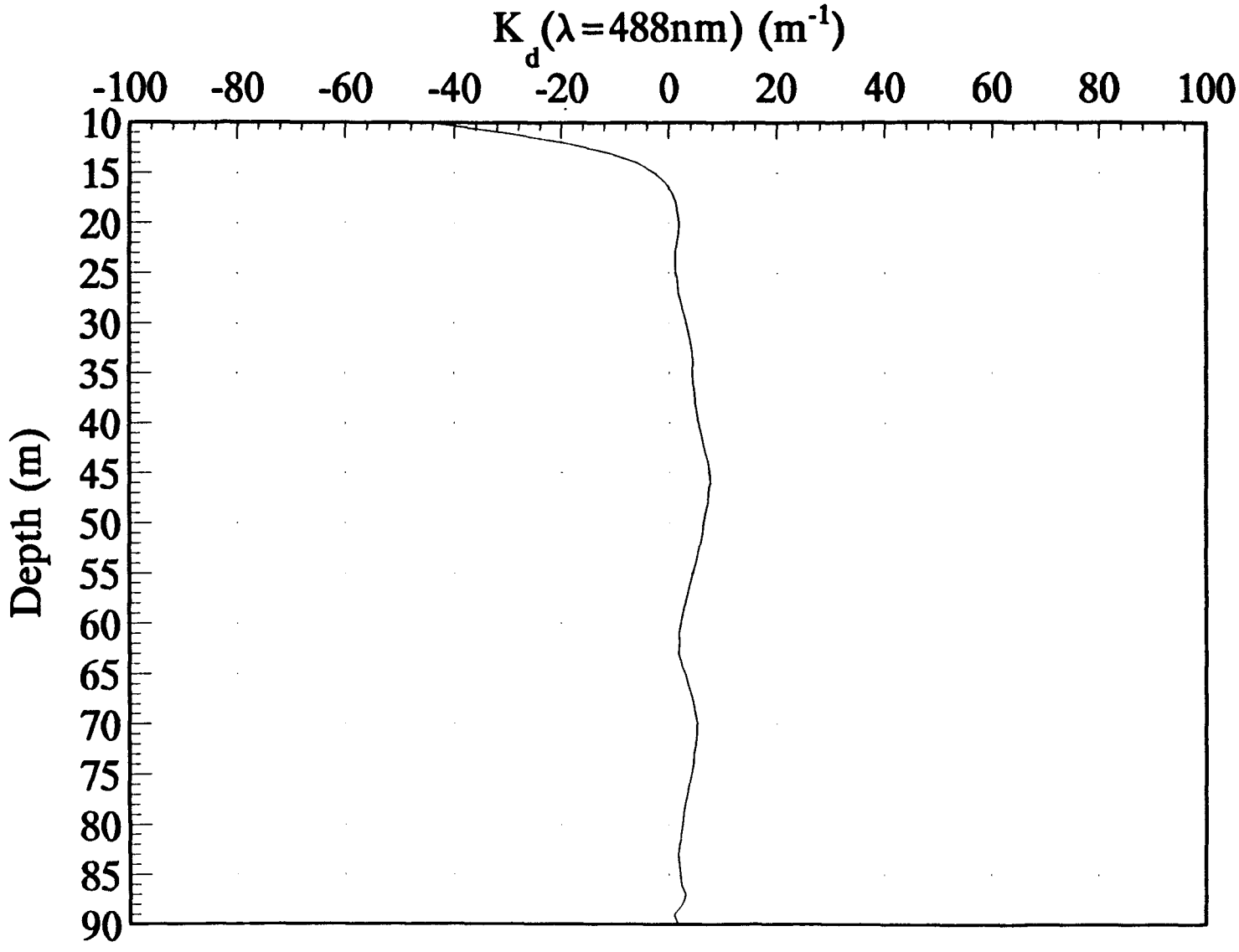

1990 Vestfjord AXKT Test
AXKT Channel 14 Drop 6

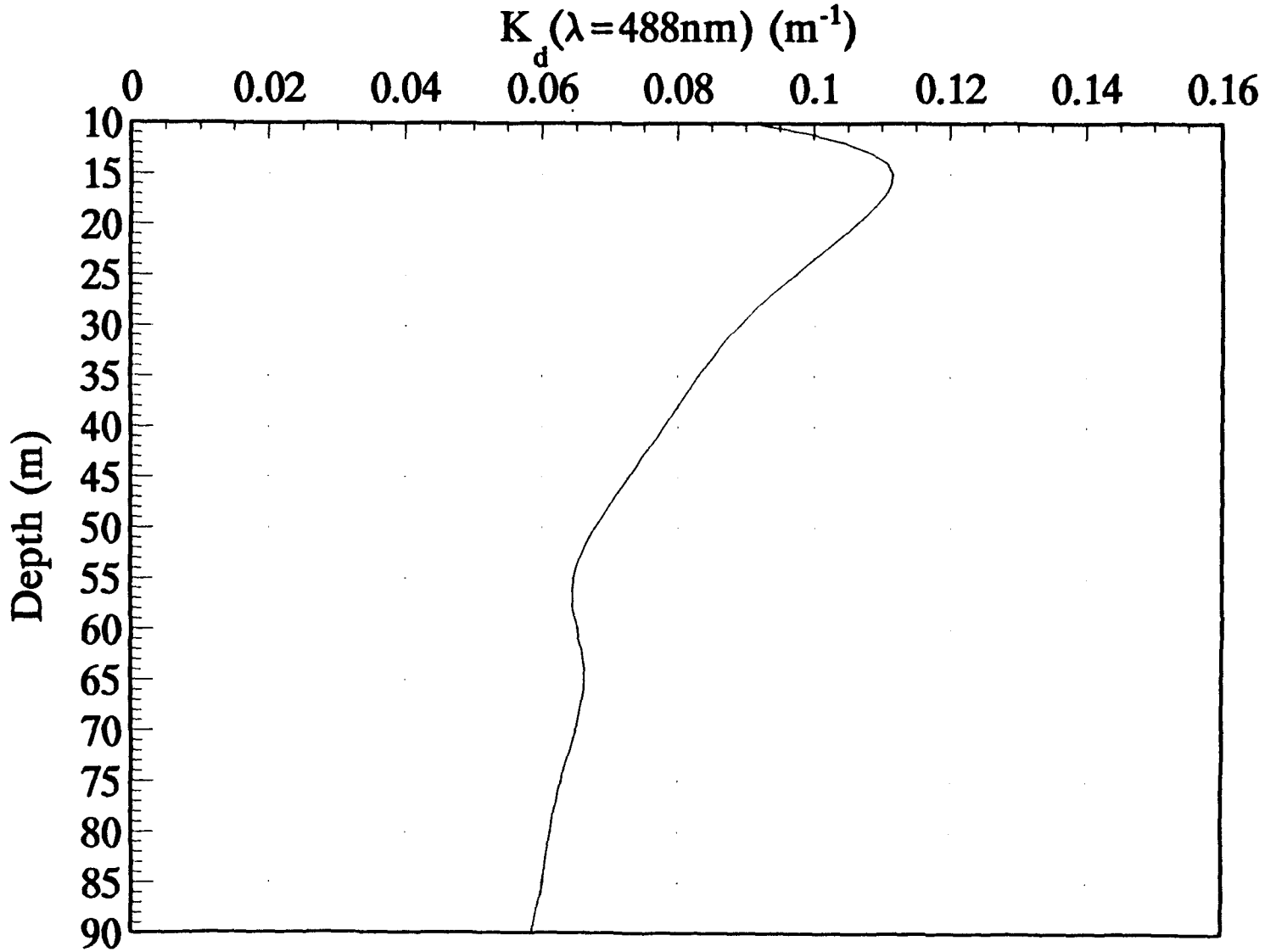

1990 Vestfjord AXKT Test
AXKT Channel 14 Drop 6 (% Difference From MER Data)

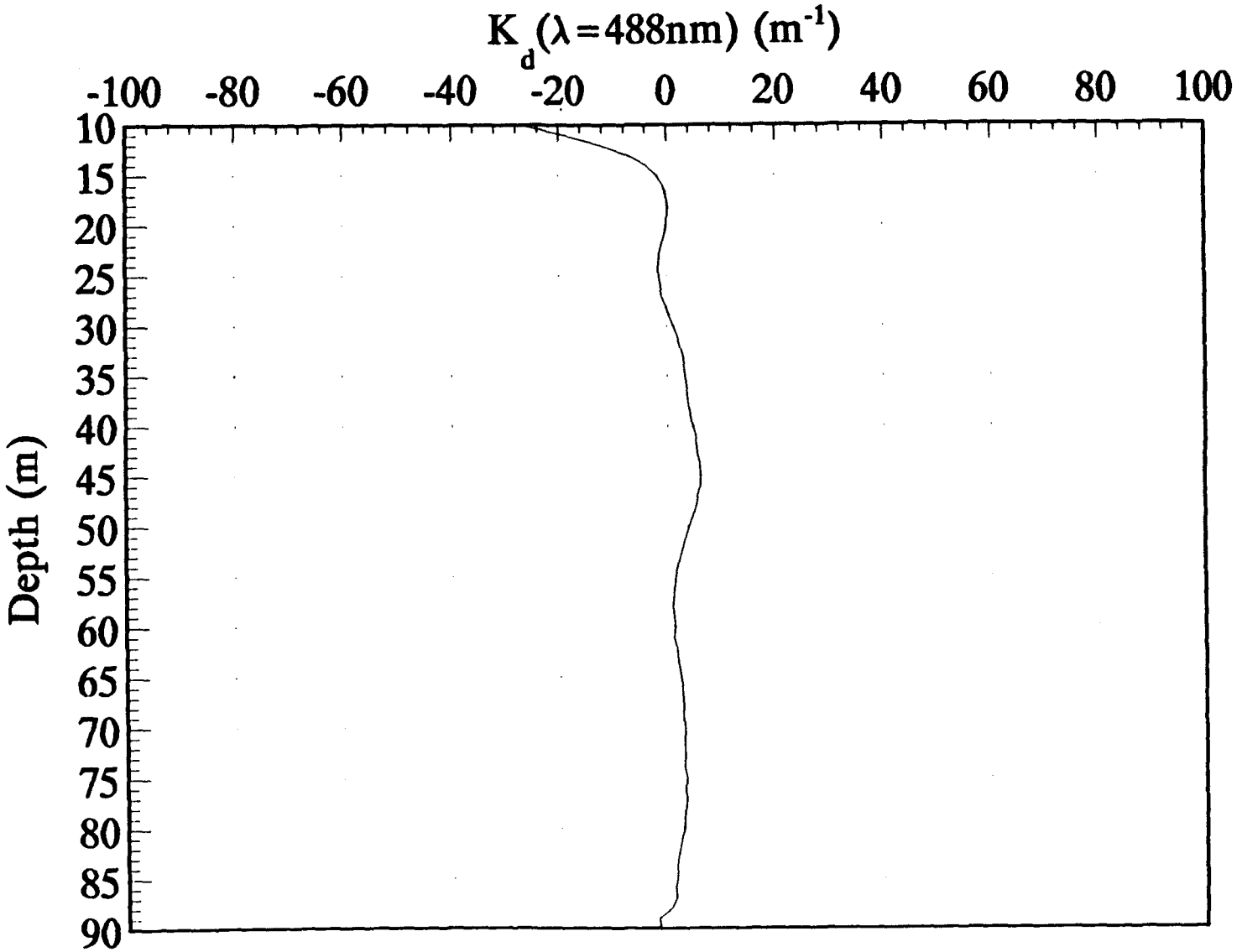

1990 Vestfjord AXKT Test
AXKT Channel 14 Drop 7

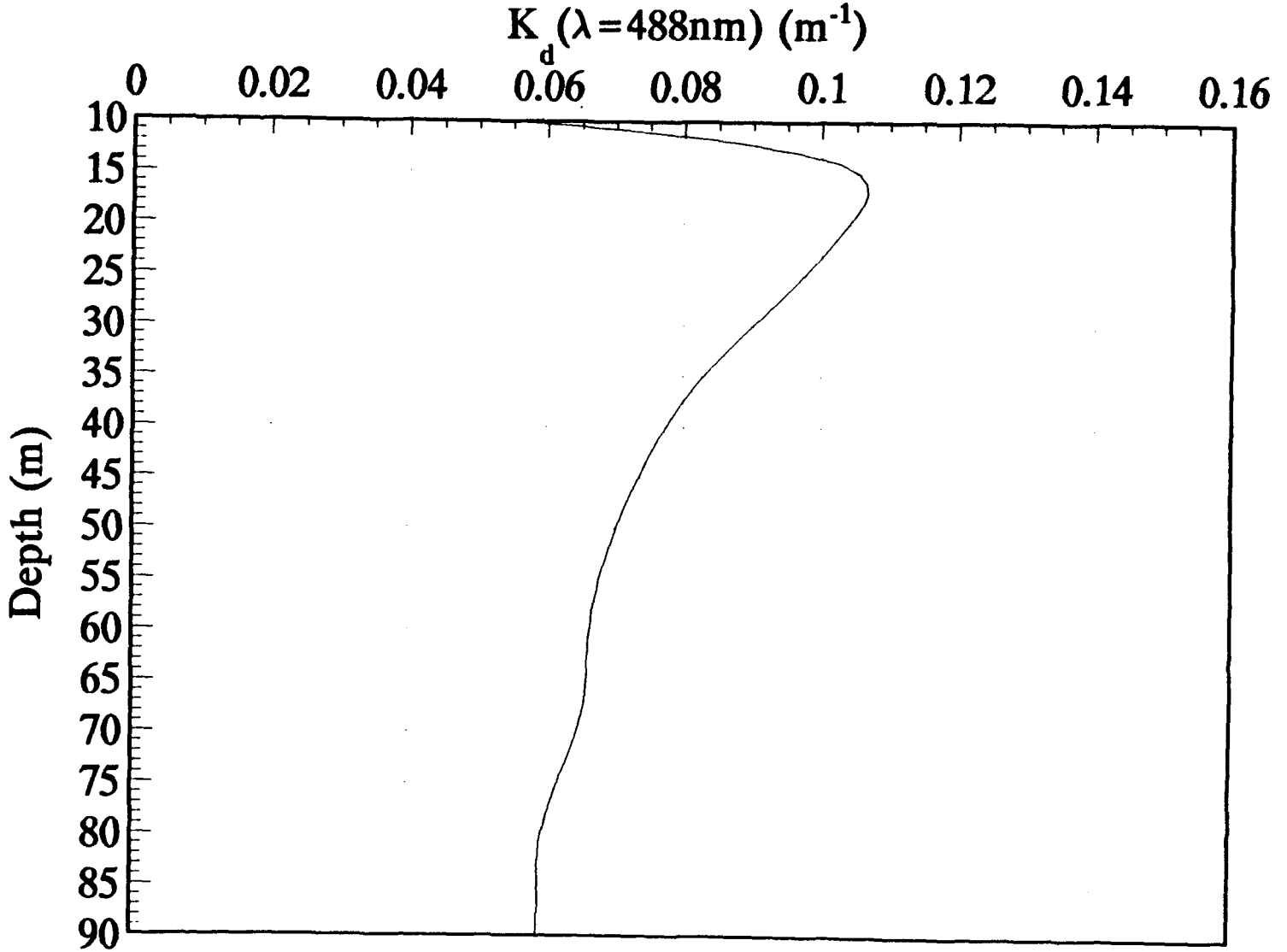

1990 Vestfjord AXKT Test
AXKT Channel 14 Drop 7 (% Difference From MER Data)

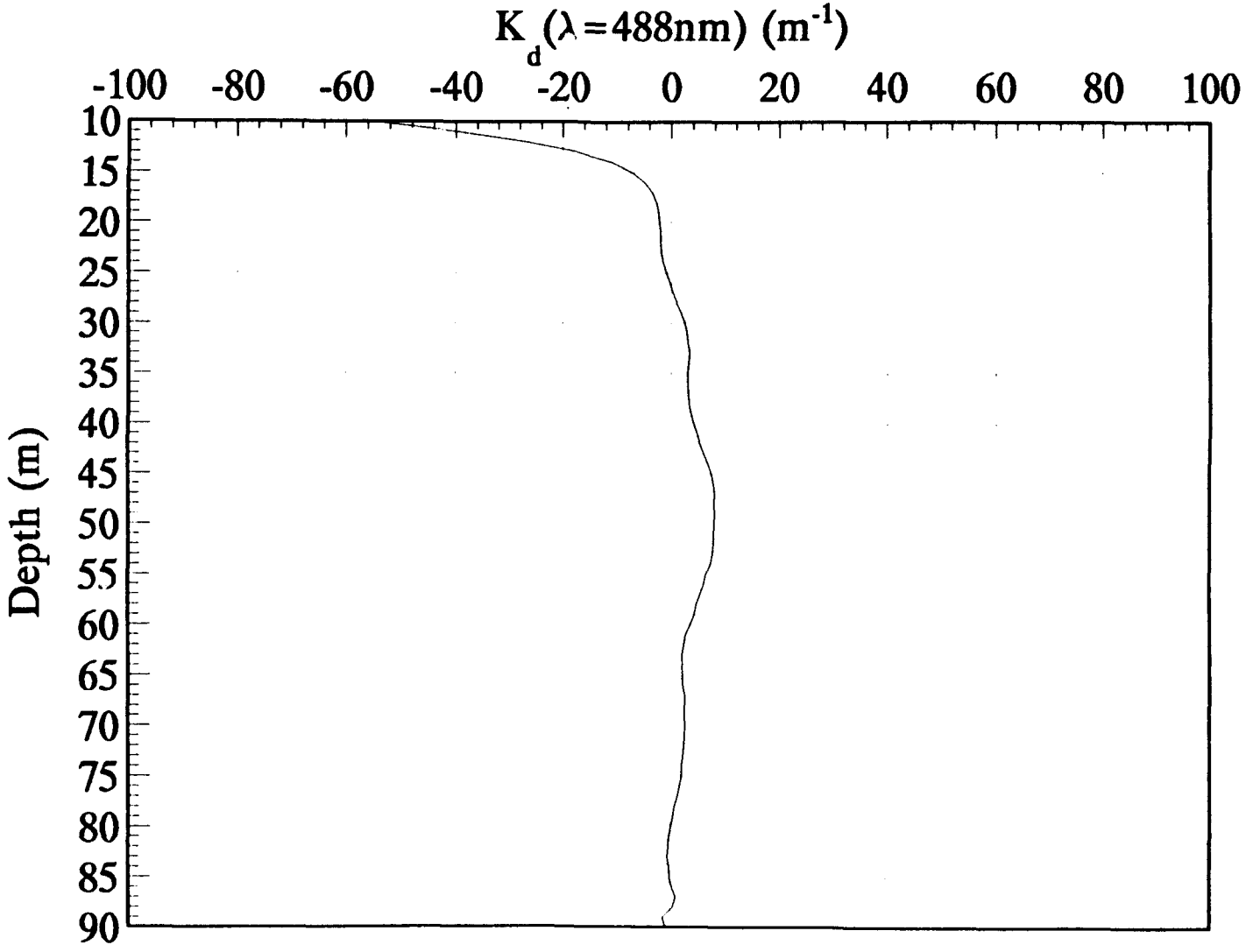

1990 Vestfjord AXKT Test
AXKT Channel 16 Drop 2

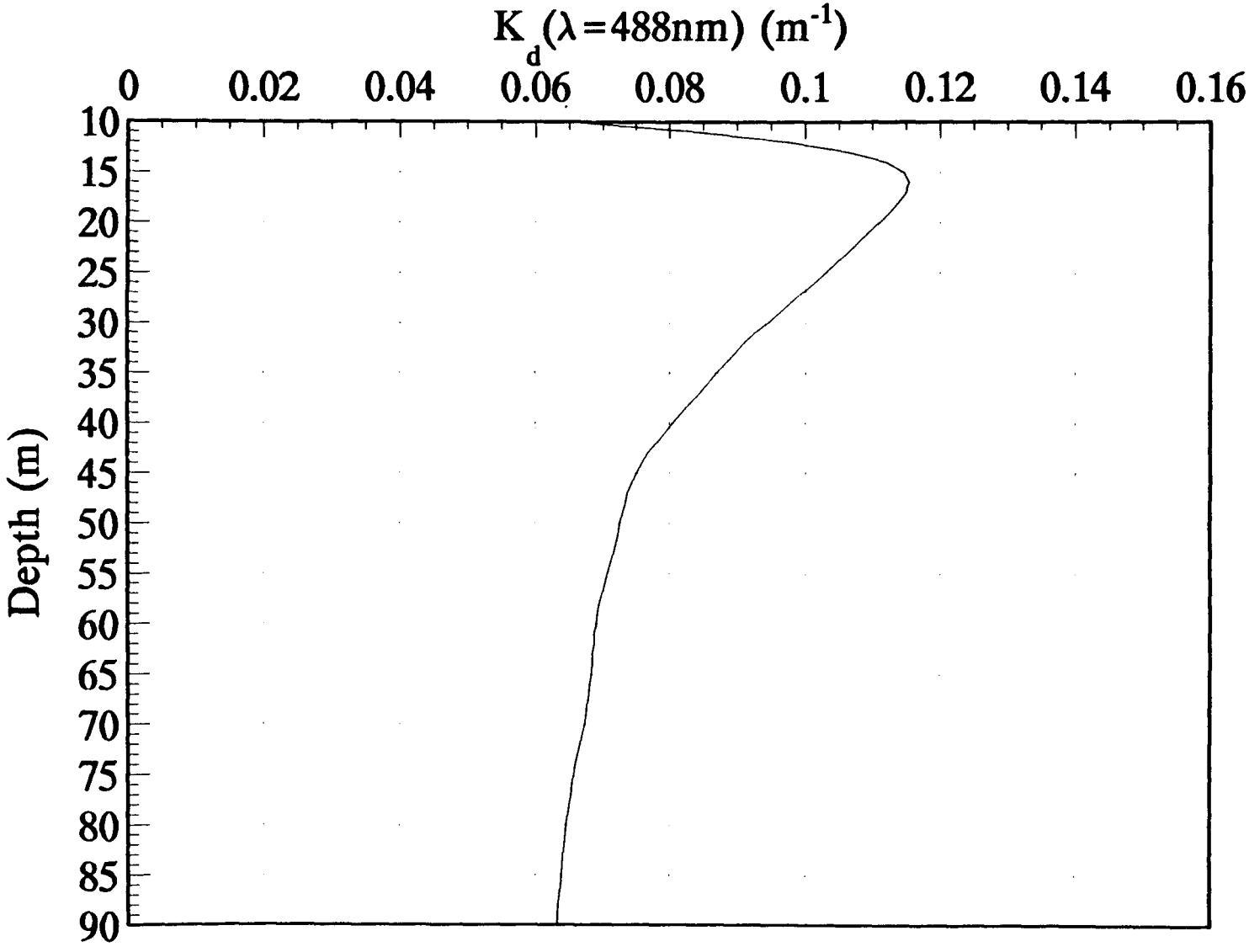

1990 Vestfjord AXKT Test
AXKT Channel 16 Drop 2 (% Difference From MER Data)

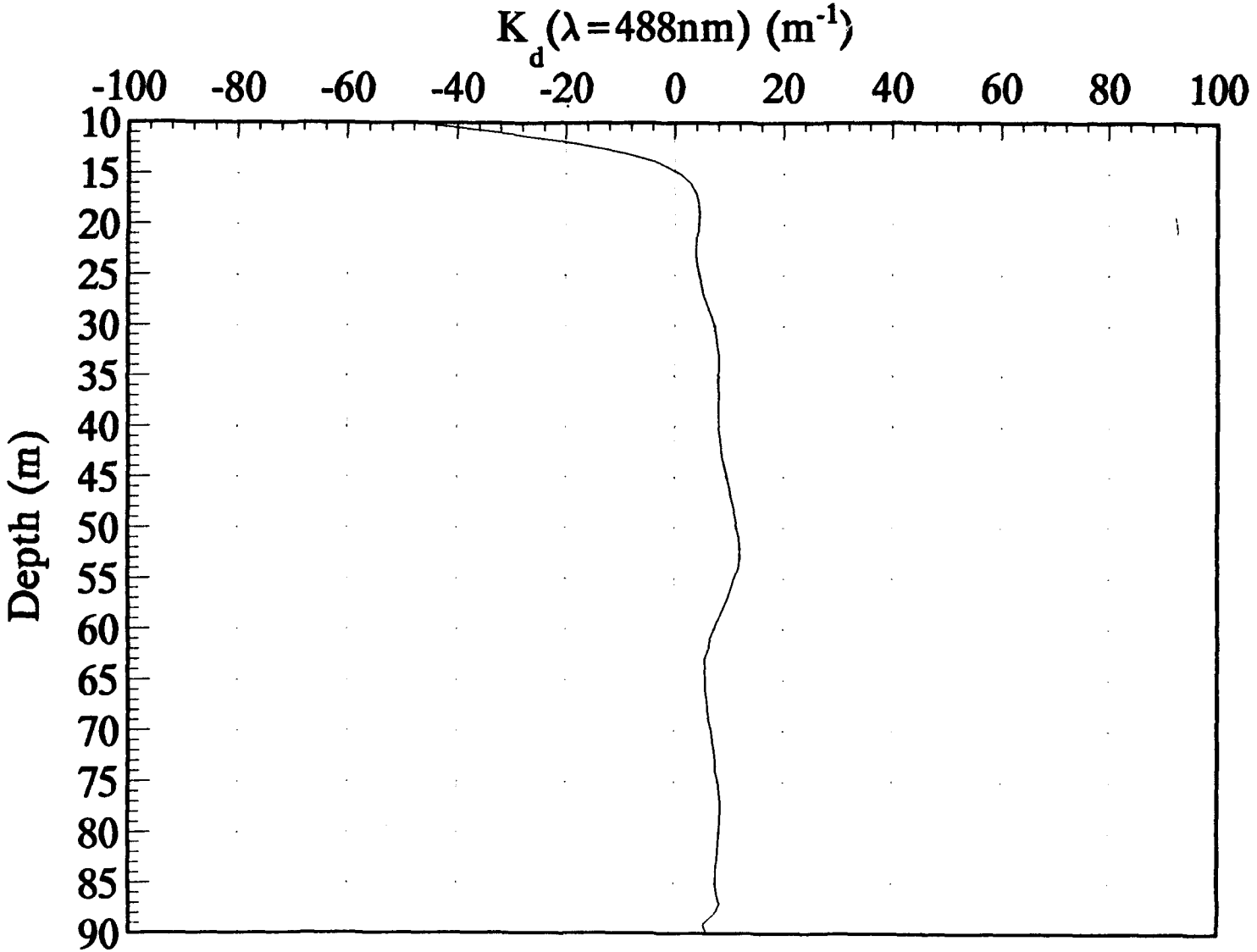

1990 Vestfjord AXKT Test
AXKT Channel 16 Drop 4

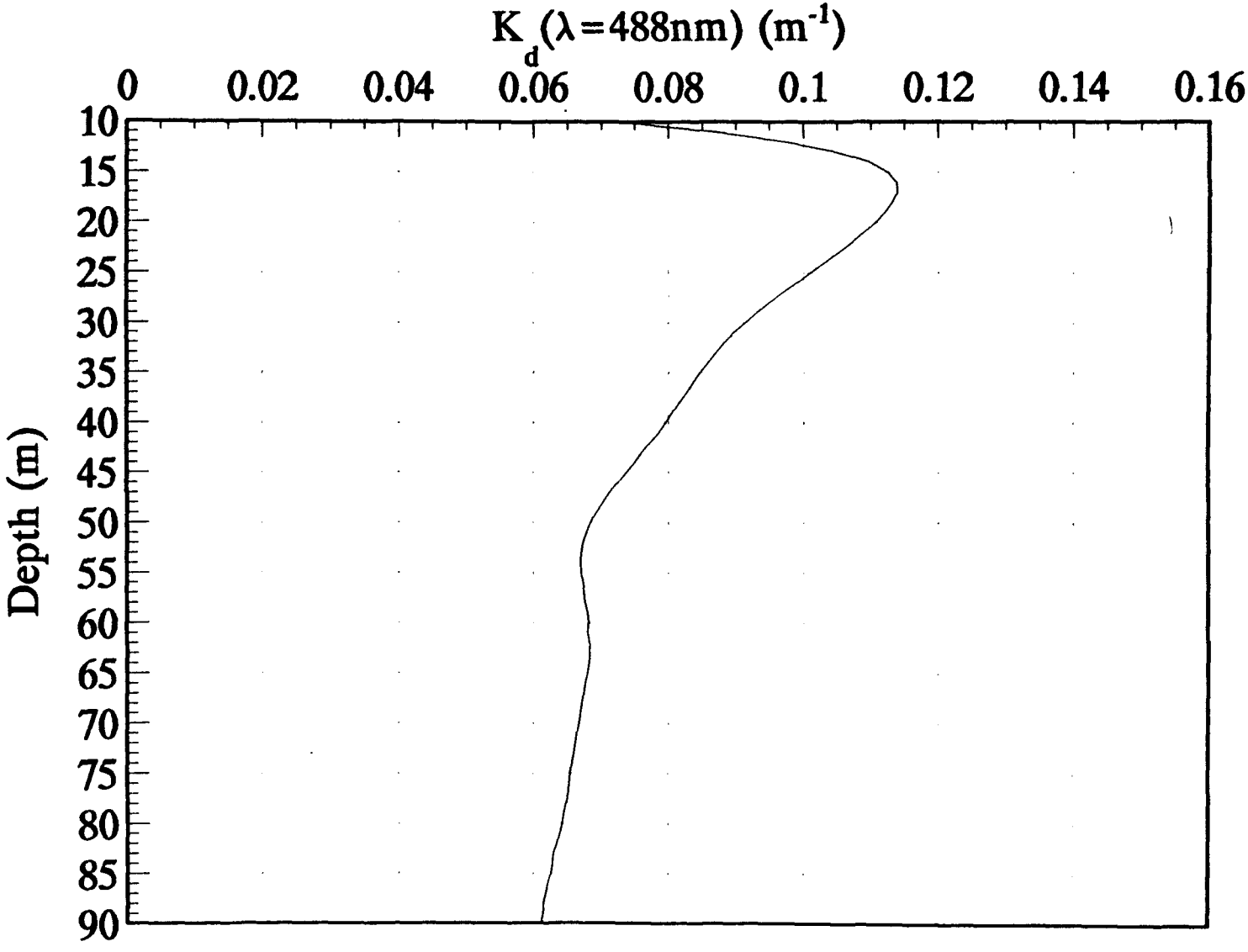

1990 Vestfjord AXKT Test
AXKT Channel 16 Drop 4 (% Difference From MER Data)

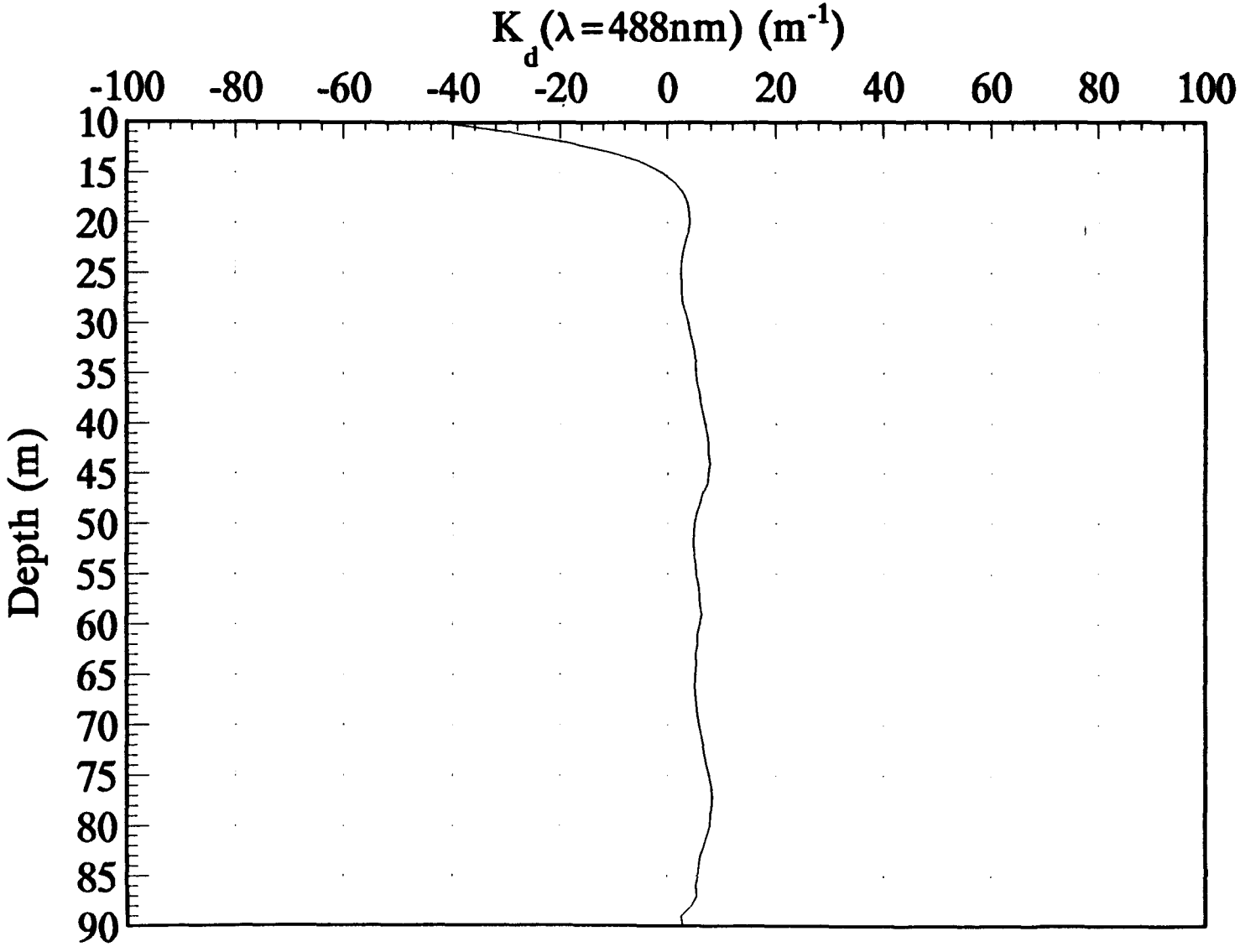

1990 Vestfjord AXKT Test
AXKT Channel 16 Drop 6

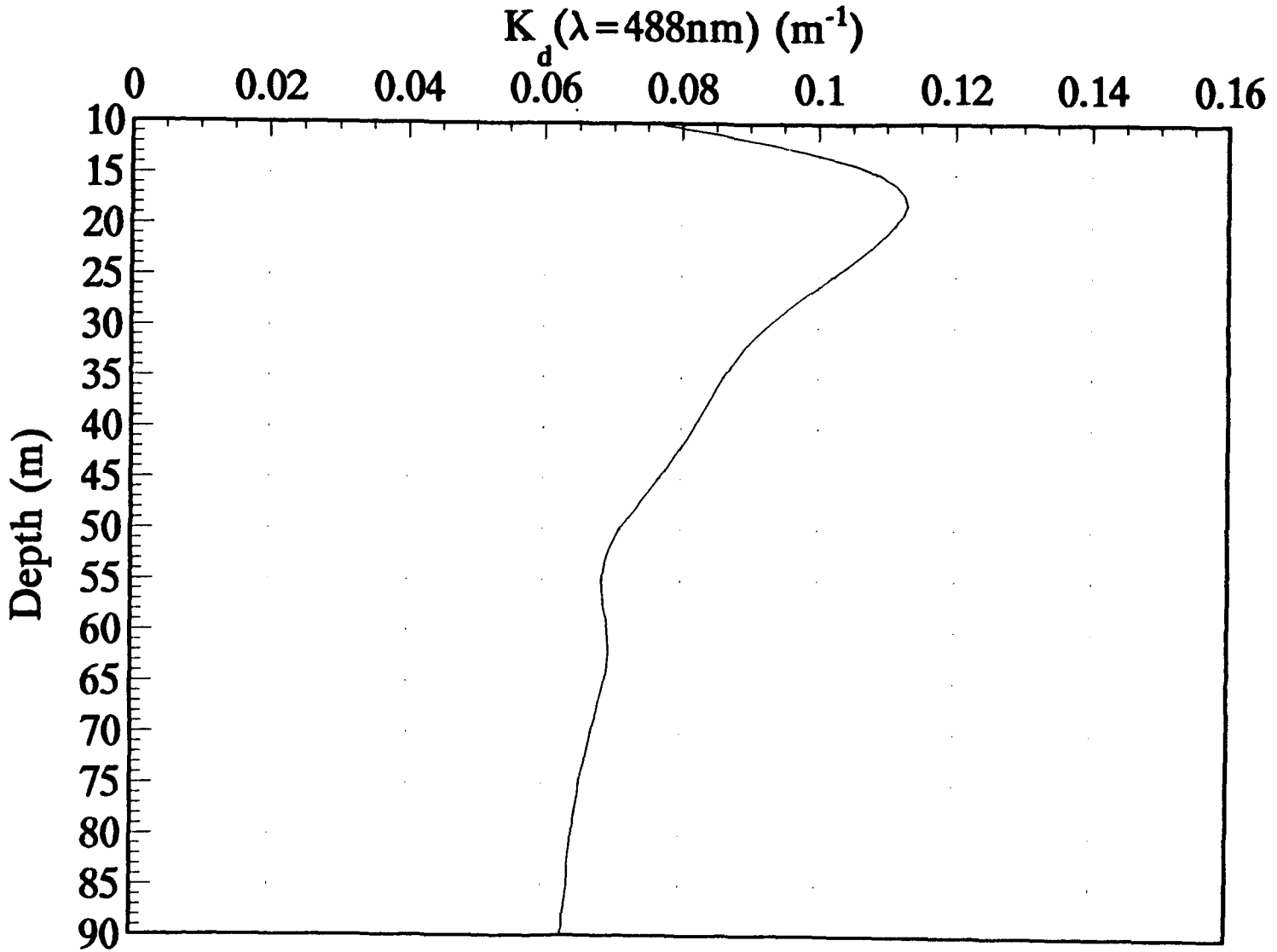

1990 Vestfjord AXKT Test
AXKT Channel 16 Drop 6 (% Difference From MER Data)

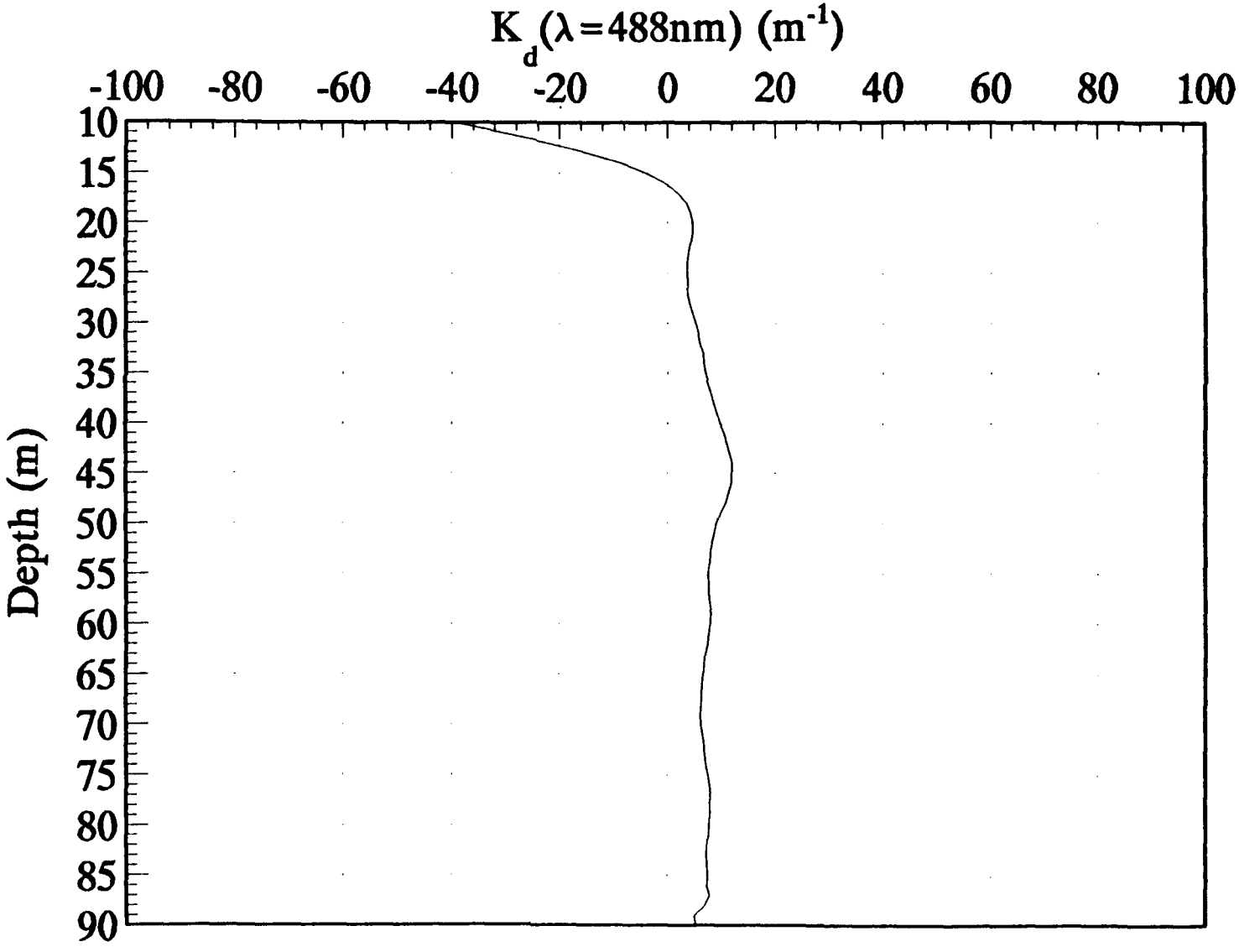

1990 Vestfjord AXKT Test
AXKT Channel 16 Drop 7

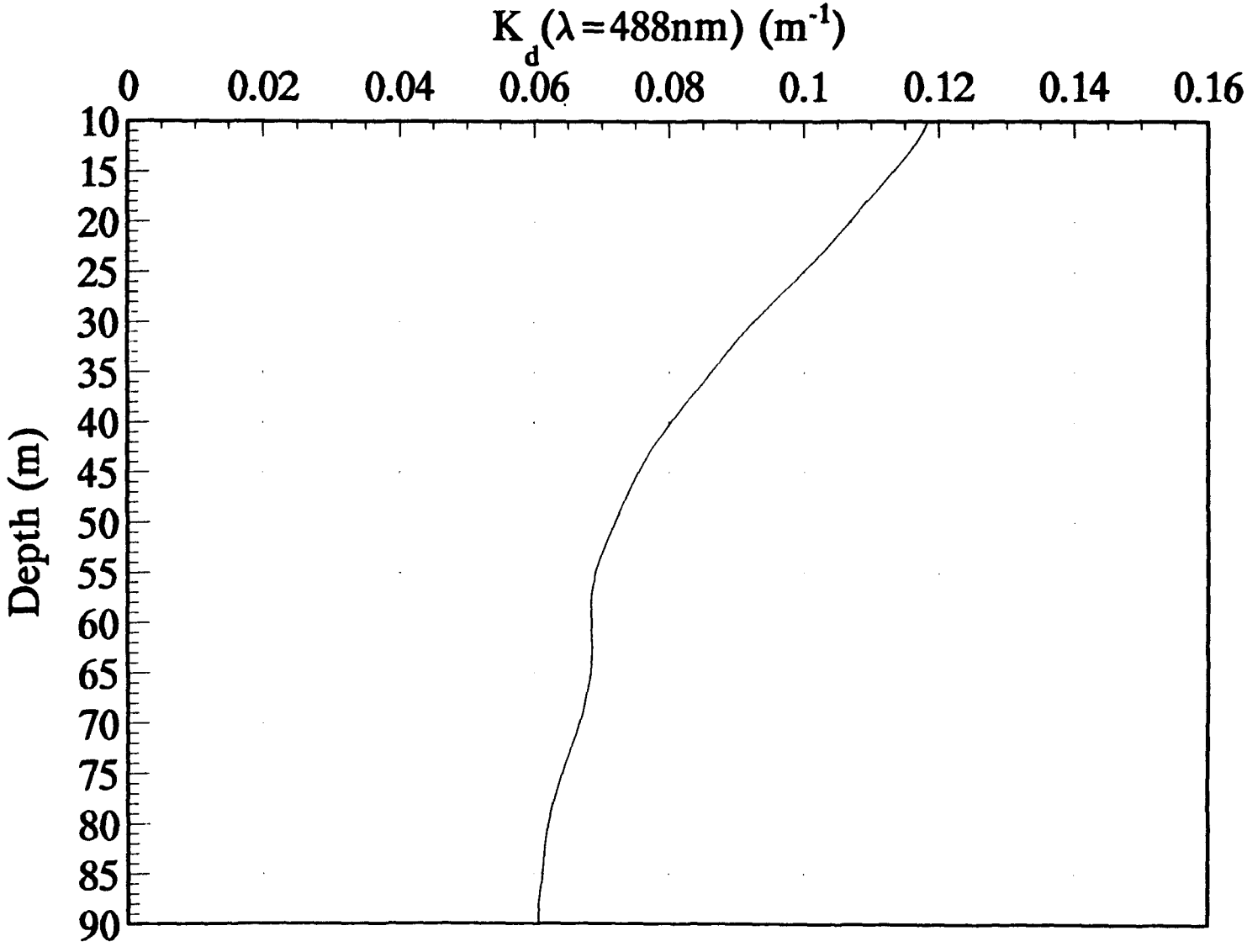

1990 Vestfjord AXKT Test
AXKT Channel 16 Drop 7 (% Difference From MER Data)

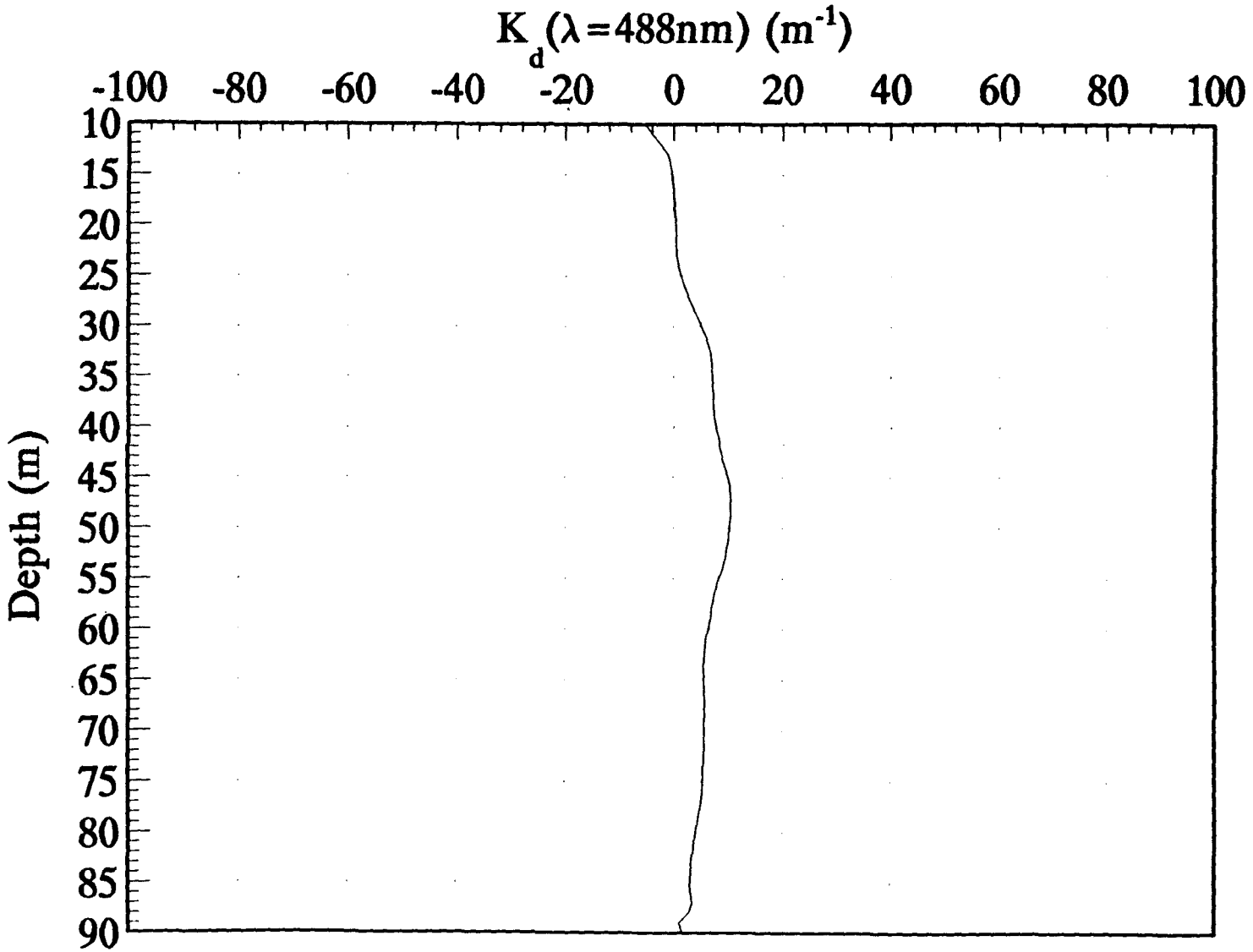

Appendix C

Comparison of MER and AXKT K_d Profiles for Pacific 1990 Test

1990 Pacific AXKT Test
MER Mean Data (+/- s.d.)

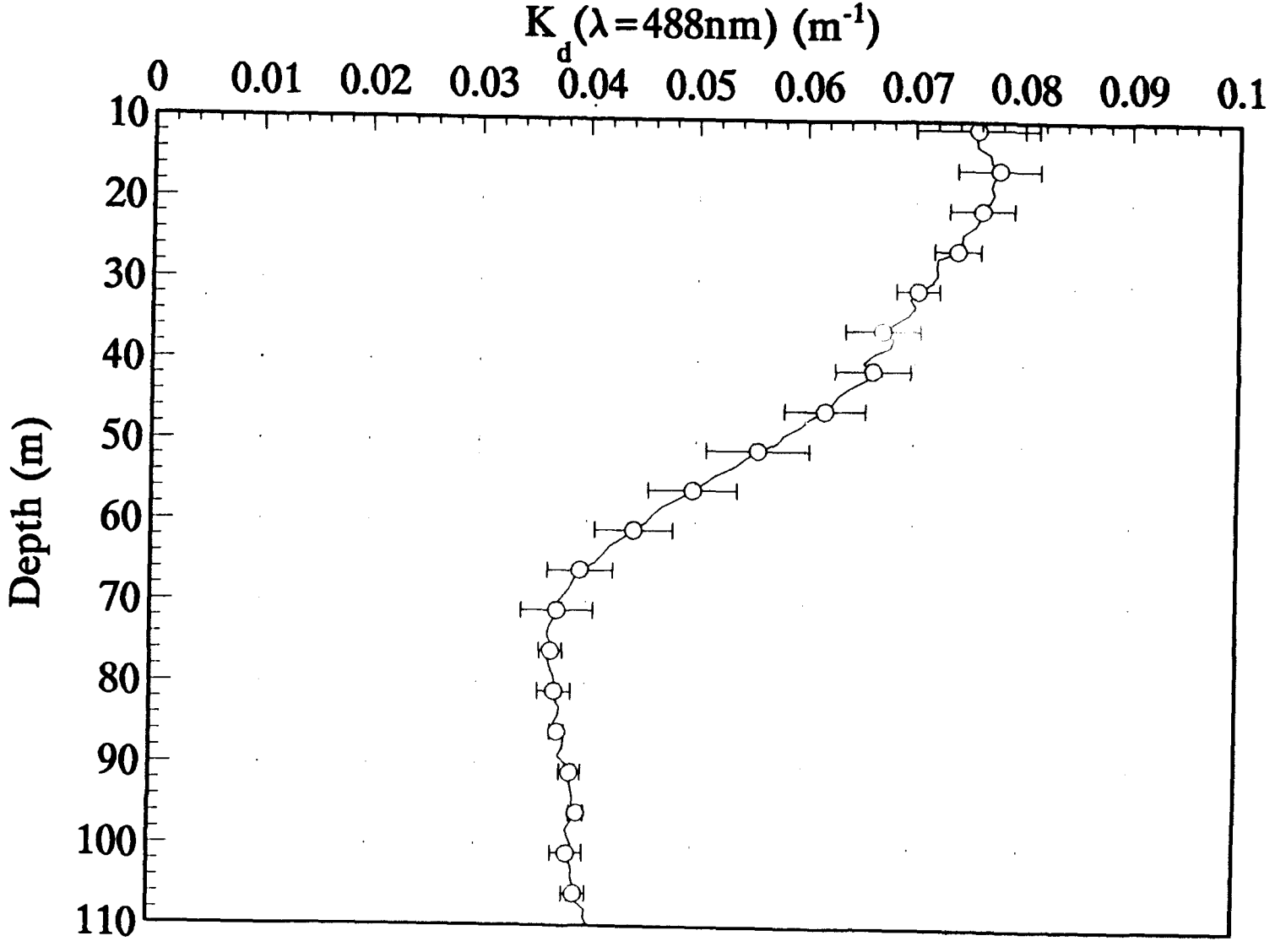

1990 Pacific AXKT Test
AXKT Channel 12 Drop 1

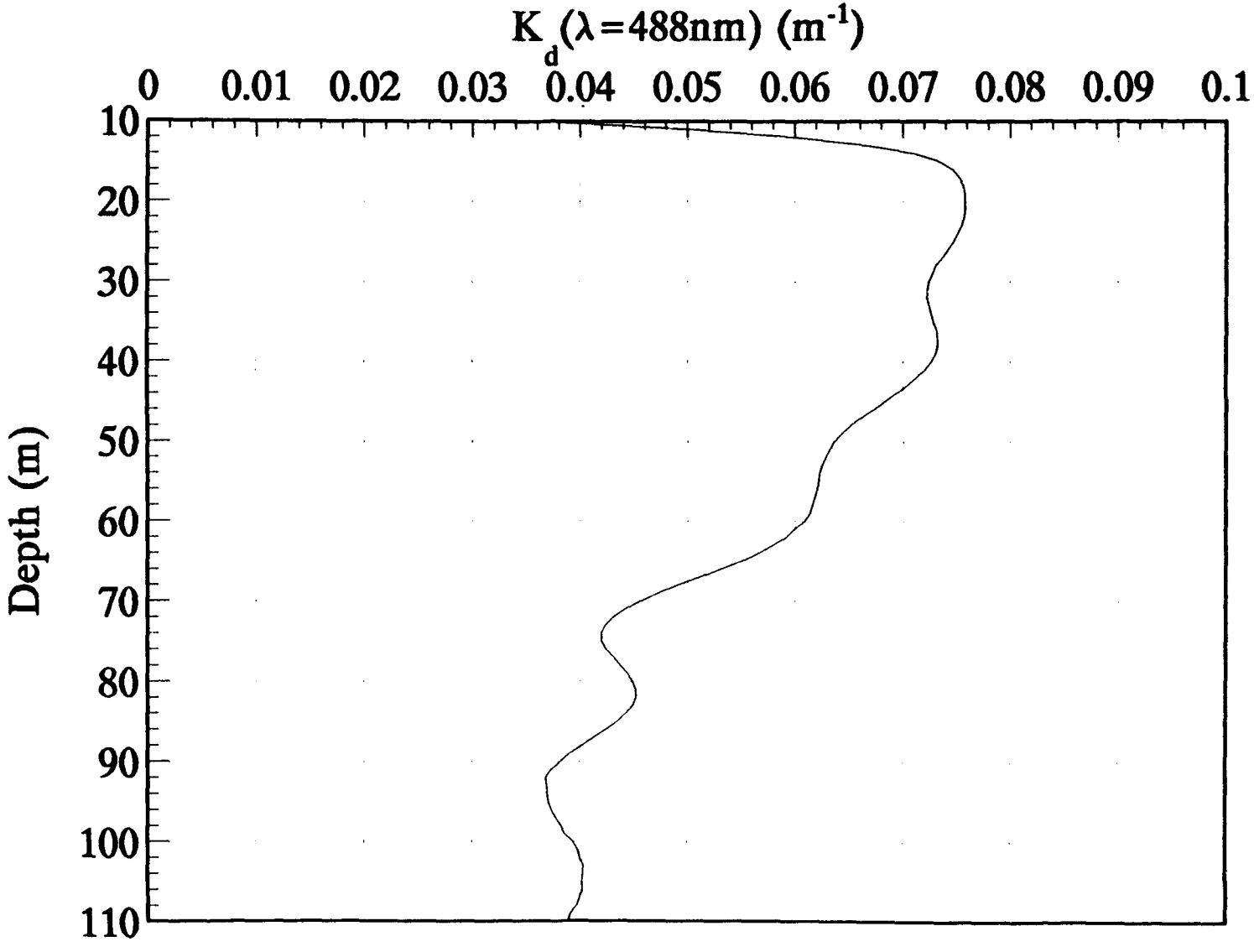

1990 Pacific AXKT Test
AXKT Channel 12 Drop 1 (% Difference From MER Data)

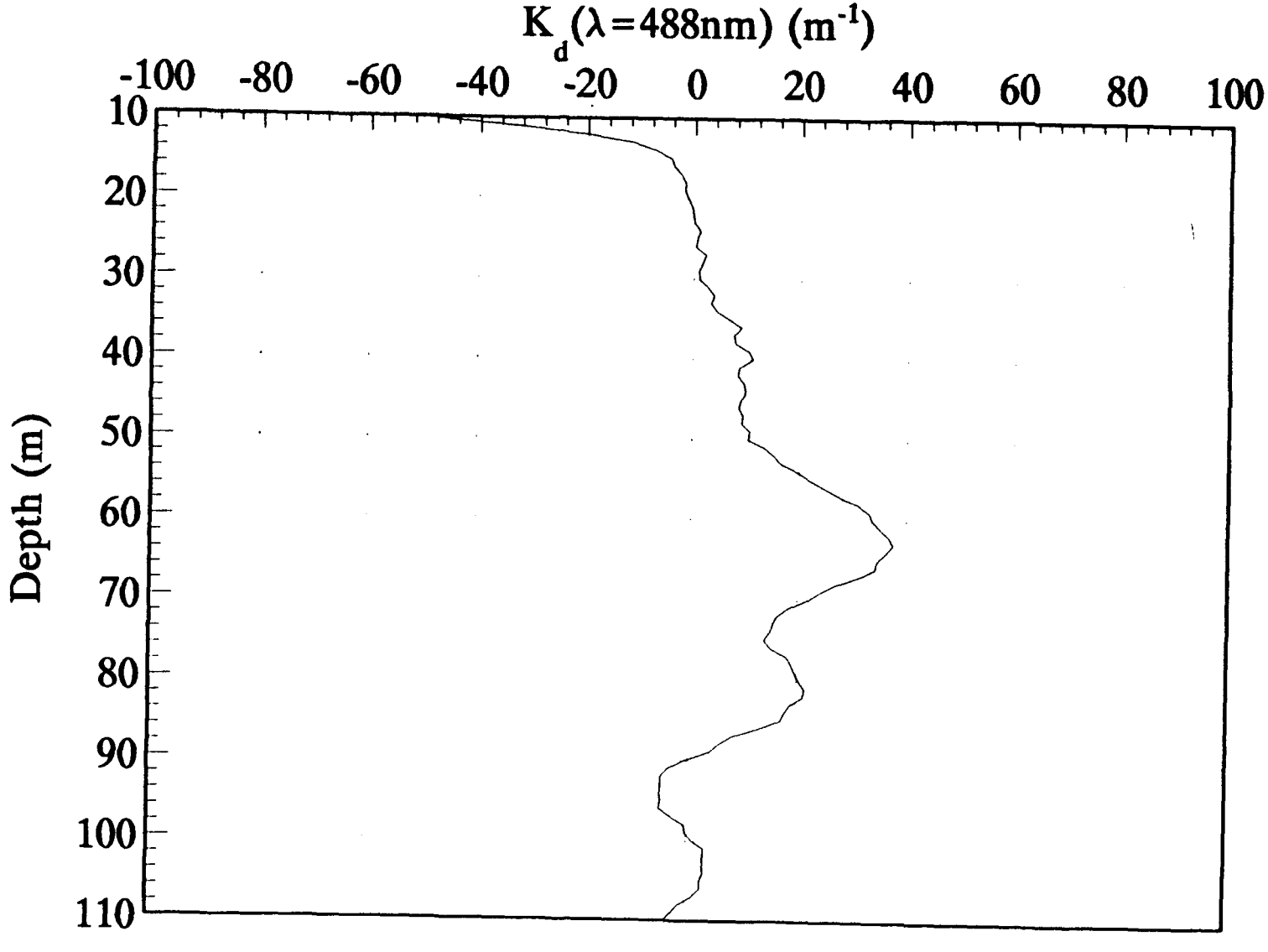

1990 Pacific AXKT Test
AXKT Channel 14 Drop 2

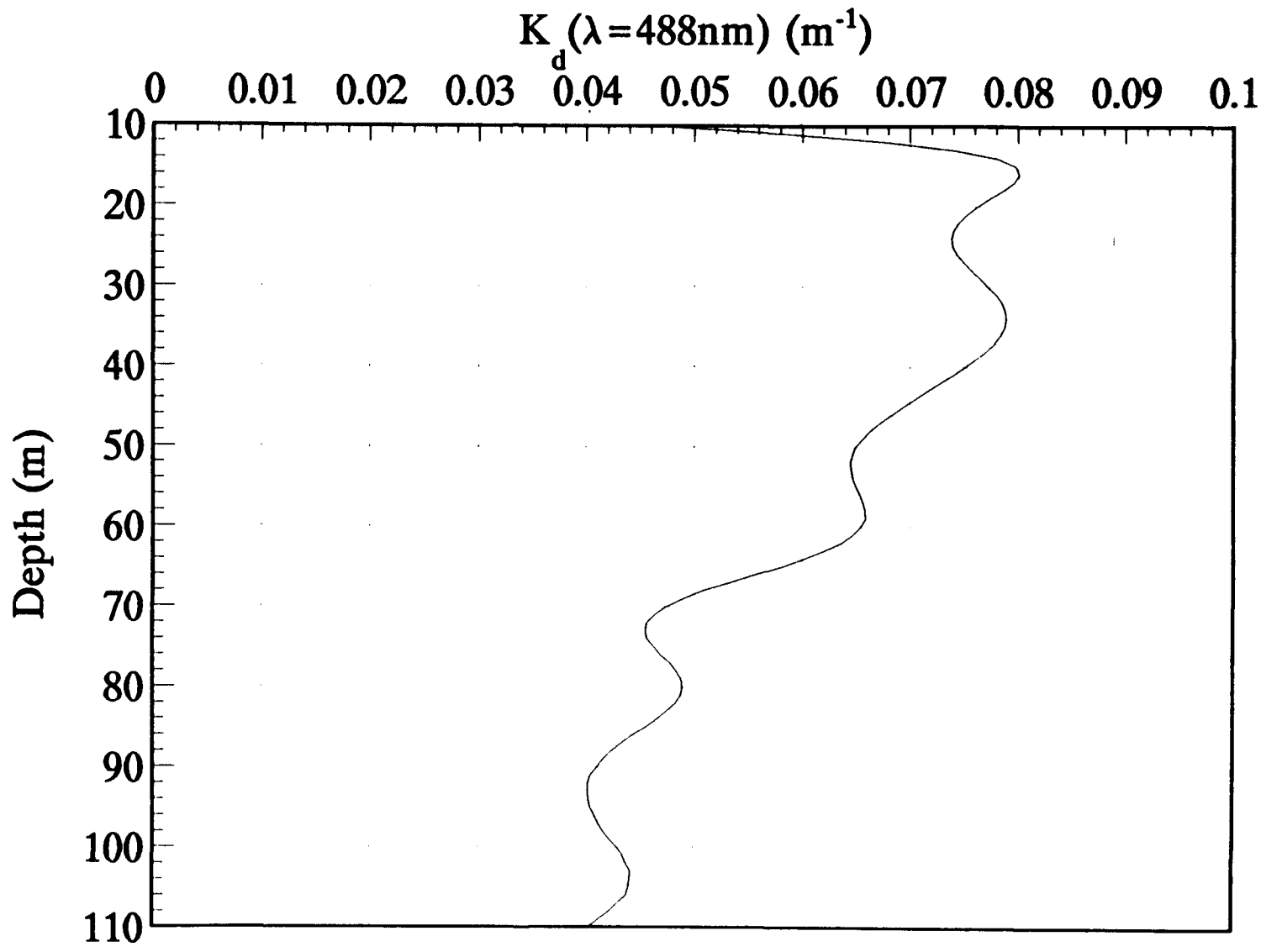

1990 Pacific AXKT Test
AXKT Channel 14 Drop 2 (% Difference From MER Data)

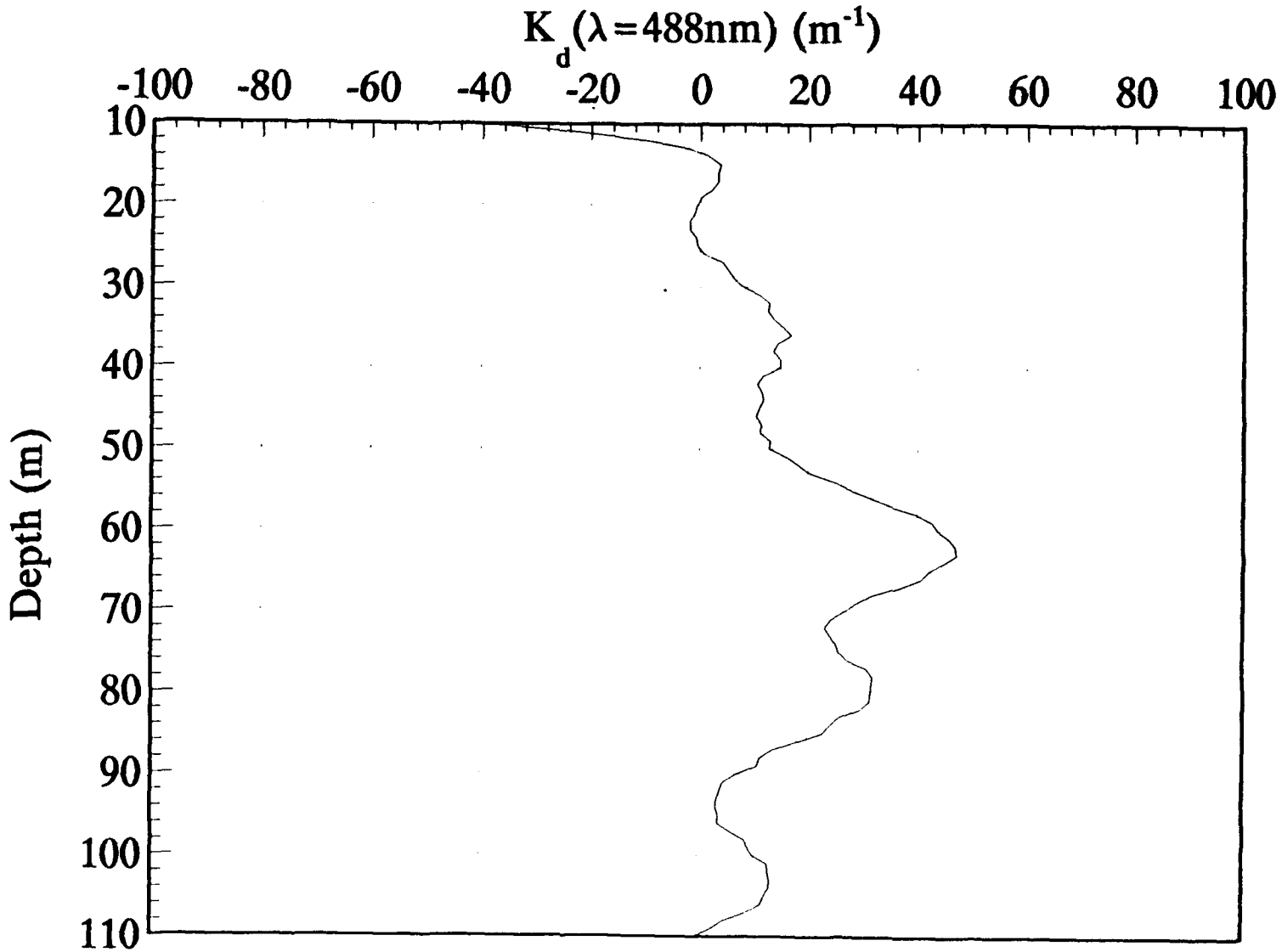

1990 Pacific AXKT Test
AXKT Channel 12 Drop 3

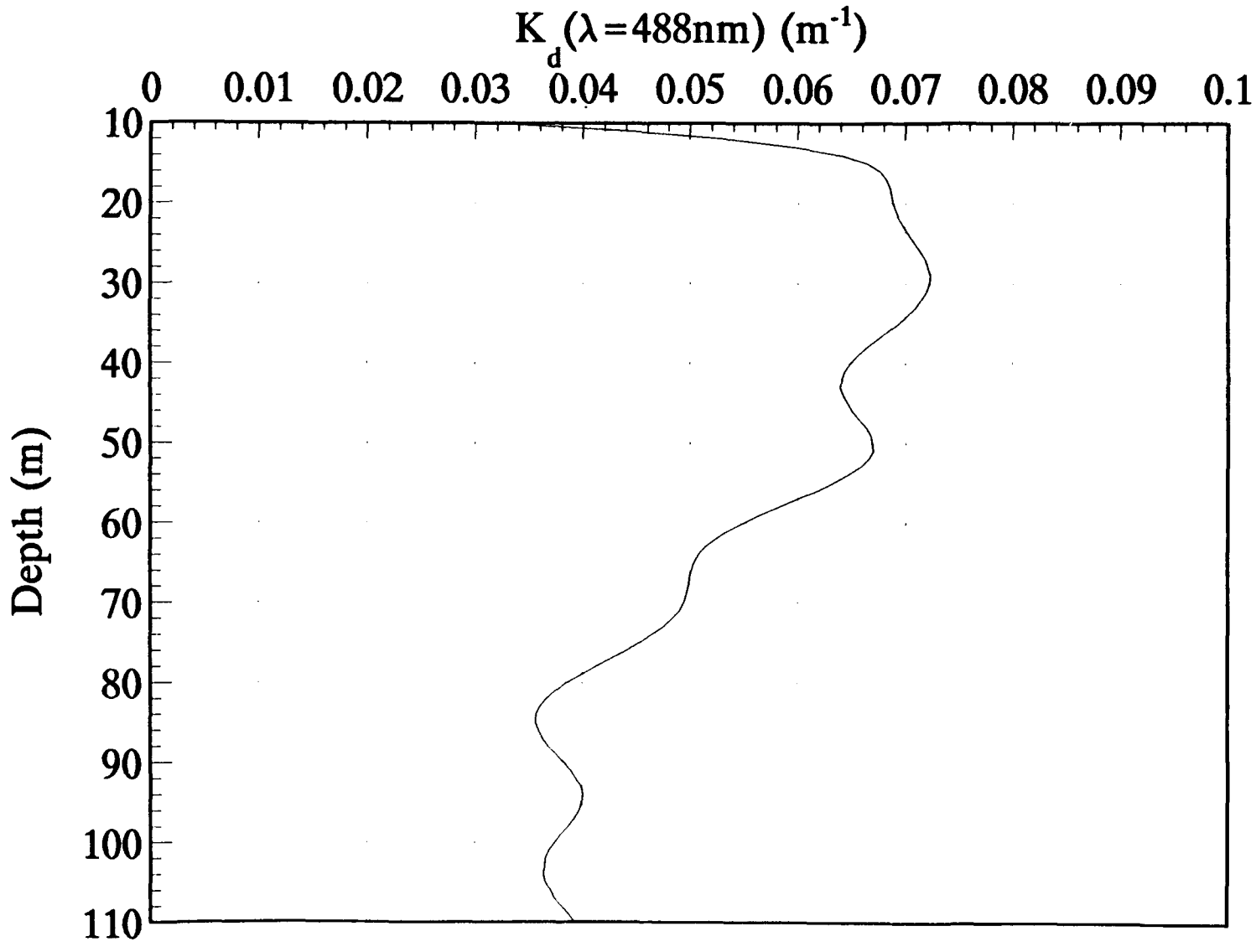

1990 Pacific AXKT Test
AXKT Channel 12 Drop 3 (% Difference From MER Data)

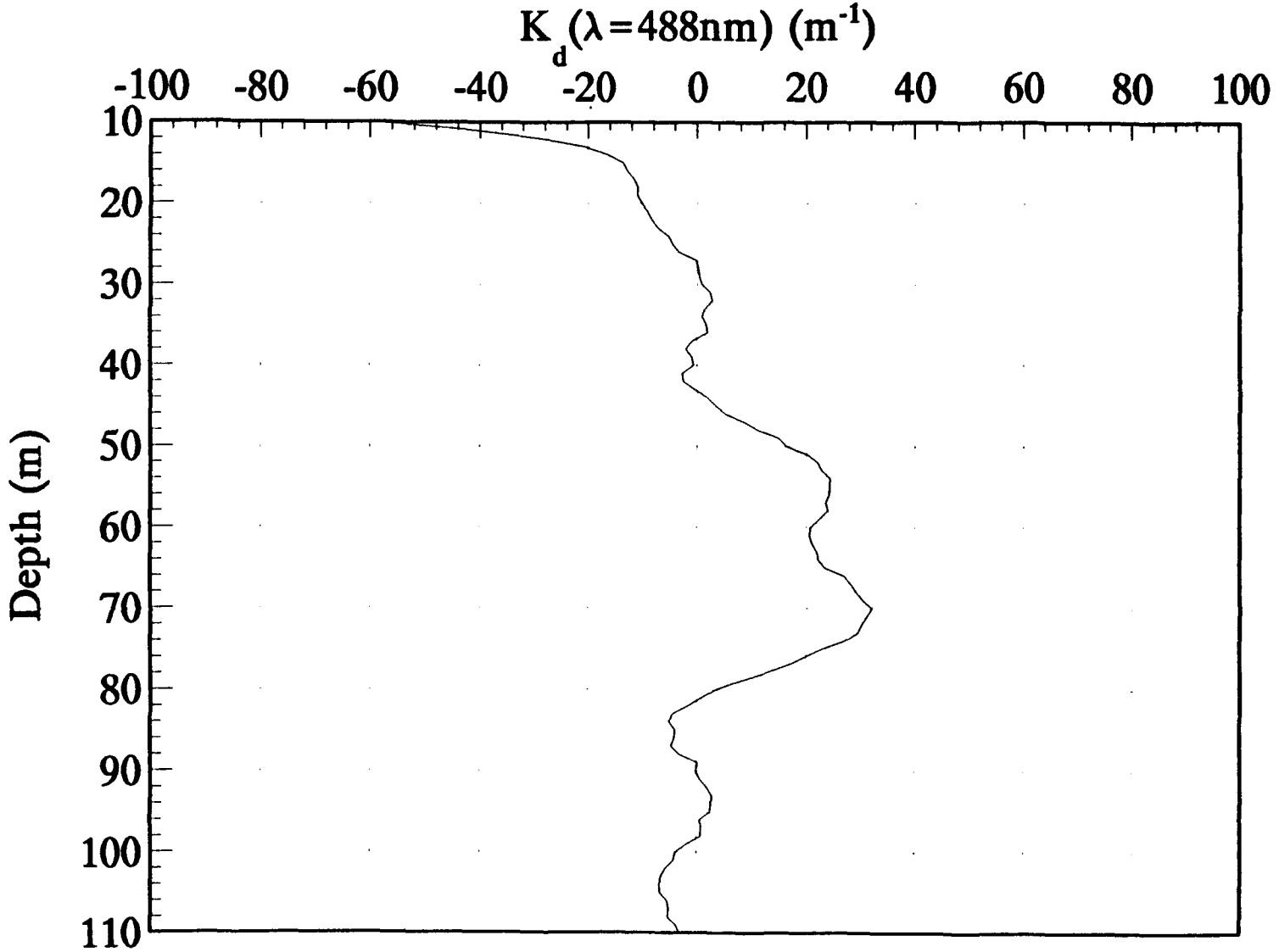

1990 Pacific AXKT Test
AXKT Channel 12 Drop 4

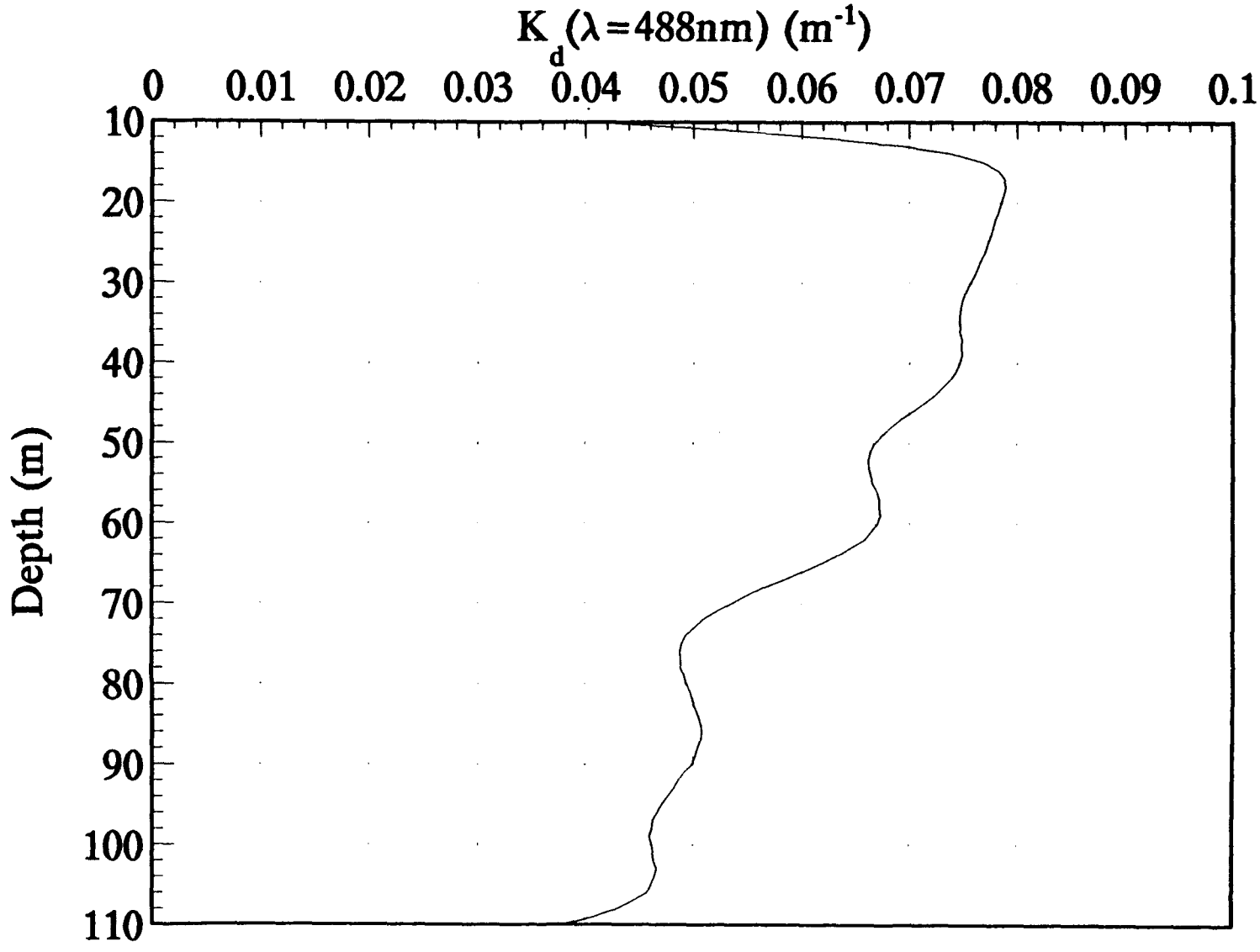

1990 Pacific AXKT Test
AXKT Channel 12 Drop 4 (% Difference From MER Data)

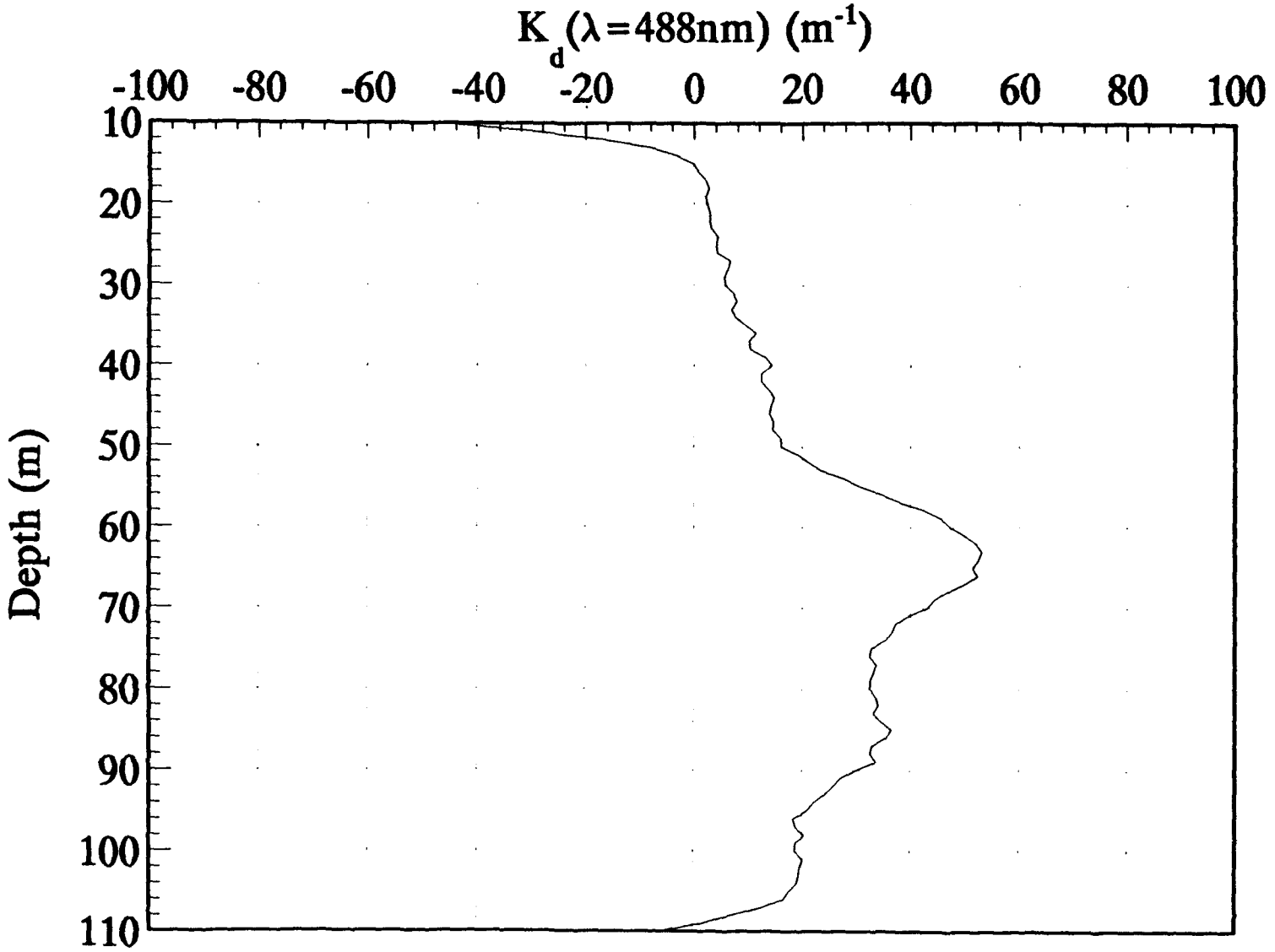

1990 Pacific AXKT Test
AXKT Channel 14 Drop 4

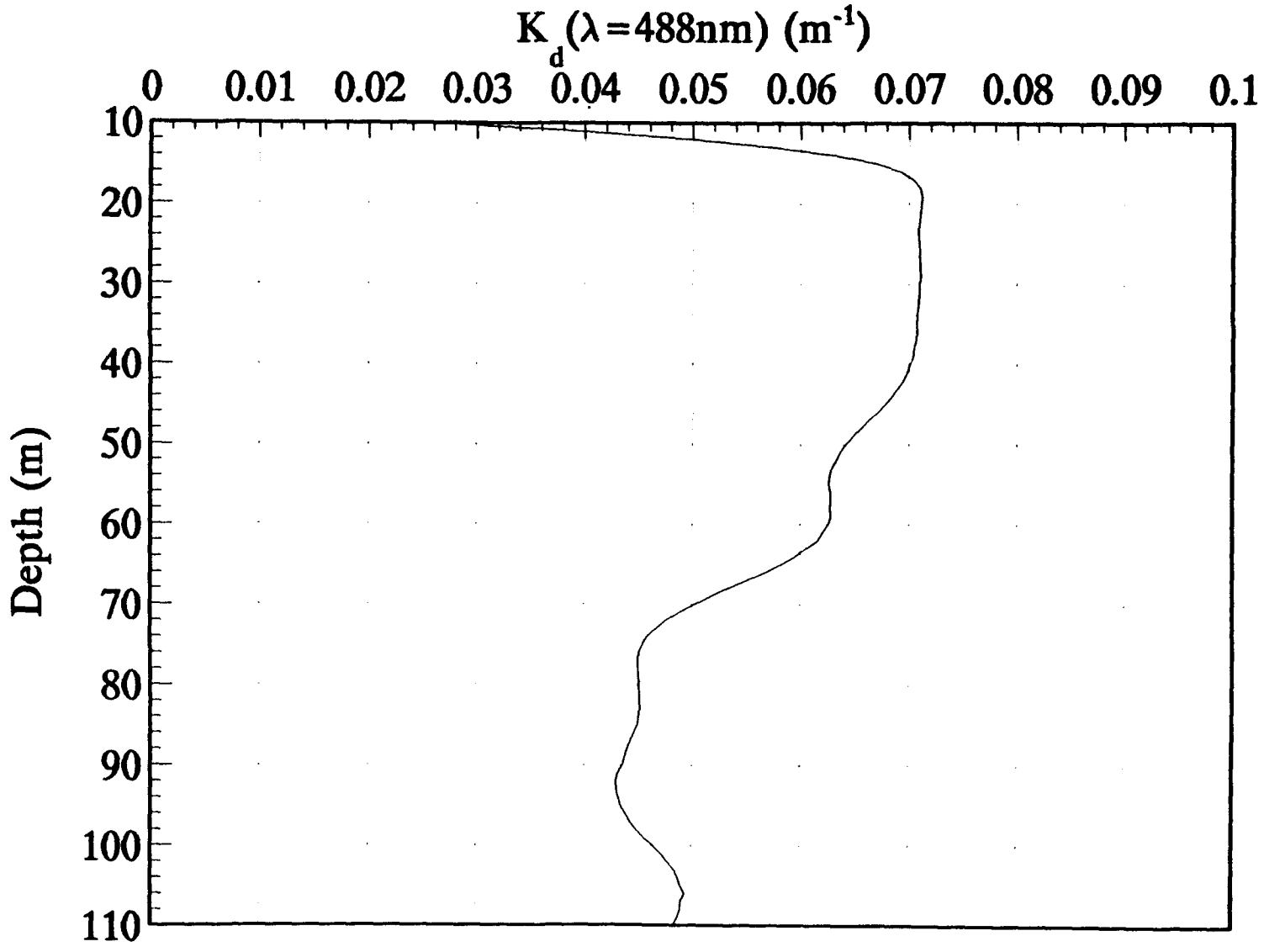

1990 Pacific AXKT Test
AXKT Channel 14 Drop 4 (% Difference From MER Data)

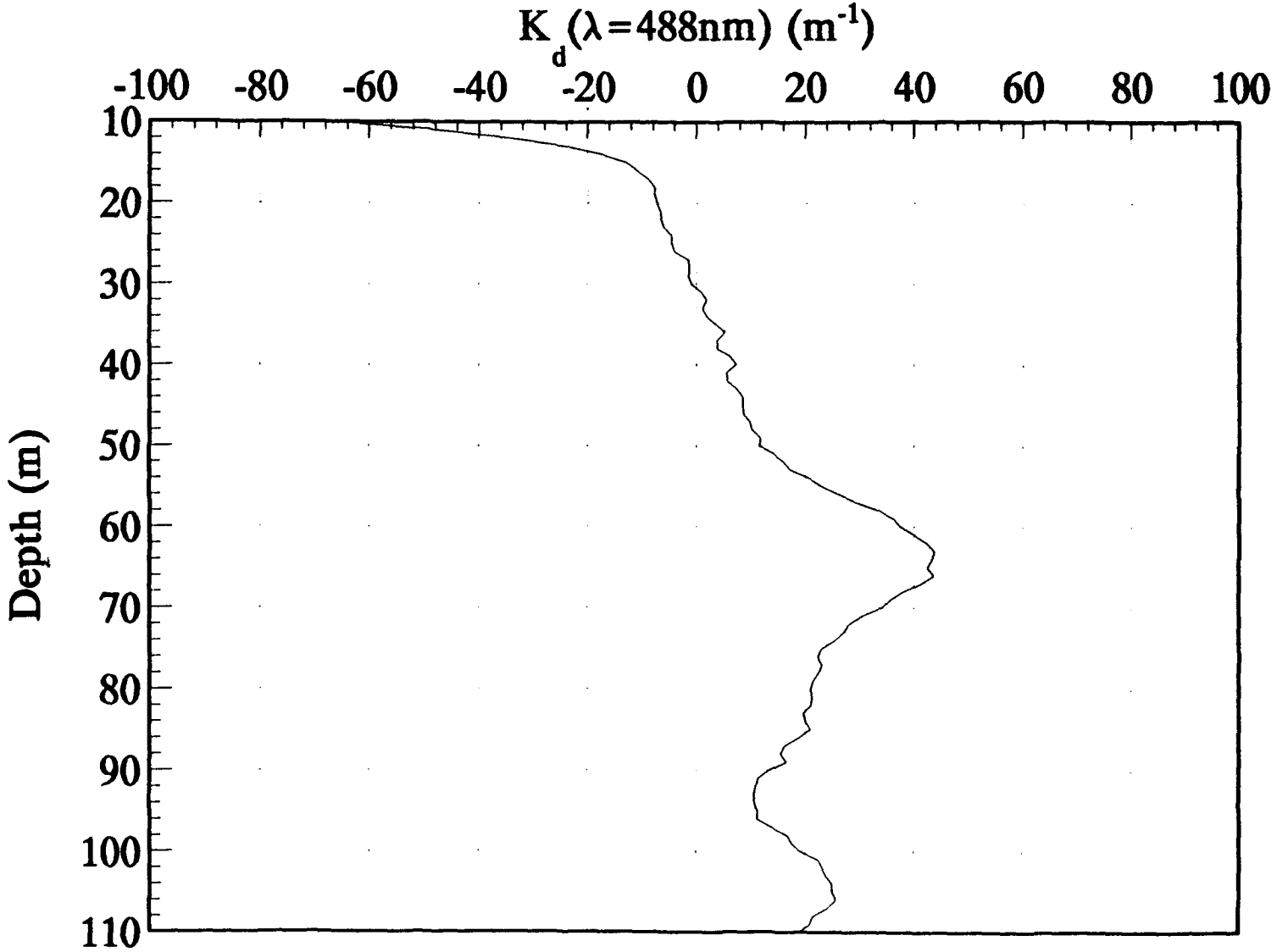

1990 Pacific AXKT Test
AXKT Channel 16 Drop 4

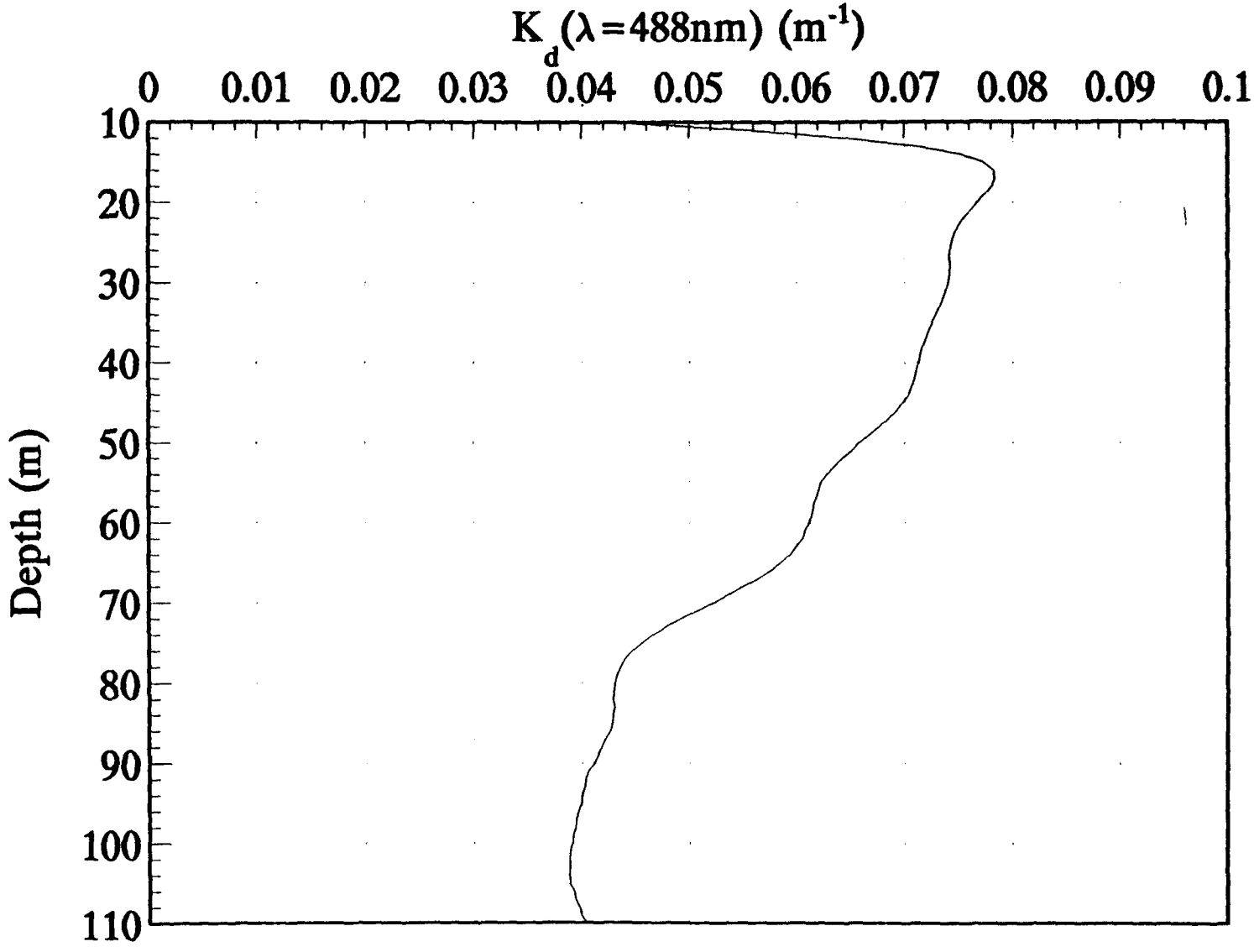

1990 Pacific AXKT Test
AXKT Channel 16 Drop 4 (% Difference From MER Data)

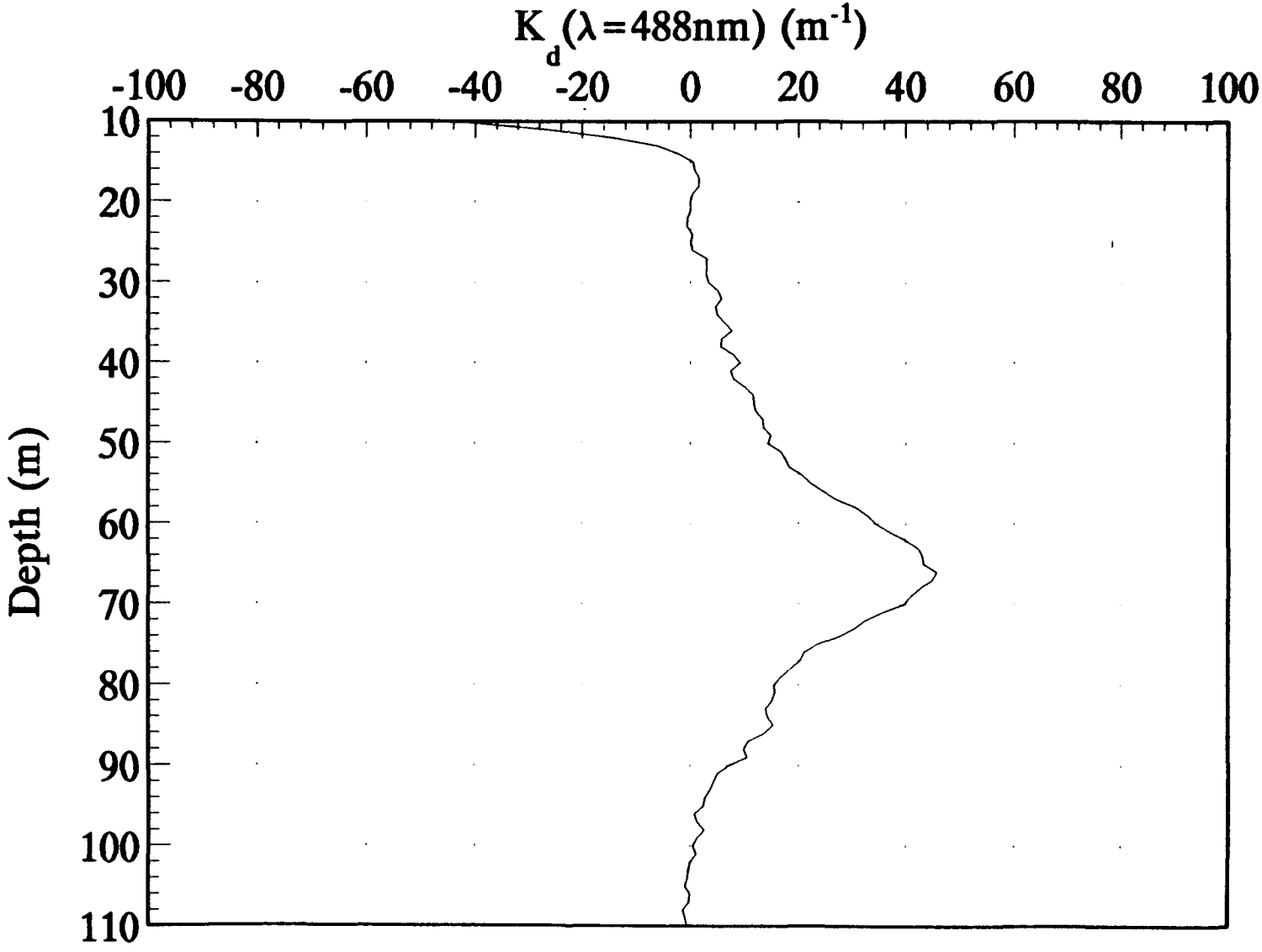

1990 Pacific AXKT Test
AXKT Channel 14 Drop 6

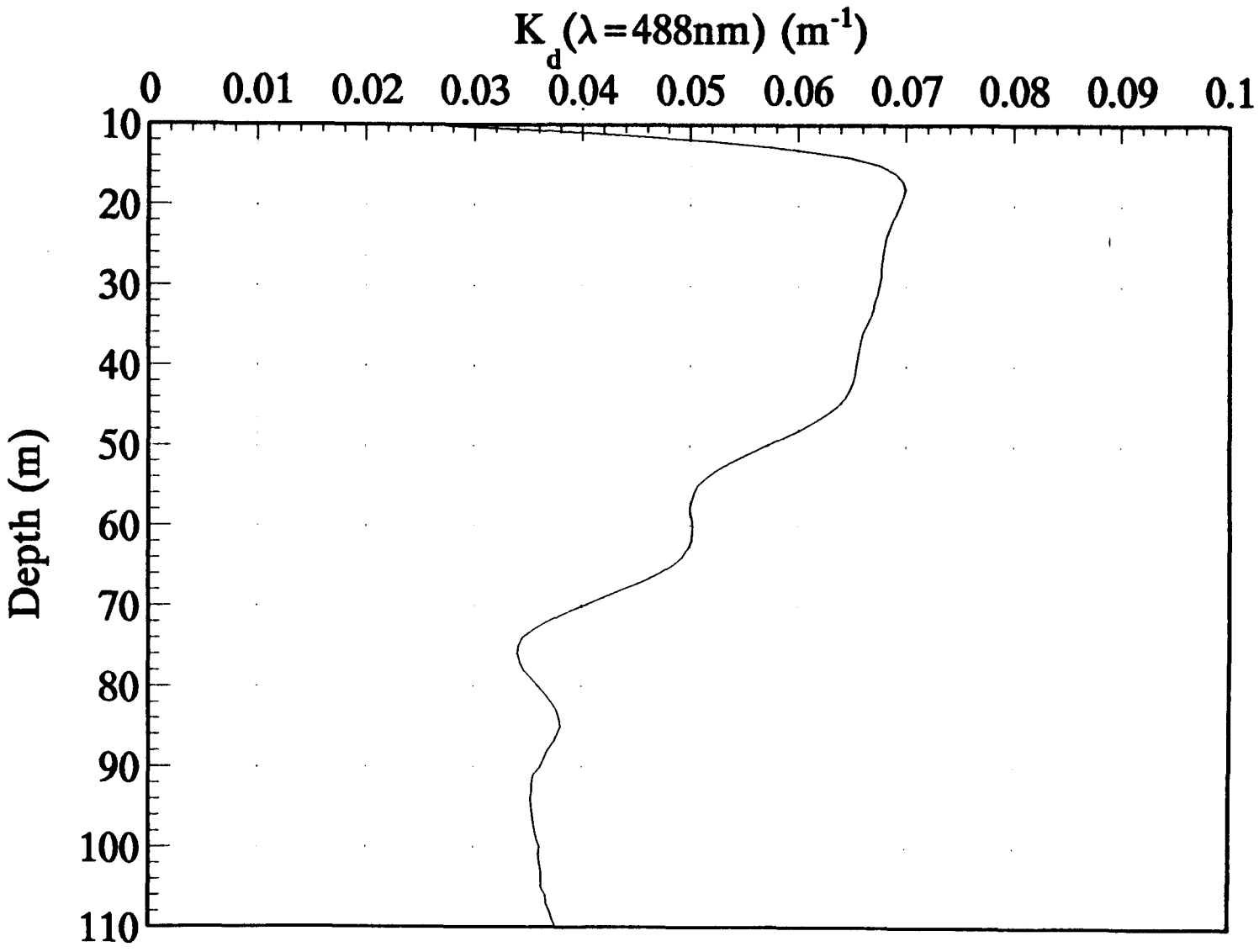

1990 Pacific AXKT Test
AXKT Channel 14 Drop 6 (% Difference From MER Data)

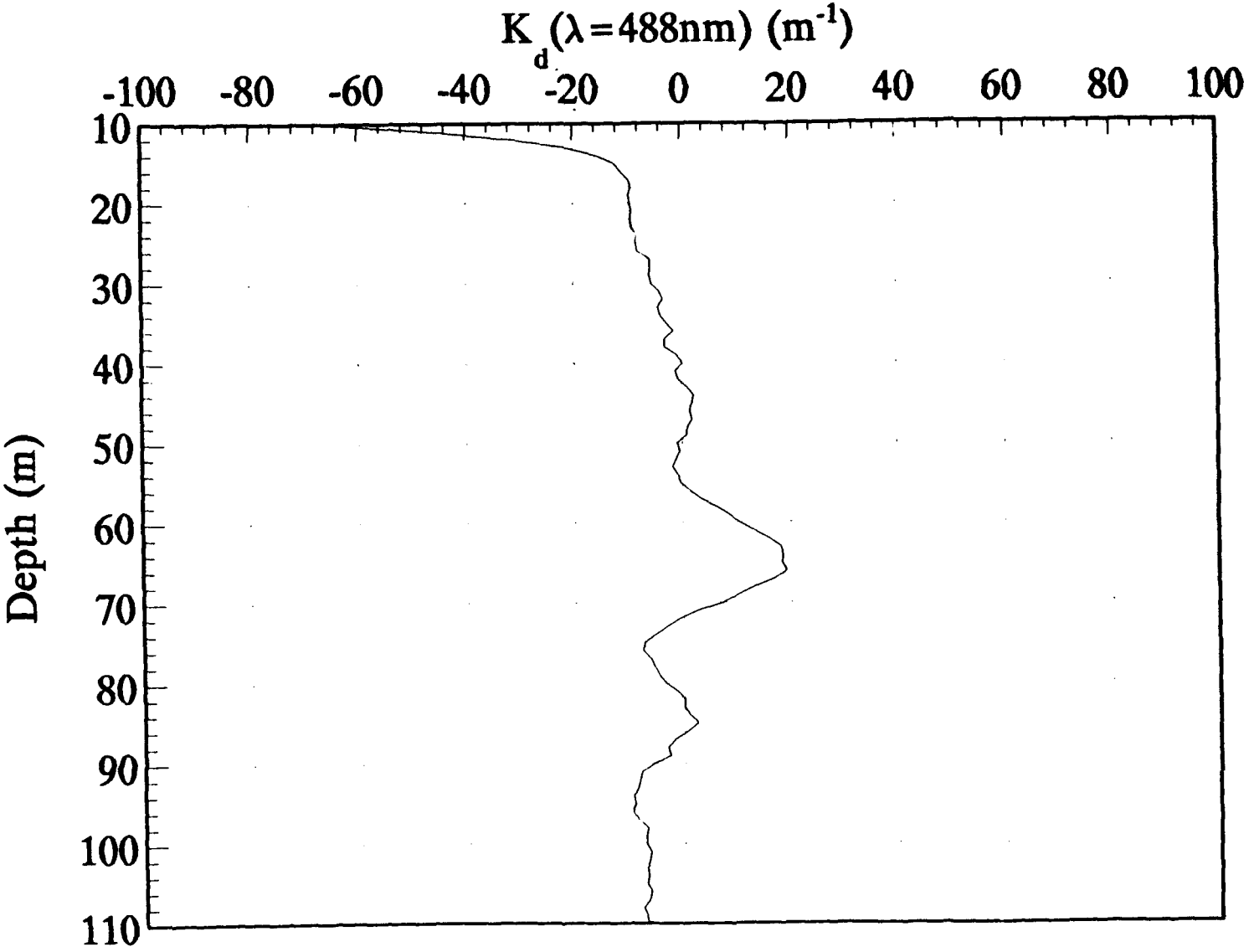

1990 Pacific AXKT Test
AXKT Channel 16 Drop 6

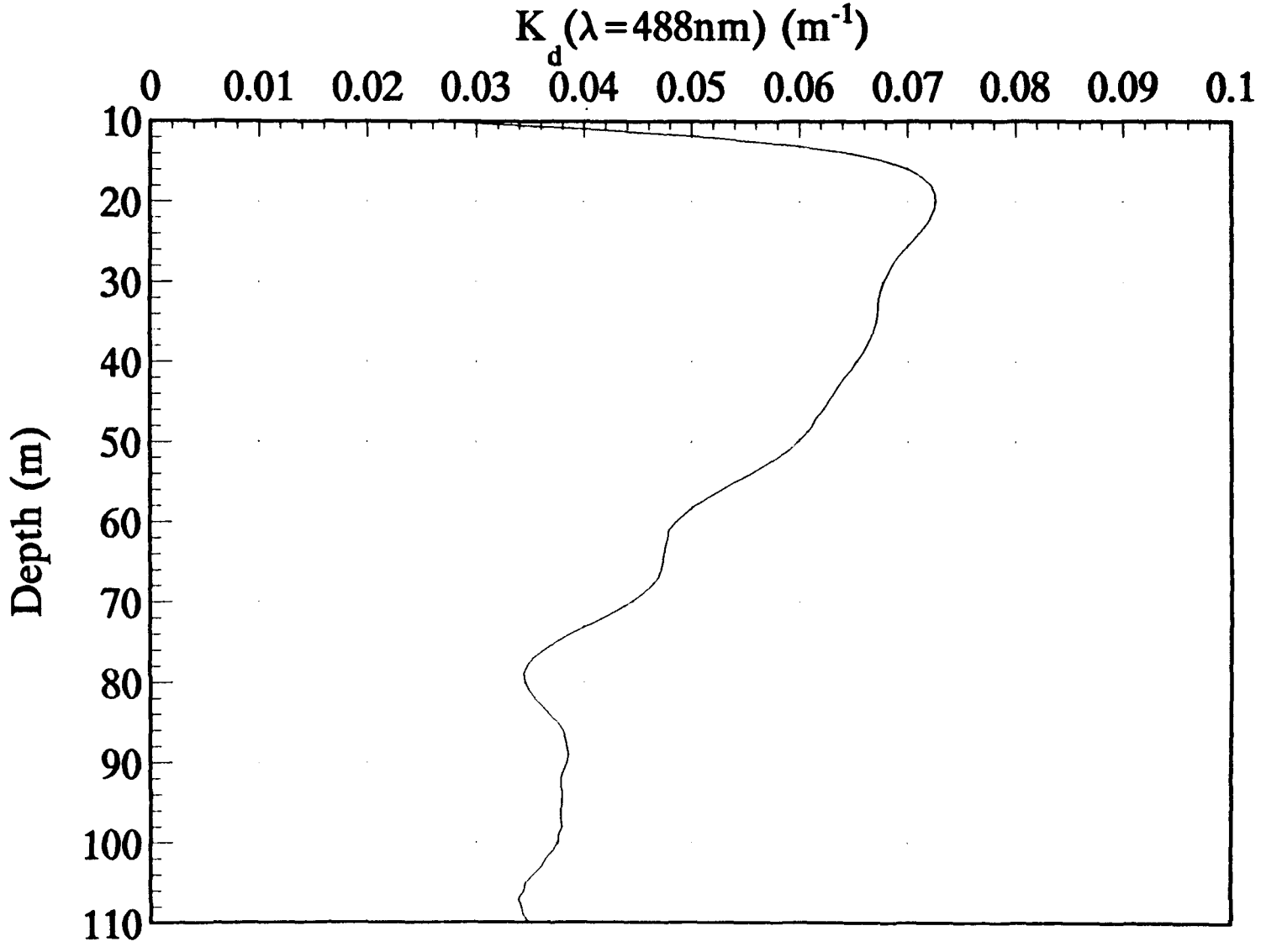

1990 Pacific AXKT Test
AXKT Channel 16 Drop 6 (% Difference From MER Data)

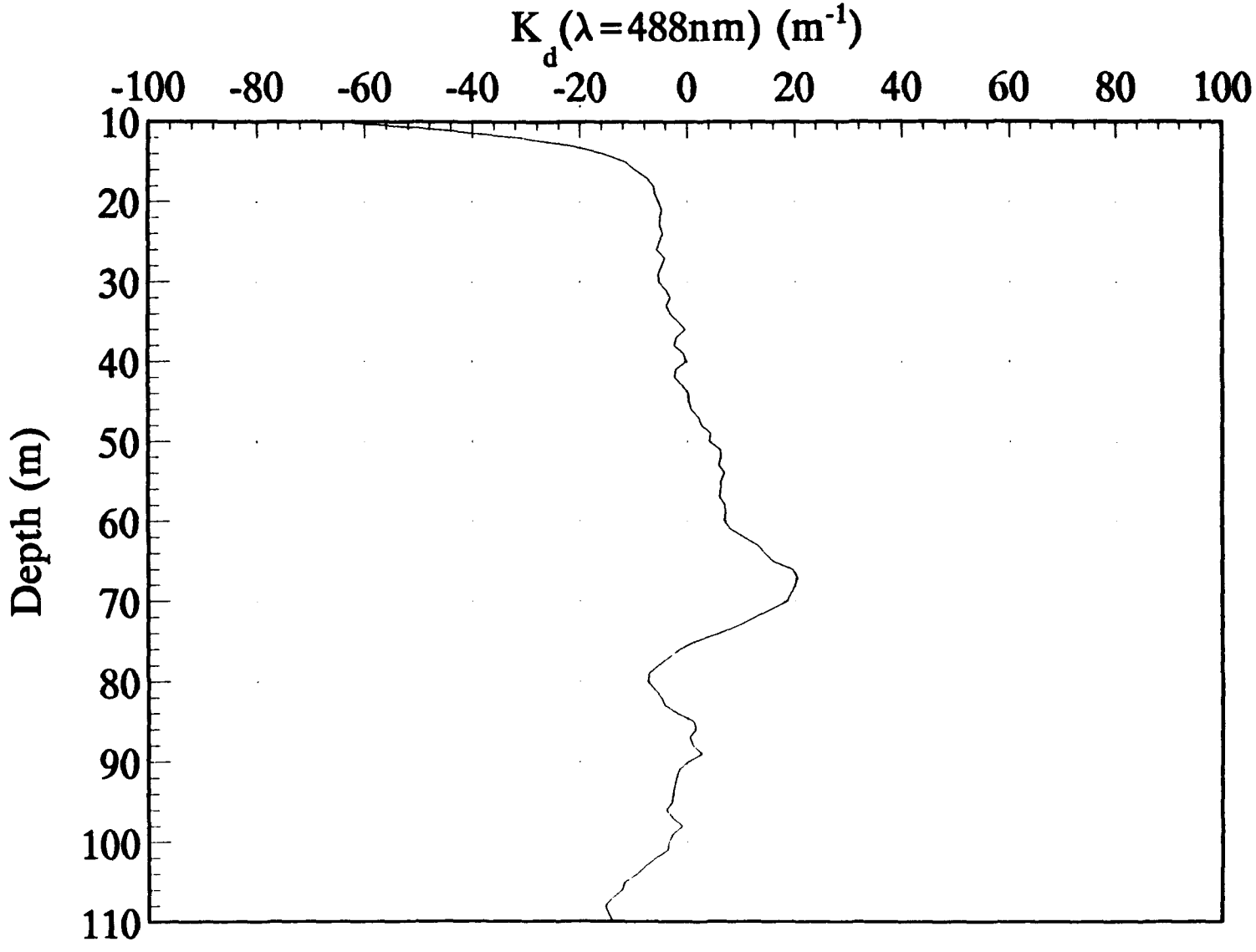

1990 Pacific AXKT Test
AXKT Channel 12 Drop 7

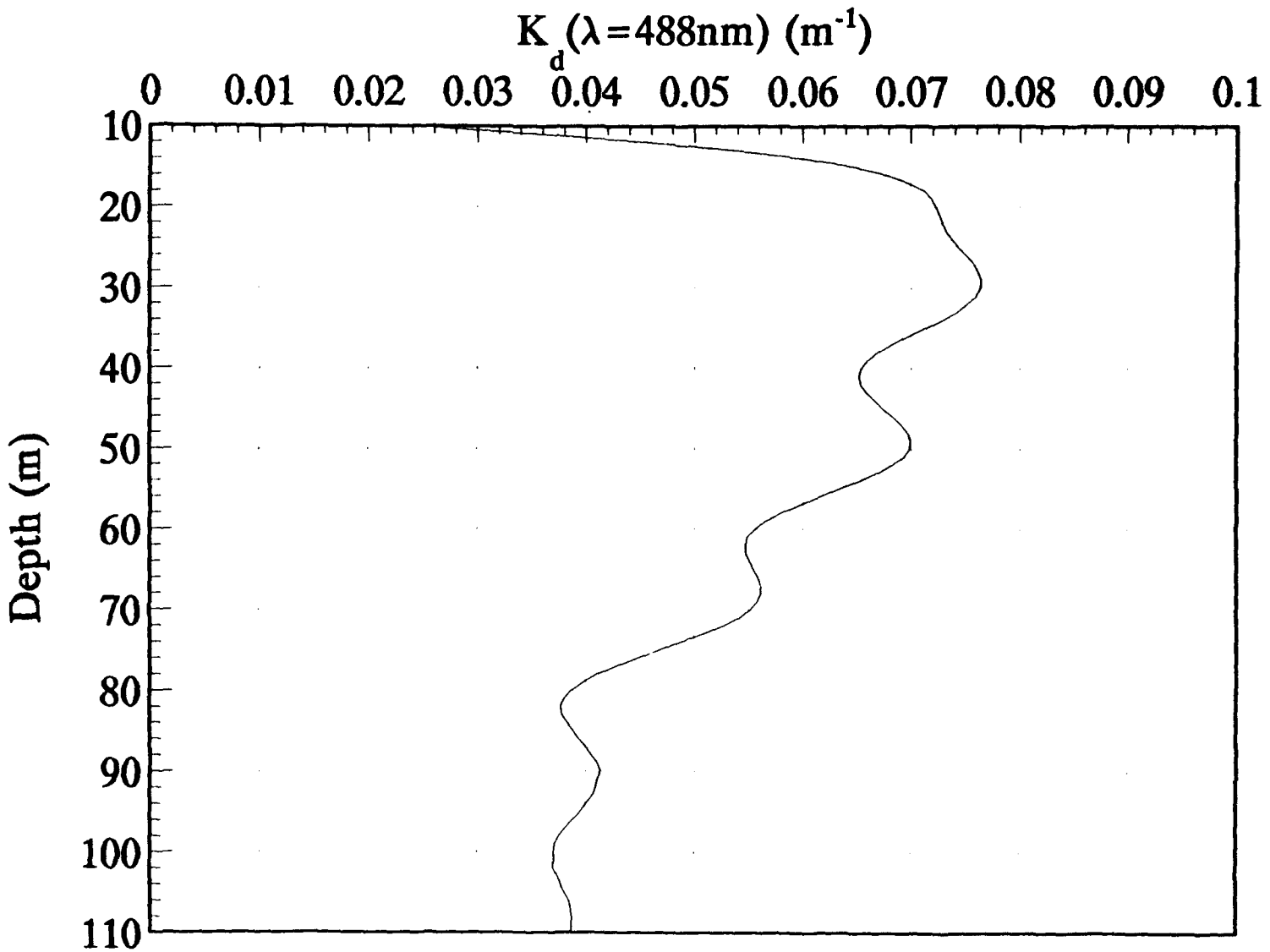

1990 Pacific AXKT Test
AXKT Channel 12 Drop 7 (% Difference From MER Data)

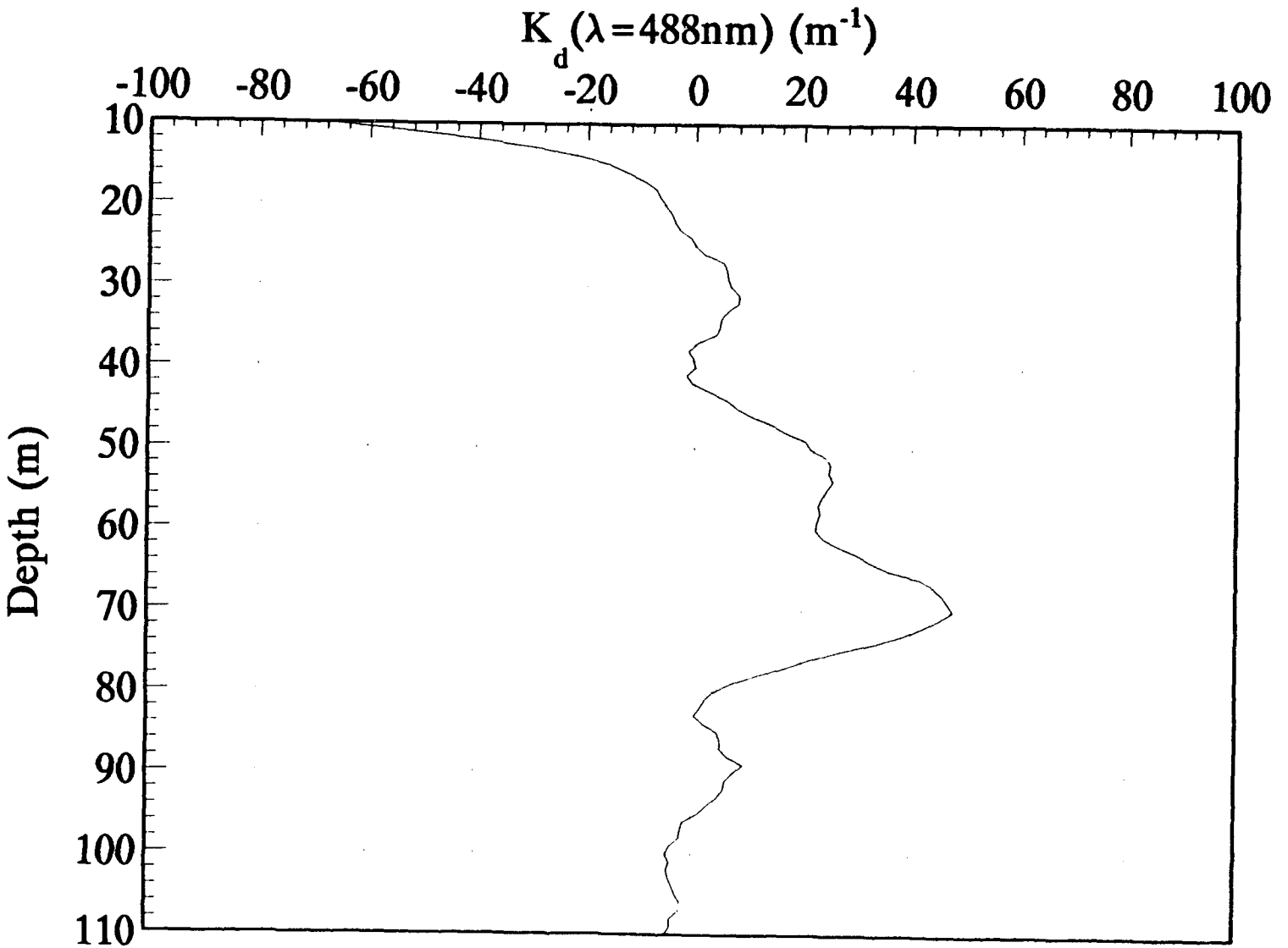

1990 Pacific AXKT Test
AXKT Channel 14 Drop 7

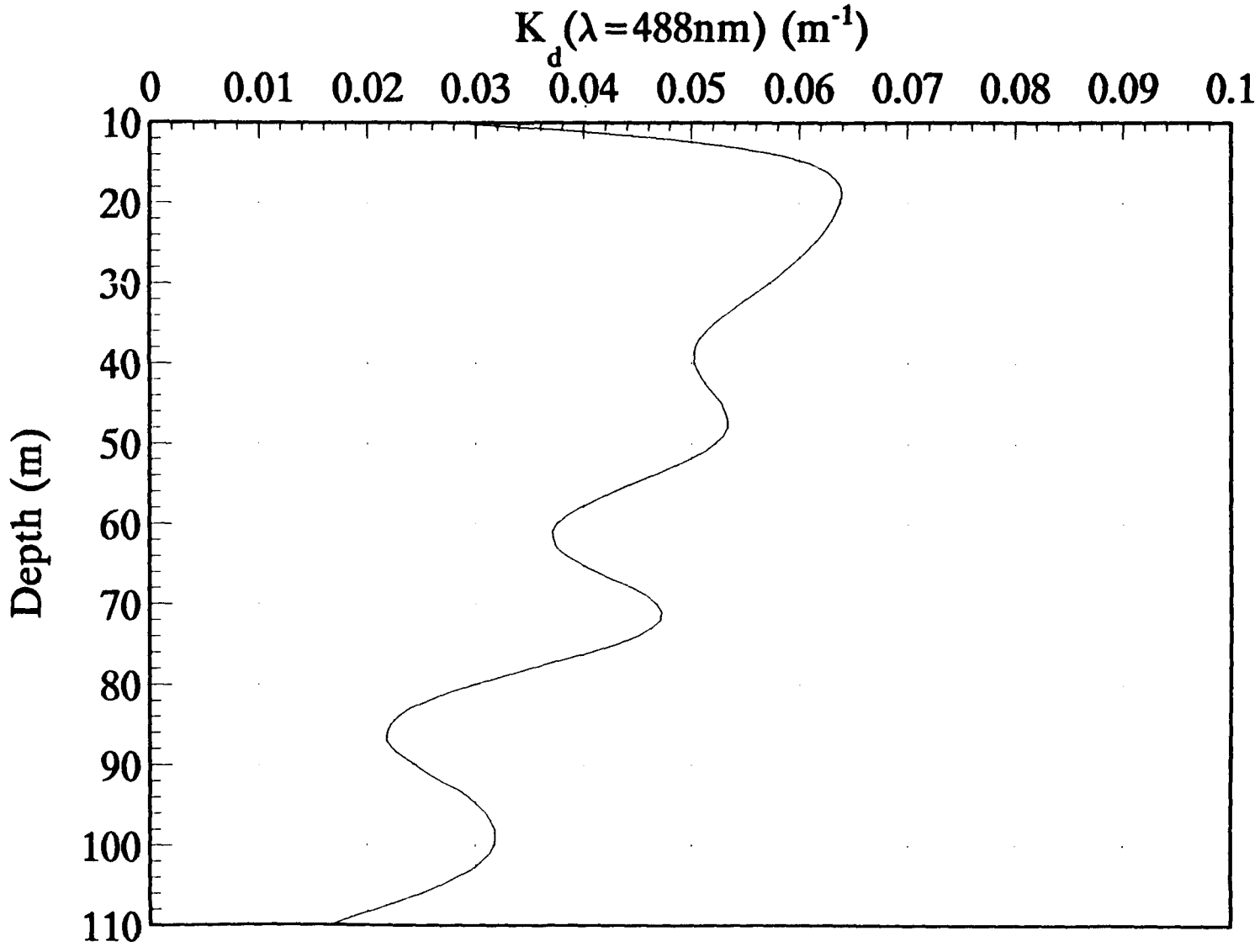

1990 Pacific AXKT Test
AXKT Channel 14 Drop 7 (% Difference From MER Data)

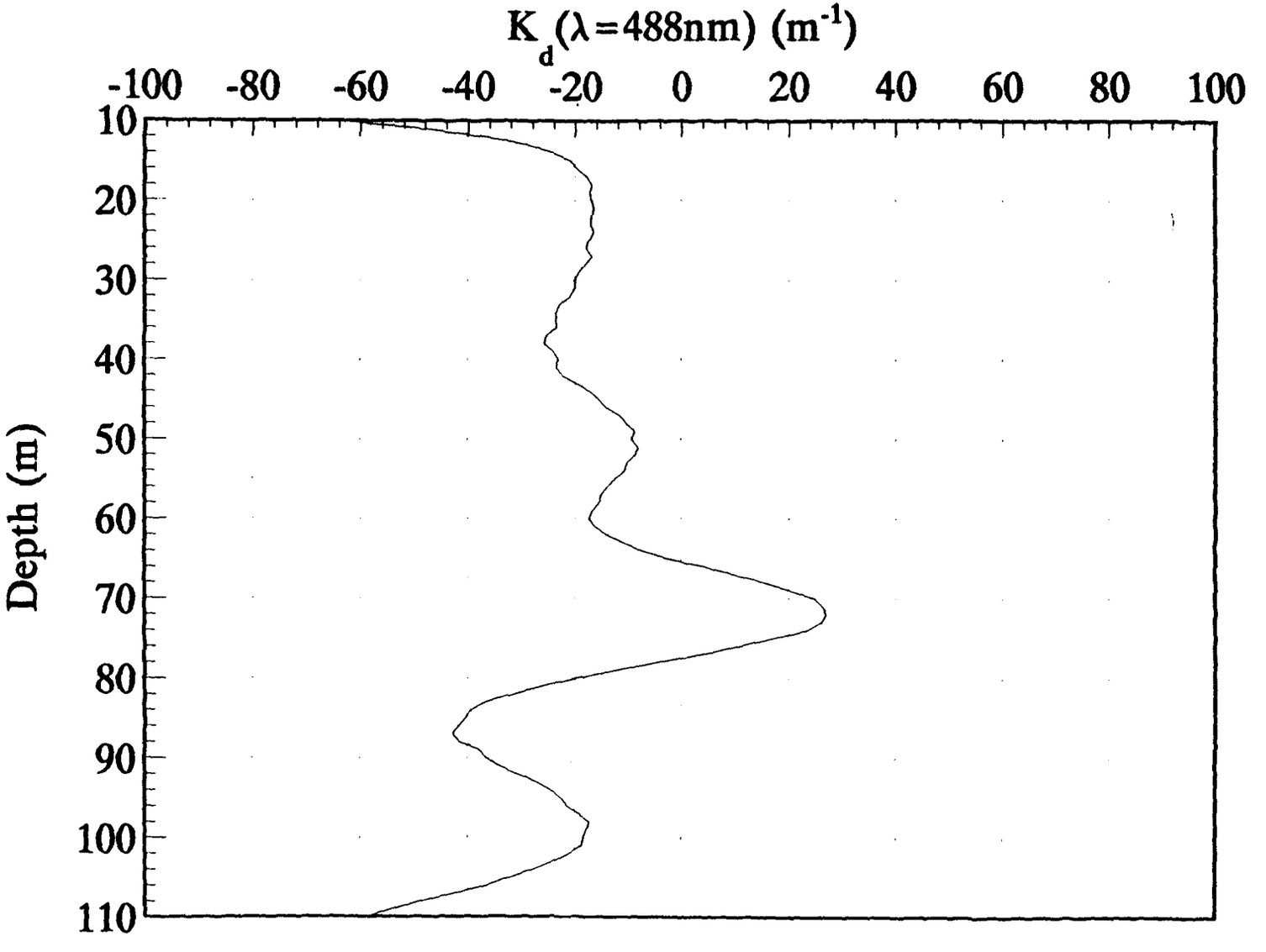

1990 Pacific AXKT Test
AXKT Channel 16 Drop 7

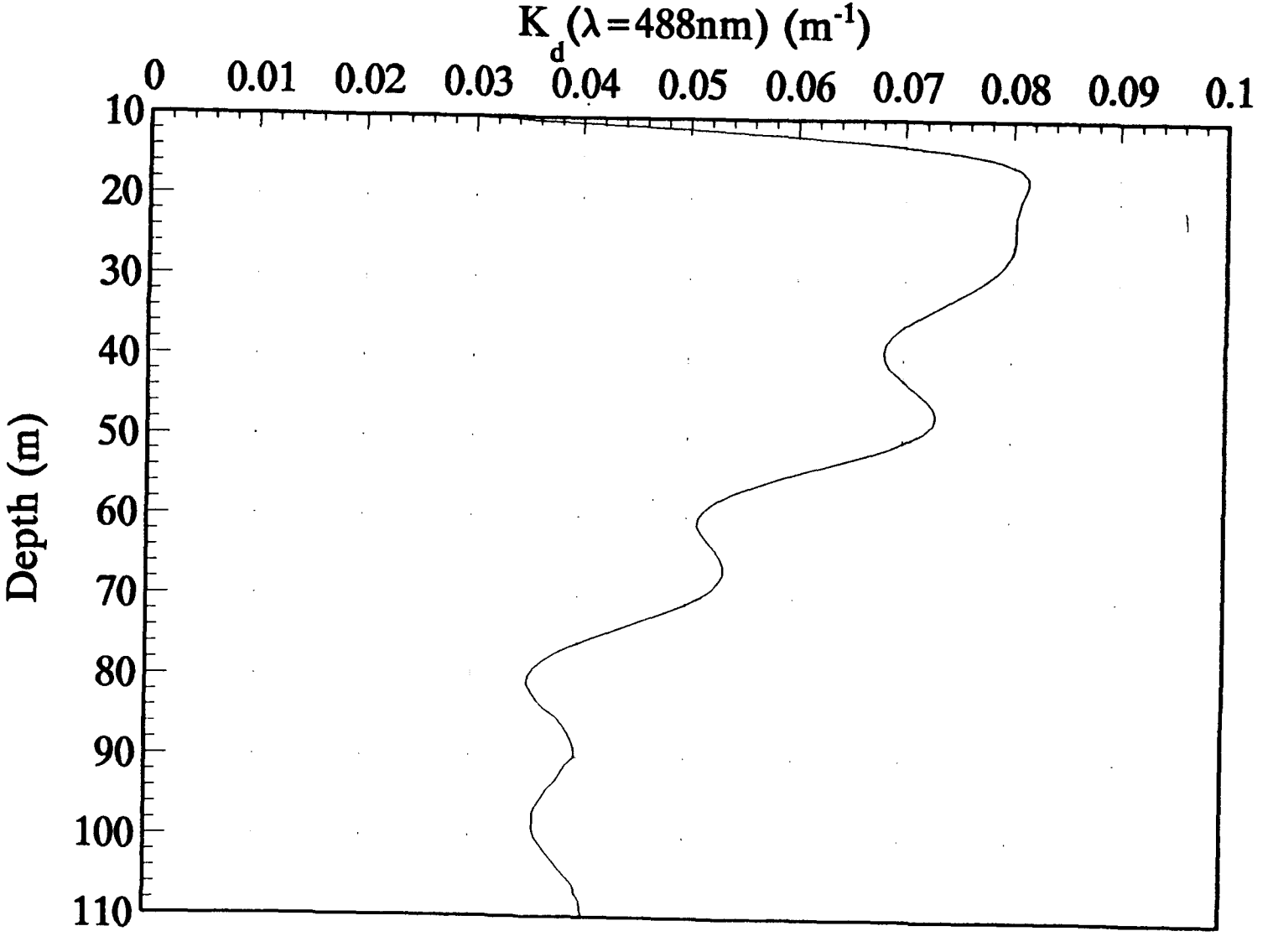

1990 Pacific AXKT Test
AXKT Channel 16 Drop 7 (% Difference From MER Data)

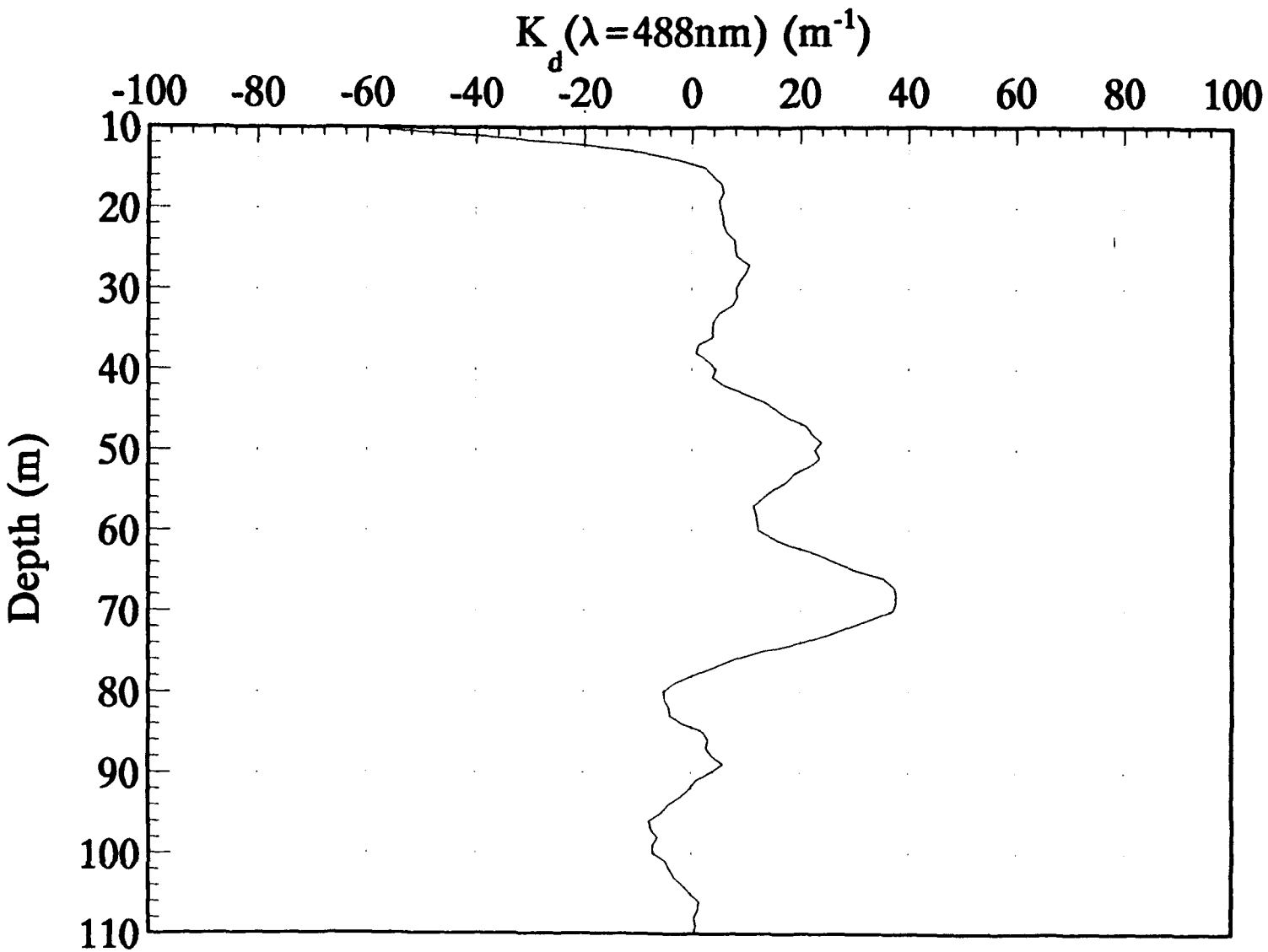

1990 Pacific AXKT Test
AXKT Channel 12 Drop 8

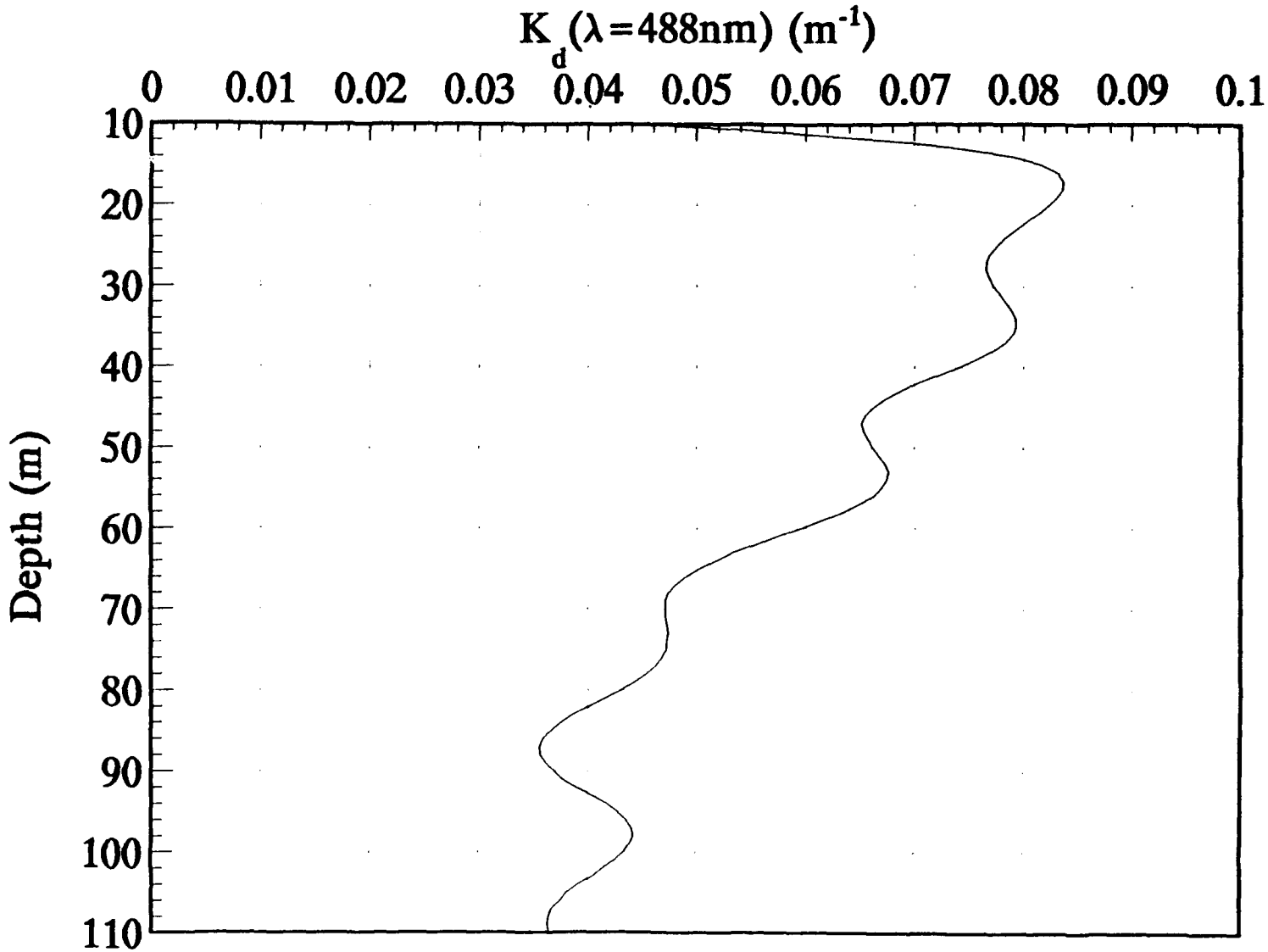

1990 Pacific AXKT Test
AXKT Channel 12 Drop 8 (% Difference From MER Data)

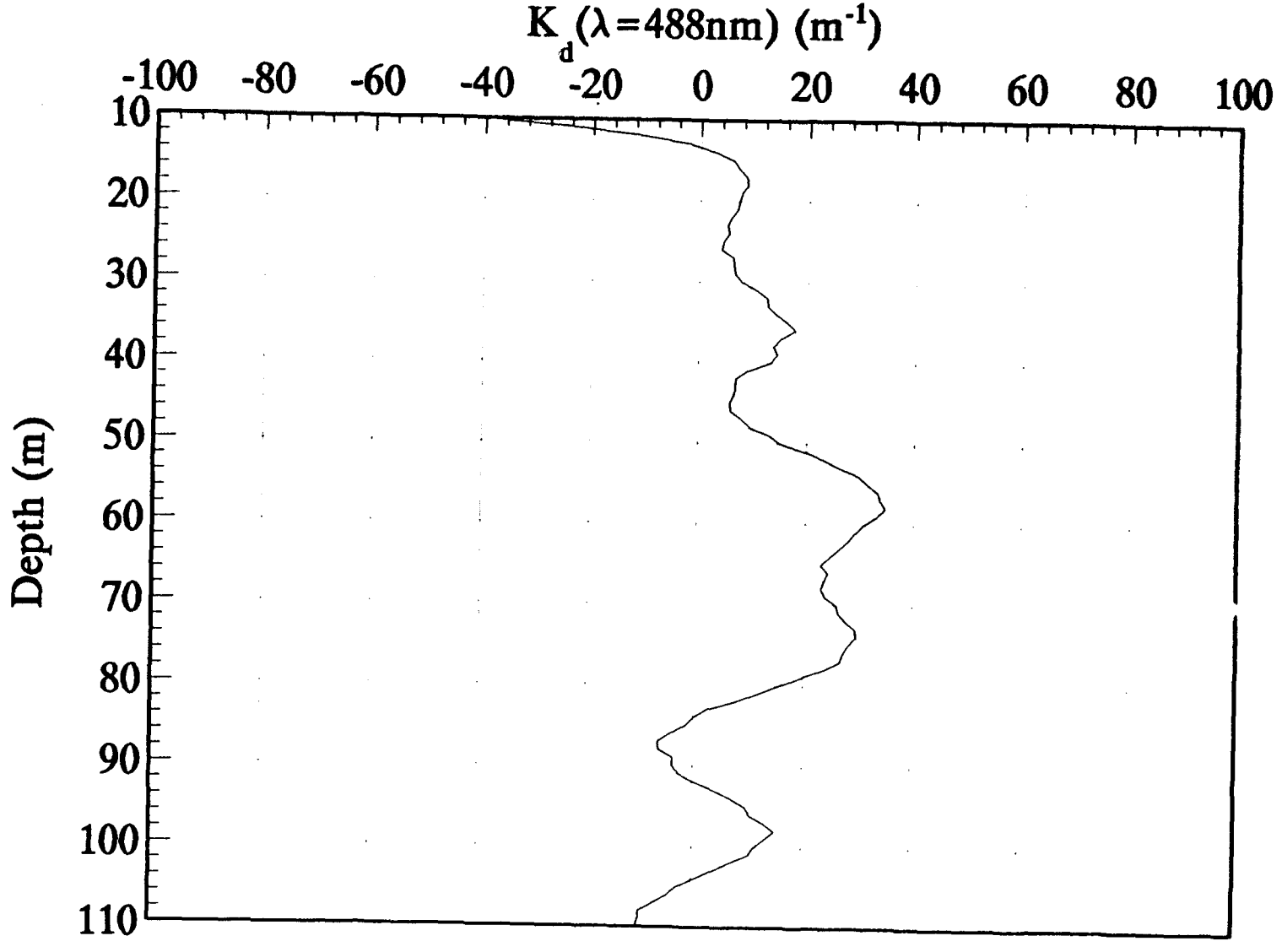

1990 Pacific AXKT Test
AXKT Channel 14 Drop 8

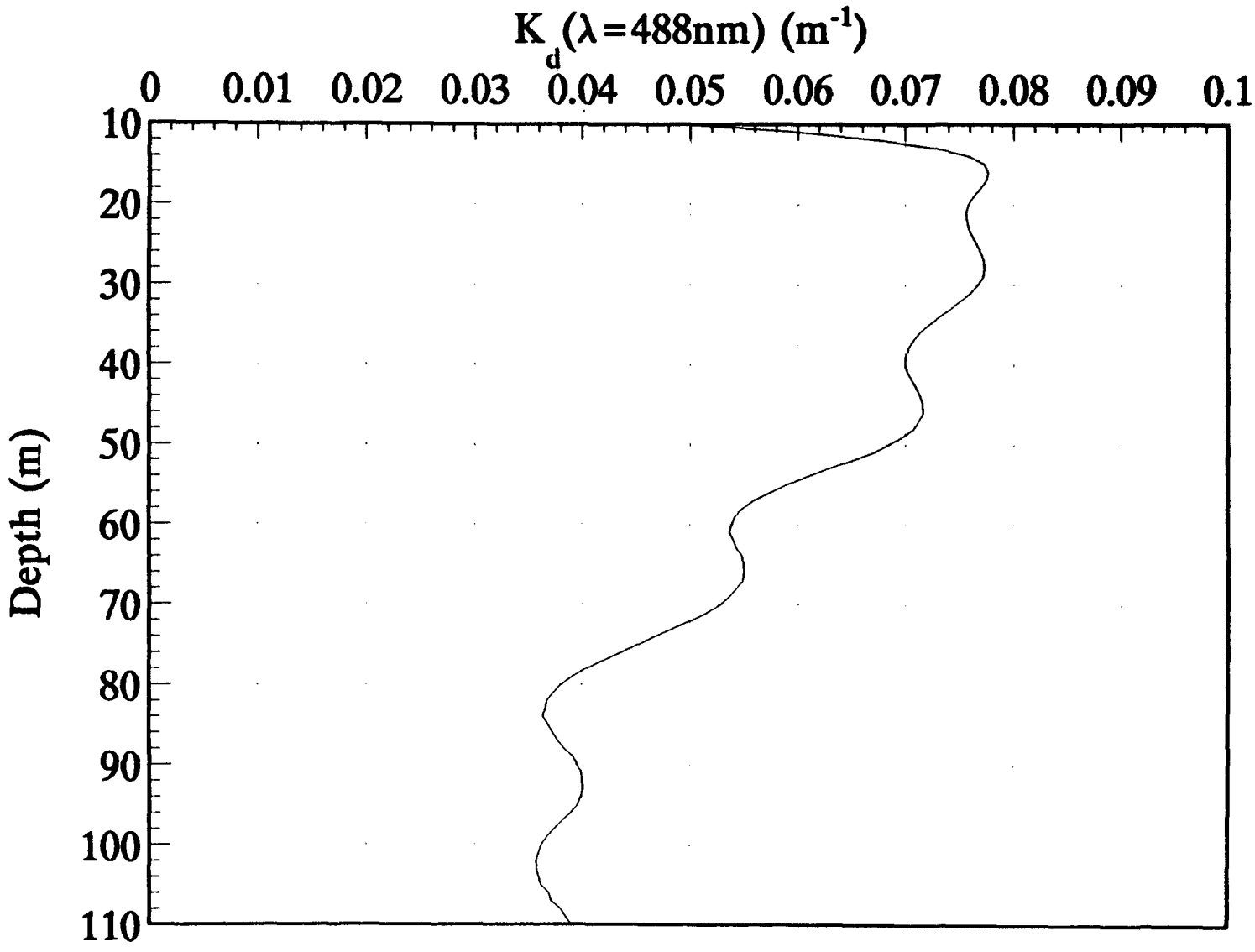

1990 Pacific AXKT Test
AXKT Channel 1 Drop 8 (% Difference From MER Data)

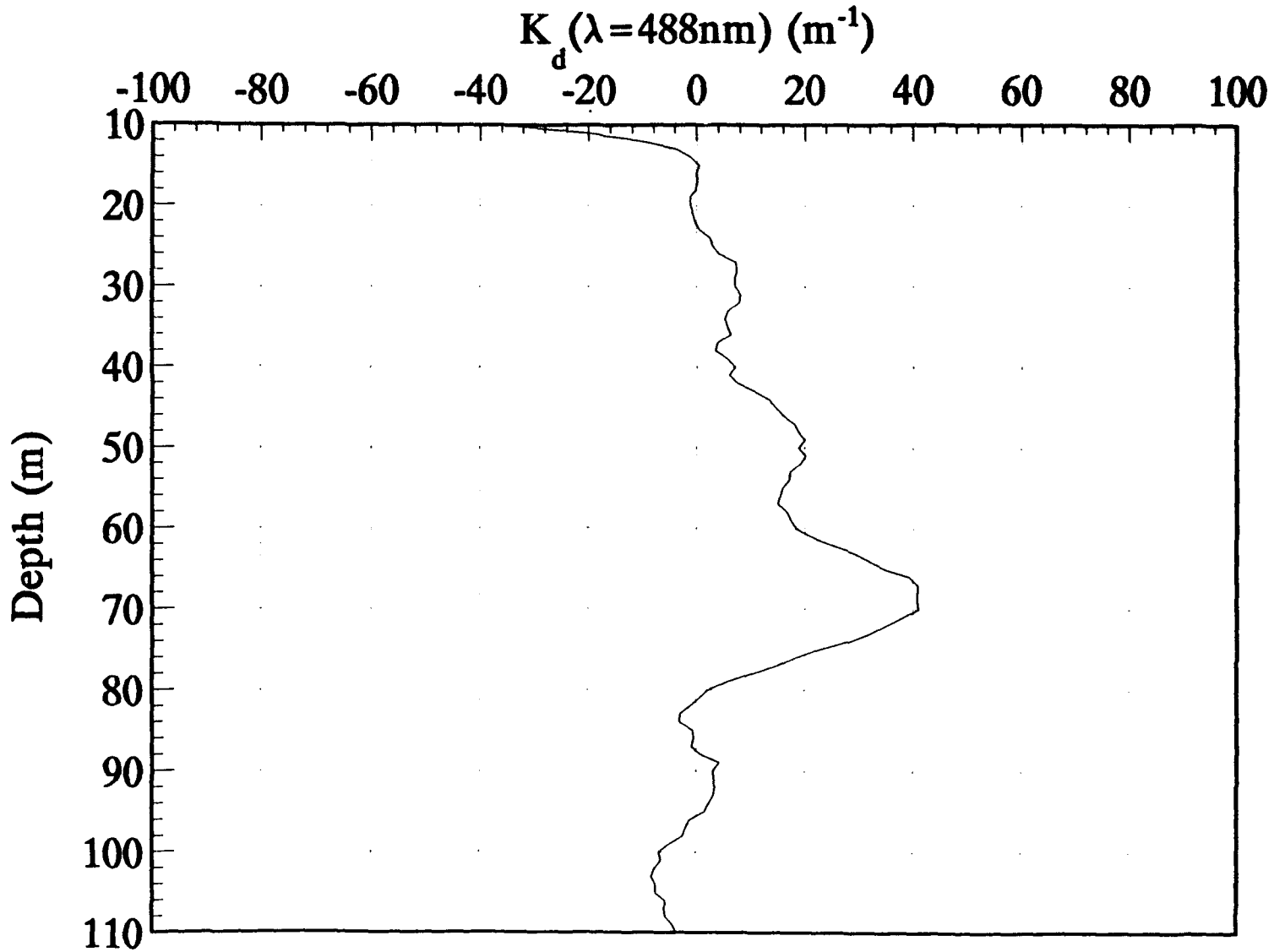

Appendix D

Comparison of MER and AXKT K_d Profiles for Pacific 1992 Test

1992 Pacific AXKT Test
MER Mean Data (+/- s.d.)

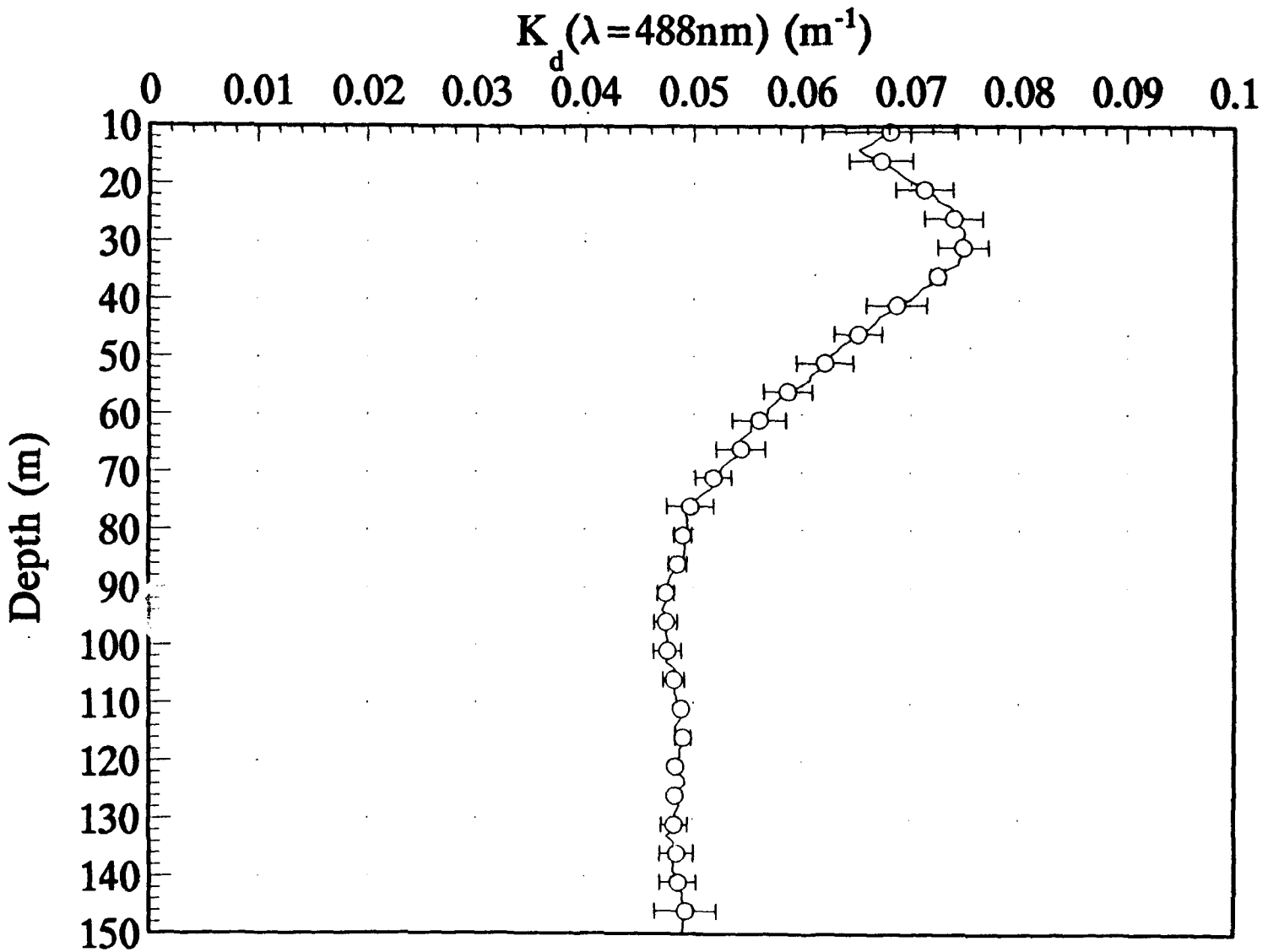

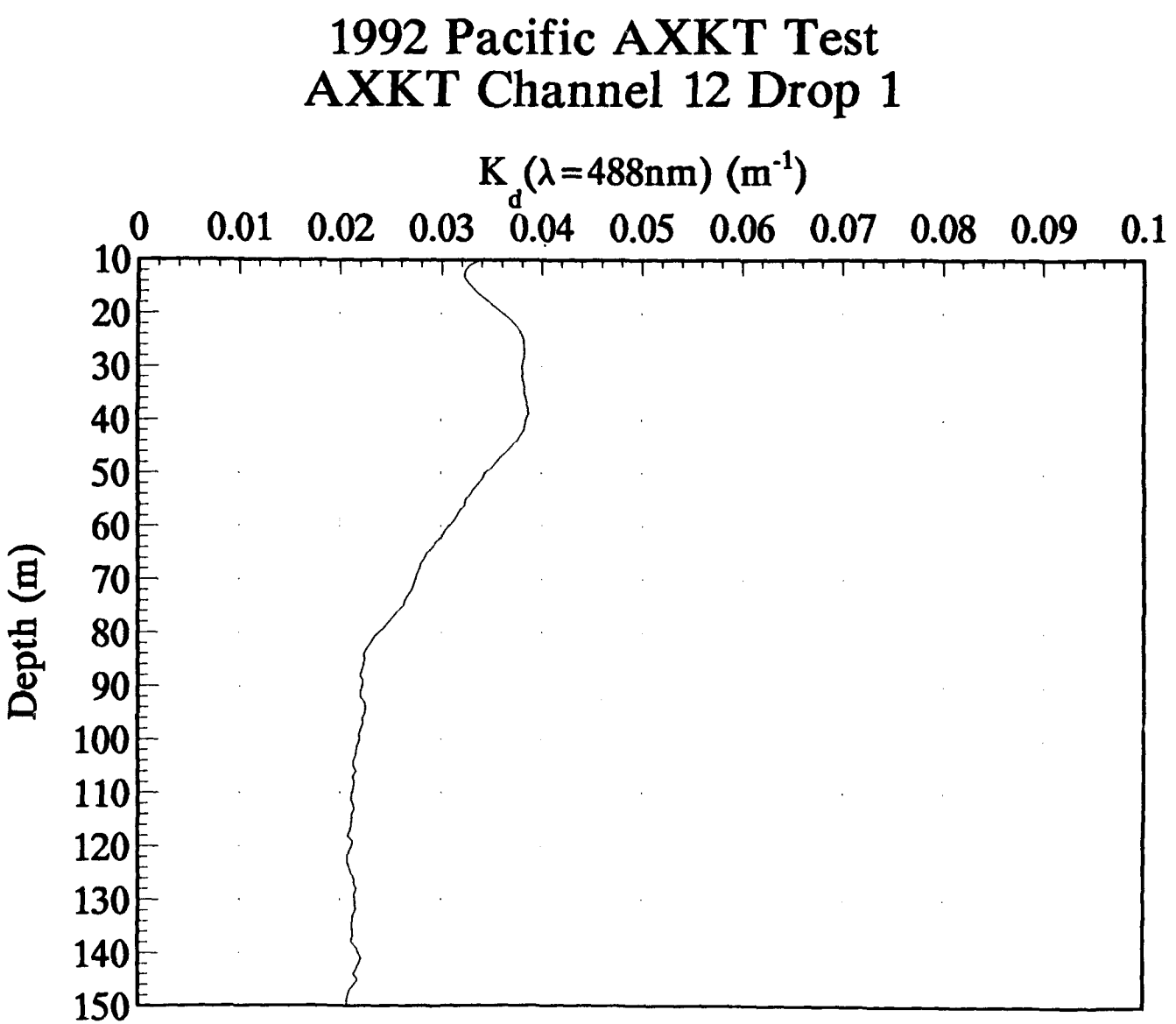
1992 Pacific AXKT Test
AXKT Channel 12 Drop 1
K d (λ=488nm) (m-1)
0
0.01
0.02
0.03
0.04
0.05
0.06
0.07
0.08
0.09
0.1
Depth (m)
10
20
30
40
50
60
70
80
90
100
110
120
130
140
150

1992 Pacific AXKT Test
AXKT Channel 12 Drop 1 (% Difference From MER Data)

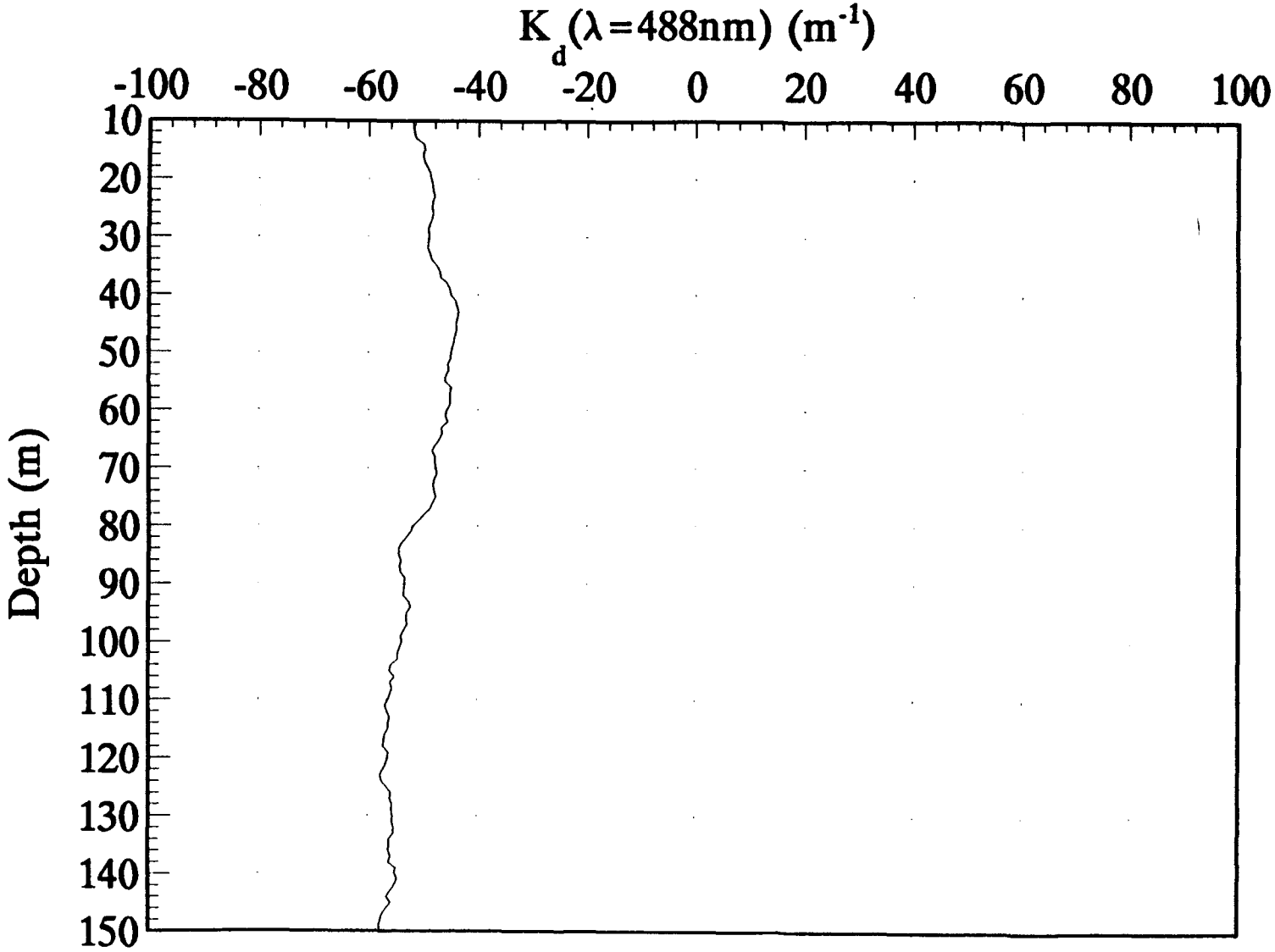

1992 Pacific AXKT Test
AXKT Channel 14 Drop 2

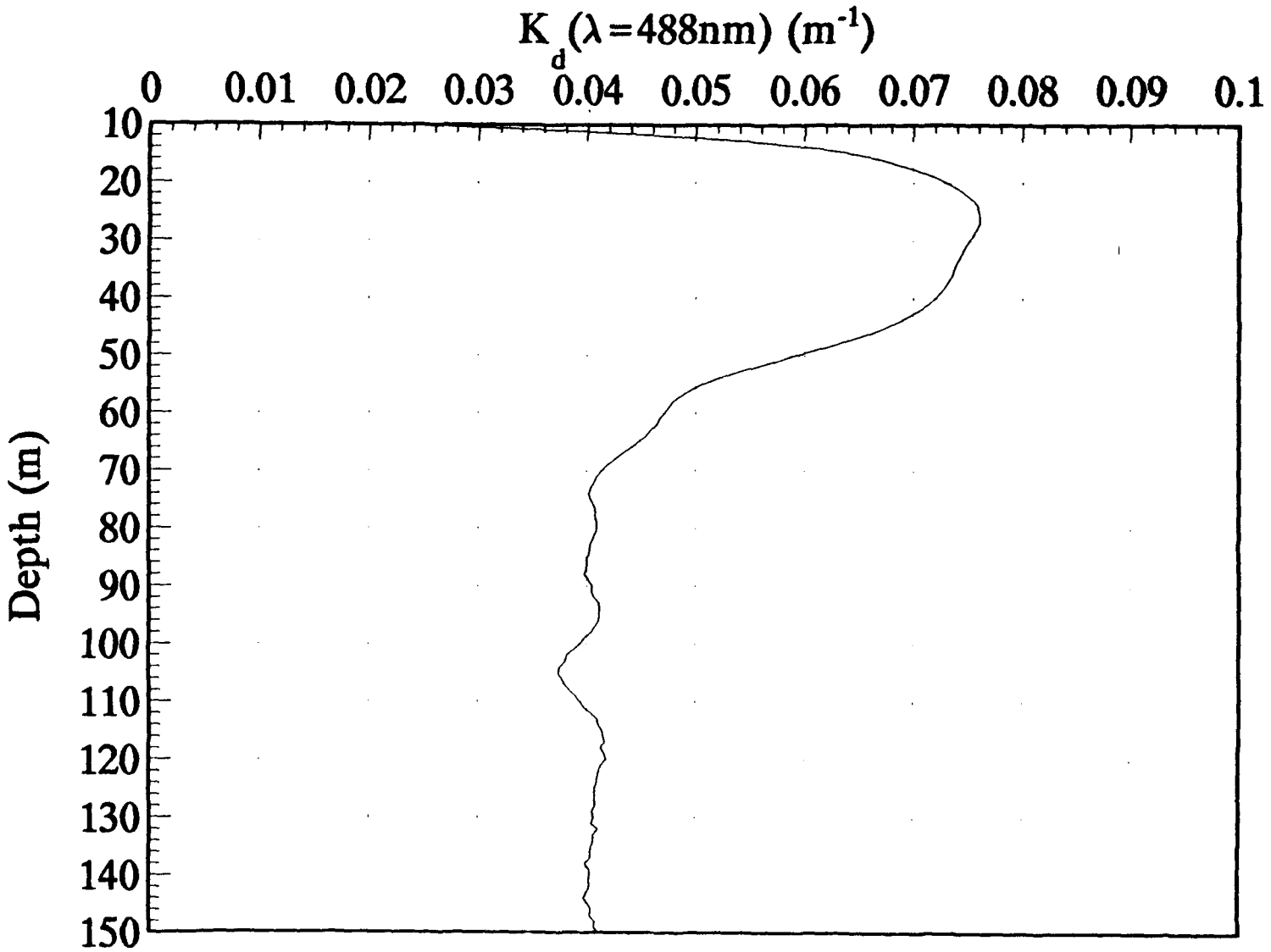

1992 Pacific AXKT Test
AXKT Channel 14 Drop 2 (% Difference From MER Data)

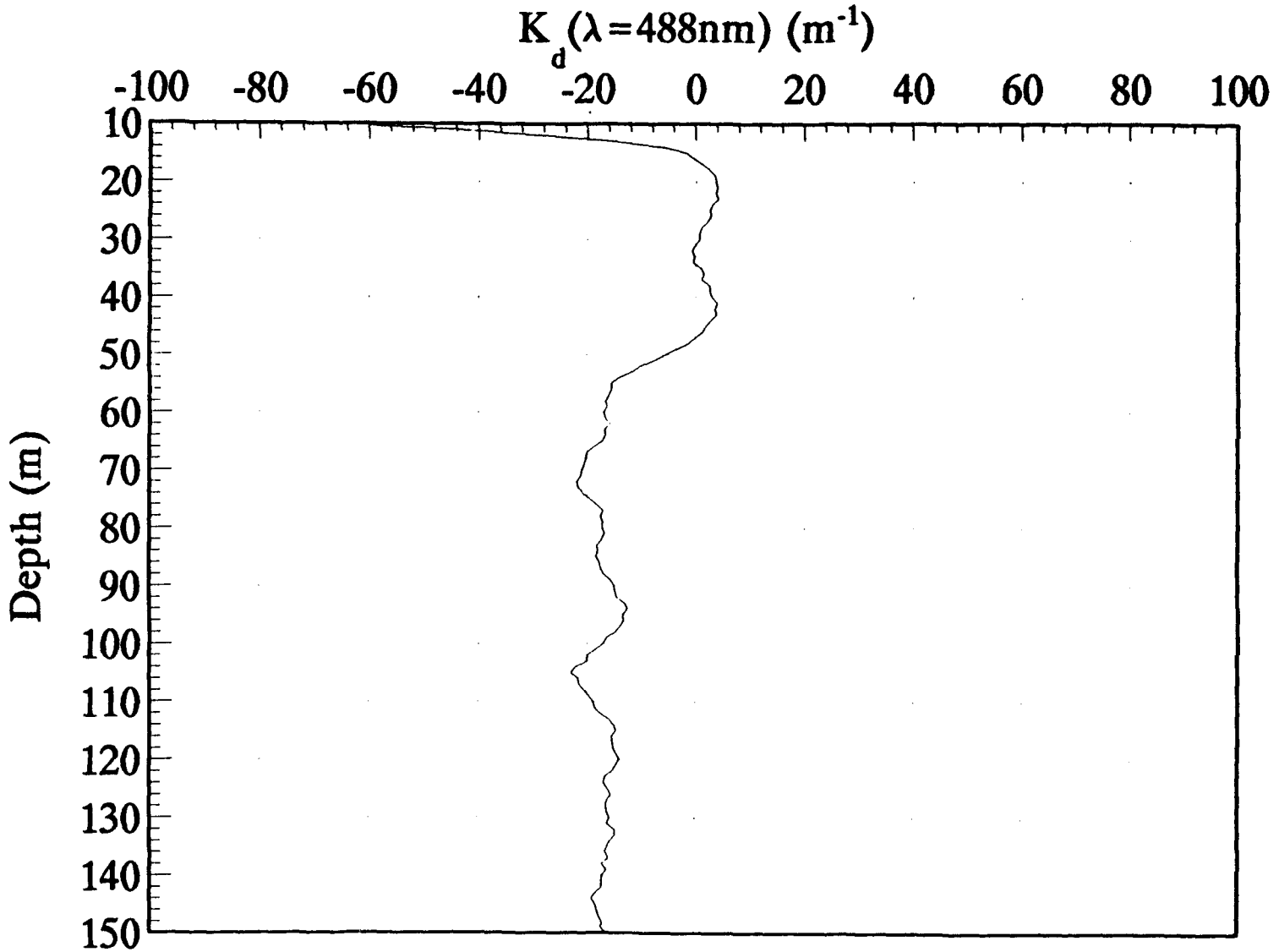

1992 Pacific AXKT Test
AXKT Channel 12 Drop 4

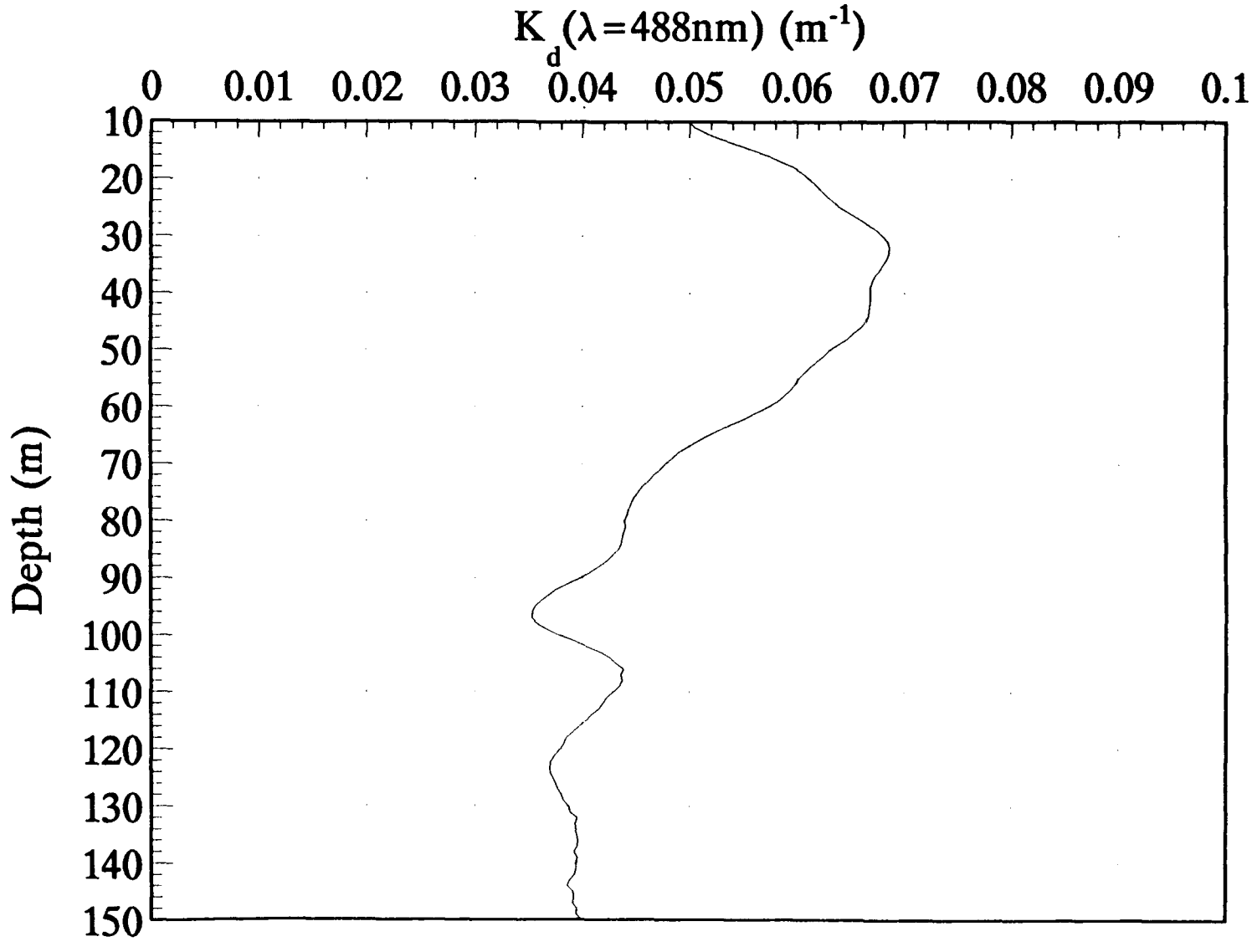

1992 Pacific AXKT Test
AXKT Channel 12 Drop 4 (% Difference From MER Data)

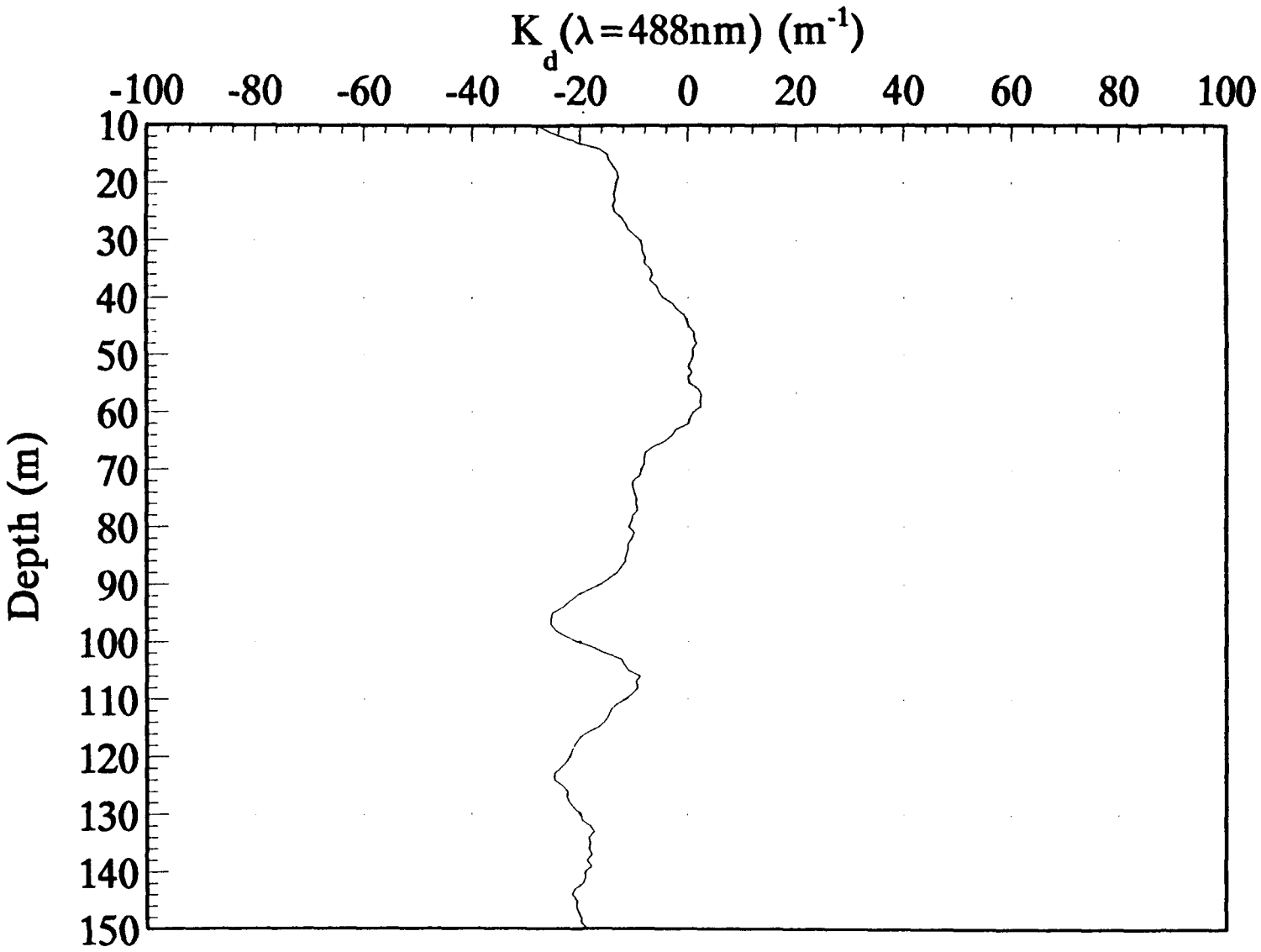

1992 Pacific AXKT Test
AXKT Channel 14 Drop 5

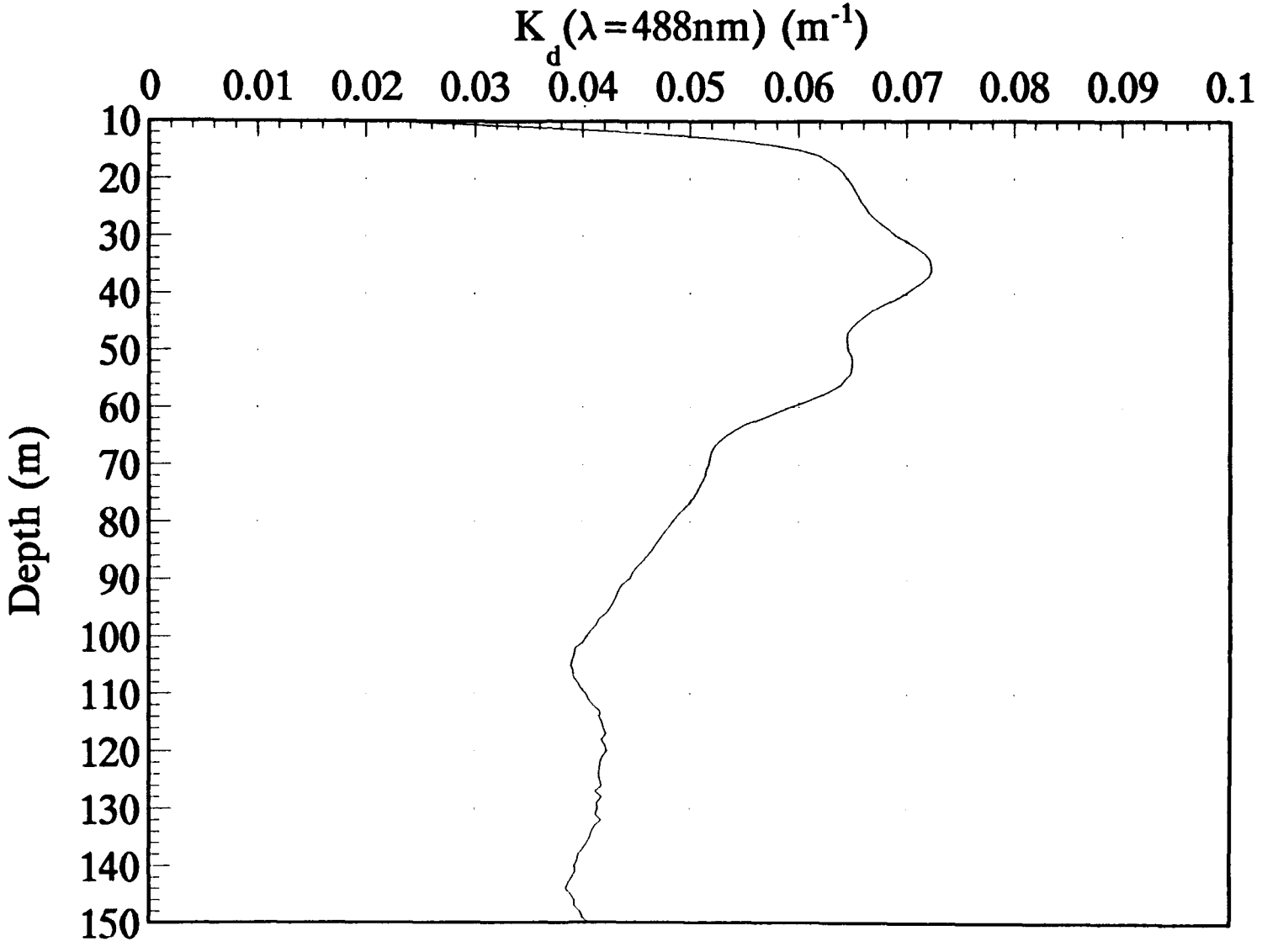

1992 Pacific AXKT Test
AXKT Channel 14 Drop 5 (% Difference From MER Data)

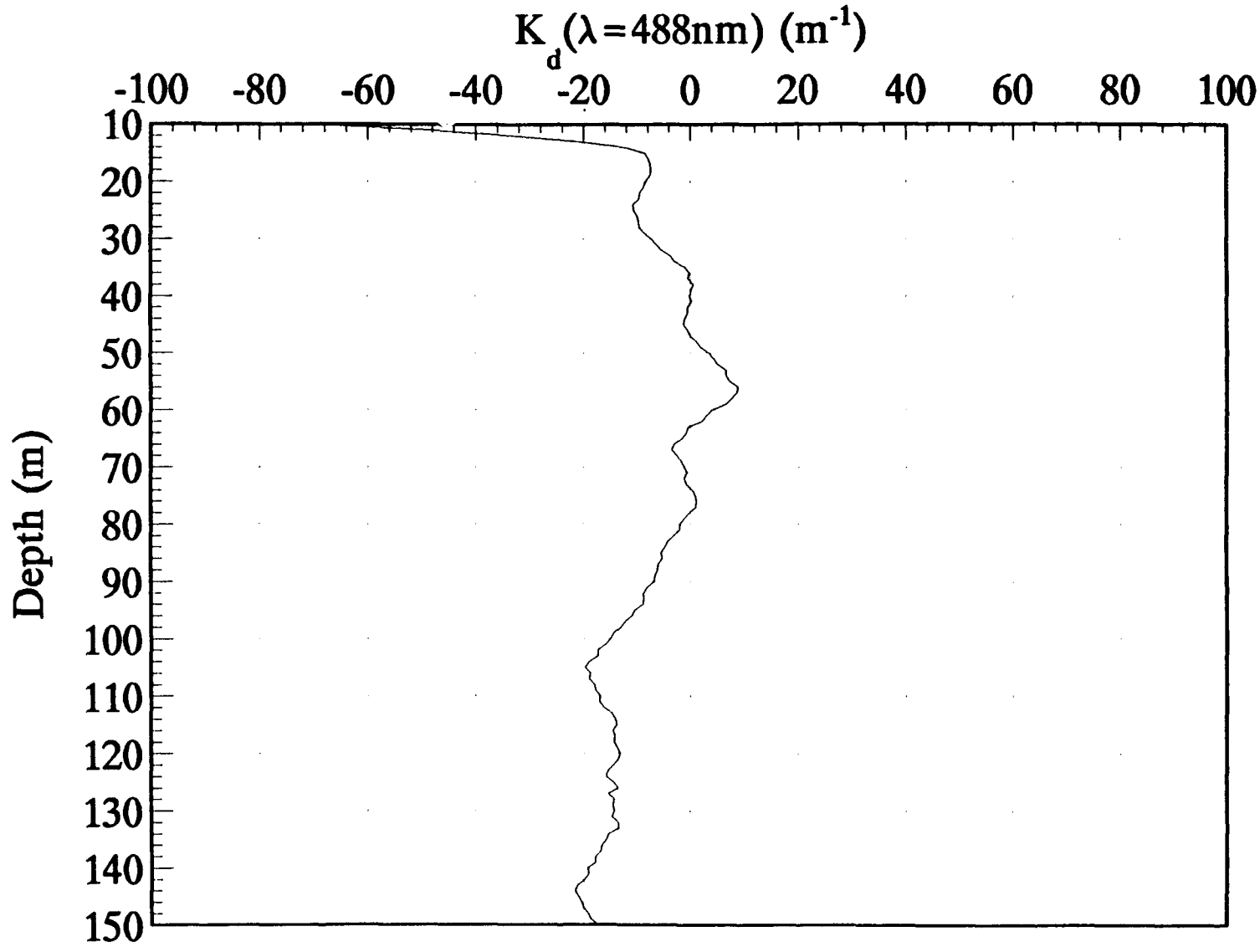

1992 Pacific AXKT Test
AXKT Channel 12 Drop 6

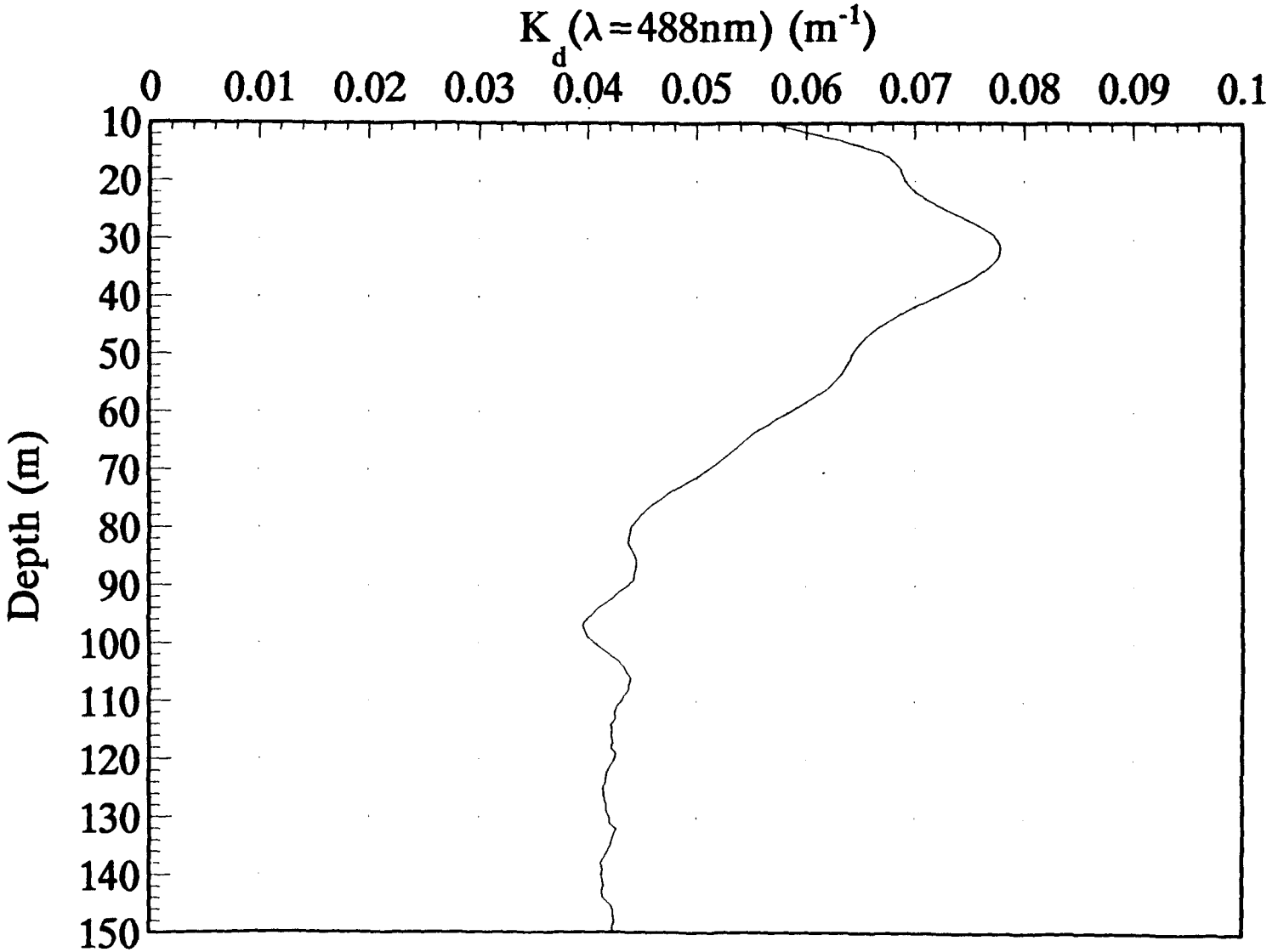

1992 Pacific AXKT Test
AXKT Channel 12 Drop 6 (% Difference From MER Data)

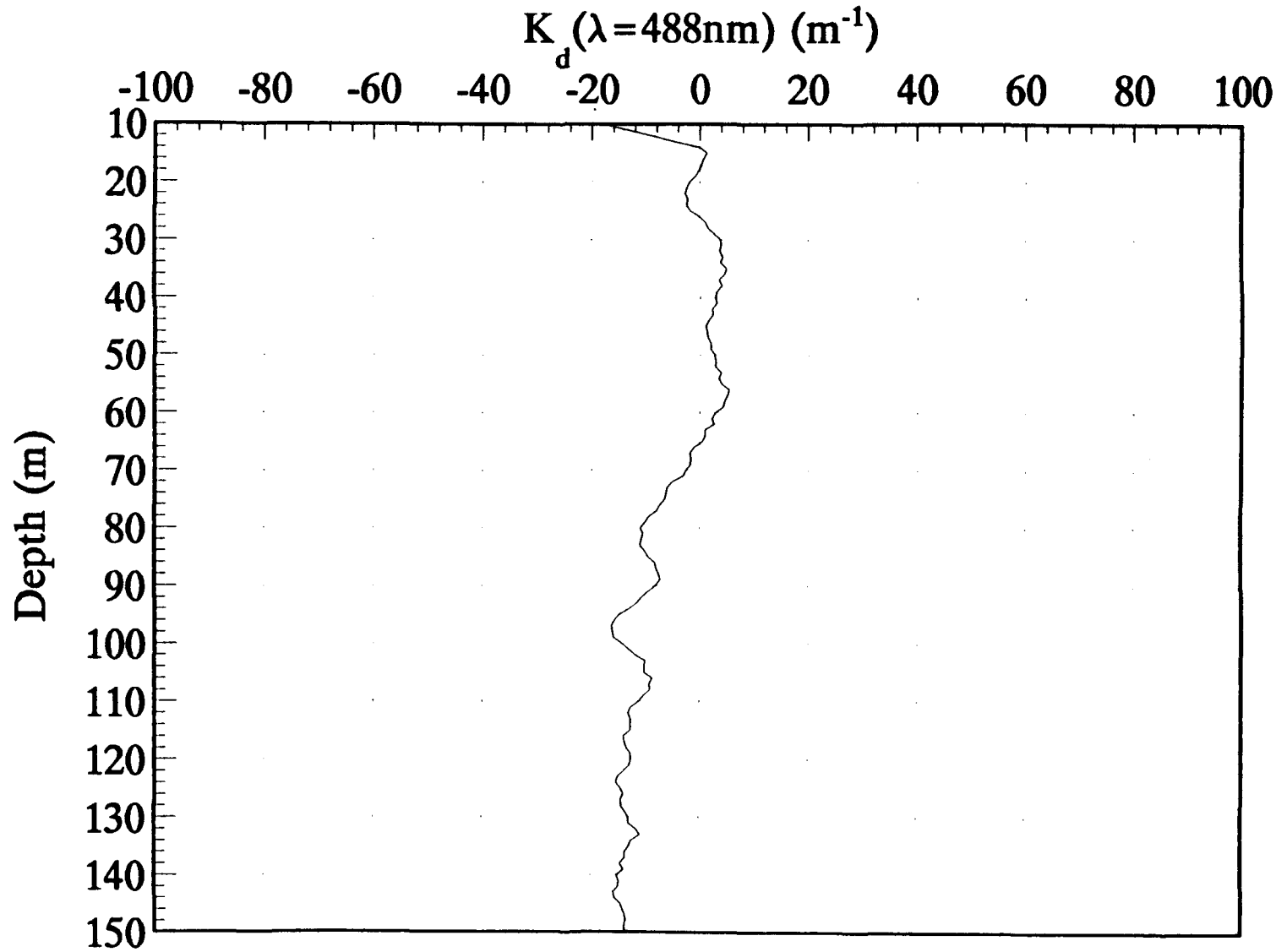

1992 Pacific AXKT Test
AXKT Channel 14 Drop 6

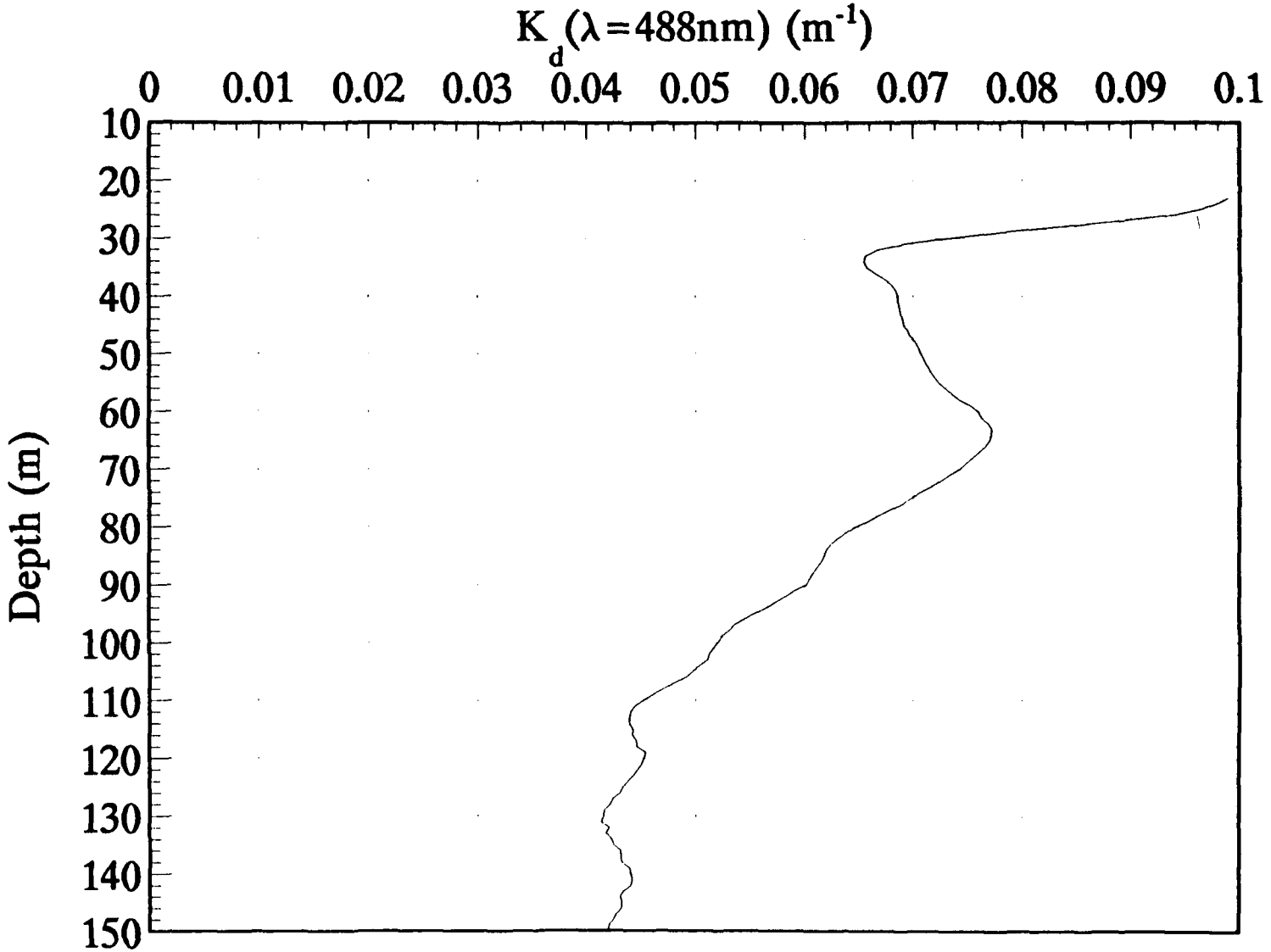

1992 Pacific AXKT Test
AXKT Channel 14 Drop 6 (% Difference From MER Data)

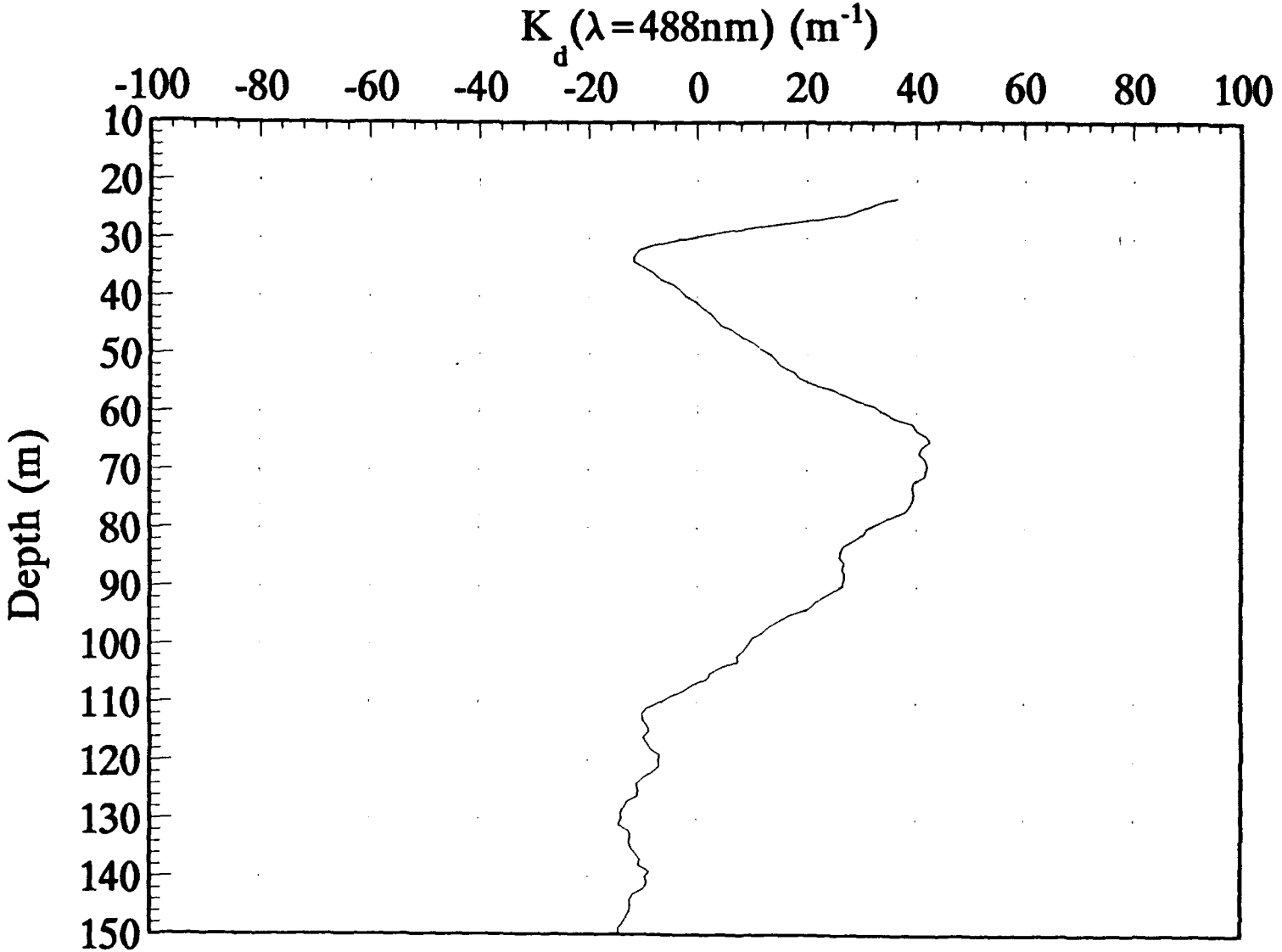

1992 Pacific AXKT Test
AXKT Channel 16 Drop 7

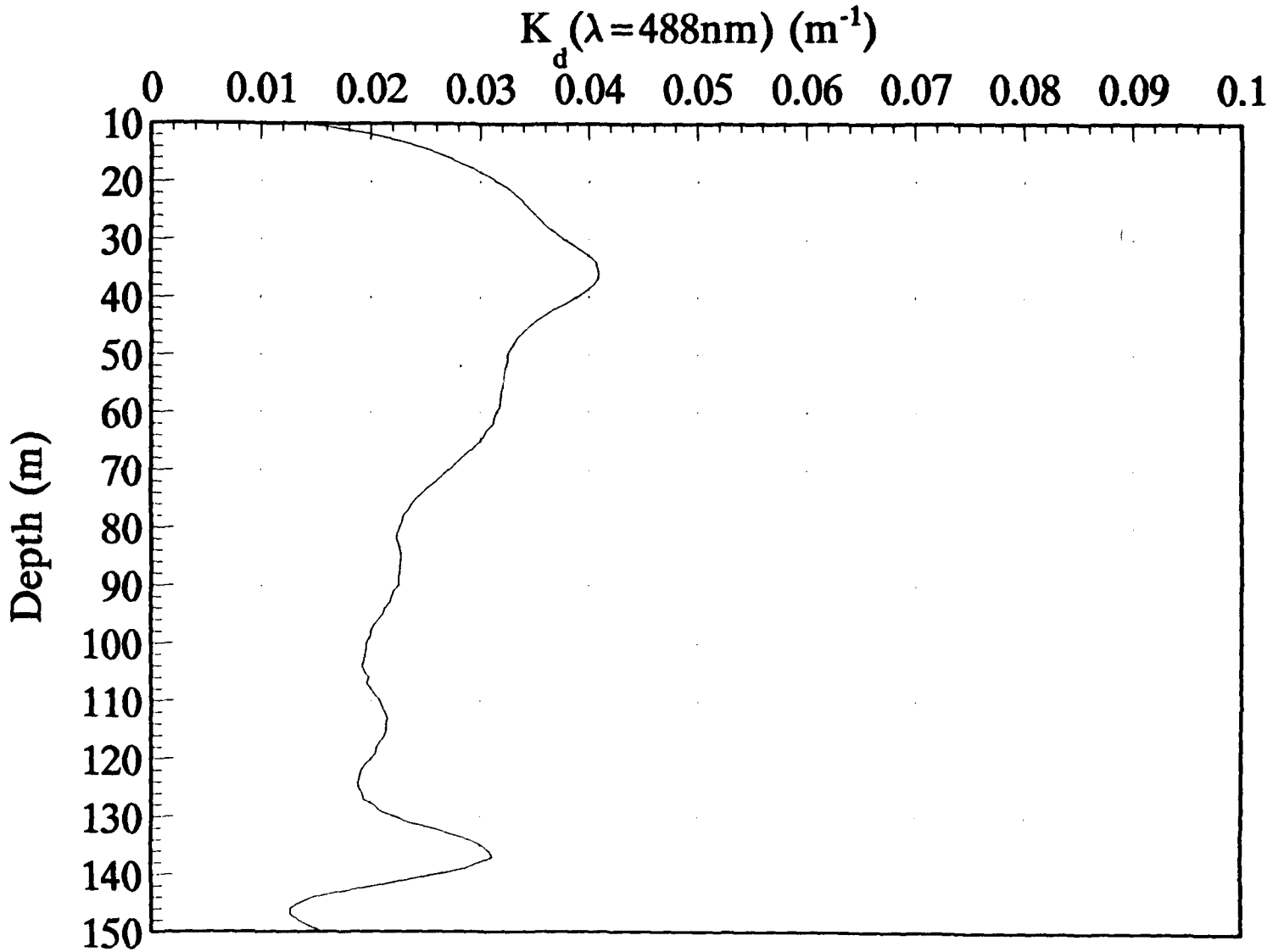

1992 Pacific AXKT Test
AXKT Channel 16 Drop 7 (% Difference From MER Data)

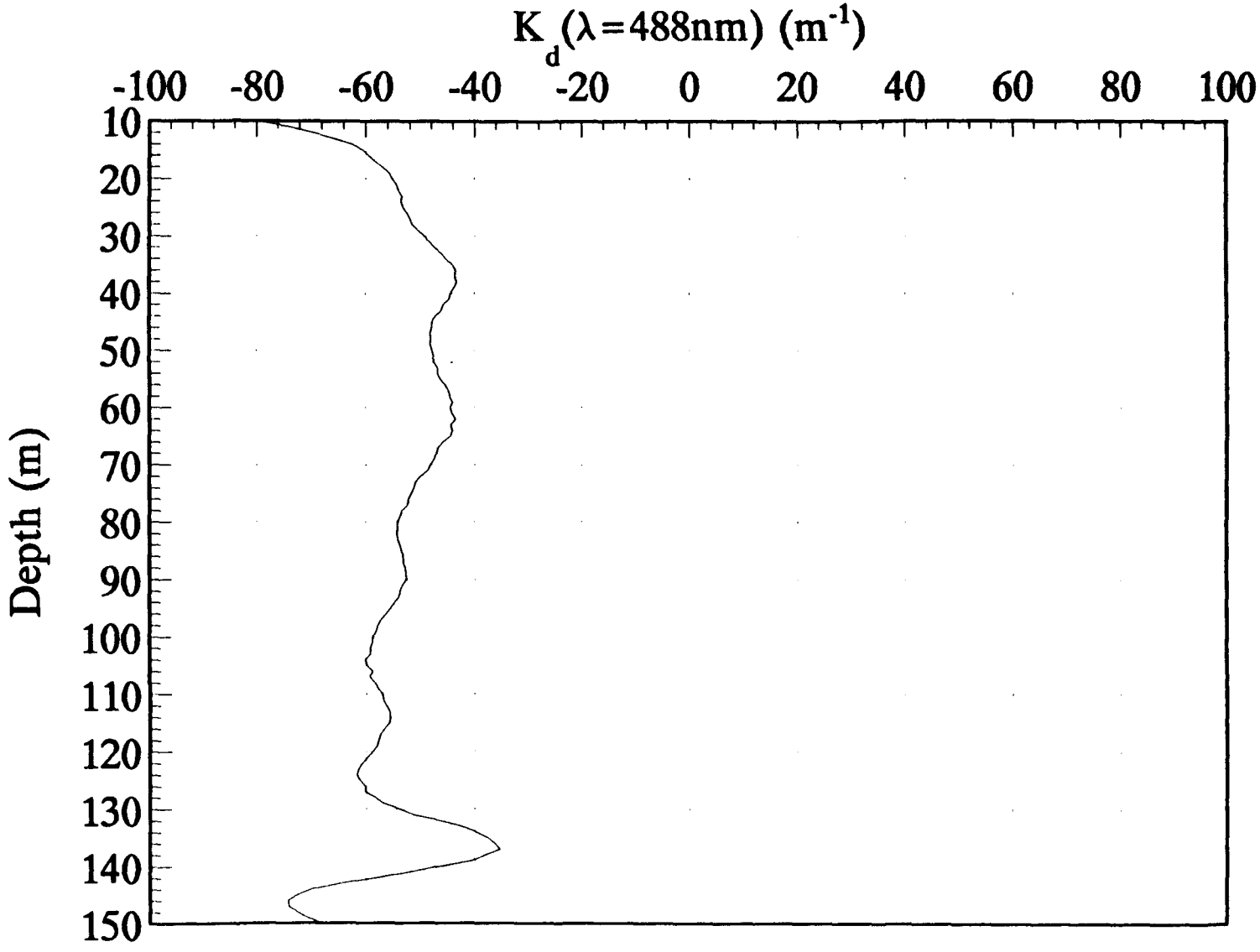

1992 Pacific AXKT Test
AXKT Channel 14 Drop 8

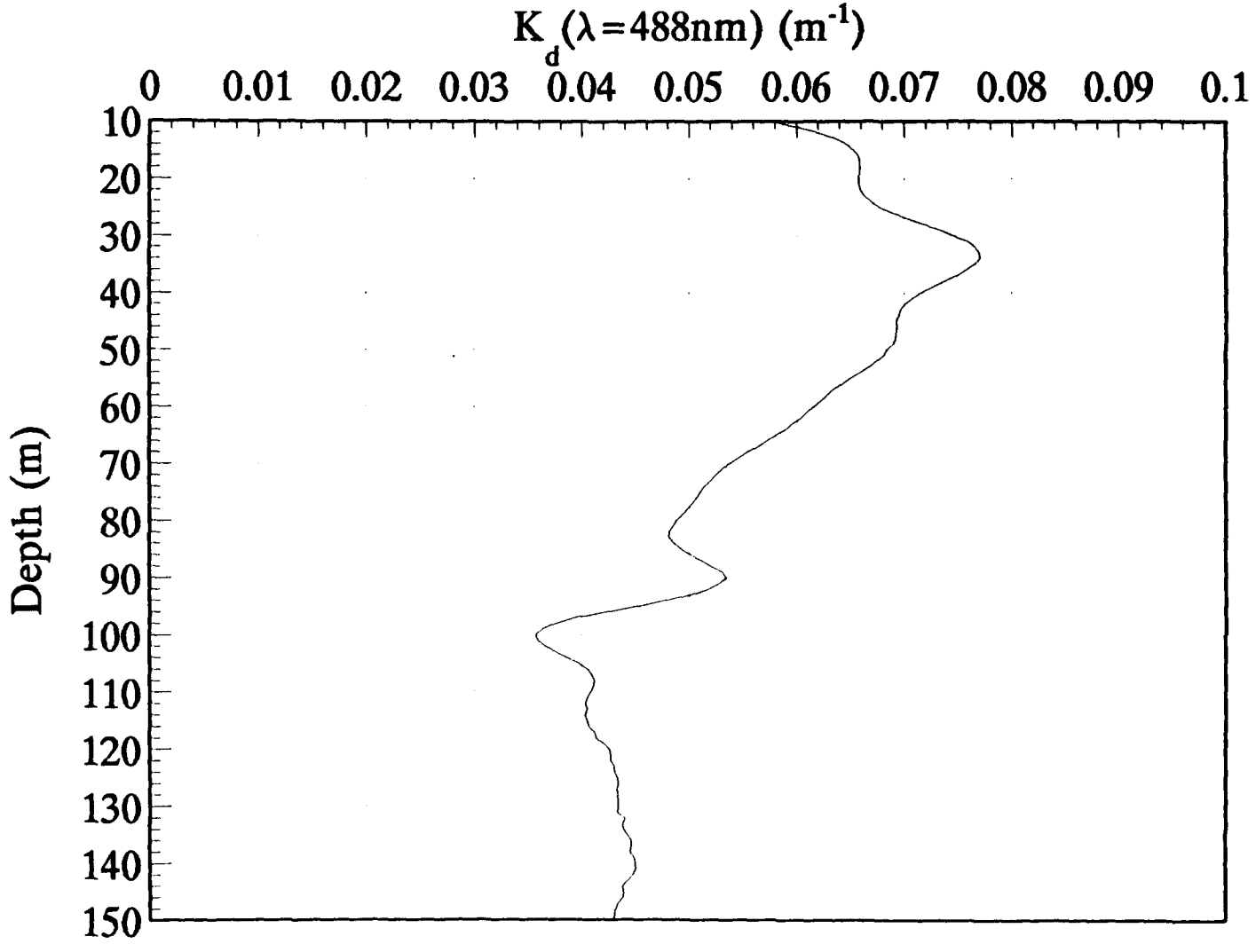

1992 Pacific AXKT Test
AXKT Channel 14 Drop 8 (% Difference From MER Data)

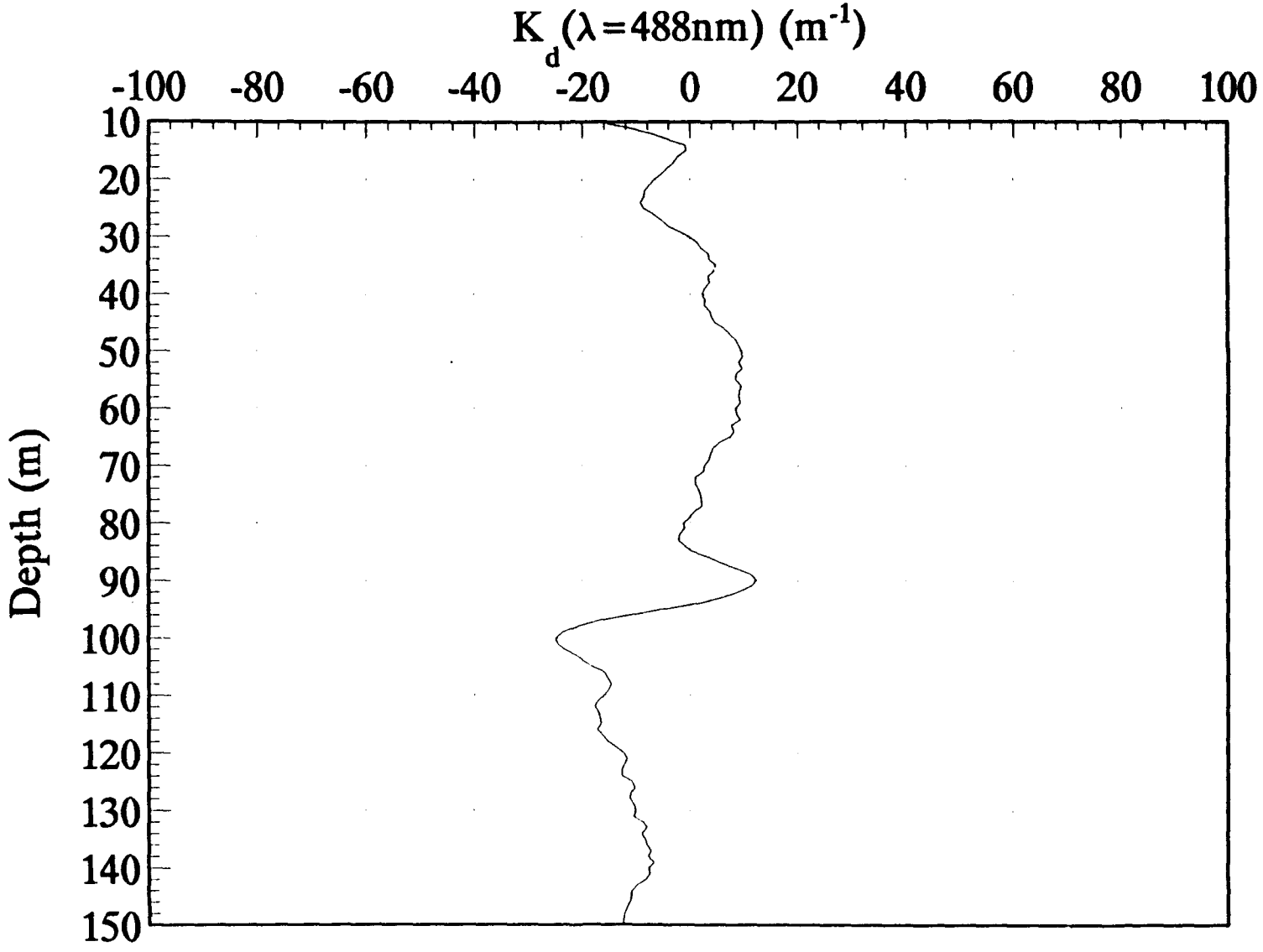

1992 Pacific AXKT Test
AXKT Channel 14 Drop 9

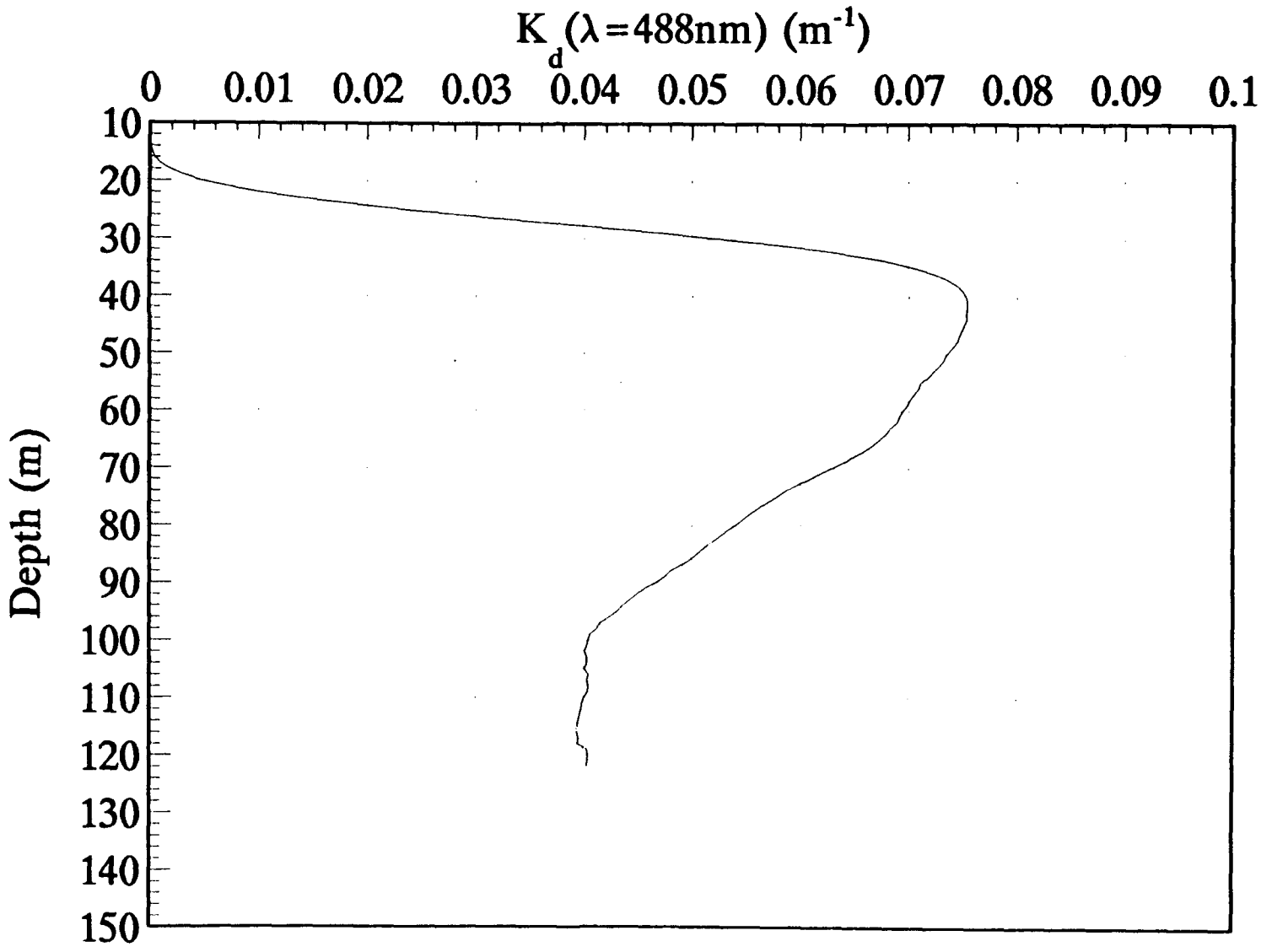

1992 Pacific AXKT Test
AXKT Channel 14 Drop 9 (% Difference From MER Data)